THE UNIVERSITY
of EDINBURGH

Main group species for catalytic hydroboration

Alessandro Bismuto

A thesis submitted for the degree of

Doctor of Philosophy

2018

Declaration of Originality

I hereby certify:

a) That the thesis has been composed by me under the supervision of Dr Stephen P. Thomas and Dr Michael J. Cowley.

b) Either that the work is my own, or, where I have been a member of a research group, that I have made a substantial contribution to the work, such contribution being clearly indicated.

c) That the work has not been submitted for any other degree or professional qualification.

Alessandro Bismuto

Abstract

Modern synthetic chemistry is unimaginable without transition metal catalysis. Yet the often high cost, toxicity and scarcity of many transition metals is driving attempts to find sustainable alternatives. Thus, the development of catalytic processes using main-group catalysts is now of broad interest. This thesis reports the development of a facile protocol for the aluminium-catalysed hydroboration of alkynes, alkenes and polar bonds using commercially-available catalysts. The catalytic hydroboration is proposed to occur by hydroalumination followed by product release through σ-bond metathesis with pinacol borane.

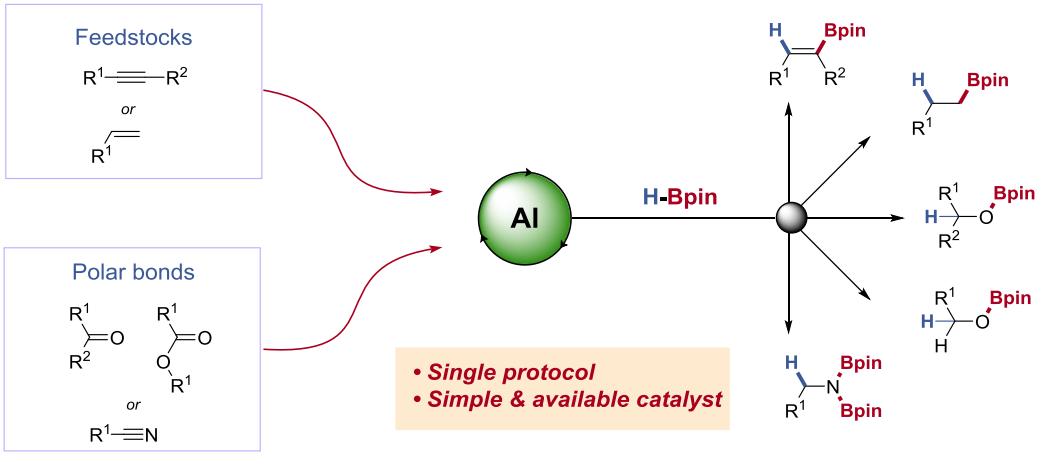

Scheme 1A. Aluminium-catalysed hydroboration.

An alternative route to alkenyl boranes is the 1,1-carboboration of alkynes using stoichiometric $B(C_6F_5)_3$. A zwitterionic intermediate in the Piers' borane-catalysed hydroboration and 1,1-carboboration of alkynes with $B(C_6F_5)_3$ has been characterised and its divergent reactivity identified. This has led to the development of a $B(C_6F_5)_3$-catalysed hydroboration of alkynes using HBpin.

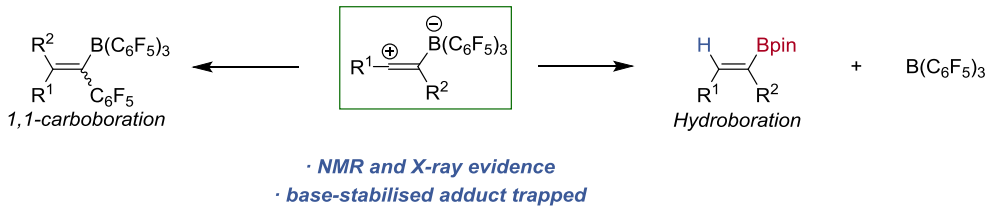

Scheme A2. Characterisation of zwitterion and $B(C_6F_5)_3$-catalysed hydroboration of alkynes.

Lay Abstract

Catalysis is a powerful method used for the synthesis of products used in everyday life, such as plastics and pharmaceuticals, and provides the ability to synthesise molecules in a controlled manner. The increasing need for sustainable chemical processes has cemented catalysis at the core of modern industrial chemistry and academic research. Synthetic chemistry today is unimaginable without transition metal catalysts, yet the often high cost, toxicity and scarcity of many such metals is driving attempts to find more benign alternatives. Thus, the development of catalytic processes employing main-group catalysts is now a subject of much-renewed interest.

This work has focussed on the use of commercially-available aluminium catalysts for chemical transformation and introduced a novel mode of reactivity to the emerging field of main-group catalysis. Aluminium is the most abundant metal in the Earth's crust and the major constituent of many common minerals, but to date has not been exploited to its full potential.

Central to advances in all catalysis is an understanding of the mechanisms of action, but this is particularly true of main group catalysis which lags behind other areas. Herein we report studies that determine main-group catalytic mechanisms, and the discovery of a novel intermediate in the preparation of functionalised alkenes which offers great potential for exploitation in new chemistries.

Acknowledgements

Firstly, I would like to express my sincere gratitude to my PhD advisors, Dr M. J. Cowley and Dr S. P. Thomas, for the continuous support during these four years. Their different background gave me the opportunity to develop diverse and valuable skills in catalysis and in inorganic chemistry. The patience, motivation, and guidance they have provided me is invaluable; I could not have imagined having better advisors and mentors for my Ph.D. study.

I also want to thank all of the members of the Thomas and Cowley group, past and present for the stimulating discussion and for sharing such a working environment. A particular thank goes to my friends, Nicola, Massimiliano and Martin, for the amazing time spent together. I would like to thank the University of Edinburgh and CRITICAT CDT for financial support. A special thanks goes to Dr K. Jones for his help and support during the first 6 months in St Andrews'. I would like to thank Juraj Bella, he has not only been a valuable friend, but also of incredible help with NMR spectroscopy; most of the work in the last chapter could have not been done without his help.

I would like to thank my partner Alessia. I met her at the beginning of my undergraduate and since then, she has been with me and supported me through most of my academic journey. She has been a rock and has kept me grounded throughout my studies. None of this could have been possible without her.

I am also grateful to John Hartwig and the members of the Hartwig group and all the staff at the University of California, Berkeley for the 6 months spent there. For this I owe thanks to the Royal Society of Chemistry for the provision of a Research Mobility Grant which made it possible. I would also like to thank the support and technical staff at the University of Edinburgh.

Last but not the least, I would like to thank my family for encouraging me in all of my pursuits and inspiring me to follow my dreams. I am grateful to my dad, his thirst for knowledge and passion about science is probably what inspired to start my scientific study. I am grateful to my mum, there are no proper words to describe her unconditional love and patience. I am grateful to my brother and my sister we have always been inseparable, as the three Musketeers "all for one and one for all" we support each other always and forever.

Table of Contents

List of Abbreviations

Ar	-	aryl
^{i}Bu	-	*iso*-butyl
^{t}Bu	-	*tertiary*-butyl
Dip	-	2,6-di*iso*propylphenyl
DEPT	-	Distortionless enhancement by polarization transfer
Et	-	ethyl
eq.	-	equivalent
EDG	-	electron donating group
EWG	-	electron withdrawing group
FLP	-	frustrated Lewis pair
HSQC	-	heteronuclear single quantum coherence
HRMS	-	high resolution mass spectrometry
IR	-	infrared
Me	-	methyl
Mes	-	2,4,6-trimethylphenyl
NMR	-	nuclear magnetic resonance
^{i}Pr	-	isopropyl
R	-	generic organic moiety
rt	-	room temperature
Ts	-	*para*-toluenesulfonate
THF	-	tetrahydrofuran
TMS	-	trimethylsilyl
VT NMR	-	variable temperature nuclear magnetic resonance

Chapter 1−Introduction

The increasing need for sustainable chemical processes has cemented catalysis at the core of modern industrial chemistry and academic research.[1] Catalysis increases the rate of a chemical reaction by the addition of a reagent, the catalyst, without its consumption. The catalyst provides a route between starting material and product with a lower activation energy than the uncatalysed process. Substances that can accomplish this remarkable role are of immense importance in chemistry and biology.

The term catalysis was first used by the Swedish chemist Jöns Jacob Berzelius in 1835 to explain a series of observations regarding enzymes. All enzymes are catalysts that expedite the biochemical reactions necessary for life. For instance, α-amylase, one of the enzymes in saliva, accelerates the conversion of starch to glucose, performing in minutes a transformation which would otherwise take weeks.[2],[3]

Catalysis is also one of the key concepts of green chemistry,[4] the design of chemical products and processes that reduce or eliminate the use and generation of waste substances. The waste usually generated in the manufacture of organic compounds, aside from solvent, is primarily based on inorganic salts. This is a direct consequence of the use of stoichiometric inorganic reagents in organic synthesis. For instance, stoichiometric reductions with metals (Na, K, and Zn) and metal hydride reagents ($LiAlH_4$, $NaBH_4$) represent a case of non-sustainable processes.

The study of catalysis is therefore of enormous importance to develop a more sustainable future. In recent years, countless efforts have been made to improve the efficiency and selectivity of catalytic systems and to design new ones, taking advantage of novel metal-ligand complexes and contributing to the growth of this field.[5]-[7] To this end, synthetic chemistry today is unimaginable without transition metal catalysts. The majority of chemical products for everyday life are made using precious and non-abundant metal catalysts in at least one step (Figure 1.1).[8],[9] For instance hydrofunctionalisation, olefins metathesis and all the cross-coupling process all require the use of precious transition metal catalysts, which makes them essential for synthetic chemistry. One of the most significant catalytic processes is the Suzuki–Miyaura

coupling reaction which uses a palladium catalyst to synthesise biaryl compounds from organohalides and boronic acids or boronic esters.[10]

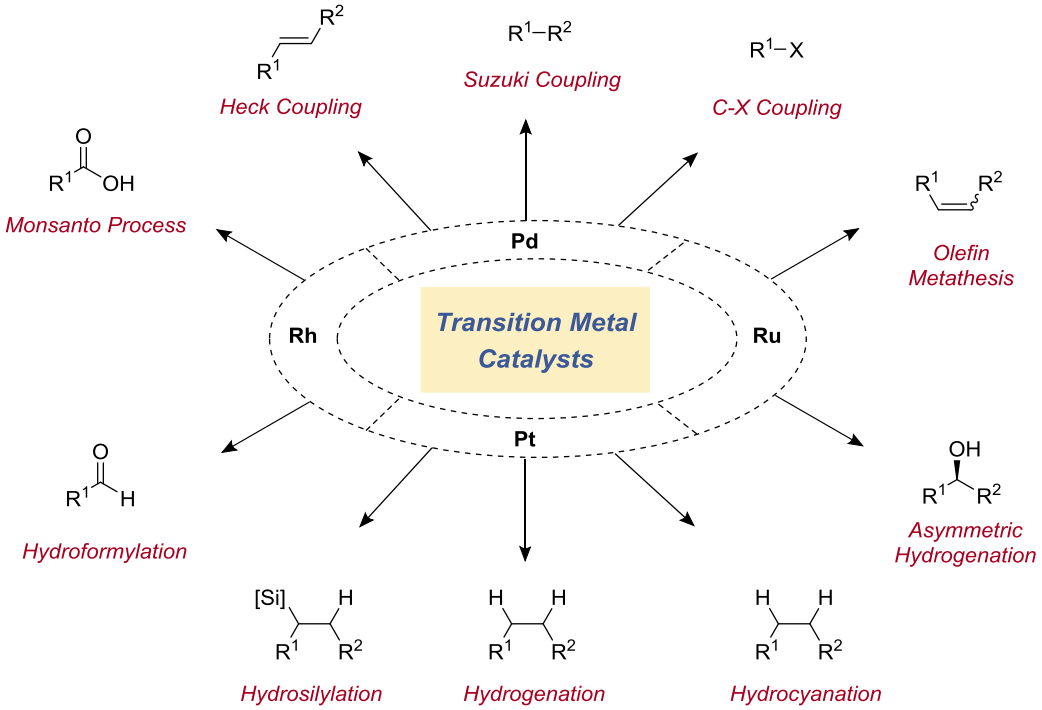

Figure 1.1. Transition-metal-catalysed processes.

Yet the often high cost, toxicity and scarcity of many transition metals[11] is driving attempts to find sustainable alternatives such as main group elements. The development of catalytic process employing main-group catalysts is now a subject of much-renewed interest.

1.1 Organo-boron and aluminium-compounds

Boron, aluminium, gallium, indium, and thallium are the elements of group 13, known as the boron group. Boron is classified as a metalloid while the rest are considered metals. The most well-known aspect of the chemistry of the Group 13 elements is the Lewis acidic behaviour of the halogenated compounds MX_3. The Lewis acidity of the MX_3 compounds in the trivalent state arises from the presence of an empty acceptor orbital on the group 13 element, most simply considered to be a valence p-orbital which comprises the lowest unoccupied molecular orbital (LUMO). Indeed, the dominance of

the +3 oxidation state and the acceptor properties that characterise the resulting inorganic halo derivatives, have defined their principal role in catalysis and in organic synthesis as a Lewis acid.[12]–[14]

Organometallic compounds of group 13 have also attracted much attention in the last century due to highly polarised bonds which give an almost carboanion character and eases further functionalisation (Figure 1.2). Organoborane species, which are more stable due to the less polarised B-R bond, have become ubiquitous in organic synthesis due to their versatility and easy functionalisation. Recently, organoaluminium compounds have also received tremendous attention due to the high abundance and low toxicity of aluminium.

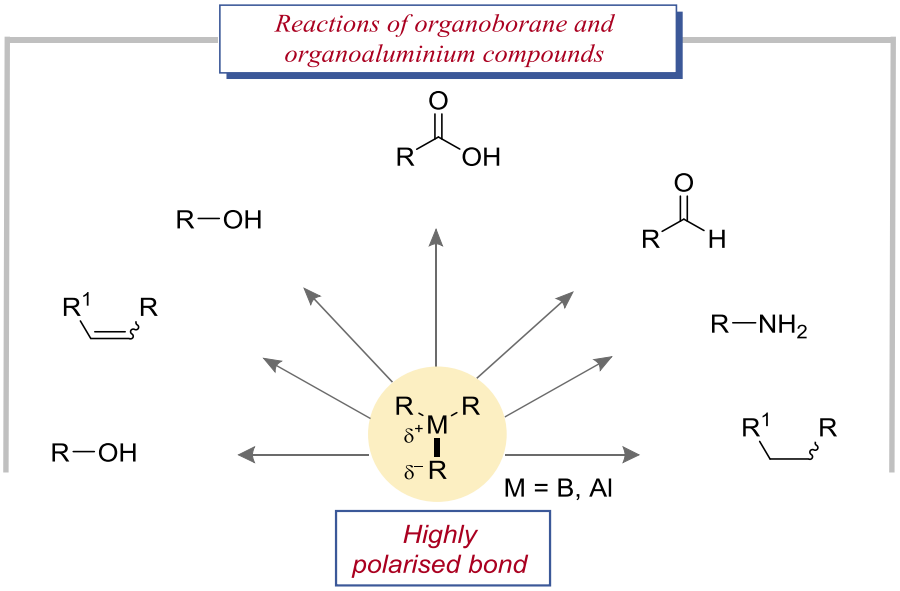

Figure 1.2. Versatile organoborane and organoaluminium in organic synthesis.

Despite the difference in polarity of C-B and C-Al bonds, boron and aluminium compounds usually share the same type of bonding.[15] The high polarity makes the compounds highly reactive to both moisture and oxygen, especially in the case of organoaluminium species. Much effort has been dedicated to characterise the structures of these compounds, both in solution and in solid state. The existence of trimethyl aluminium has roots before the 19th century, but the solid state structure was only reported in the 1960s, as one of the first methyl bridging metal systems (Figure 1.2).[16] The lower homologs of trialkylaluminium or trialkylborane compounds are well known to

form dimers with symmetrical alkyl bridges. A common description of this structure is a sp^3–hybridised representation for both Al and C with the overlap of the hybrid orbital of the bridging carbon atom with two metal orbitals to form a 3-centre-2-electron bond (Figure 1.3). It is worth noting that the long history of studies on the nature of the bridge bonding in Al_2Me_6 is well documented and it is still debated.[17],[18]

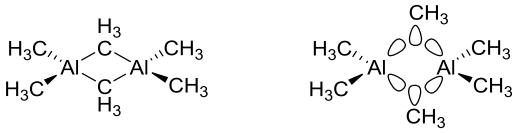

Figure 1.3. Structure and molecular orbitals description of Al_2Me_6.

The bonding nature can be strongly influenced by the substituents on the aluminium centre; increasing the bulk of the alkyl substituents limits its ability to form alkyl bridges through 3-centre-2-electron bonding. As a consequence, the introduction of sterically hindered *tert*-butyl groups results in $^tBu_3Al$ being a monomer in solution and in the solid state.[19],[20] The polarity of these group 13-organo derivatives leads to reactivity like a carbanion; highly versatile in organic synthesis and which together with the Lewis acidic metal centre, has further potential for catalysis.

Another important class of aluminium and boron compounds are the hydrides: borane and alane, which share many properties with the above-mentioned alkyl species. These compounds feature single or multiple E-H bonds with an empirical formula of BH_3 and AlH_3. Diborane (B_2H_6) was first synthesised in the 19th century by hydrolysis of metal borides, but it was never chracterised. At the beginning of the previous century, Alfred Stock investigated boron hydrides chemistry leading to experimental procedures for the synthesis and manipulation of the highly reactive and volatile boron compunds. The possible structure of this species was amply debated with different bonding models and hybridisations proposed. Ethane and ethene-like structure were initially proposed, with a tetrahedral or a trigonal planar boron, respectively.[21] Eventually experimental and theoretical investigations agreed that diborane adopts a D_{2h} structure containing four terminal and two bridging hydrogen atoms. The bridging hydrogen atoms provide one electron, another example of 3-centre 2-electron bonding.[21]

In contrast, alane (AlH_3) is a polymer. Hence, its formula is sometimes represented as $(AlH_3)_n$. Monomeric AlH_3 has been isolated at low temperature in a solid noble gas matrix and featured a planar geometry. The dimer Al_2H_6 has been isolated in solid hydrogen and is isostructural with diborane (B_2H_6).[22]

Both alane and borane share a tedious synthesis and difficulty in storage. Different strategies have been adopted to make them more practical while maintaining the fundamental reducing reactivity. Two major strategies were developed: donor-stabilised adducts and the use of the tetra-substituted anionic salt forms (Figure 1.4). Borane and alane are readily stabilised by σ-donors such as amines and sulfides, which shift the equilibrium to the monomeric form and therefore increase their stability.[23] Some of these adducts are commercially available and have been widely used in organic synthesis over the last 50 years.

Anionic borohydride and aluminium-hydride compounds were first synthesised by reaction of an alkali metal hydride and the corresponding group 13 halo derivative.[24] These anionic forms are usually more stable and more powerful reducing agents than borane or alane and have been extensively used in the reduction of unsaturated polar bonds. The higher solubility in organic solvents has facilitated the use of organo- and hydrido- species compare to their inorganic counterparts MX_3. For the above-mentioned reasons, boron and aluminium excel among main group elements for the versatily in organic synthesis.

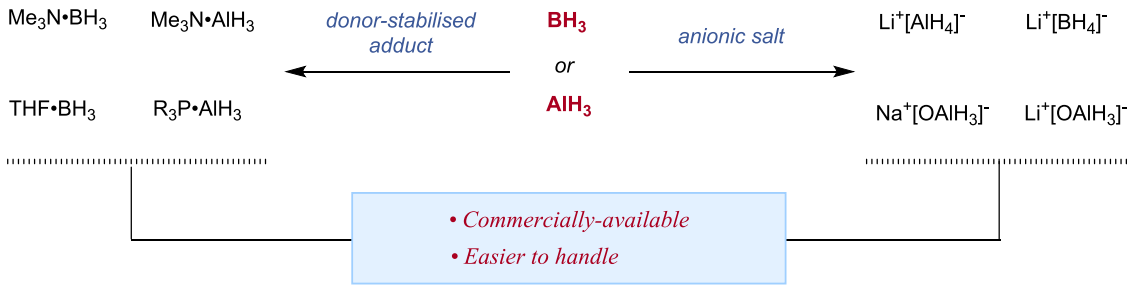

Figure 1.4. Stabilised borane and alane species.

1.2 Hydroboration Reactions

In 1960s, Brown and coworkers discovered that the addition of an H-B bond across an unsaturated bond led to a new class of reaction: hydroboration.[25]–[27] The earliest reported hydroboration reagent is diborane B_2H_6 which showed extremely good reduction activity towards unsaturated bonds.[28],[29] Diborane is in equilibrium with borane, and the reaction was proposed to be initiated through coordination of the carbonyl lone-pair into the empty p-orbital of borane. Subsequent hydride migration to the keto functionality leads to the formation of the alkoxy borane product (Scheme 1.1).[29] Brown and co-workers also demonstrated diborane's efficiency for the hydroboration of olefins (Scheme 1.1).[30],[31] The addition of BH_3 (and other hydroboration reagents) to alkenes and alkynes takes place *via* a concerted mechanism and in a *syn*-fashion, in direct contrast to the hydroboration of ketones which is a step-wise process. The *anti*-Markovnikov bonding is generally preferred, with the boron moiety attached to the less substituted carbon.

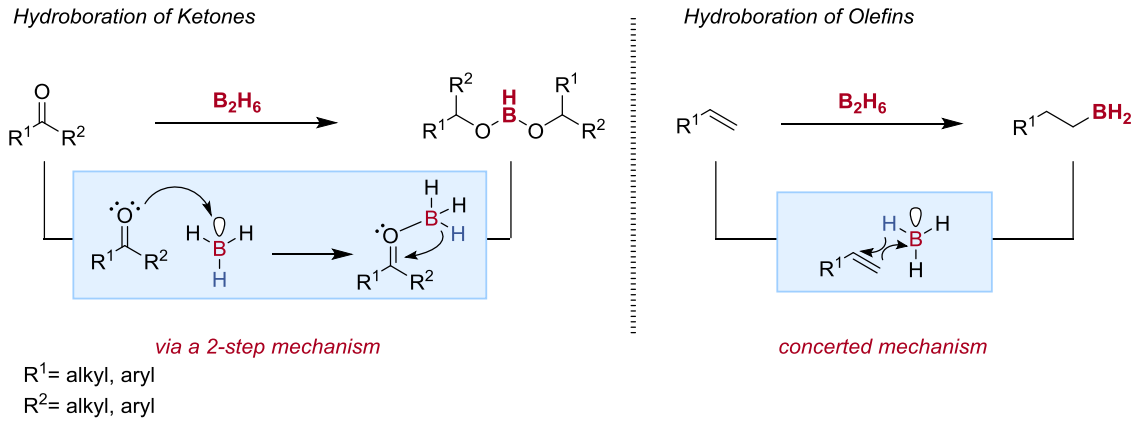

Scheme 1.1. Hydroboration of polar and non-polar bonds.

The mechanism of this transformation was further investigated by Brown and Zweifel using BH_3·THF for the hydroboration of different *para*-substituted styrene derivatives (Scheme 1.2).[32] The *para*-substituent played a crucial role in determining regioselectivity. For instance, *para*-methoxy styrene showed a ratio of *anti*-Markovnikov to Markovnikov product of 66:34 while *para*-trifluoromethyl styrene a ratio of 94:6. Examining the two possible transition states it was postulated that electron-donating groups tend to proceed with boron addition at the terminal carbon position through the

more stable transition-state (**I**). The reverse case gives increased selectivity towards the linear product, transition-state (**II**). As a result, alkyl alkenes or alkynes usually result in a better selectivity (94:6) than arene derivatives (80:20), however in all the cases the selectivity is strongly influenced by both electronic and steric parameters.

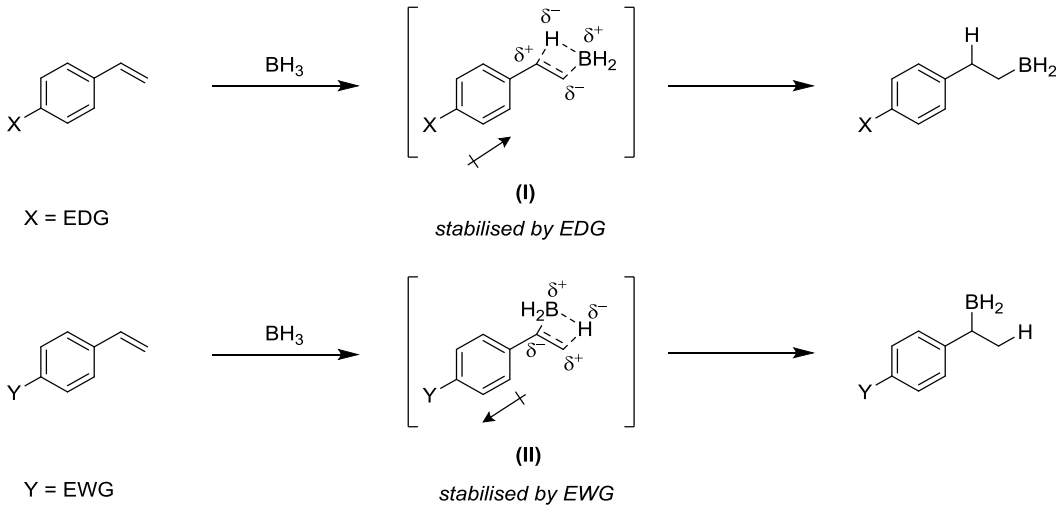

Scheme 1.2. Hydroboration of polar and non-polar bonds.

Although diborane is highly reactive, it is a gas at room temperature and requires technically demanding handling and specialist equipment. Hence several hydroborating agents such as borane-THF,[33] Me_2S-borane complex,[34] thexylborane,[35] disiamylborane,[36] and *B*-H-9-BBN[37] (Figure 1.5) have been developed to stabilise borane and to ease the practicality of this transformation. All of these products lead to alkyl borane species which are usually difficult to purify as they are not stable under column chromatography conditions. A recent advance was the introduction of new hydroboration reagents with the ultimate goal of forming boronic esters, which are easier to handle and to purify.

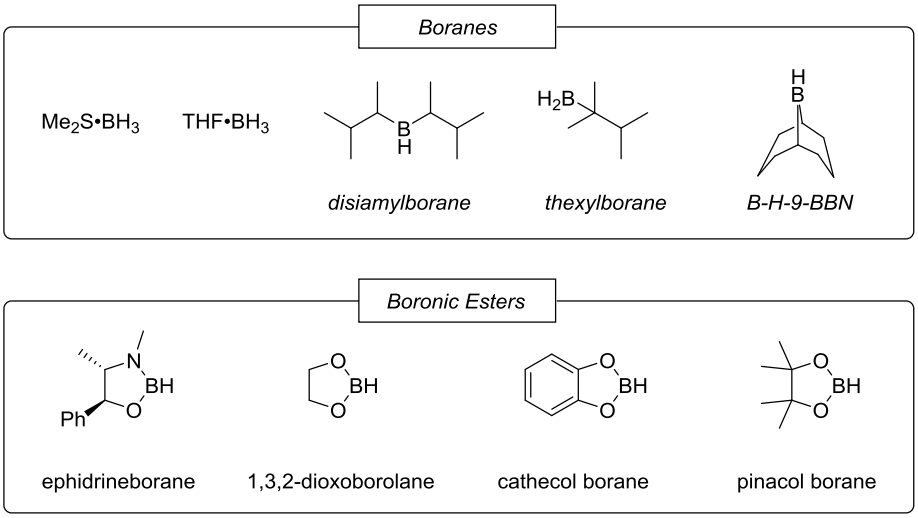

Figure 1.5. Versatile organoborane and boronic ester reagents.

Among these, catechol borane, HBcat, was the first, commercially available, reagent capable of performing the hydroboration of alkenes and alkynes.[38]–[40] Catechol borane can be easily accessed from catechol and BH_3·THF and can be purified by distillation. It can be handled and stored in a pure form and the corresponding hydroboration products are typically formed in an *anti*-Markovnikov fashion (Scheme 1.3). The versatility of catechol borane has been widely demonstrated in both uncatalysed and metal-catalysed hydroboration processes.

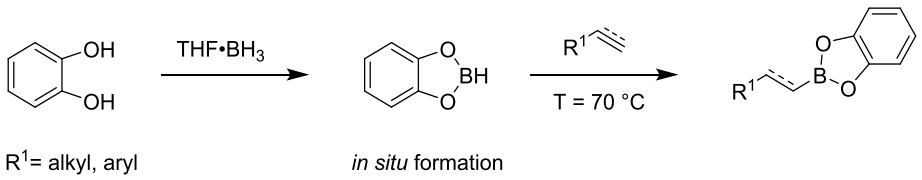

Scheme 1.3. Hydroboration of alkenes and alkynes using catechol borane.

Despite its vast use, catechol borane is not a perfect reagent; it is air-sensitive and readily decomposes at room temperature to borate, B_2cat_3, and borane (Scheme 1.4).[41],[42] The borane formed can lead to uncatalysed hydroboration, or in combination with metal catalysts lead to isomerisation and uncontrolled hydroborations leading to a mixture of products. Additionally, the hydroboration products, catechol boronic esters, are not

stable to traditional purification techniques such as column chromatography and distillation.

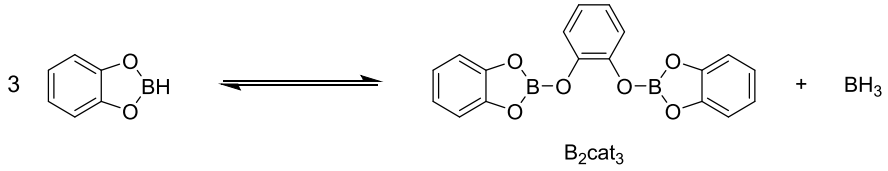

Scheme 1.4. Hydroboration of olefins using catechol borane.

Pinacol borane was first introduced as a hydroborating reagent by Knochel[43] and is probably the most used boronic ester synthetically. Pinacol borate esters are usually stable to column chromatography and air and moisture and they can often be formed under mild conditions. Boronic esters were traditionally accessed by conversion *in situ* from other boron containing species. It is worth nothing that, unlike borane, boronic esters do not react spontaneously with alkenes or alkynes (Figure 1.6). However, because of the greater stability of boronic esters and following the discovery of the Suzuki cross-coupling reaction, much attention has been focused on developing catalytic protocols for the hydroboration of alkenes and alkynes. Usually catalytic reactions are mechanistically different from uncatalysed reactions, and offer the possibility of the chemo-, regio- and stereo selectivity as defined by the catalyst rather than the substrate.

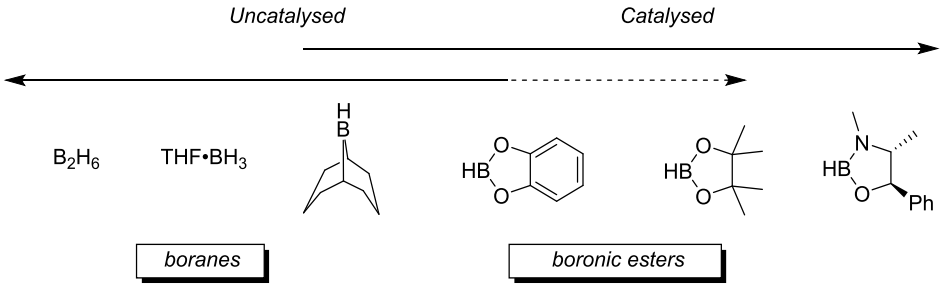

Figure 1.6. Catalysed *vs* uncatalysed hydroboration.

Srebnik reported the first example of rhodium-catalysed hydroborations using pinacol borane, albeit with poor selectivity.[44] Following this discovery, several protocols have been developed which have improved regioselectivity and group tolerance. Most of them have been catalysed by precious transition metals such as rhodium, iridium and palladium (Scheme 1.5).[45] The mechanism of this transformation has been widely

analysed and discussed alongside the development of new ligands to improve the efficiency and the selectivity of the process.[46]–[49]

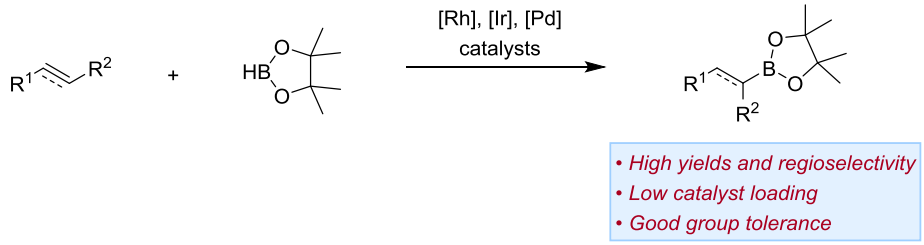

Scheme 1.5. Precious transition-metal-catalysed hydroboration of alkenes and alkynes.

1.3 Hydroalumination

In contrast to organomagnesium and organolithium compounds, which have been widely used in organic synthesis, organoaluminium compounds were almost unknown before the last century. The introduction of alkyl aluminium species by Ziegler and co-workers in 1952[50] is particularly significant as they provide complementary synthetic capabilities to zinc, magnesium, and lithium alkyls but, often with better chemo- and regioselectivity. Rare examples of carboalumination of α,β-unsaturated ketones and hydroalumination of highly polar aldehydes had been observed as early as the 1930s.[51] However, in 1950, the extensive research undertaken by Ziegler and co-workers on metal hydride additions to ethylene led to the discovery of both carbalumination and hydroalumination of unconjugated alkenes and alkynes,[52] as well as a wide variety of carbonyl[53] and related compounds.[54]

Hydroalumination, the addition of an Al-H bond to an unsaturated system, is a diffuse method for the stereoselective reduction of organic compounds.[55],[56]
Wilke and co-workers investigated the mechanism of the transformation and established that such additions can occur in a kinetically controlled *syn* fashion.[57] An important contribution directed towards the reaction mechanisms and the structures of the intermediates came from Eisch and others.[58],[59] They investigated reactions of aluminium hydride species and terminal and internal alkynes. They proposed that hydroalumination proceeds by initial coordination of the substrate (alkene or alkyne) to the p-orbital of the monomeric, three-coordinate aluminium hydride, followed by

concerted *cis* addition (Scheme 1.6). The rate of the reaction may be controlled by use of an electron-donor solvent such as tetrahydrofuran. Stronger Lewis bases can drastically slow or completely prevent the addition of H-Al bonds to carbon-carbon multiple bonds.

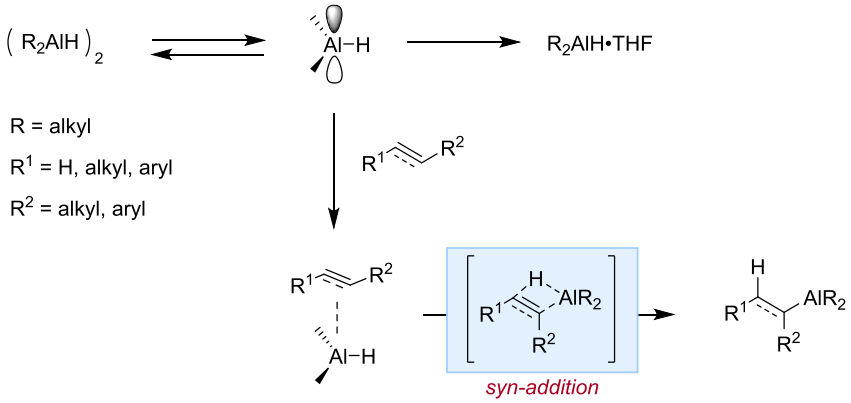

Scheme 1.6. Hydroalumination of alkenes or alkynes.

Stereoselectivity can vary depending on the steric and electronic nature of the substituent or the temperature, in some cases leading to a *trans*-hydroalumination. Eisch and co-workers analysed the effect of the bulk of trimethylsilyl substituent on the stereoselectivity of hydroalumination of acetylene derivatives.[60] They proposed that the hydroalumination of silyl acetylenes still occurred in a *syn*-fashion, but the silylvinylaluminium intermediate formed can rearrange using the p-orbital of the aluminium leading to the more stable *(Z)*-alkenyl aluminium isomer (Scheme 1.7). This is supported by the observation that the addition of a base inhibited the isomerisation which is due to coordination to the empty p-orbital of the hydroalumination product.

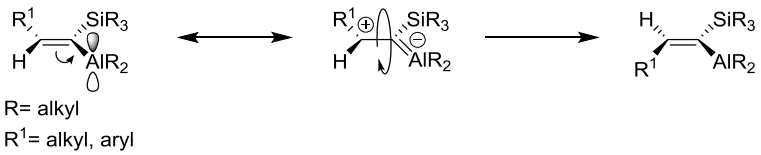

Scheme 1.7. Isomerisation of alkenyl aluminium species.

Despite the attention given to hydroalumination, the organoaluminium products have rarely been isolated, and their identities were typically deduced from the hydrocarbons obtained on hydrolytic work-up or other functionalisation.

Within the past 50 years, Uhl and co-workers have reported detailed studies on the physical and chemical properties of the hydroalumination.[61],[62] The isolation of these products was often facilitated by steric shielding by bulky bis(trimethylsilyl)methyl groups which helped the characterisation of hydroalumination products.

The reaction of terminal alkynes and Al-H species does not always result in hydroalumination; alkyne deprotonation with formation of alkynylaluminium compounds and dihydrogen is also a possibility. Steric hindrance on the aluminium and the acidity of the alkyne are often key contributors to the chemoselectivity of the two competing processes, which lead to the formation of two fundamentally different products. Power and co-workers have recently reported a thorough study on the reactivity of a sterically hindered primary alane $(Ar^{iPr_8}AlH_2)_2$ (Ar^{iPr_8} = (2,4,6-tri*iso*propylphenyl)-3,5-di*iso*propylphenyl) towards alkenes and alkynes (Scheme 1.8).[63] They demonstrated that sterically crowded substituents on the aluminium centre favoured the hydroalumination product over the deprotonation of terminal aryl alkynes. Reactivity studies of primary organoaluminium hydrides showed facile hydroalumination with both terminal alkynes and terminal alkenes, although no reaction was observed with internal alkenes even upon increasing the reaction temperature. Surrounding the aluminium with more steric bulk resulted in an enhancement of the rate of the reaction as a consequence of an increased concentration of monomeric species in solution.

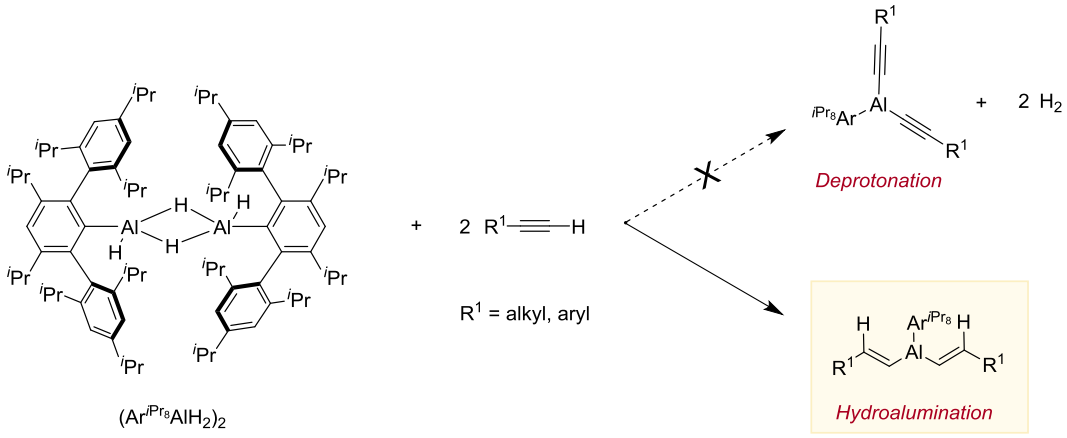

Scheme 1.8. Hydroalumination using sterically hindered aluminium $(Ar^{iPr8}AlH_2)_2$.

The hydroalumination of alkenes, instead, has only been applied to a relatively small extent. The reaction rates reported are slower compared with those of alkynes and the

reactions often only proceed at elevated temperatures.[64] Thus, several transition metal-catalysed processes have been reported, mostly using zirconium,[65] titanium,[66],[67] and nickel.[67] For instance, the hydroalumination of α-olefins and norbornene derivatives with $^{i}Bu_2AlH$ can be carried out at room temperature in the presence of $ZrCl_4$.

Notably, regardless of efficiency, all of the above-mentioned examples exclusively give formation of the *anti*-Markovnikov hydroalumination product. A breakthrough was reported by Hoveyda and co-workers who developed a nickel-catalysed stereospecific hydroalumination of alkynes (Scheme 1.9).[68] Tuning the phosphine ligand allowed selective formation of either the linear or the branched hydroalumination product. This protocol allows the synthesis of α-alkenyl aluminium species in good yields and high selectivity. The resultant species can be functionalised in a stereospecific manner to give the halide or the boronic esters, which would otherwise require tedious synthesis.

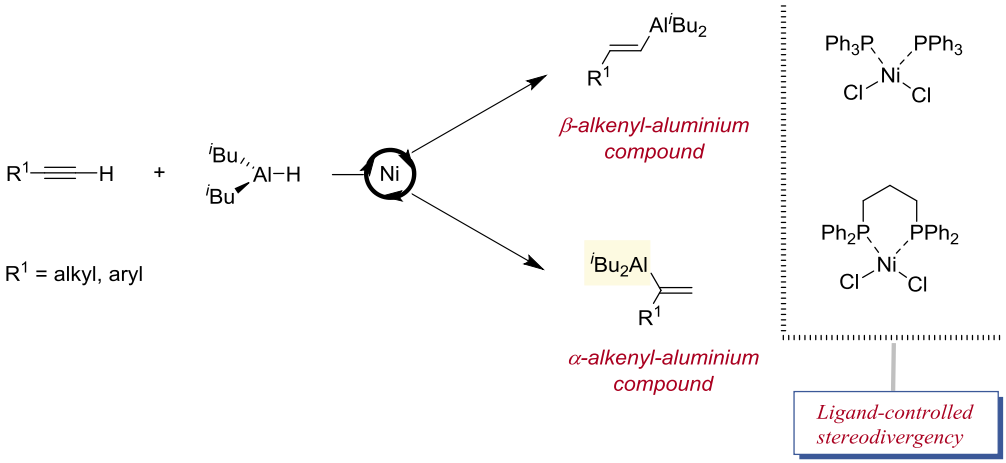

Scheme 1.9. Nickel-catalysed stereodivergent hydroalumination.

1.4 Main-group-catalysed Hydroboration

Understanding the synthesis and the structure of transition-metal hydride complexes has been the focus of research for many years, leading to their use in numerous catalytic applications.[69] Although main group hydride species have been equally well studied, their use in organic synthesis is often limited to stoichiometric applications. The turning point can be attributed to Harder and co-workers who reported a well-defined and highly soluble calcium hydride complex generated by σ-bond metathesis with phenyl silane.[70]

By analogy with Rare-Earth metal chemistry, it was hypothesised that this step could be used in catalysis. Thus, in the same year, using a similar complex, Harder and co-workers reported the first example of calcium-catalysed hydrosilylation of olefins (Scheme 1.10).[71] The catalysis was initiated by *in situ* formation of a Ca-H bond which inserted into the olefin generating a metal alkyl bond which released the product upon further reaction with phenyl silane. A proposed alternative mechanism involved the formation a highly reactive penta-coordinate silane, generated by reaction of the Ca-H complex with phenyl silane, which could insert in to the olefin bond by a concerted mechanism releasing the product and regenerating the catalyst.

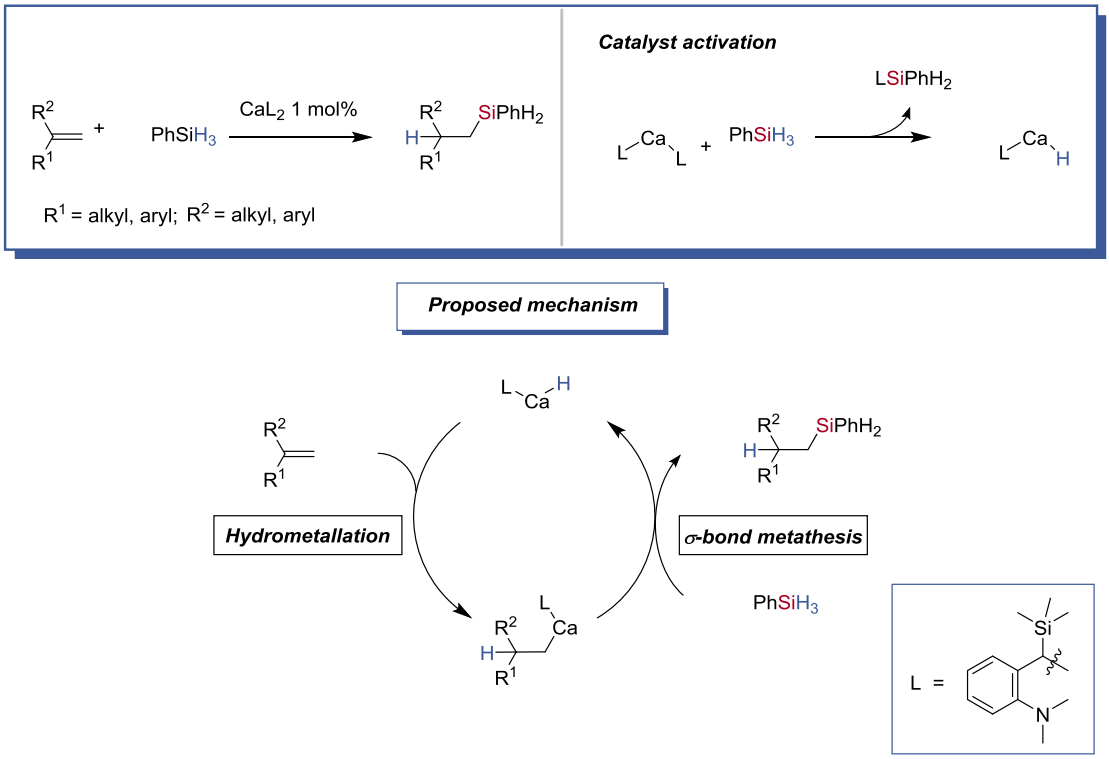

Scheme 1.10. Calcium-catalysed hydrosilylation of alkenes.

Based on the same concept, Hill and co-workers have investigated Mg-NacNac complexes [(*N,N'*-bis-2,6-(Dip)NC(CH_3)CHC(CH_3)N(Dip)], for catalytic hydrosilylation (Scheme 1.11). Although the same hydride exchange was proposed, no hydrosilylation was observed. However, the use of the more Lewis-acidic pinacol borane as opposed to phenyl silane triggered turnover, paving the way for a series of catalytic hydroborations of unsaturated polar bonds. Aldehydes and ketones[72] were the first substrates to

achieve good isolated yields under mild conditions and low catalyst loadings (Scheme 1.11).[72] Catalyst activation is proposed to occur by hydride exchange between the magnesium alkyl complex and pinacol borane, generating the Mg-H species *in situ*. The latter has been previously reported by Jones[73] as the major product of the reaction of phenylsilane with alkyl-MgNacNac. Any attempts to isolate the dimer from the reaction mixture failed and Mg-H and ^{n}BuBpin species were only confirmed spectroscopically (δ ^{1}H = 3.53, δ ^{11}B = 34.53). This compound was postulated to exist in equilibrium with another species where only one hydride is effectively bound to magnesium while the other remains covalently bound to boron and the overall system is stabilised by oxygen coordination, which explains the difficult NMR interpretation (Scheme 1.11).

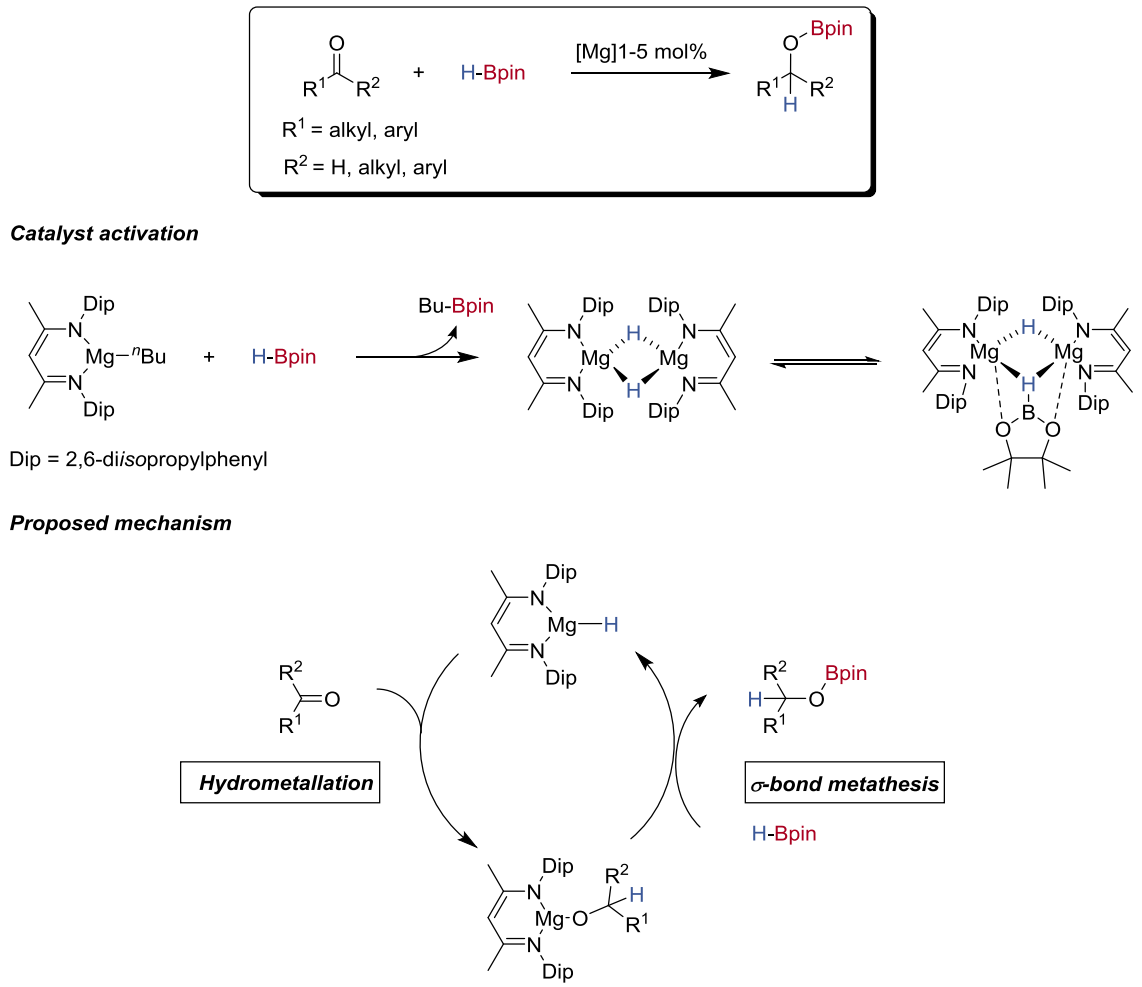

Scheme 1.11. Magnesium-catalysed hydroboration of unsaturated polar bonds.

The same Mg complex was reported as a catalyst for imines[74] and nitriles functionalities.[75] A range of alkyl and aryl imines and nitriles were successfully hydroborated using 10 mol% catalyst loading under mild conditions. As before, the reaction proceeds *via in situ* Mg-H formation followed by hydride attack and generation of the product by reaction with pinacol borane, which simultaneously regenerates the catalyst.

Recently Sadow and co-workers disclosed the catalytic hydroboration of esters using a magnesium bisoxazoline complex (Scheme 1.12).[76] The reaction proceeds at room temperature with low catalyst loading and good functional group tolerance. The mechanism of this transformation was extensively studied through both stoichiometric and kinetic studies. The stoichiometric reaction of the magnesium complex with HBpin gave no conclusive information. However, carrying out the reaction in the presence of an excess of pinacol borane gave formation of a borohydride species. Surprisingly, X-ray analysis revealed pinacol borate coordinated to the magnesium centre through one of the oxygen atoms of the pinacol moiety with the boron bearing a dihydride substuent. Reaction of ethyl acetate and the magnesium compound resulted in the formation of the corresponding magnesium ethoxide with production of acetone through a series of insertion and β-ethoxide elimination reactions.

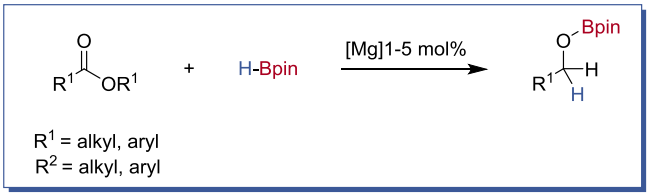

Stochiometric investigations

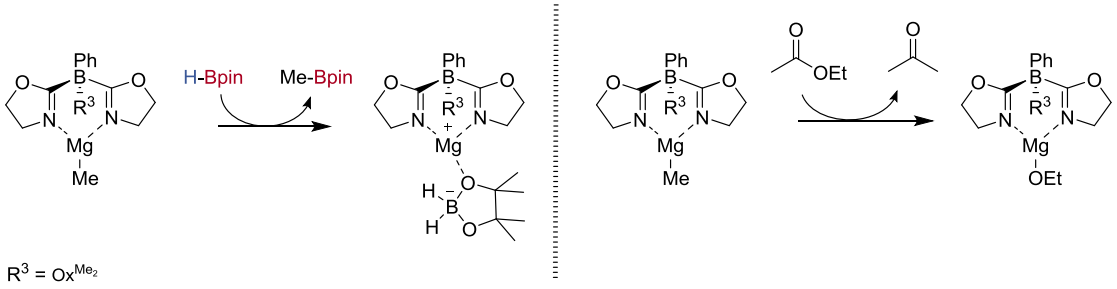

Scheme 1.12. Magnesium-catalysed hydroboration of unsaturated polar bonds.

Somewhat surprisingly, the kinetic analysis ruled out Mg-H as the catalyst resting state, suggesting an alternative mechanism (Scheme 1.13). Zero-order, half-order and first-order dependencies were found for HBpin, ethyl acetate, and the catalyst, respectively. This proves a lack of any Mg-HBpin or Mg-substrate species being involved in the rate-determining step as it would result in an overall second-order rate law. Half-order [EtOAc] dependency indicates a reversible interaction between the catalyst and ester to give two equivalents of the corresponding aldehyde before the rate-limiting step.[76] Sadow and co-workers also provided evidence of a magnesium zwitterion species as the catalyst resting state which was shown to give the borate ester products on addition of EtOAc. This latter observation is consistent with the zero-order dependency on [HBpin] as the hydride reducing equivalent is already present in the zwitterionic catalyst resting state.

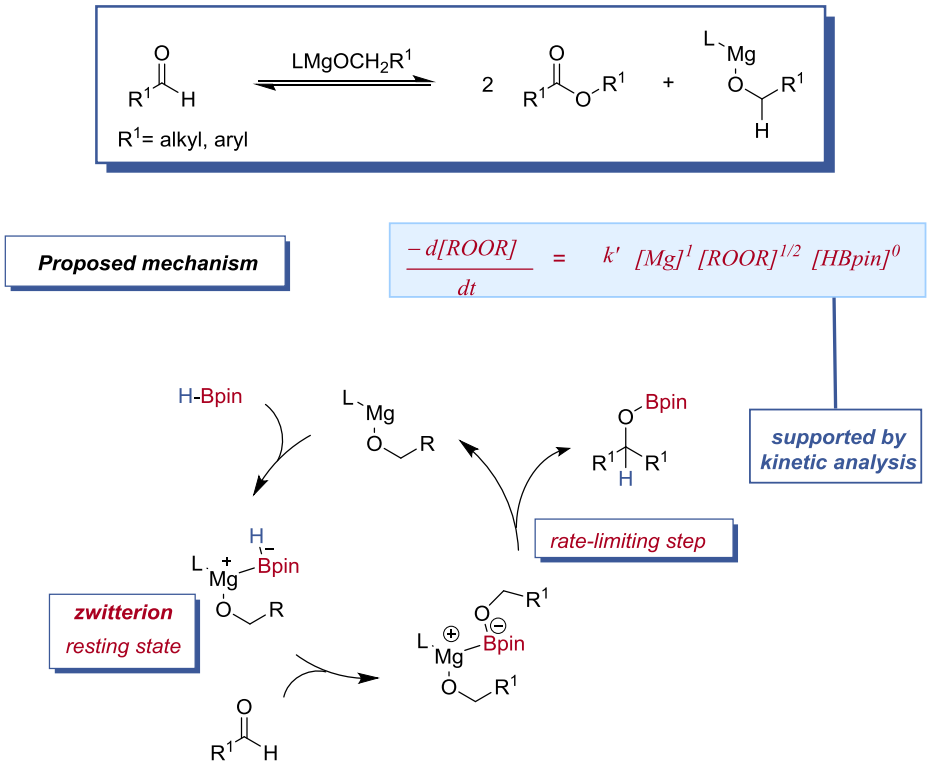

Scheme 1.13. Magnesium-catalysed hydroboration of unsaturated polar bonds.

Compared with examples from group 2, group 1 compounds have only recently been investigated for hydroboration reactions.[77] Particularly relevant works are form Okuda's,[78],[79] and Sen's[80] groups. Okuda and co-workers reported the synthesis and

catalytic activity of group 1 borohydride salts for the hydroboration of ketones and aldehydes. Interestingly, X-ray analysis of the complexes showed a significant difference in the bond character between the metal and the counter ion. While lithium is solvated by a molecule of THF, displaying a separate ion-pair coordination, both sodium and potassium form a contact-ion mode through a non-covalent interaction with phenyl borate rings. This resulted in completely different catalyst activity with lithium being almost 50 times more active than the others in this transformation. A possible mechanism was proposed whereby substrate activation was provided by hydride insertion to form an alkoxy borate species and turnover determined by σ-bond metathesis with pinacol borane (Scheme 1.14). An in depth study of the reaction mechanism showed that rate of insertion of the borohydride complexes is independent of the metal. However, it was proposed that the cationic metal centre plays a crucial role as a mediator for HBpin hydride abstraction.

Sen and co-workers reported the hydroboration of ketones and aldehydes using a 2,6-*tert*-butyl phenolate lithium complex.[80] The reaction proceeded under mild conditions with very high turnover frequencies (TOF) (benzophenone, TOF = 66,000 h^{-1}) and good group tolerance. Nitro, free amino, halo, and heterocycles substituents were all tolerated under the reaction conditions. As stoichiometric investigations gave no conclusive information, to obtain mechanistic insight full quantum chemical calculations were performed (Scheme 1.14). The pathway was proposed to be initiated by coordination of pinacol borane to the lithium through the endocyclic oxygen of the pinacol group. In the next step, the carbonyl oxygen atom of benzaldehyde attacks the boron centre of HBpin, with the hydride being transferred from the boron centre to the carbonyl carbon with subsequent formation of the boronic esters alongside catalyst regeneration.

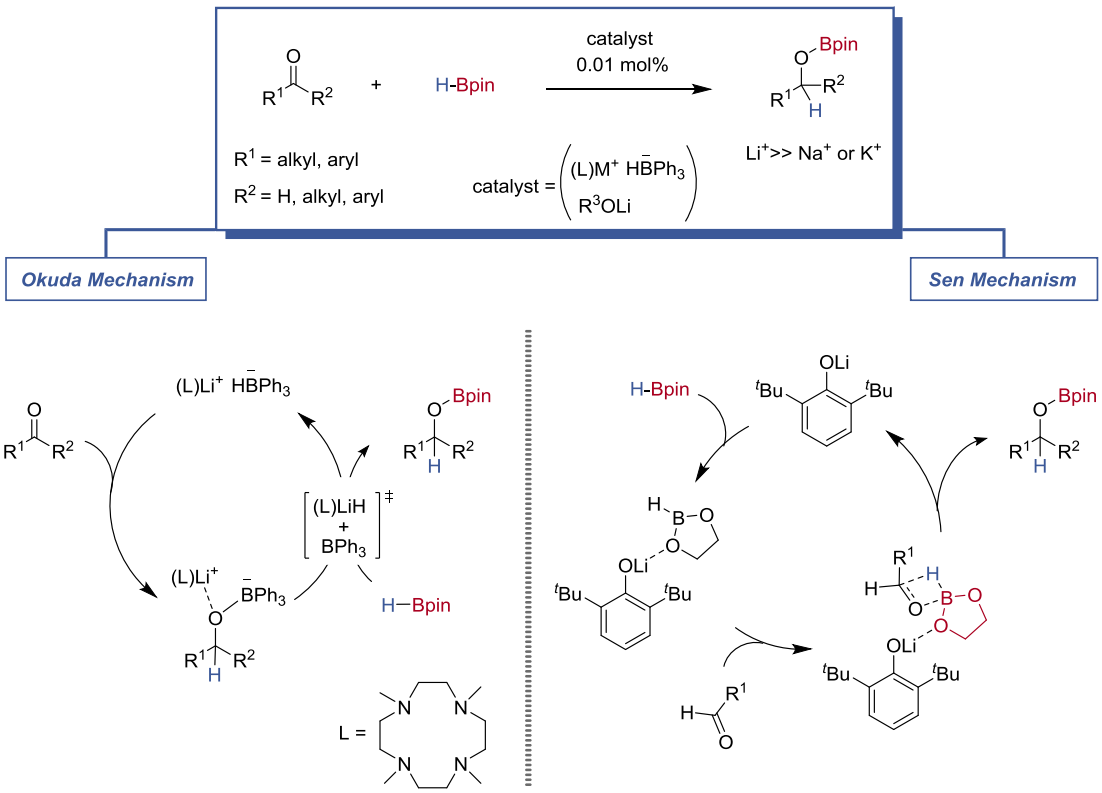

Scheme 1.14. Li-catalysed hydroboration of unsaturated polar bonds.

Recently, significant advances have been made in the field of low-valent main group chemistry in which some compounds appear to be as reactive as established transition-metal catalysts.[81] In 2014, Jones reported low-valent tin and germanium complexes for the hydroboration of ketones and aldehydes under mild conditions and at very low catalyst loadings (0.1 mol%, Scheme 1.15).[82] The empty p-orbital on the metal centre enhances the reactivity of the system, allowing hydride exchange with pinacol borane to generate the active catalyst *in situ* and release the product, as previously described (Scheme 1.15).

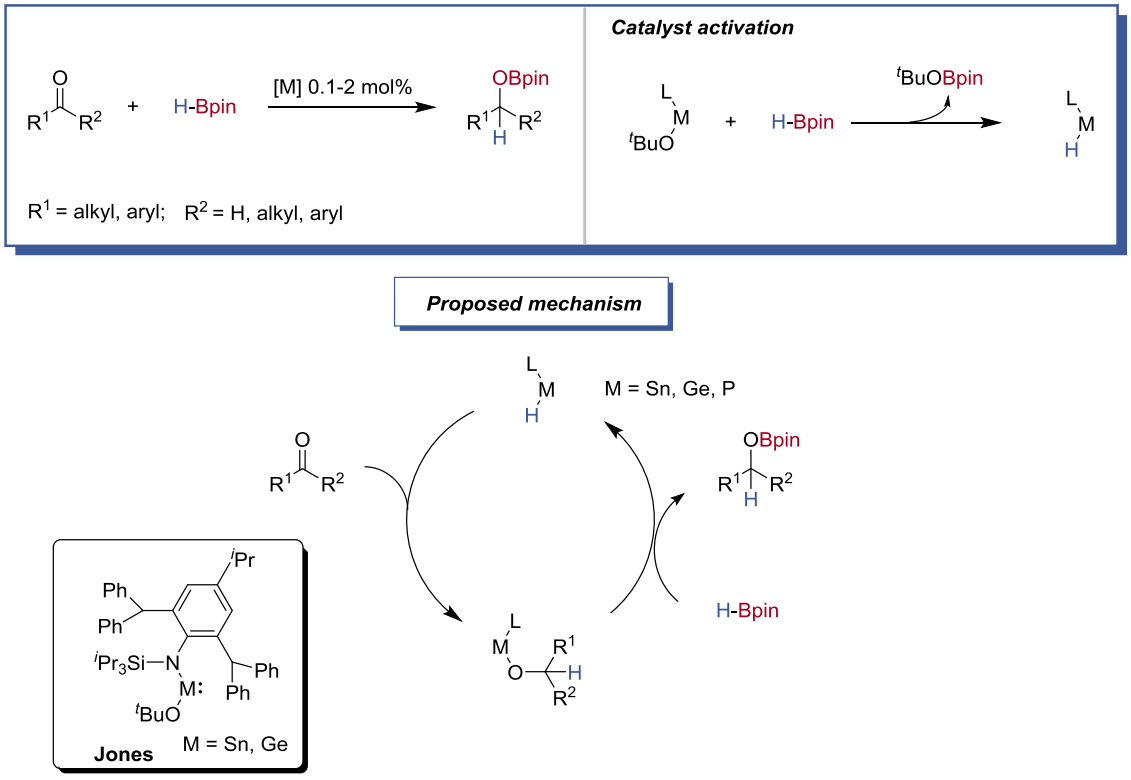

Scheme 1.15. Group 14 and 15 catalysts for hydroboration.

The hydroboration of polar bonds is less challenging and less applicable than the analogous reaction with olefins. In 2017, during the course of this PhD project, a particularly relevant protocol was published which extended the substrate scope of this transformation to unsaturated C-C bond. Zhao and co-workers used several nucleophiles, including NaOH (5-10 mol%), to initiate the hydroboration of aldehydes, ketones, imines, terminal alkynes, and alkenes (Scheme 1.16).[83] However, despite efficiency of the NaOH protocol for the hydroboration of polar bonds, there were limited examples of alkene and alkyne substrates. A stoichiometric reaction between sodium hydroxide and pinacol borane gave an insoluble precipitate and provided no significant information about the reaction mechanism. It was proposed that the reaction may lead to borohydride formation which could serve as an active hydride source. Carrying out the same reaction using *B*-H-9-BBN dimer instead of pinacol borane, confirmed formation of a borohydride species which was isolated by addition of 15-crown-5. The latter was then used to further investigate the mechanism of the hydroboration of aldehydes. In the case

of *B*-H-9-BBN experimental and theoretical studies suggest that the catalytically active species is a bridged sodium-boron hydride species generated *in situ* from the reaction mixture. The latter could engage a benzaldehyde molecule, through the phenyl substituent, and undergo concerted hydroboration.

However, when HBpin is used as borane source, they could not rule out a mechanism involving the formation of an 'ate' complex upon coordination of the hydroxide to pinacol borane.[84]

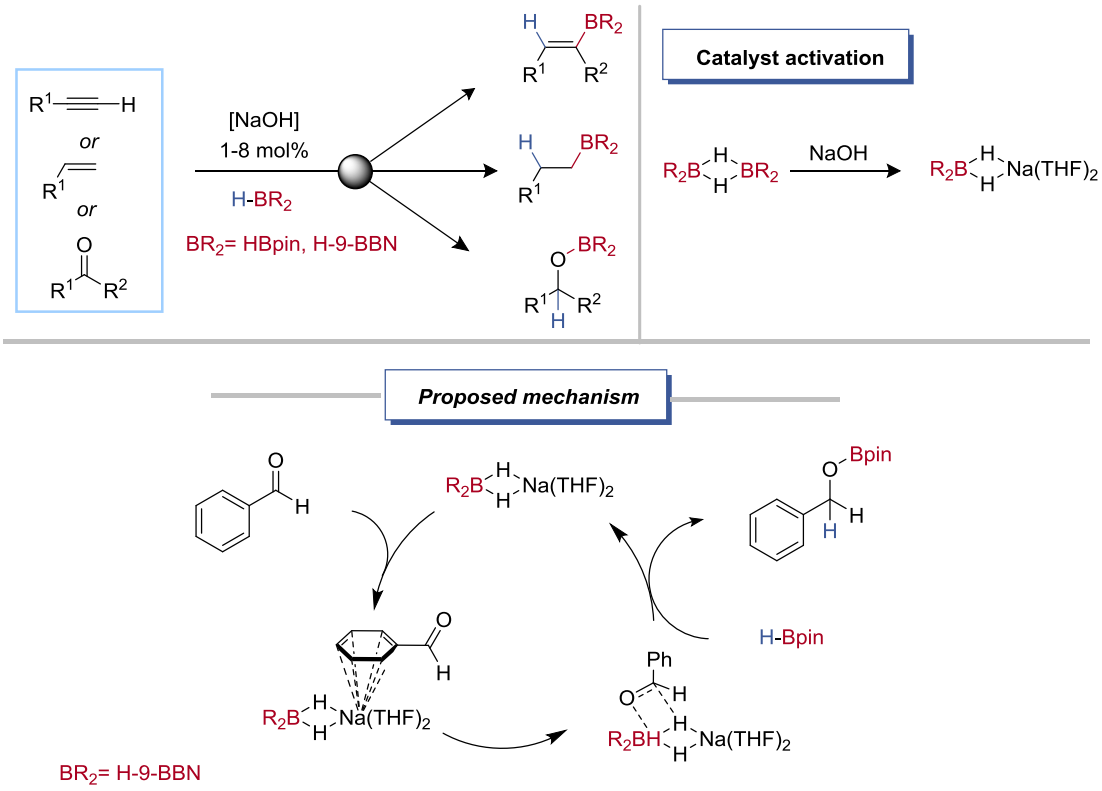

Scheme 1.16. NaOH-initiated hydroboration.

1.5 Aluminium-catalysed Hydroboration

Woodward and co-workers reported pioneering work on the hydroboration of acetophenone catalysed by BINOL-derived aluminium hydrides using catechol borane.[85] After 15 years the field has been revived with a renewed interest in aluminium-catalysed hydroboration.[86] Roesky described the first example of a Al-NacNac monohydride complex for hydroboration of aldehydes and ketones using pinacol borane

(Scheme 1.17).[87] Surprisingly, catalyst activation through hydride exchange does not require high temperatures or pressures, even if the process should, in principle, be less favoured due to the comparable Lewis acidity between the catalyst and pinacol borane. The mechanism of hydroboration was studied by density functional theory (DFT) calculations. The reaction was suggested to proceed *via* addition of the aldehyde to aluminium to form a five-coordinate intermediate that undergoes intramolecular hydride insertion on the carbonyl group to give an aluminium alkoxide. A subsequent (2 σ + 2 σ) heterolytic splitting of the H–B bond on the Al–O bond leads to the aluminium hydride regeneration and releases the product of hydroboration. Later, Nembenna and co-workers described the efficient hydroboration of a variety of aldehydes and ketones catalysed by a well-defined aluminium hydride (Scheme 1.17).[88] This process tolerates fluoro-, chloro-, bromo-, and nitro-substituents in aromatic substrates and allows for chemoselective reduction of aldehydes in the presence of ketones. It was suggested that the reaction proceeds *via* Al–H insertion into the C-O moiety followed by σ-bond metathesis with pinacol borane.

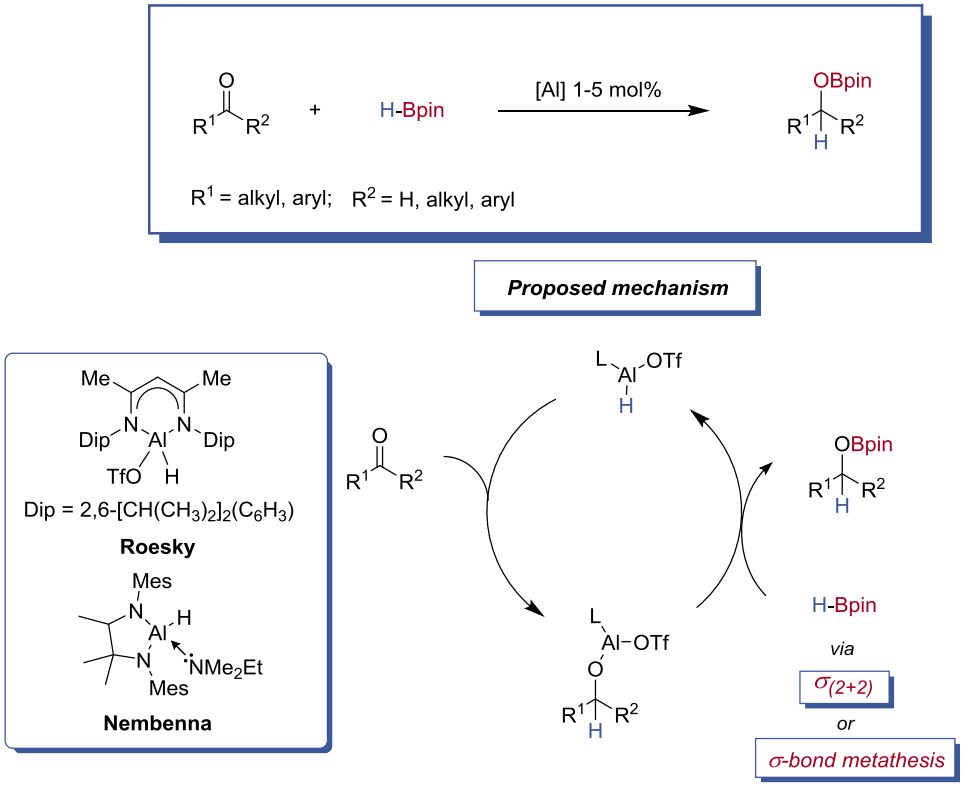

Scheme 1.17. Aluminium catalysts for hydroboration of aldehydes and ketones.

Through the use of an aluminium *NacNac* dihydride complex, the substrate scope was extended to less reactive and less polar substrates such as alkynes using an aluminium dihydride system and HBpin (Scheme 1.18).[89] The reaction occured with moderate catalyst loadings and at room temperature, however only terminal alkynes underwent successfully hydroboration. Interestingly, this reaction is proposed to occur by a different mechanism compared to that reported for other main-group systems (Scheme 1.10). Stoichiometric experiments suggested that catalyst activation is achieved by alkyne deprotonation generating *in situ* the alkynyl derivative DipNacNacAl(H)(C-CPh), and dihydrogen. The latter is proposed to react through a (2 σ + 2 π) cycloaddition with HBpin to form an alkenylaluminium boronic ester intermediate. Subsequent σ-bond metathesis with another molecule of alkyne gives catalyst turnover and product release. DFT studies revealed the rate-determining step of this process to be Al–C/H–C metathesis with a very high activation barrier ($\Delta G^{\ddagger}$ = 45.3 kcal mol^{-1}). However, the reaction occurred at room temperature which suggests that a different mechanism with a lower activation barrier

may be operative. Inoue and co-workers reported al an N-heterocyclic imine (NIH) aluminium hydride for the hydroboration of aldehydes, ketones, imines, and terminal alkynes.[90] The mechanism proposed for the hydroboration of alkynes is similar to that reported by Roesky's group, but the reaction was carried out at 80 ºC.

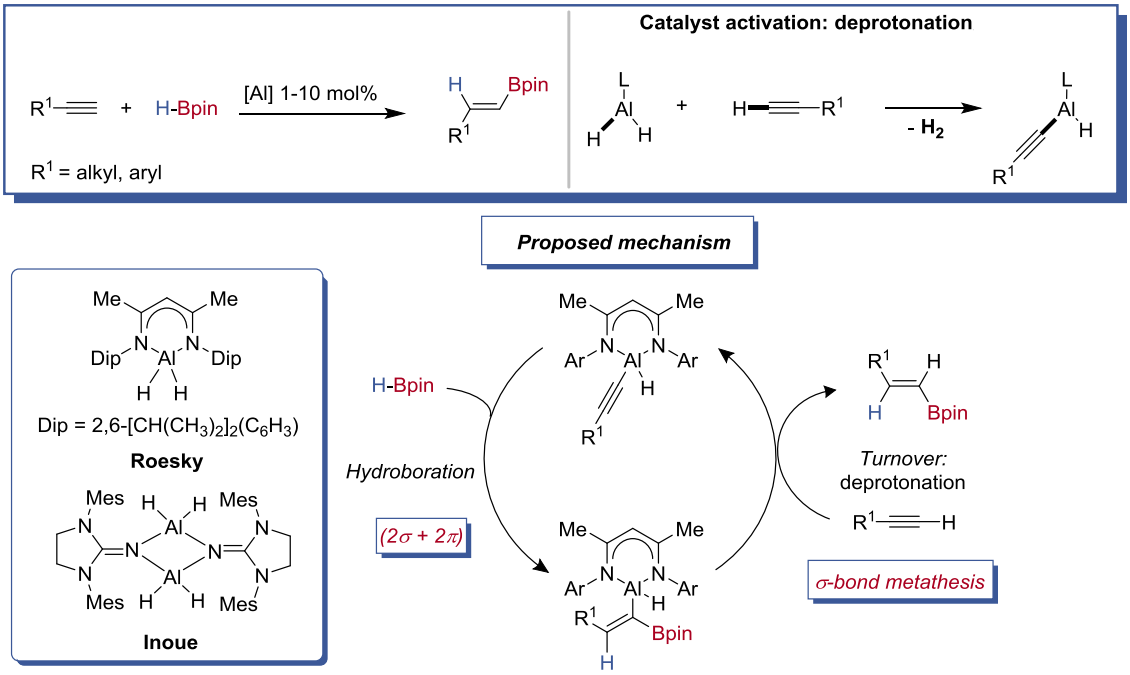

Scheme 1.18. Aluminium catalysts for hydroboration.

1.6 General Aims

Although the catalytic activity of main group species as Lewis acids is well established, main-group compounds have not usually been considered as viable catalysts for hydrofunctionalisation. However, significant efforts have been made to develop main group systems to mimic typical transition metal reactivity.

The advent of Frustrated Lewis Pairs (FLPs) has provided a new strategy for the activation of small molecules and the interest in those systems continues to grow. While the FLP concept has provided a strategy for the design and application of main group

elements in synthesis and catalysis, the catalytic reactivity of main group hydrides only recently emerged.[70],[71]

Despite the encouraging results, the potential of main-group catalysis of these systems is mostly limited to unsaturated polar bonds, leaving out inexpensive and readily available materials such as alkenes and alkynes. Furthermore, the non-commercially available catalysts limit the applicability of these aluminium hydride species as a general protocol for hydroboration.

The aim of this project is to develop new catalysts for the hydroboration of unsaturated carbon-carbon bonds using commercially-available or easier to handle aluminium sources. The concept is based on the well-known reactivity of $^{i}Bu_2Al$-H and $LiAlH_4$[92] as reducing agents in organic synthesis. In fact, the hydroalumination step constitutes a possible method of further functionalising alkenes and alkynes with different electrophiles (Scheme 1.19).

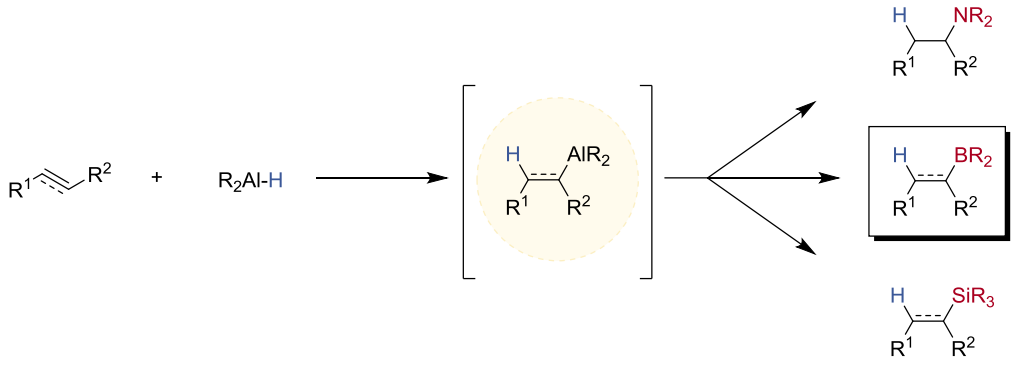

Scheme 1.19. Possible hydrofunctionalisation using alkenylaluminium species.

To the best of our knowledge this process has only ever been stoichiometric, therefore this thesis focuses on developing its catalytic variant.

1.7 References

[1] S. Bhaduri and D. Mukesh, *Homogeneous Catalysis: Mechanism and Industrial Apllications*, John Wiley & Sons, Inc., New York, USA, 2002.

[2] R. Buckow, U. Weiss, V. Heinz and D. Knorr, *Biotechnol. Bioeng.*, 2007, **97**, 1–11.

[3] A. P. A. de Oliveira, M. A. Silvestre, N. F. L. Garcia, H. F. Alves-Prado, A. Rodrigues, M. F. Da Paz, G. G. Fonseca and R. S. R. Leite, *Sci. World J.*, 2016, **2016**, 1–10.

[4] P. T. Anastas, *ChemSusChem*, 2009, **2**, 391–392.

[5] J. G. de Vries and S. D. Jackson, *Catal. Sci. Technol.*, 2012, **2**, 2009.

[6] D. J. Cole-Hamilton, *Science*, 2003, **299**, 1702–1706.

[7] Q. L. Zhou, *Angew. Chem. Int. Ed.*, 2016, **55**, 5352–5353.

[8] K. C. Taylor, in *Studies in Surface Science and Catalysis*, 1987, vol. 30, pp. 97–116.

[9] J. Kašpar, P. Fornasiero and N. Hickey, *Catal. Today*, 2003, **77**, 419–449.

[10] C. C. C. Johansson Seechurn, M. O. Kitching, T. J. Colacot and V. Snieckus, *Angew. Chem. Int. Ed.*, 2012, **51**, 5062–5085.

[11] K. Huddersman, *Appl. Organomet. Chem.*, 1991, **2**, 140–141.

[12] D. A. Atwood, J. A. Jegier and D. Rutherford, *J. Am. Chem. Soc.*, 1995, **117**, 6779–6780.

[13] B. B. Snider, *Acc. Chem. Res.*, 1980, **13**, 426–432.

[14] L. R. Domingo, A. Asensio and P. Arroyo, *J. Phys. Org. Chem.*, 2002, **15**, 660–666.

[15] C. Eaborn and J. D. Smith, *J. Chem. Soc. Dalt. Trans.*, 2001, 1541–1552.

[16] R. G. Vranka and E. L. Amma, *J. Am. Chem. Soc.*, 1967, **89**, 3121–3126.

[17] A. Almenningen, S. Halvorsen and A. Haaland, *Acta Chem. Scand.*, 1971, 25, 1937–1945.

[18] H. G. Stammler, S. Blomeyer, R. J. F. Berger and N. W. Mitzel, *Angew. Chem. Int. Ed.*, 2015, **54**, 13816–13820.

[19] A. Keys, P. T. Brain, C. A. Morrison, R. L. Callender, B. A. Smart, D. A. Wann, H. E. Robertson, D. W. H. Rankin and A. R. Barron, *Dalt. Trans.*, 2008, **3**, 404–410.

[20] A. R. Cowley, A. J. Downs, S. Marchant, V. A. Macrae, R. A. Taylor and S.

Parsons, *Organometallics*, 2005, **24**, 5702–5709.

[21] S. H. Bauer, *J. Am. Chem. Soc.*, 1937, **59**, 1096–1103.

[22] J. W. Turley and H. W. Rinn, *Inorg. Chem.*, 1969, **8**, 18–22.

[23] C. L. Raston, *J. Organomet. Chem.*, 1994, **475**, 15–24.

[24] A. E. Finholt, A. C. Bond and H. I. Schlesinger, *J. Am. Chem. Soc.*, 1947, **69**, 1199–1203.

[25] V. H. Brown, *Hydroboration New York: W. A. Benjamin Inc. 290*, 1962.

[26] V. H. C. Brown, *Boranes in Organic Chemistry, Cornell University Press. Ithica - London*, 1972.

[27] V. H. C. Brown, *Organic synthesis via Borane, John Wiley & Sons Inc: New York,* 1975.

[28] H. I. Schlesinger and A. B. Burg, *J. Am. Chem. Soc.*, 1931, **53**, 4321–4332.

[29] H. C. Brown, H. I. Schlesinger and A. B. Burg, *J. Am. Chem. Soc.*, 1939, **61**, 673–680.

[30] H. C. Brown and B. C. Subba Rao, *J. Am. Chem. Soc.*, 1956, **78**, 5694–5695.

[31] H. C. Brown and G. Zweifel, *J. Am. Chem. Soc.*, 1960, **82**, 4708–4712.

[32] H. C. Brown and R. L. Sharp, *J. Am. Chem. Soc.*, 1966, **88**, 5851–5854.

[33] J. A. Livasy, 1952, **5211**, 2750–2751.

[34] L. M. Beaun, R. A. Bhaun, H. R. Crissman, M. Oppehman and R. M. Adams, *J. Org. Chem.*, 1971, **36**, 2388–2389.

[35] G. Zweifel and H. C. Brown, *J. Am. Chem. Soc.*, 1963, **85**, 2066–2072.

[36] H. C. Brown and A. W. Moerikofer, *J. Am. Chem. Soc.*, 1961, **83**, 3417–3422.

[37] H. C. Brown, E. F. Knights and C. G. Scouten, *J. Am. Chem. Soc.*, 1974, **96**, 7765–7770.

[38] H. C. Brown and S. K. Gupta, *J. Am. Chem. Soc.*, 1971, **93**, 1816–1818.

[39] H. C. Brown and S. K. Gupta, *J. Am. Chem. Soc.*, 1975, **97**, 5249–5255.

[40] C. F. Lane and G. W. Kabalka, *Tetrahedron*, 1976, **32**, 981–990.

[41] S. A. Westcott, H. P. Blom, T. B. Marder, R. T. Baker and J. C. Calabrese, *Inorg. Chem.*, 1993, **32**, 2175–2182.

[42] J. V. B. Kanth, M. Periasamy and H. C. Brown, *Org. Process Res. Dev.*, 2000, **4**, 550–553.

[43] C. E. Tucker, J. Davidson and P. Knochel, *J. Org. Chem.*, 1992, **57**, 3482–3485.

[44] S. Pereira and M. Srebnik, *J. Am. Chem. Soc.*, 1996, **118**, 909–910.

[45] K. Burgess and M. J. Ohlmeyer, *Chem. Rev.*, 1991, **91**, 1179–1191.

[46] D. M. Khramov, E. L. Rosen, Er, Joyce A.V., P. D. Vu, V. M. Lynch and Bielawski, Christopher W., *Tetrahedron*, 2008, **64**, 6853–6862.

[47] Y. Yamamoto, R. Fujikawa, T. Umemoto and N. Miyaura, *Tetrahedron*, 2004, **60**, 10695–10700.

[48] J. Huang, W. Yan, C. Tan, W. Wu and H. Jiang, *Chem. Commun.*, 2018, **54**, 1770–1773.

[49] C. M. Vogels and S. A. Westcott, in *Encyclopedia of Inorganic Chemistry*, John Wiley & Sons, Ltd, Chichester, UK, 2006, vol. 3, pp. 1–9.

[50] Von Karl Ziegler, Wolf-Rainer Kroll, Wolfgang Larbig, Otto-Walter Steudel, *Met. Verbindungen , XXXII*, 1960, 53–89.

[51] H. Gilman and R. H. Kirby, *J. Am. Chem. Soc.*, 1941, **63**, 2046–2048.

[52] K. Ziegler, H. -G Gellert, H. Martin, K. Nagel and J. Schneider, *Justus Liebigs Ann. Chem.*, 1954, **589**, 91–121.

[53] J. Schneider, V. K. Ziegler, K. Schneider, H. Prof and H. Meerwein, *Justus Liebigs Ann. Chem.*, 1959, **226**, 9–16.

[54] S. Pastskiewicz and A. S. D. Ewa, *Ratio*, 1964.

[55] I. Marek and J.-F. Normant, *Chem. Rev.*, 1996, **96**, 3241–3268.

[56] J. Malek, *Reductions by metal alkoxyaluminum hydrides. Part II. Carboxylic acids and derivatives, nitrogen compounds, and sulfur compounds.*, 1988, vol. 36.

[57] G. Wilke and H. Muller, *Liebigs Ann. Chem.*, 1960, **629**, 222–240.

[58] J. J. Eisch and W. C. Kaska, *J. Am. Chem. Soc.*, 1963, **85**, 2165–2166.

[59] J. J. Eisch and W. C. Kaska, *J. Am. Chem. Soc.*, 1966, **88**, 2213–2220.

[60] J. Eisch and M. W. Foxton, *J. Org. Chem.*, 1971, **36**, 3520–3526.

[61] M. Layh and W. Uhl, *Polyhedron*, 1990, **9**, 277–282.

[62] U. Marcus, W. Uhl, *J. Organomet. Chem.*, 1991, **415**, 181–190.

[63] J. C. Fettinger, P. a. Gray, C. E. Melton and P. P. Power, *Organometallics*, 2014, **33**, 6232–6240.

[64] S. Aldridge and A. J. Downs, *The Group 13 Metals Aluminium, Gallium, Indium and Thallium: Chemical Patterns and Peculiarities*, 2011.

[65] H. Makabe and E.-I. Negishi, *European J. Org. Chem.*, 1999, 969–971.

[66] E. C. Ashby and S. A. Noding, *Tetrahedron Lett.*, 1977, **1**, 4579–4582.
[67] E. C. Ashby and S. A. Noding, *J. Org. Chem.*, 1980, **45**, 1035–1041.
[68] F. Gao and A. H. Hoveyda, *J. Am. Chem. Soc.*, 2010, **132**, 10961–10963.
[69] G. G. Hlatky and R. H. Crabtree, *Coord. Chem. Rev.*, 1985, **65**, 1–48.
[70] S. Harder and J. Brettar, *Angew. Chem. Int. Ed.*, 2006, **45**, 3474–3478.
[71] F. Buch, J. Brettar and S. Harder, *Angew. Chem. Int. Ed.*, 2006, **45**, 2741–2745.
[72] M. Arrowsmith, T. J. Hadlington, M. Hill and G. Kociok-Kohn, *Chem. Commun.*, 2012, **48**, 4567–4569.
[73] S. P. Green, C. Jones and A. Stasch, *Angew. Chem. Int. Ed.*, 2008, **47**, 9079–9083.
[74] M. Arrowsmith, M. S. Hill and G. Kociok-Köhn, *Chem. Eur. J.*, 2013, **19**, 2776–2783.
[75] C. Weetman, M. D. Anker, M. Arrowsmith, M. S. Hill, G. Kociok-Köhn, D. J. Liptrot and M. F. Mahon, *Chem. Sci.*, 2016, **7**, 628–641.
[76] D. Mukherjee, A. Ellern and A. D. Sadow, *Chem. Sci.*, 2014, **5**, 959.
[77] V. A. Pollard, S. A. Orr, R. McLellan, A. R. Kennedy, E. Hevia and R. E. Mulvey, *Chem. Commun.*, 2018, **54**, 1233–1236.
[78] H. Osseili, D. Mukherjee, T. P. Spaniol and J. Okuda, *Chem. - A Eur. J.*, 2017, **23**, 14292–14298.
[79] H. Osseili, D. Mukherjee, K. Beckerle, T. P. Spaniol and J. Okuda, *Organometallics*, 2017, **36**, 3029–3034.
[80] M. K. Bisai, T. Das, K. Vanka and S. S. Sen, *Chem. Commun.*, 2018.
[81] K. Revunova and G. I. Nikonov, *Dalt. Trans.*, 2015, **44**, 840–866.
[82] T. J. Hadlington, M. Hermann, G. Frenking and C. Jones, *J. Am. Chem. Soc.*, 2014, **136**, 3028–3031.
[83] Y. Wu, C. Shan, J. Ying, J. Su, J. Zhu, L. L. Liu and Y. Zhao, *Green Chem.*, 2017, **19**, 4169–4175.
[84] I. P. Query, P. A. Squier, E. M. Larson, N. A. Isley and T. B. Clark, *J. Org. Chem.*, 2011, **76**, 6452–6456.
[85] A. J. Blake, A. Cunningham, A. Ford, S. J. Teat and S. Woodward, *Chem. Eur. J.*, 2000, **6**, 3586–3594.
[86] G. I. Nikonov, *ACS Catal.*, 2017, **7**, 7257–7266.

[87] Z. Yang, M. Zhong, X. Ma, S. De, C. Anusha, P. Parameswaran and H. W. Roesky, *Angew. Chem. Int. Ed.*, 2015, **54**, 10225–10229.

[88] V. K. Jakhar, M. K. Barman and S. Nembenna, *Org. Lett.*, 2016, **18**, 4710–4713.

[89] Z. Yang, M. Zhong, X. Ma, K. Nijesh, S. De, P. Parameswaran and H. W. Roesky, *J. Am. Chem. Soc.*, 2016, **138**, 2548–2551.

[90] D. Franz, L. Sirtl, A. Pothig and S. Inoue, *Zeitschrift fur Anorg. und Allg. Chemie*, 2016, **642**, 1245–1250.

[91] G. C. Welch, R. R. San Juan, J. D. Masuda and D. W. Stephan, *Science*, 2006, **314**, 1124–1126.

[92] G. Wilke and H. Müller, *Chem. Ber.*, 1956, **89**, 444–447.

Chapter 2 − Aluminium-catalysed hydroboration of alkynes

Catalysis is a simple, powerful method of improving the efficiency of molecular synthesis, as well as reducing waste and energy consumption. In recent years, countless efforts have been made to improve the efficiency and selectivity of catalytic systems and to design new ones.[1]–[5]

The Suzuki-Miyaura cross-coupling reaction offers a unique method for the preparation of biaryl compounds which are one of the most ubiquitous substructures of pharmaceutical and natural products and has led to a significant increase in the use of organoboron species in synthesis. Organoboron species were originally synthesised using alkylithium and magnesium reagents or by hydroboration using stoichiometric borane sources.[6] However, the poor functional group tolerance of these reactions has led to the development of alternative methods based on transition metal catalysts. Rhodium[7],[8] ruthenium,[9] and palladium[10] have been successfully used to catalyse hydroboration, achieving high yield and good group tolerance (Scheme 2.1). Yet the often high cost, toxicity and scarcity of many transition metals is driving attempts to find sustainable alternatives such as main group elements.

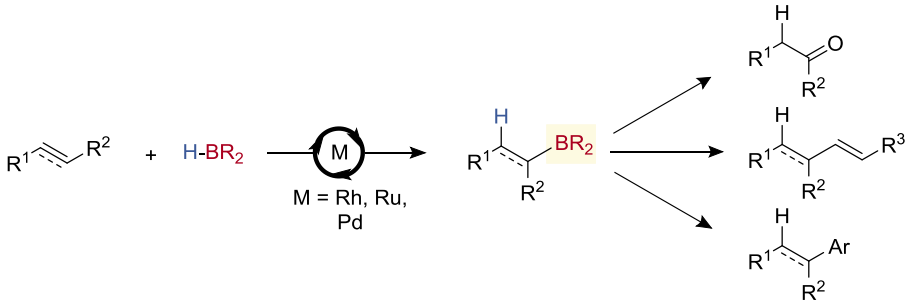

Scheme 2.1 Transition-metal-catalysed hydroboration to access alkenyl boron synthons.

Aluminium is one of the most abundant elements in the Earth's crust[11] and its application in material Science is vast. However, the typical use of this element in catalysis has been restricted to Lewis acid catalysed reactions.[12],[13] This lack of broader reactivity stems from the absence of easily accessible *d*-orbitals at aluminium which hampers oxidative addition and reductive elimination reactions, which usually form the basis of a catalytic cycle. Despite this, substrate activation can still be provided through

σ-bond metathesis and insertion steps, enabling the development of new catalytic applications.[14]

2.1 Project Aims

Aluminium hydride species have been widely used for the reduction of unsaturated bonds which upon treatment with an electrophile give the functionalised olefin products (Scheme 2.2). However, this process has only been reported using stoichiometric organoaluminium compounds.

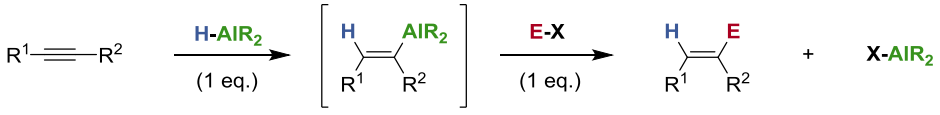

Scheme 2.2 Aluminium-hydride reactivity.

The aim of this project was to develop new catalysts for the hydrofunctionalisation of unsaturated carbon-carbon bonds, using commercially-available or easily handled aluminium sources. A new mode of operation was envisaged in which substrate activation would be achieved by hydroalumination and turnover by use of an electrophile with a hydride substituent.[15] In this way, stoichiometric quantities of aluminium hydride reagents would be avoided.

Given that group 13 species undergo ligand exchange, we thus identified borane reagents as possible reaction partners, and a potential hydride source. Ideally a readily available, air- and moisture-stable hydride source would be used. Transmetallation of alkenyl aluminum species with pinacol borane (HBpin), which fulfils these criteria, would result in the formation of synthetically useful alkenyl boronic esters (Scheme 2.3).

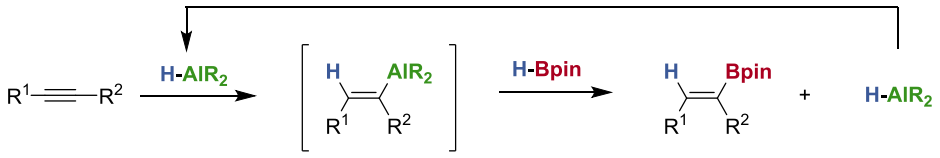

Scheme 2.3 Aluminium hydride regeneration: concept of this work.

2.2 Reaction Development

An initial reaction with 1-octyne and with 1.5 equivalents of pinacol borane (HBpin) using a substoichiometric amount of commercially-available $^{i}Bu_2Al$-H (20 mol%) at room temperature displayed <5% conversion after 24 hours (Table 2.1). Upon increasing the temperature to 110 °C almost full conversion to the (*E*)-alkenyl boronic ester species was observed by ^{1}H NMR in just 2 hours. A number of Al(III) compounds were trialled as catalysts for the reaction (entry 2). Interestingly, trialkyl aluminium species, $AlMe_3$ and $AlEt_3$, were also able to perform this transformation in moderate to good yield (entries 3 and 4) without any evidence of carboalumination or other side reactions. More Lewis acidic systems (entries 5 and 6) led to lower yield and unidentified side reactions involving HBpin. Performing the reaction in the absence of aluminium, both at room temperature and at 110 °C, resulted in only trace amounts of product even after 24 hours.

Table 2.1. Screening of aluminium species.

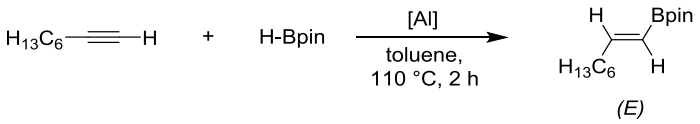

(E)

Entry	[Al] (20 mol%)	Yield (%)
1	$^{i}Bu_2Al$-H	4[a]
2	$^{i}Bu_2Al$-H	90
3	$AlMe_3$	35
4	$AlEt_3$	75
5	$AlCl_3$	23
6	$Al(OTf)_3$	11
7	None	2

Reaction conditions: 0.030 mmol (0.2 eq.) catalyst, 0.15 mmol (1 eq.) octyne and 0.225 mmol (1.5 eq.) HBpin in 0.60 mL toluene-d_8, heated at 110 °C for 2 h. [a]Reaction performed at room temperature for 24 h. Yield determined by ^{1}H NMR of the crude reaction mixture using 1,3,5-trimethoxybenzene as an internal standard.

Although these catalysts are commercially available, alkyl aluminium species are pyrophoric reagents and highly oxygen and moisture sensitive. Selecting an appropriate base to stabilise the compounds could lead to an easier-to-handle catalyst. Inspired by the work of Bradley and Woodward,[16],[17] who reported the synthesis of $(AlMe_3)_2$·DABCO (DABCO = 1,4-diazabicyclo[2.2.2]octane) as a non-pyrophoric and robust compound, the synthesis of the corresponding triethylaluminium-base adduct was attempted. The addition of triethylaluminium to a solution of DABCO at 0 °C and stirring for 1 hour at room temperature led to precipitation $AlEt_3$·DABCO which was isolated in 70% yield (Scheme 2.4). A single cubic crystal suitable for X-ray analysis was obtained from a hexane at −20 °C (Figure 2.1).

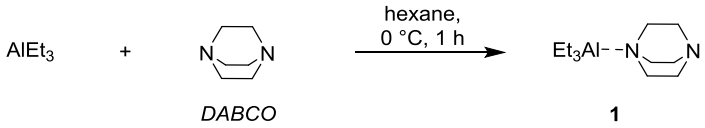

Scheme 2.4. Synthesis of $AlEt_3$·DABCO.

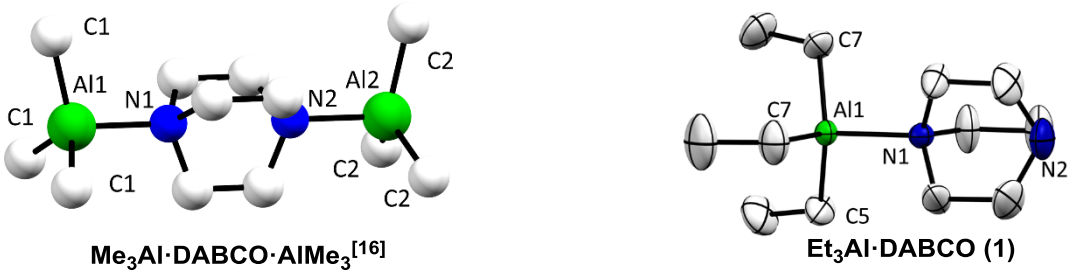

Me_3Al·DABCO·$AlMe_3$[16] **Et_3Al·DABCO (1)**

Figure 2.1 Comparison of molecular structure of Et_3Al·DABCO (**1**) and $[Al(Me)_3]_2$·DABCO in the solid state. Ellipsoids are set to 50% probability; hydrogen atoms are omitted for clarity. Selected both lengths (Å) for $[Al(Me)_3]_2$·DABCO: Al(1)–N(1) 2.065(8), Al(2)–N(2) 2.066(8), Al(1)–C(1) 1.954(11), Al(2)–C(2) 1.968(7), Al(1)–C(5) 1.636(4). Selected both lengths (Å) for $AlEt_3$·DABCO (**1**): Al(1)–N(1) 2.045(4), Al(1)–C(7) 1.981(4), Al(1)–C(5) 1.985(7).

Interestingly the synthesis of $(AlMe_3)_2$·DABCO is usually carried out using an excess of DABCO, but the product could only be isolated as dinuclear aluminium compound. In contrast to the trimethylaluminium DABCO adduct, $AlEt_3$·DABCO (**1**) is a 1:1 adduct in both solution, using ^1H NMR spectroscopy, and the solid state, by single crystal X-ray crystallography.[15]

When compared to $Me_3Al{\cdot}DABCO{\cdot}AlMe_3$, the aluminium-carbon bonds are elongated and aluminium-nitrogen bonds shorter [(Al-C = 1.981(4) (Å) *vs* 1.954(11) (Å)) and (Al-N = 2.045(4) (Å) *vs* 2.065(8) (Å)] displaying a stronger nitrogen coordination.

As $^{i}Bu_2Al$-H was a marginally more active catalyst, the isolation of the DABCO adduct was attempted. Using the same procedure as that for $AlEt_3{\cdot}DABCO$, the adduct was isolated as an amorphous solid, albeit in considerably lower yield 45%. After several attempts, a single, colourless, needle-shaped crystal suitable for X-ray analysis was obtained from slow cooling from benzene/hexane mixture (Figure 2.2).

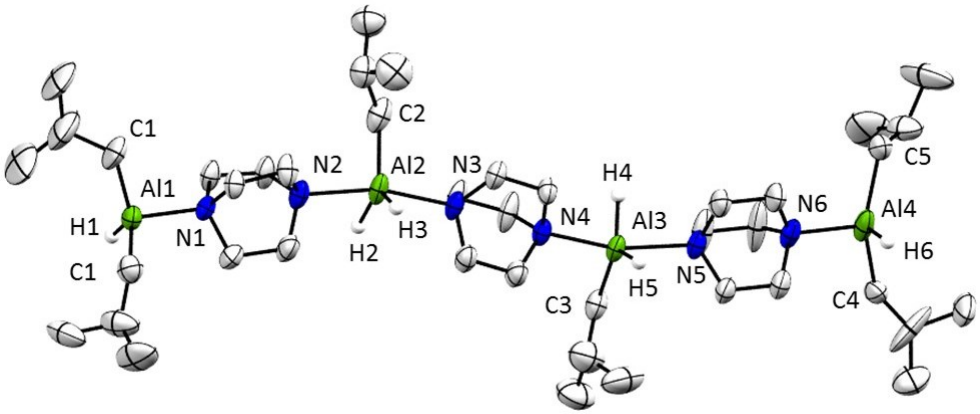

$[^{i}Bu_2AlH\text{-}^{i}BuAlH_2]_2{\cdot}(DABCO)_3$ (2)

Figure 2.2. Crystal structure of $[^{i}Bu_2AlH\text{-}^{i}BuAlH_2]_2{\cdot}(DABCO)_3$ **(2)**. Ellipsoids are set to 50% probability; hydrogen atoms are omitted for clarity with the exception of Al-H bonds. Selected both lengths (Å) for **2**: Al(1)–N(1) 2.032(3), Al(1)–C(1) 1.961(5), Al(1)–C(1) 1.978(12), Al(1)–H(1) 1.524(12), Al(2)–N(2) 2.244(3), Al(2)–N(3) 2.203(3), Al(2)–C(2) 2.033(6), Al(2)–H(2) 1.540(4), Al(2)–H(3) 1.564(4), Al(3)–N(4) 2.194(3), Al(3)–N(5) 2.250(3), Al(3)–C(3) 2.001(5), Al(3)–H(4) 1.628(4), Al(3)–H(5) 1.608(4), Al(4)–N(6) 2.033(4), Al(4)–C(4) 1.906(10), Al(4)–C(5) 1.886(9), Al(4)–H(6) 1.487(4).

The crystalline material proved to be very air-sensitive with immediate decomposition upon contact with air. $[^{i}Bu_2AlH\text{-}^{i}BuAlH_2]_2{\cdot}(DABCO)_3$ (**2**) was isolated as an aluminium-amine 4:3 adduct species in the solid state bearing two coordination motifs of aluminium. The terminal Al(1) and Al(4) showed a tetrahedral geometry with aluminium-nitrogen and aluminium-carbon bonds and angles in agreement with those reported for dative bonds. The internal Al(2) and Al(3) instead display a distorted trigonal bipyramid geometry with

two DABCO molecules in the axial positions and two hydrides and the *iso*butyl group in the equatorial position. The geometry of the aluminium centre shows one of the least deviation reported from an ideal trigonal bipyramidal geometry (τ = 0.967)[18] with significant longer aluminium-carbon and aluminium-nitrogen bonds compared to $Me_3Al{\cdot}DABCO{\cdot}AlMe_3$ [(Al-C = 1.954(11) (Å) *vs* 2.033(6) (Å)) and (Al-N = 2.065(8) (4) (Å) vs 2.203(3) (Å)]. The bonding situation in this five-coordinate aluminium complex is best described as donation from the lone-pair electrons of the apical ligands into a vacant 3p orbital, as typical for hypervalent systems. The interaction leads to the formation of a three-centre four-electron (3c-4e) hypervalent bonding system.[19],[20] Surprisingly, the Al(2) and Al(3) bear two hydride ligands instead of one as the result of ligand exchange presumably with subsequent formation of $^{i}Bu_3Al{\cdot}DABCO$ (Scheme 2.5).

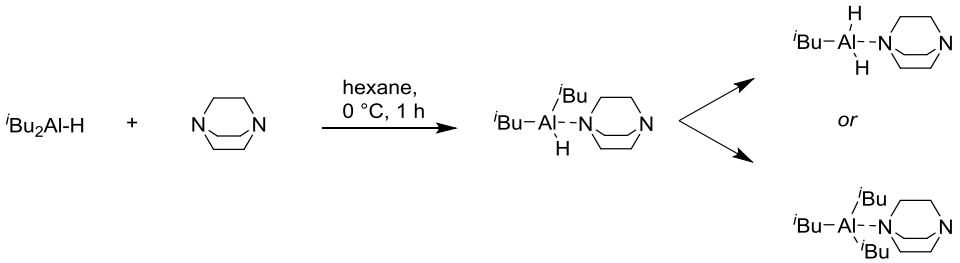

Scheme 2.5. Reaction of $^{i}Bu_2Al$-H and DABCO and ligand exchange reaction.

To the best of our knowledge, few examples of five-coordinated alkyl aluminium species have been reported[21]–[23] with dihydride being rare. ^{1}H NMR analysis of crystalline $[^{i}Bu_2AlH\text{-}^{i}BuAlH_2]_2{\cdot}(DABCO)_3$ was observed as a 1:1 Lewis acid-base adduct ($^{i}Bu_2Al$-H·DABCO) in solution. Alkyl aluminium species were then screened at lower catalyst loading with $^{i}Bu_2Al$-H, $^{i}Bu_2Al$-H·DABCO, and $Et_3Al{\cdot}DABCO$ found to be the best catalysts (Table 2.2).

Table 2.2 Catalysts screening.

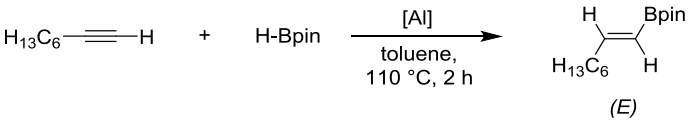

Entry	[Al] (10 mol%)	Yield (%)
1	$AlMe_3$	23
2	$AlEt_3$	59
3	$^{i}Bu_2Al$-H	73
4	$^{i}Bu_2Al$-H·DABCO	74
5	Et_3Al·DABCO	72
6	$(AlMe_3)_2$·DABCO	36

Reaction conditions: 0.015 mmol (0.1 eq.) catalyst, 0.15 mmol (1 eq.) octyne and 0.225 mmol (1.5 eq.) HBpin in 0.60 mL toluene-d_8, heated at 110 °C for 2 h. Yield determined by ^{1}H NMR of the crude reaction mixture using 1,3,5-trimethoxybenzene as an internal standard.

Due to the easier synthesis of Et_3Al·DABCO compared to $^{i}Bu_2Al$-H·DABCO the screening of all the other reaction conditions such as solvent, equivalents of HBpin and reaction concentration were then performed using 10 mol% of Et_3Al·DABCO and 1-octyne as a benchmark substrate. All the reactions were carried out in solvent under reflux and the majority of these experiments gave low yield, below 15% (Table 2.3). Toluene was therefore selected as the solvent for the next optimisation. This choice was also motivated by the Pfizer solvent selection guide,[24] which indicates toluene as one of the most environmentally-friendly apolar solvents.

Table 2.3. Solvent screening.

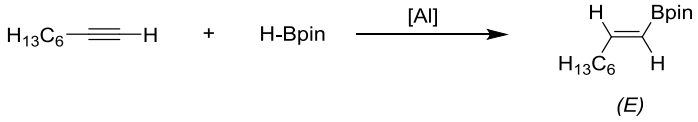

(E)

Entry	Solvent	T (°C)	Yield (%)
1	dichloromethane	45	10
2	2-methyl-THF	80	12
3	cyclopentyl methyl ether	106	4
4	toluene	110	72

Reaction conditions: 0.015 mmol (0.1 eq.) $AlEt_3$·DABCO, 0.15 mmol (1 eq.) octyne and 0.225 mmol (1.5 eq.) HBpin in 0.60 mL of the indicated solvent heated at the boiling point for 2 h. Yield determined by ^{1}H NMR of the crude reaction mixture using 1,3,5-trimethoxybenzene as an internal standard.

Decreasing the loading of HBpin from 1.5 to 1.2 equivalents did not show a significant difference in yield, while moving to 3 equivalents gave an improved yield (Table 2.4, entries 1-3). Nevertheless, in order to improve the sustainability of the process, 1.2 equivalents were selected as the optimal condition. Furthermore, increasing the concentration of the reaction resulted in a lower yield of the product (Entries 4, 5). Performing the reaction at lower temperature resulted in lower yield with only trace amount of product observed when the reaction was carried out at room temperature (Entries 6, 7).

Table 2.4. Screening of reaction conditions.

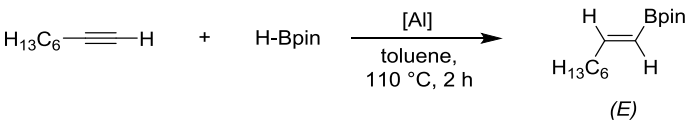

Entry	HBpin (eq.)	Reaction concentration	T (°C)	Yield (%)
1	1.2	0.25 M	110	70
2	1.5	0.25 M	110	72
3	3.0	0.25 M	110	84
4	1.2	0.50 M	110	65
5	1.2	1.00 M	110	60
6	1.2	0.25 M	60	28
7	1.2	0.25 M	25	trace

Reaction conditions: 0.015 mmol (0.1 eq.) $AlEt_3$·DABCO, (1 eq.) octyne and (1.2-3.0 eq) HBpin in 0.60 mL of solvent heated to 110 °C for 2 h. Yield determined by ^1H NMR of the crude reaction mixture using 1,3,5-trimethoxybenzene as an internal standard.

Optimised reaction conditions were: 1.2 equivalents HBpin in a 0.25 M solution of substrate in toluene. Using these conditions, a screening of different bases was carried out, generating the Al-base species *in situ* (Table 2.5). Using a base-stabilised aluminium hydride species (entry 1) did not make a significant difference in terms of yield. Using aromatic amine adducts (entries 3, 4, 5) or aromatic phosphine (entry 6) led to similar conversions, except for DMAP (2,6-dimethylpyridine) where the conversion dropped to

40%. However, aromatic amine-aluminium adducts have been reported as highly reactive and pyrophoric species, and are therefore incompatible with our aims. Overall, DABCO was found to be the most effective base (Table 2.5).

Table 2.5. Base screening.

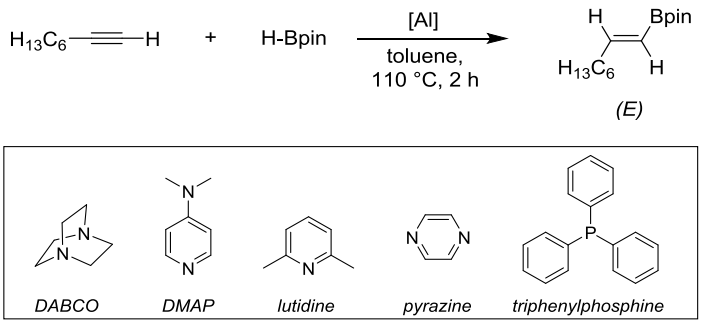

Entry	[Al] (10 mol%)	Yield (%)
1	$^{i}Bu_2Al$-H·DABCO	74
2	Et_3Al·DABCO	72
3	Et_3Al·DMAP	40
4	Et_3Al·pyrazine	56
5	Et_3Al·lutidine	71
6	Et_3Al·PPh_3	65

Reaction conditions: 0.015 mmol (0.1 eq.) alkyl aluminium, 0.015 mmol (0.1 eq.) of the corresponding base, 0.15 mmol (1 eq.) octyne and 0.18 mmol (1.2 eq.) HBpin in 0.60 mL toluene-d_8 at 110 °C for 2 h. Yield determined by ^{1}H NMR of the crude reaction mixture using 1,3,5-trimethoxybenzene as an internal standard.

2.3 Substrate Scope

Encouraged by these results, we explored the substrate scope and functional group tolerance of this hydroboration protocol using both $^{i}Bu_2Al$-H and $Et_3Al{\cdot}DABCO$ (10 mol%) as the catalyst (Scheme 2.6). In all reactions the stereoselectivity was determined by ^{1}H NMR $^{3}J_{H\text{-}H}$ coupling constants and by comparison to reported literature data. Terminal aliphatic alkynes bearing primary (**4a**), secondary (**4b**), and tertiary alkyl groups (**4c**) were successfully converted to the (*E*)-alkenyl boronic esters in good yields and stereoselectivity. No significant change in catalyst activity was observed with the increase of steric hindrance. Internal alkyl alkynes (**4d**-**4f**), also gave the (*Z*)-boronic esters in good yield, both symmetrical and unsymmetrical examples, with particularly good selectivity in the case of 4-methyl-2-pentenyl boronic ester **4f** (90:10), presumably due to different steric hindrance present.

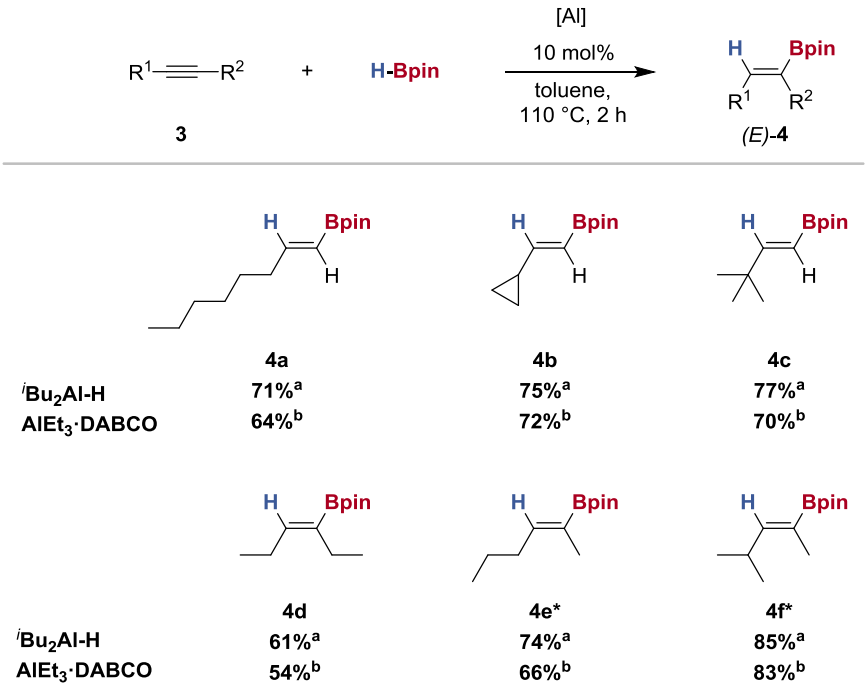

Scheme 2.6. Substrates scope. Conditions: alkyne (0.75 mmol), [Al] (10 mol%), HBpin (1.2 eq.), toluene (0.25 M), 2 h, 110 °C. [a] Yield of isolated product when using $^{i}Bu_2Al$-H (10 mol%), toluene (0.25 M), 2 h, 110 °C. [b] Yield of isolated product when using $Et_3Al{\cdot}DABCO$ (10 mol%), toluene (0.25 M), 2 h, 110 °C.*__4e__ and *__4f__ were isolated as an inseparable mixture of regioisomers (__4e__, 70:30) and __(4f__, 90:10).

Terminal aryl alkynes all underwent successful hydroboration to the (*E*) alkenyl boronic ester (**4g**-**4j**). Variation of the electronic character of the alkyne aryl substituent showed that equal catalyst activity was achieved across arenes bearing both electron-donating (**4h**-**4i**) and or electron-withdrawing (**4j**) substituents and without exhibiting protodeborylation (Scheme 2.7). Diphenylacetylene (**3k**) gave the (*Z*)-alkenyl boronic ester (**4k**) in a moderate yield, presumably caused by the steric hindrance. Chemoselectivity was observed for terminal alkynes over internal alkenes (**4l**).

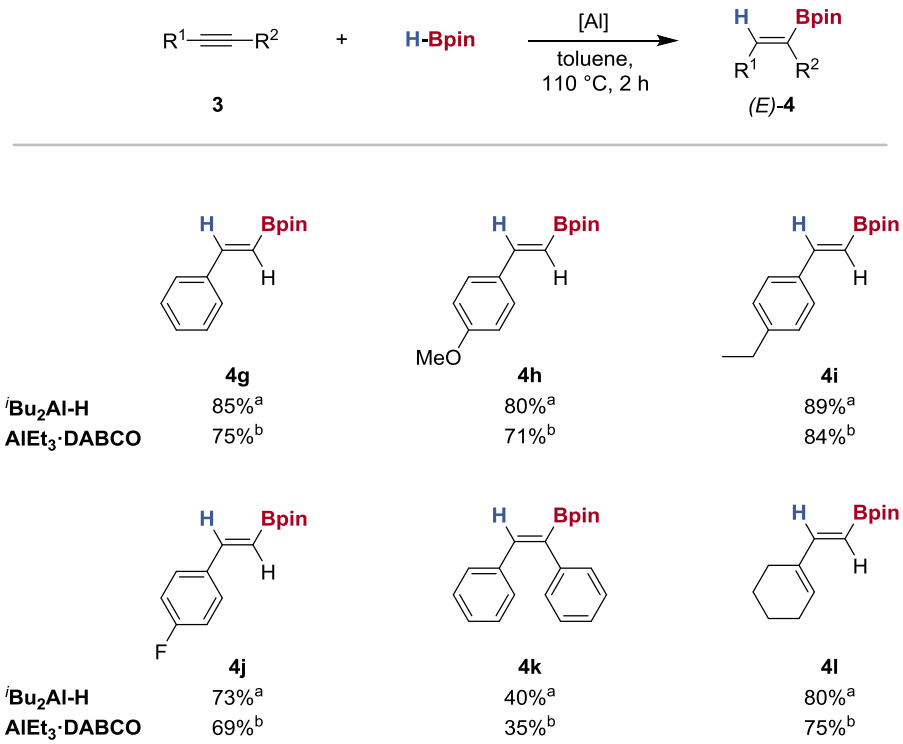

Scheme 2.7. Substrates scope. Conditions: alkyne (0.75 mmol), [Al] (10 mol%), HBpin (1.2 eq.), toluene (0.25 M), 2 h, 110 °C.[a] Yield of isolated product when using $^{i}Bu_2Al$-H (10 mol%), toluene (0.25 M), 2 h, 110 °C.[b] Yield of isolated product when using $AlEt_3$·DABCO (10 mol%), toluene (0.25 M), 2 h, 110 °C.

It is worth noting that across all 15 substrates, both $^{i}Bu_2Al$-H and Et_3Al·DABCO showed equal catalytic activity; strongly suggesting a shared mode of operation. Unfortunately, alcohol and amino functionalities were not tolerated, presumably due to catalyst deactivation caused by strong coordination of these substrates (Scheme 2.8).

Hydroboration of internal and terminal alkenes failed. The hydroalumination of these substrates in fact is more challenging and usually requires stronger donating substituents or harsher conditions.[25]

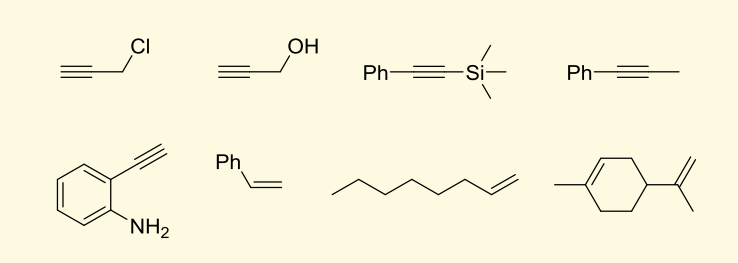

Scheme 2.8 Unsuccessful substrates.

2.4 Mechanistic Studies

We next began to investigate the mechanism of this transformation. As we observed catalysis with both DIBAL-H and alkyl aluminium species, we envisaged the formation of an aluminium hydride as a first step when using trialkyl aluminium species. In addition, group 13 alkyl derivatives have shown to undergo a facile alkyl group exchange.[26],[27] This redistribution provides a convenient method of preparing heteroleptic trialkyl compounds (Scheme 2.9).

Scheme 2.9. Al-alkyl group exchange.

Along this line, we hypothesised that the Al-H species could be generated *in situ* by σ-bond metathesis with one molecule of HBpin. Hence, a series of stoichiometric reactions of $AlMe_3$, $AlEt_3$ and $Et_3Al{\cdot}DABCO$ with pinacol borane were carried out in deuterated toluene. The reactions of HBpin with trimethylaluminium showed immediate conversion of HBpin to mostly Me_3B ($\delta^{11}B$ = 83) and a small amount of MeBpin ($\delta^{11}B$ = 34.4) with diagnostic resonances (Figure 2.3).

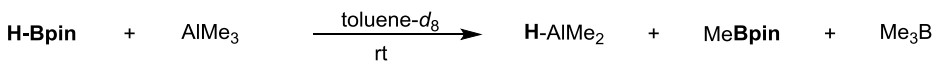

Scheme 2.10. Al-H *in situ* generation: reaction of $AlMe_3$ and HBpin.

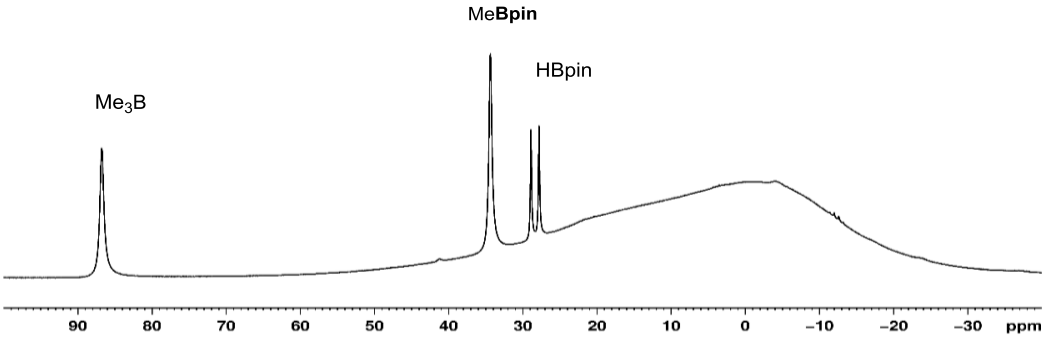

Figure 2.3. ^{11}B NMR spectrum of reaction of $AlMe_3$ and HBpin.

The same type of pattern was also observed when the reaction was performed with triethylaluminium, the formation of a diagnostic broad singlet in the ^{1}H NMR spectrum (δ ^{1}H = 3.53) was also observed (Figure 2.4). By analogy to other aluminium-alkyl hydrides,[28] this resonance can be assigned to a new Al-H bond, supporting the proposed hydride exchange.

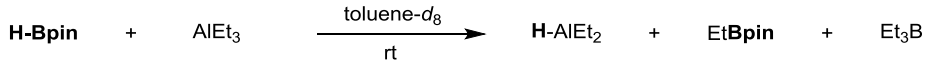

Scheme 2.11. Al-H *in situ* generation: reaction of $AlEt_3$ and HBpin.

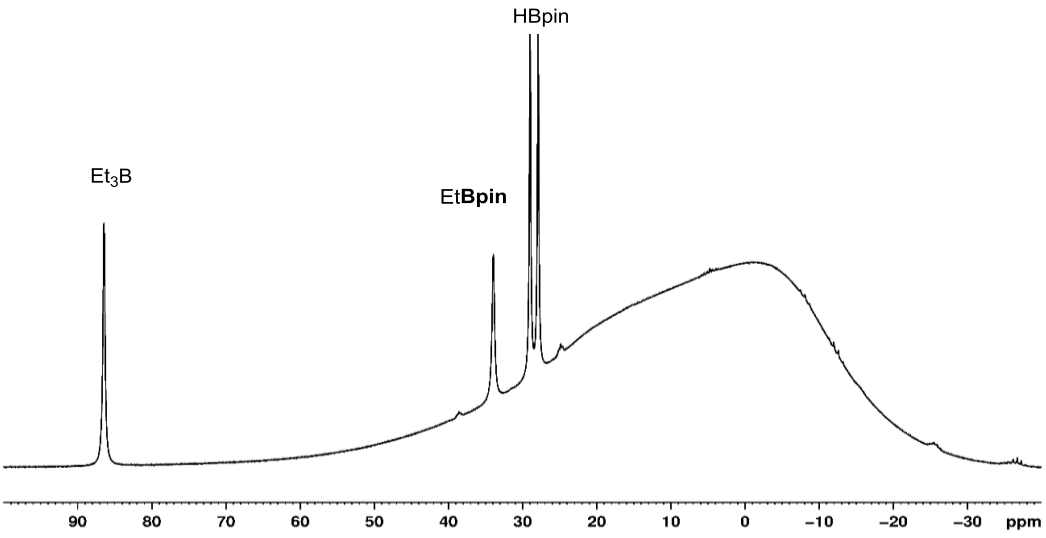

Figure 2.4. ^{11}B NMR spectrum of reaction of $AlEt_3$ and HBpin.

The formation of these unexpected borane species (BMe_3, BEt_3) may be a result of an over-exchange mechanism between aluminium and boron which could potentially lead to catalytically incompetent species. Although the reactivity of $AlMe_3$, and $AlEt_3$ may be expected to be similar, their solution structure differs in the aggregation state (monomer, dimer, etc.) as often happens with alkyl zinc species.[29],[30] In the case of triethyl aluminium, this may result in increased concentration of monomeric structure available which could lead to a more selective Al-H hence a more effective catalyst for this transformation.

Performing the reaction with $Et_3Al{\cdot}DABCO$ resulted in a slower, but more selective reaction towards formation of EtBpin, suggesting that DABCO is preventing HBpin decomposition to alkyl borane species (Figure 2.5).

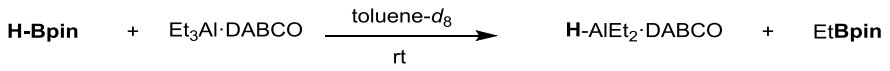

Scheme 2.12. Al-H *in situ* generation: reaction of $Et_3Al{\cdot}DABCO$ and HBpin.

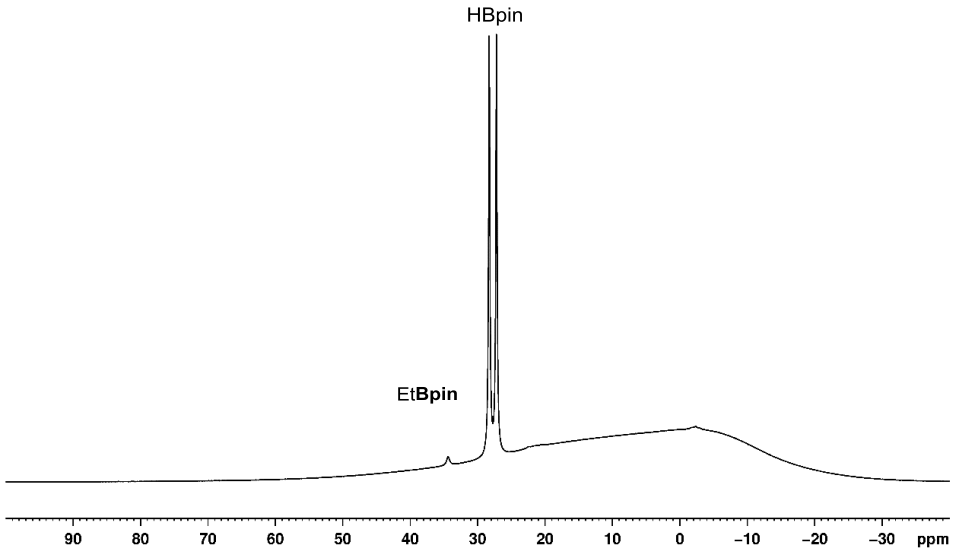

Figure 2.5. ^{11}B NMR spectrum of reaction of $Et_3Al{\cdot}DABCO$ and HBpin.

No conclusive information about the aluminium species could be obtained due to the broad ^{1}H NMR signals related to multiple boron alkyl species. It is worth noting that after 24 hours all the reactions showed upfield resonances in the ^{11}B NMR corresponding to unidentified four-coordinate boron species as a result of side reactions. In the case of

the Et_3Al·DABCO reaction with HBpin**,** it was possible to crystallise, under the reaction mixture conditions, one of these four-coordinate species, $EtBH_2$·DABCO (Figure 2.6). Based on the multiplicity of the signal in the ^{11}B NMR ($\delta\ ^{11}B = -2.1$, t, $J_{B\text{-}H}$ = 93.73 Hz) we could identify this species, which shows a diagnostic proton boron coupling constant.

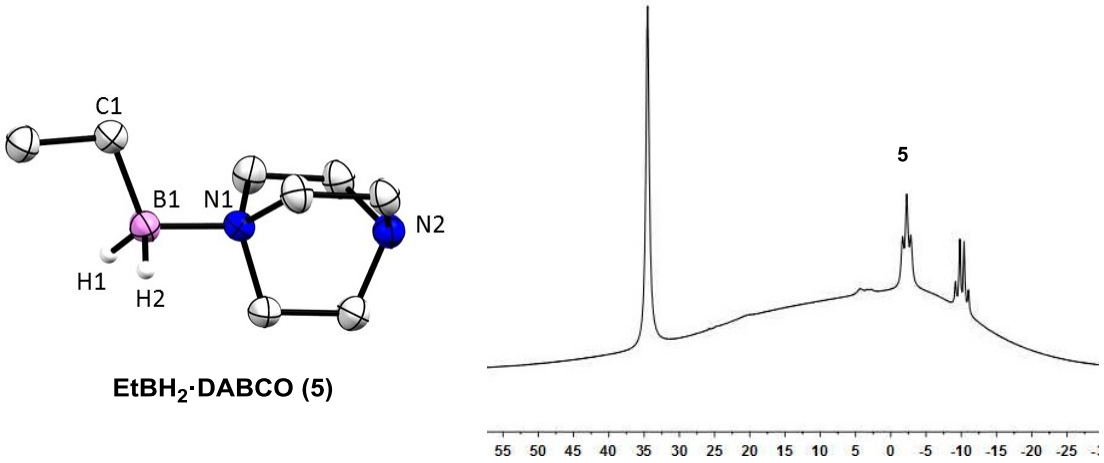

$EtBH_2$·DABCO (5)

Figure 2.6. Crystal structure of $EtBH_2$·DABCO (**5**) and ^{11}B NMR spectrum of the reaction of Et_3Al·DABCO and HBpin after 24 h. Ellipsoids are set to 50% probability; hydrogen atoms are omitted for clarity with the exception of B-H bond. Selected both lengths of $EtBH_2$·DABCO (**5**) (Å): B(1)–N(1) 1.635(2), B(1)–C(1) 1.961(5), B(1)–H(1) 1.147(12), B(1)–H(2) 1.134(12).

All attempts to isolate and fully characterise $EtBH_2$·DABCO failed. Once identified this species we were able to then assign the further negative resonance, ($\delta\ ^{11}B = -10$, q, $J_{B\text{-}H}$ = 97.65), to BH_3·DABCO based on previously reported value.[31] However as all the reactions of alkyl aluminium species and pinacol borane showed a similar pattern, it is proposed that both trialkyl and dialkyl aluminium species converge to a closely related active catalyst, by formation of alkyl-Bpin and subsequent formation of Al-H species.

Once formed, the aluminium hydride undergoes hydroalumination,[12] hence in order to isolate the hydroalumination product, stoichiometric reactions using $^{i}Bu_2Al$-H (as a model aluminium hydride species) and alkynes (aliphatic and aromatic) were performed. Both alkyl and aryl alkyne underwent successful hydroalumination in more than 50% conversion however all the attempts to isolate the product and grow a crystal suitable for X-ray analysis failed (Scheme 2.13). Unfortunately, diphenyl acetylene displayed no reactivity even after several days.

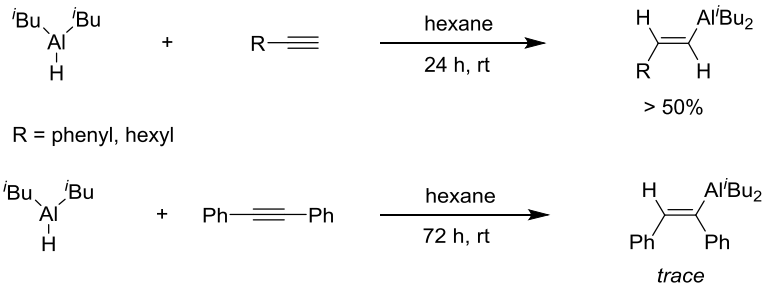

Scheme 2.13. Hydroalumination of terminal and internal alkynes.

Finally performing the reaction using, 3,3-dimethyl-1-butyne as the substrate, resulted in almost full conversion within 30 minutes at room temperature (Scheme 2.14). Product formation was confirmed by ^{1}H NMR and $^{13}C\{H\}$ NMR showing diagnostic olefinic proton and carbon resonances (δ ^{1}H NMR = 7.51, 5.89), (δ $^{13}C\{H\}$ NMR = 194.06, 118.52) (Figure 2.7) and it was possible to isolate it as a crystalline solid in 60% yield. The alkenyl aluminium dimer was synthesised accordingly to a modification of a previously reported procedure by Uhl and co-workers.[32]

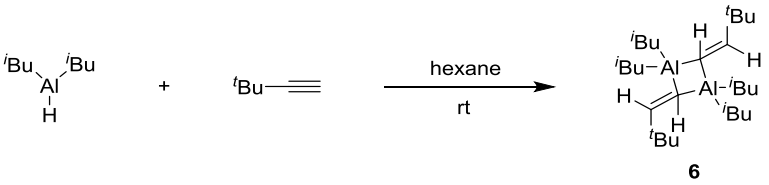

Scheme 2.14. Hydroalumination of 3,3-dimethyl-1-butyne.

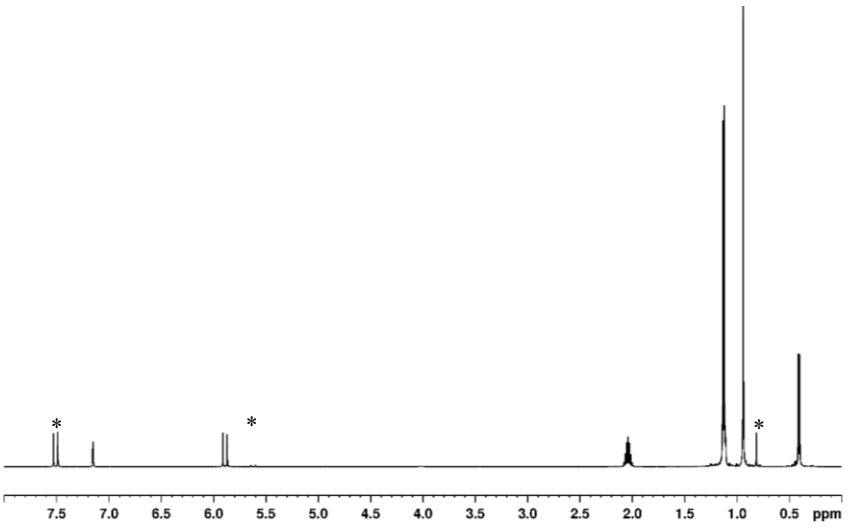

Figure 2.7. ^{1}H NMR spectrum of the alkenyl aluminium (**6**), * = trans isomer.

Interestingly, performing the hydroalumination of 3,3-dimethyl-1-butyne using $^{i}Bu_2Al$-H·DABCO adduct generated *in situ*, no vinyl aluminium species was observed even after 24 hours, likely due to the base coordination inhibiting hydroalumination. Detailed mechanistic studies have in fact shown that Lewis bases can prevent the hydroalumination by coordination.[33] The three-coordinate nature of the aluminium centre and the electrophilic character is essential to the coordination of the unsaturated bond and the subsequent Al-H insertion. However, since aluminium-base adducts have displayed catalytic competence, it could be concluded that the adduct is partially dissociated under catalytic conditions.

With the alkenyl aluminium (**6**), the next step of the catalytic cycle and the role of the base were investigated, carrying out stoichiometric reactions with HBpin, alkenyl aluminium species (**6**) and DABCO (Scheme 2.15).

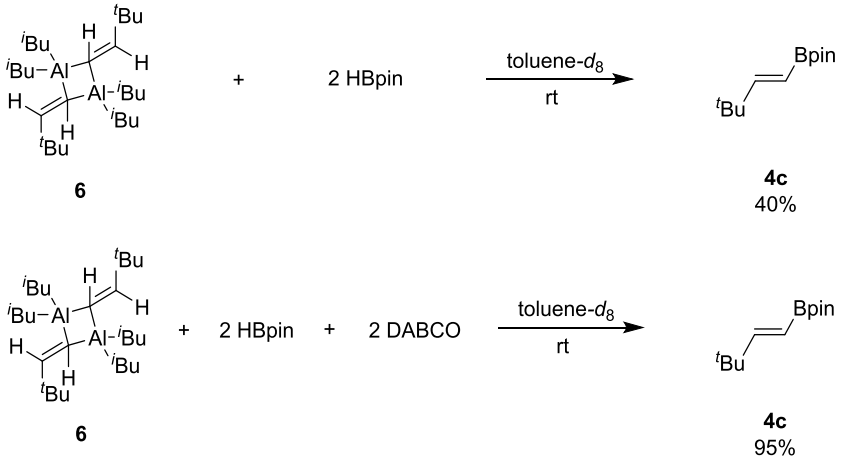

Scheme 2.15. Reaction of the alkenyl aluminium (**6**) and HBpin; reaction of the alkenyl aluminium (**6**) and HBpin in the presence of DABCO.

Treating the alkenyl aluminium (**6**) with HBpin showed 40% conversion after 5 minutes, without any further increase even after 24 hours. In the presence of DABCO the same reaction goes to full conversion in 30 minutes.

In the base free reaction, the ^{11}B NMR clearly showed the formation of trialkylboron species and $^{i}BuBpin$, which was not observed in the reaction carried out in the presence of DABCO (Figure 2.8). However, in the presence of DABCO, ^{11}B NMR showed a negative resonance corresponding to BH_3·DABCO ($\delta\,^{11}B = -10$, q, J = 97.65 Hz) as well

as HBpin·DABCO (δ ^{11}B = 25, d, *J* = 171.40 Hz)[34] confirming that the base could coordinate both the aluminium and boron during the process. A possible explanation for higher conversion in the presence of DABCO is that the base breaks up the dimeric alkenyl aluminium species (**6**) to give the DABCO alkenyl aluminium adduct. A shift in the ^{1}H NMR of the alkenyl proton from δ = 7.51 ppm to δ = 6.34 ppm could support this. The presence of DABCO lowers the concentration of the dimeric alkenyl aluminium species which resulted in a decrease in the overall rate of reaction, but a higher overall yield.

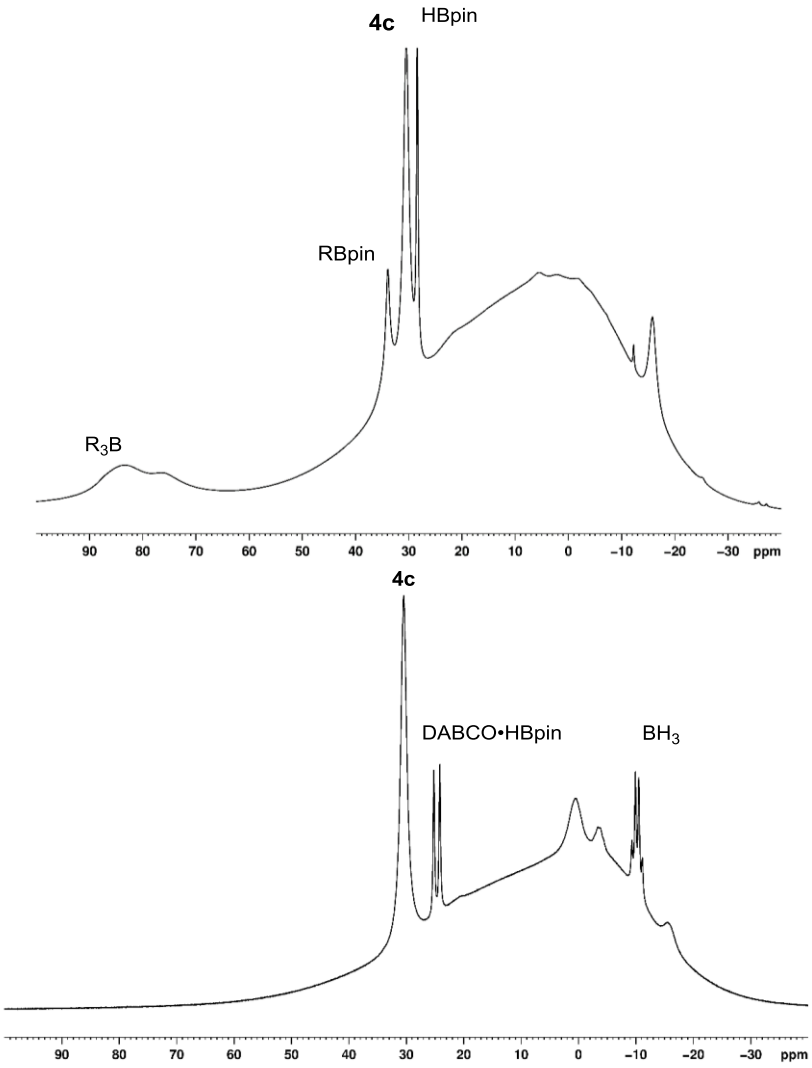

Figure 2.8. ^{11}B NMR spectra comparison of reactions of alkenyl aluminium (**6**) and HBpin. *Top spectrum*: reaction carried out without base; *bottom spectrum*: reaction carried out with 2 eq. of DABCO.

To further support the proposed mechanism, alkenyl aluminium (**6**) was tested as a catalyst using 2.5 mol% at 110 °C for 2 hours in the hydroboration of 3,3-dimethyl-1-butyne (Scheme 2.16). Formation of the boronic ester was observed in 68% yield, confirming that the hydroalumination product either lies on the catalytic cycle or is a catalyst resting state. Carrying out the reaction with 1 equivalent of DABCO gave the same yield. The role of the base in the catalytic systems is complex and still requires further investigation.

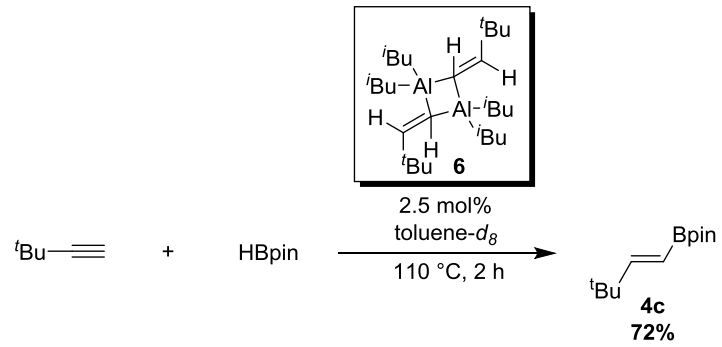

Scheme 2.16. Catalytic competence of the alkenyl aluminium (**6**).

Based on the above experiment, a proposed mechanism for the aluminium-catalysed hydroboration of alkynes is reported (Scheme 2.17). Based on the mechanistic studies we propose that the active catalyst, R_2Al-H, is generated by σ-bond metathesis with HBpin. The aluminium hydride then undergoes hydroalumination with the alkyne to give a highly reactive alkenyl aluminium intermediate. This then reacts with a further equivalent of HBpin, through σ-bond metathesis, to regenerate the catalyst and release the product.

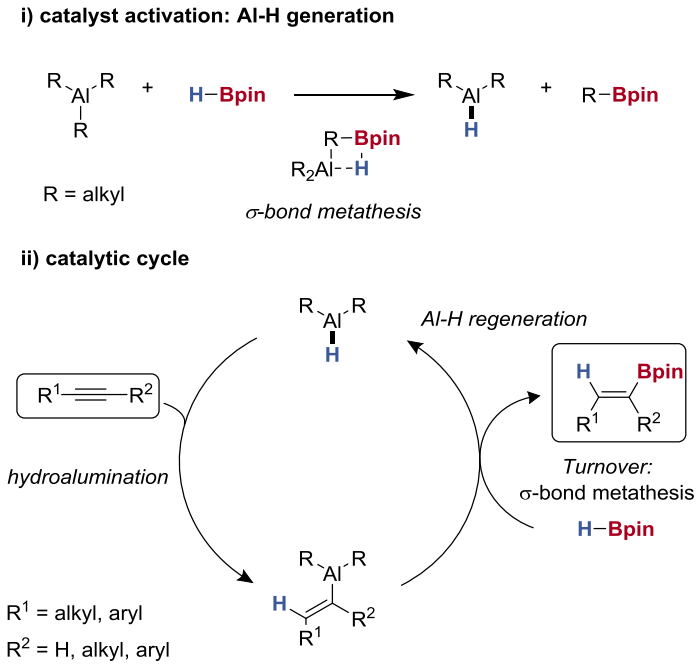

Scheme 2.17. Proposed mechanism for aluminium-catalysed hydroboration.

At the same time as our work, Roesky and co-workers have reported a catalytic hydroboration of terminal alkynes using a *N,N'*-bis-2,6-di*iso*propylphenyl diketiminate (NacNac) supported aluminum dihydride.[35] In this case, catalyst activation is provided through alkyne deprotonation with an activation barrier of 33 kcal mol^{-1} to form the alkynyl aluminium species (Scheme 2.18). The rate-determining step in this mechanism was predicted computationally to be the protonation of the borylated alkenyl group at the aluminum centre by the incoming terminal alkyne, with an activation barrier of 45.3 kcal mol^{-1}.[35] Although this mechanism is a possibility for the hydroboration of terminal alkyne catalysed by the NacNacAlH_2 system, it cannot explain the ability of $^{i}Bu_2$Al-H and Et_3Al·DABCO to catalyse hydroboration of internal alkynes.

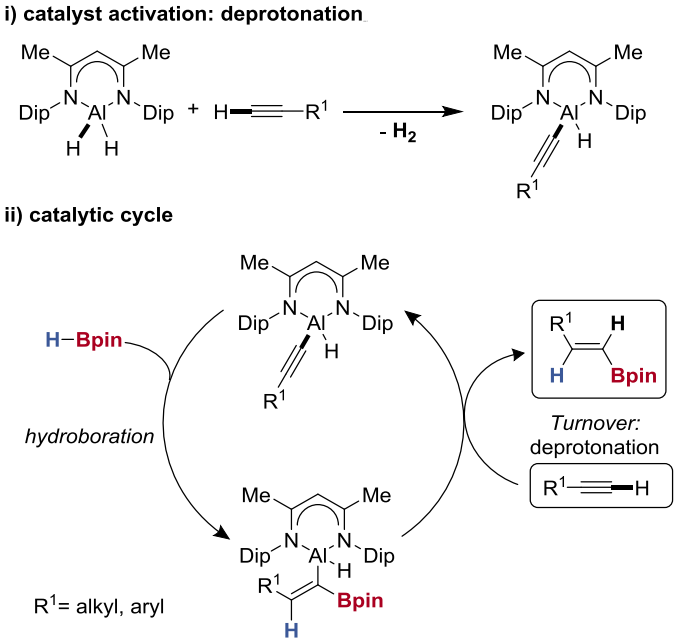

Scheme 2.18. Mechanism of NacNacAlH$_2$-catalysed hydroboration.

In order to confirm that substrate activation was provided by hydoalumination over deprotonation, d_1-3,3-dimethylbutyne was synthesised and tested under catalytic conditions (Scheme 2.19). In this case, if deprotonation is occurring the formation of H-D will be observed; the proton-deuterium coupling is characterised by a diagnostic resonance multiplicity (1:1:1 triplet). The reaction was initially performed in a J Young's NMR tube to monitor any H-D evolution and then scaled up to isolate the product. As expected, no H-D species was observed, however a diagnostic triplet (δ ^{1}H = 6.93, $J_{H\text{-}D}$ = 2.57 Hz; ^{2}H NMR δ = 5.64, $J_{H\text{-}D}$ = 2.57 Hz) belonging to deuterated *E*-alkenyl boronic ester was observed (Figure 2.9).

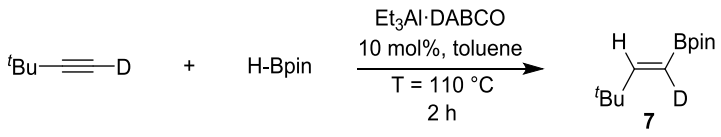

Scheme 2.19. Hydroboration d_1-3,3-dimethylbutyne.

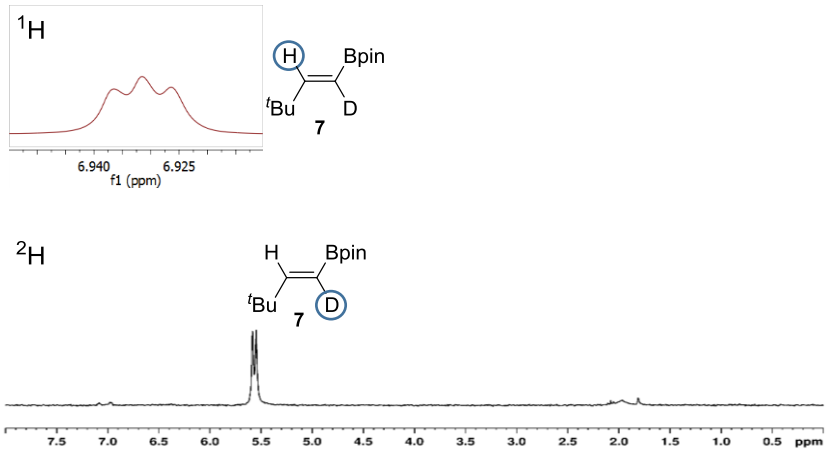

Figure 2.9. Hydroboration of d_1-3,3-dimethylbutyne. *Top spectrum*: ^{1}H NMR spectrum of the alkenyl boronic ester (**7**). *Bottom spectrum*: ^{2}H NMR spectrum of the alkenyl boronic ester (**7**).

To further support the proposed mechanism, we synthesised d_1,-pinacol borane and used it under catalytic conditions with 3,3-dimethylbutyne as the substrate and $Et_3Al{\cdot}DABCO$ as the catalyst (Scheme 2.20). The reaction gave deuterium incorporation into the product at α position (δ ^{1}H NMR = 5.64, $J_{H\text{-}D}$ = 2.57 Hz) (δ ^{2}H NMR = 6.93, $J_{H\text{-}D}$ = 2.57 Hz) which showed deuterium transfer from the boron to the aluminium (Figure 2.10). Additionally, the stereoselectivity could also be confirmed with the hydroaluminiation step operating in a *syn* fashion.

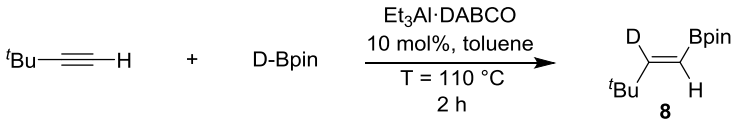

Scheme 2.20. Hydroboration of 3,3-dimethylbutyne using d_1-pinacol borane.

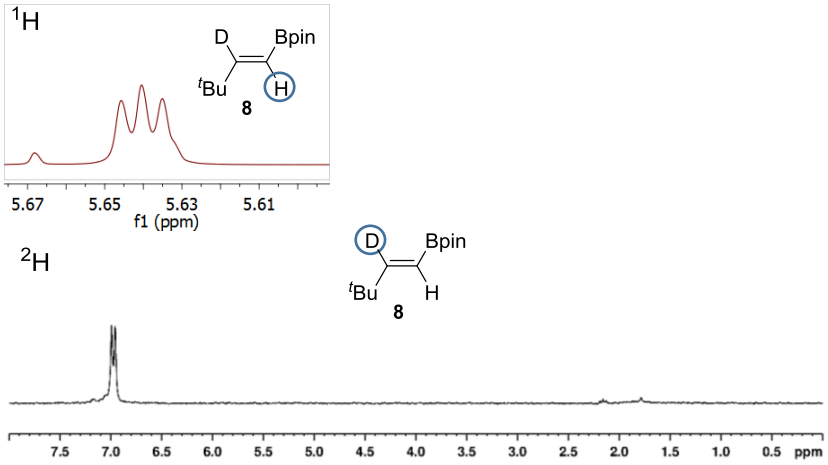

Figure 2.10 Hydroboration of 3,3-dimethylbutyne using d_1-pinacol borane. *Top spectrum*: ^{1}H NMR spectrum of the alkenyl boronic ester (**8**). *Bottom spectrum*: ^{2}H NMR spectrum of the alkenyl boronic ester (**8**).

The isolated product of the catalysis with DBpin contained some non-deuterated alkenyl boronic ester (8%, δ ^{1}H NMR = 5.65 ppm) that can be rationalised as the product of a-hydride elimination from one of the alkylaluminium species (Scheme 2.21). This generated the Al-H bond which determined non-deuterated vinylboron compounds.[36]

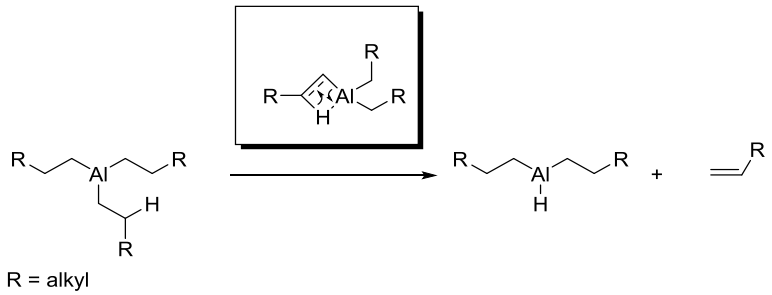

Scheme 2.21. Aluminium hydride decomposition pathway.

To summarise the mechanistic studies, it is proposed that the active catalyst is generated *in situ* through σ-bond metathesis with one molecule of HBpin, substrate activation occurs *via* hydroalumination. Further σ-bond metathesis with pinacol borane allowed product release and Al-H regeneration. Experimental evidence suggest that it differs from very recent proposals by Roesky and co-workers which were supported by computational studies.

2.5 Conclusions and Future work

A facile system for aluminium-catalysed hydroboration of alkynes using commercially-available and user-friendly materials, which represents a significant advance for main-group catalysis (Scheme 2.22). Both aryl and alkyl-alkynes have been shown to be hydroborated under the developed reaction conditions, in good yield and with moderate group tolerance. We were also able, for the first time, to use an aluminium catalyst in the hydroboration of internal alkynes. Unfortunately, the selective hydroboration of alkyne functionality in the presence of functional groups containing potentially reducible carbon-heteroatom multiple bonds such as a ketone was not possible. Mechanistic studies support the generation of aluminium hydride reagents *in situ* from bench-stable precursors. The aluminium hydrides act as the active catalysts in the reaction, whilst turnover strongly depends upon the hydroalumination step.

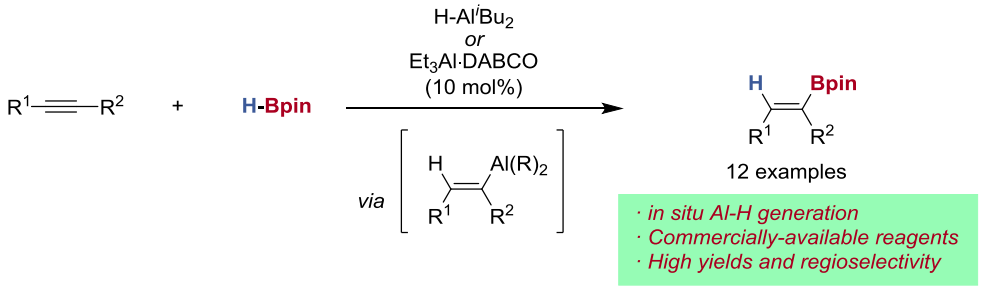

Scheme 2.22. Aluminium-catalysed hydroboration of alkynes.

Future work should focus on hydrofunctionalisation processes such as hydrofluorination and hydroamination. Aluminium-catalysed intramolecular hydroamination of aminoalkenes is an established process.[37] The mechanism is based on amine deprotonation with subsequent coordination formation of an aluminium nitrogen bond. Alkene insertion into aluminium nitrogen bond followed by protonolysis step gave the product regenerating the catalyst (Scheme 2.23). However, due to the high activation energy required for the insertion step, the substrate scope is limited to intramolecular hydroamination.

An alternative pathway which could eventually lead to intermolecular hydroamination of alkenes is described below (Scheme 2.23). An appropriate hydride source generates the aluminium hydride species *in situ*, which then activates the substrates through

hydroalumination step and releases the product by σ-bond metathesis. The active catalyst is then regenerated by hydride exchange with phenylsilane.

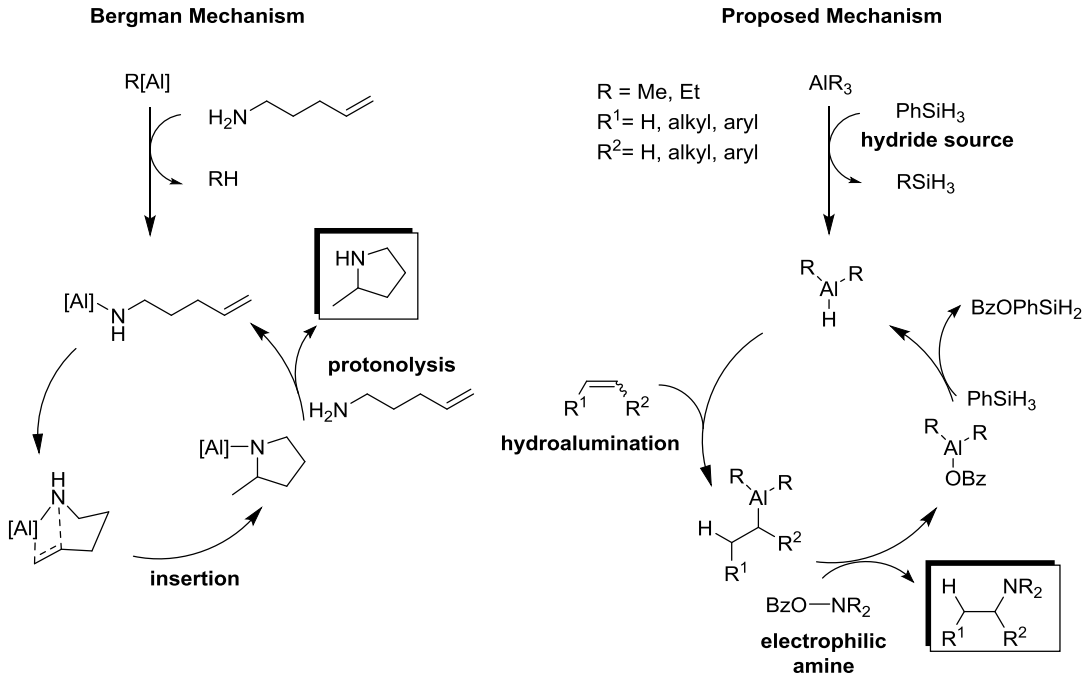

Scheme 2.23. Different pathway for aluminium-catalysed hydroamination.

This work has been published in *Angewandte Chemie International Edition* (*Angew. Chem. Int. Ed.*, 2016, **55**, 15356–15359, doi.org/10.1002/anie.201609690, see Appendix 1).

2.6 References

[1] N. Miyaura and A. Suzuki, *Chem. Rev.*, 1995, **95**, 2457–2483.

[2] B. W. Glasspoole and C. M. Crudden, *Nat. Chem.*, 2011, **3**, 912–913.

[3] J. F. Hartwig, *Acc. Chem. Res.*, 2012, **45**, 864–873.

[4] F.-S. Han, *Chem. Soc. Rev.*, 2013, **42**, 5270–98.

[5] A. J. J. Lennox and G. C. Lloyd-Jones, *Chem. Soc. Rev.*, 2014, **43**, 412–443.

[6] H. C. Brown and B. Singaram, *Pure Appl. Chem.*, 1987, **59**, 879–894.

[7] D. Männig and H. Nöth, *Angew. Chem. Int. Ed.*, 1985, **24**, 878–879.

[8] S. a. Westcott, H. P. Blom, T. B. Marder and R. T. Baker, *J. Am. Chem. Soc.*, 1992, **114**, 8863–8869.

[9] K. Burgess and M. Jaspars, *Organometallics*, 1993, **12**, 4197–4200.

[10] Y. Matsumoto, M. Naito and T. Hayashi, 1992, **26**, 2732–2734.

[11] M. J. Winter, *J. Chem. Educ.*, 2011, **88**, 1507–1510.

[12] S. Aldridge and A. J. Downs, *The Group 13 Metals Aluminium, Gallium, Indium and Thallium: Chemical Patterns and Peculiarities*, 2011.

[13] H. W. Roesky, *Inorg. Chem.*, 2004, **43**, 7284–7293.

[14] K. Revunova and G. I. Nikonov, *Dalton Trans.*, 2015, **44**, 840–66.

[15] A. Bismuto, S. P. Thomas and M. J. Cowley, *Angew. Chem. Int. Ed.*, 2016, **55**, 15356–15359.

[16] A. M. Bradford, D. C. Bradley, M. B. Hursthouse and M. Motevalli, *Organometallics*, 1992, **11**, 111–115.

[17] K. Biswas, O. Prieto, P. J. Goldsmith and S. Woodward, *Angew. Chem. Int. Ed.*, 2005, **44**, 2232–2234.

[18] A. W. Addison and T. N. Rao, *J. Chem. Soc. Dalt. Trans.*, 1984, **1**, 1349.

[19] G. A. Papoian and R. Hoffmann, *Angew. Chem. Int. Ed.*, 2000, **39**, 2408–2448.

[20] M. L. Munzarová and R. Hoffmann, *J. Am. Chem. Soc.*, 2002, **124**, 4787–4795.

[21] T. W. Myers, A. L. Holmes and L. A. Berben, *Inorg. Chem.*, 2012, **51**, 8997–9004.

[22] T. W. Myers, N. Kazem, S. Stoll, R. D. Britt, M. Shanmugam and L. a. Berben, *J. Am. Chem. Soc.*, 2011, **133**, 8662–8672.

[23] J. Lewiński, J. Zachara, T. Kopeć and Z. Ochal, *Polyhedron*, 1997, **16**, 1337–1341.

[24] K. Alfonsi, J. Colberg, P. J. Dunn, T. Fevig, S. Jennings, T. a. Johnson, H. P.

Kleine, C. Knight, M. a. Nagy, D. a. Perry and M. Stefaniak, *Green Chem.*, 2008, **10**, 31–36.

[25] George Zweifel, John T. Snow, Charles C. Whitney, *J. Am. Chem. Soc.*, 1968, **90**, 7139–7141.

[26] M. Bochmann and M. J. Sarsfield, *Organometallics*, 1998, **17**, 5908–5912.

[27] J. Klosin, G. R. Roof, E. Y. X. Chen and K. A. Abboud, *Organometallics*, 2000, **19**, 4684–4686.

[28] L. V. Parfenova, P. V. Kovyazin, I. E. Nifant'ev, L. M. Khalilov and U. M. Dzhemilev, *Organometallics*, 2015, **34**, 3559–3570.

[29] D. Seyferth, *Organometallics*, 2001, **20**, 2940–2955.

[30] J. T. B. H. Jastrzebski, J. Boersma and G. van Koten, *PATAI'S Chem. Funct. Groups*, 2009, 31–135.

[31] W. Biffar, H. Nöth and D. Sedlak, *Organometallics*, 1983, **2**, 579–585.

[32] W. Uhl, E. Er, A. Hepp, J. Kösters, M. Layh, M. Rohling, A. Vinogradov, E. U. Würthwein and N. Ghavtadze, *Eur. J. Inorg. Chem.*, 2009, **22**, 3307–3316.

[33] J. J. Eisch and Hordis, Charles K, *Organometallics*, 1971, **23**, 2974–2981.

[34] P. Eisenberger, A. M. Bailey and C. M. Crudden, *J. Am. Chem. Soc.*, 2012, **134**, 17384–17387.

[35] Z. Yang, M. Zhong, X. Ma, K. Nijesh, S. De, P. Parameswaran and H. W. Roesky, *J. Am. Chem. Soc.*, 2016, **138**, 2548–2551.

[36] B. E. Bent, R. G. Nuzzo and L. H. Dubois, *J. Am. Chem. Soc.*, 1989, **111**, 1634–1644.

[37] J. Koller and R. G. Bergman, *Chem. Commun.*, 2010, **46**, 4577–4579.

Chapter 3− Aluminium-catalysed hydroboration of alkenes

The alkene functional group is one the most prevalent in nature, thus, their use as a platform for accessing many diversely functionalised products is crucial. During the last 50 years, many methods have been developed using transition metals for the hydrofunctionalisation of alkenes.[1]–[5]

Alkyl boronic esters are of great synthetic utility due to their easy conversion into other functional groups.[6]–[8] A range of stereospecific transformations are well known for secondary and tertiary boronic esters, such as oxidations, protodeboronation, and the formation of new C–C bonds.[9]

In contrast to transition metal catalysts which have been extensively used in alkenes hydroboration, there are only a few examples using main-group elements[10],[11] and no example of an aluminium-based catalyst, although the stoichiometric reactivity is well established (Scheme 3.1).

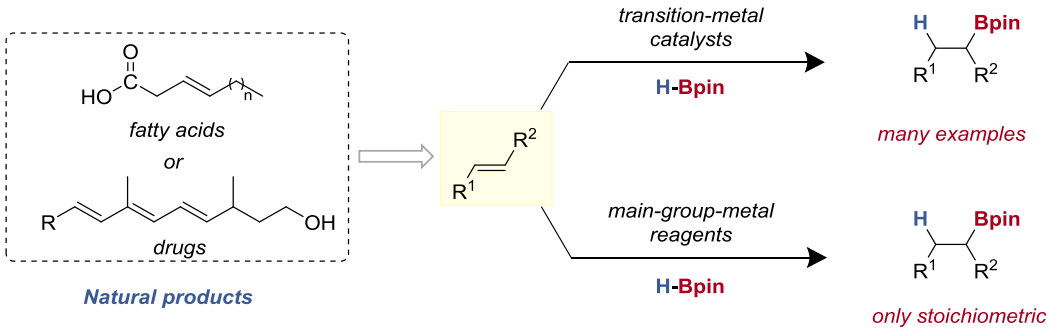

Scheme 3.1. State-of-the-art of catalytic hydroboration of alkenes.

3.1 Project Aims

As previously established (see chapter 1), the development of more sustainable chemical systems is of critical importance. Industrial catalysis is dominated by heavy, precious transition metals,[12],[13] thus considerable efforts have been invested in Earth-abundant metals[14],[15] including main-group metal alternatives. Many effective systems for transition-metal-catalysed hydroboration of unsaturated polar and non-polar bonds have been reported achieving good yield and functional group tolerance. However, there

are few examples of alkyne hydroboration, [16],[17] and none of the hydroboration of alkenes using an aluminium catalyst.

The aim of this project was to develop an aluminium-catalysed hydroboration of alkenes. Alkyne hydroalumination has already been shown as a route to alkenyl boronic esters (see chapter 2). However, the analogous reaction with alkenes is far more challenging and very limited in scope (see chapter 1, Hydroalumination).[18],[19] In spite of this, it was hypothesised that with an appropriate aluminium design, tuning steric bulk and Lewis acidity, alkene hydroalumination could potentially be accessed and used as a first-step in the catalytic hydroboration of alkenes.

3.2 Reaction Development

An initial reaction with styrene and pinacol borane using the conditions developed for alkyne hydroboration, or the control reaction displayed only trace amount of alkyl boronic ester (Table 3.1, entries 1-3). In order to increase the reactivity of the aluminium reagent $Me_3N{\cdot}AlH_3$ and the more hydridic bis(2-methoxyethoxy)aluminium hydride (Red-Al) were tested. The linear alkyl boronic ester was obtained in slightly better yields (Entries 3 and 4). In order to improve the yield of the reaction, different solvents were screened using commercially-available Red-Al (10 mol%). Performing the reaction in THF resulted in 30% yield of the alkyl boronic ester (Entry 8), as observed by ^{1}H NMR, indicating that catalyst turnover could be achieved. Inspired by recent works, which showed an increase of product yield under solvent-free conditions,[11] a further reaction was performed in the absence of solvent. Notably this time, the hydroboration of styrene proceded in 95% yield to give the *anti*-Markovnikov (linear) alkyl boronic ester in 4 hours, showing an aluminium species to be catalytically competent for the hydroboration of alkenes.

Table 3.1. Reaction development.

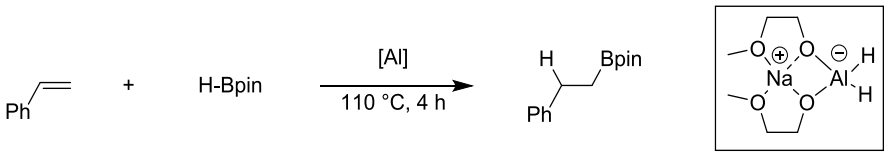

Red-Al

Entry	[Al] (10 mol%)	Solvent	Yield (%)
1[a]	none	toluene	1
2[a]	$^{i}Bu_2Al$-H	toluene	3
3[a]	Et_3Al·DABCO	toluene	3
4[a]	Red-Al	toluene	9
5[a]	Me_3N·AlH_3	toluene	9
6[a]	Red-Al	dichloromethane	2
7[a]	Red-Al	2-methyl-THF	12
8[a]	Red-Al	THF	30
9[b]	Red-Al	*none*	95

Reaction conditions: [a] 0.015 mmol (0.1 eq.) catalyst, 0.15 mmol (1 eq.) styrene and 0.18 mmol (1.5 eq.) HBpin in 0.60 mL of the solvent, heated to 110 °C for 4 h. [b] 0.045 mmol (0.1 eq.) catalyst, 0.45 mmol (1 eq.) styrene and 0.54 mmol (1.5 eq.) HBpin in heated at 110 °C for 4 h. Yield determined by ^{1}H NMR of the crude reaction mixture using 1,3,5-trimethoxybenzene as an internal standard.

Encouraged by these results, a series of aluminium compounds were trialled for the hydroboration of styrene under solvent-free conditions (Table 3.2). $AlEt_3$ and Et_3Al·DABCO compounds successfully promoted this transformation (Entries 1 and 2) with significant lower activity with observed for the more Lewis acidic Et_2AlCl (Entry 3). Neutral aluminium hydrides resulted in an improved yield (Entry 4), with almost full conversion to the alkyl boronic ester when Me_3N·AlH_3 was used (Entry 5). As the anionic aluminium (Red-Al) species had proved to be a successful catalyst for the hydroboration of styrene, a significant advance would be to extend it the most used aluminium hydride reagent in organic synthesis; $LiAlH_4$. The latter is not only 100 times less expensive than $^{i}Bu_2Al$-H or any other alkyl aluminium species, but it reduces any additional operational complexity. Interestingly, $LiAlH_4$ successfully promoted the hydroboration of styrene with

full conversion in less than 4 hours (Entry 7). In order to test the activity of the catalyst, further screening at lower catalyst loadings were then carried out. Both $Et_3Al{\cdot}DABCO$ and commercially-available $^{i}Bu_2Al\text{-}H$ gave the linear boronic ester, albeit in decreased yield (40% and 55% respectively, Entries 8 and 9). All the other hydride species resulted in good yield using 5 mol% of catalyst loading (Table 3.2, entries 9-12,)

Table 3.2. Catalysts screening.

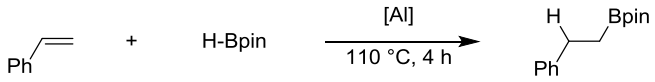

Entry	[Al]	loading	Yield (%)
1	Et_3Al	10 mol%	75
2	$Et_3Al{\cdot}DABCO$	10 mol%	66
3	$AlEt_2Cl$	10 mol%	35
4	$^{i}Bu_2Al\text{-}H$	10 mol%	85
5	$Me_3N{\cdot}AlH_3$	10 mol%	95
6	Red-Al	10 mol%	94
7	$LiAlH_4$	10 mol%	95
8	$^{i}Bu_2Al\text{-}H$	5 mol%	55
9	$Et_3Al{\cdot}DABCO$	5 mol%	40
10	$Me_3N{\cdot}AlH_3$	5 mol%	83
11	Red-Al	5 mol%	86
12	$LiAlH_4$	5 mol%	86

Reaction conditions: (0.05 - 0.1 eq.) catalyst, 0.45 mmol (1 eq.) styrene and 0.54 mmol (1.2 eq.) HBpin in heated at 110 °C for 4 h. Yield determined by ^{1}H NMR of the crude reaction mixture using 1,3,5-trimethoxybenzene as an internal standard.

Given the low price and the simple procedure, $LiAlH_4$ was selected as the catalyst for further work. In order to optimise the protocol, a screening of all the other reaction parameters was undertaken. Decreasing the loading of HBpin from 1.2 to 1.1 equivalents did not show a significant difference in product yield, while moving to 1.5 equivalents gave an improved yield (Table 3.3, entries 1-4). Nevertheless, in order to improve the

sustainability of the process, 1.1 equivalents were selected as optimal condition. The reaction was also tested at different temperatures. Performing the reaction at 30 °C or at 60 °C resulted in lower yield (Entries 5, 6 respectively) while 80 °C gave a moderate yield (Entry 7). So, 110 °C was chosen as the ideal temperature.

Table 3.3. Screening of reaction conditions.

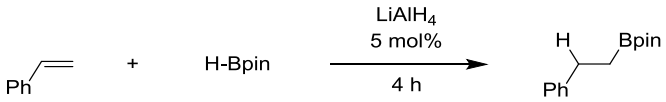

Entry	HBpin (eq.)	T (°C)	Yield (%)
1	1.0	110	73
2	1.1	110	82
3	1.2	110	86
4	1.5	110	99
5	1.1	30	12
6	1.1	60	30
7	1.1	80	68

Reaction conditions: 0.022 mmol (0.05 eq.) $LiAlH_4$, 0.45 mmol (1 eq.) styrene and (1.0-1.5 eq.) HBpin heated at the indicated temperature for 4 h. Yield determined by ^1H NMR of the crude reaction mixture using 1,3,5-trimethoxybenzene as an internal standard.

A final investigation was then carried out monitoring the hydroboration of styrene using 5 mol% of $LiAlH_4$. No evidence of an induction period was observed.

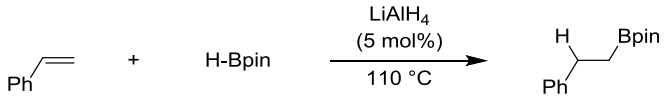

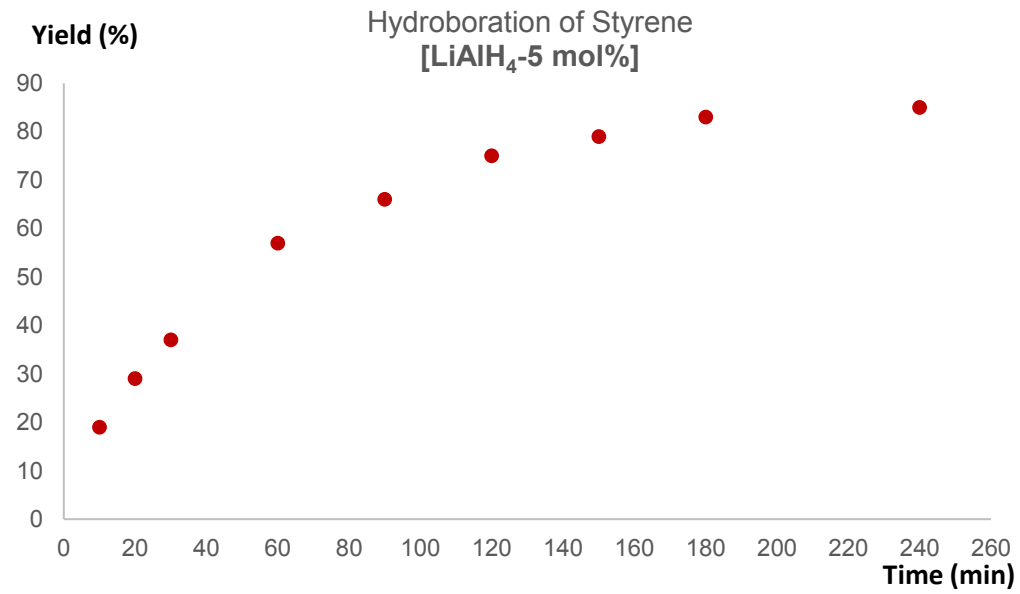

Figure 3.1. Kinetic profile monitoring of the linear hydroboration of styrene and HBpin using 5 mol% of $LiAlH_4$.

Screening of the reaction parameters (solvent, temperature, etc.) led to optimised reaction conditions of alkene (1 equivalent), HBpin (1.1 equivalents) and $LiAlH_4$ (5 mol%), at 110 °C for 3 hours. However, in order to maximise product formation and considering the low cost of $LiAlH_4$, the following reactions were performed using 10 mol% of catalyst.

3.3 Substrate Scope

With these conditions, the substrate scope and functional group tolerance of this hydroboration protocol were explored (Scheme 3.2). In all the cases the regioselectivity was determined by NMR spectroscopy. Terminal alkyl-substituted alkenes all underwent successful hydroboration to the linear alkyl boronic ester with excellent control of regioselectivity (Scheme 3.2, **10a-10h**). Very little variation in catalyst activity was observed across alkenes bearing primary, secondary, and tertiary alkyl substituents (**10a-10c**). Good functional group tolerance was observed with halide- (**10e**), and tosyl- (**10f**) and silyl-substituents (**10g**). The successful hydroboration of 1,1-dichloro-2-vinylcyclopropane (**10h**) proceeded without cleavage of the C-Cl.

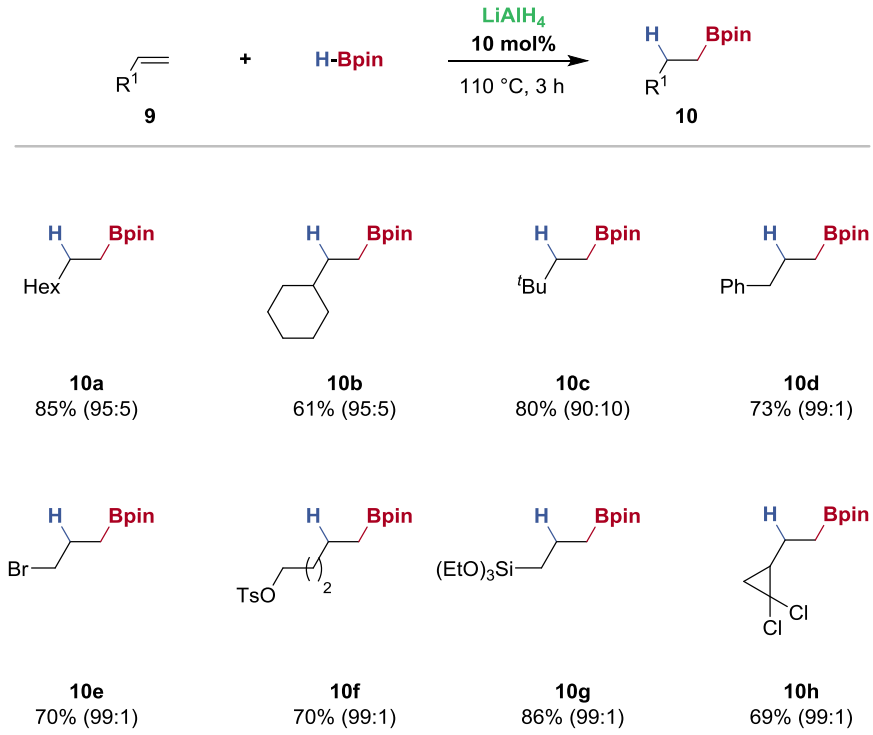

Scheme 3.2. Substrate scope. Isolated yield using $LiAlH_4$ (10 mol%), neat, 3 h, 110 °C; ratios in parentheses report the distribution of regioisomers (linear/branched).

The hydroboration of 1,1-dichloro-2-vinylcyclopropane (**9h**) and of allyl bromide (**9e**) proceeded without the observation of protodehalogenation or cyclopropyl ring-opening; in contrast to methods using stoichiometric $LiAlH_4$ (Scheme 3.3).[20],[21]

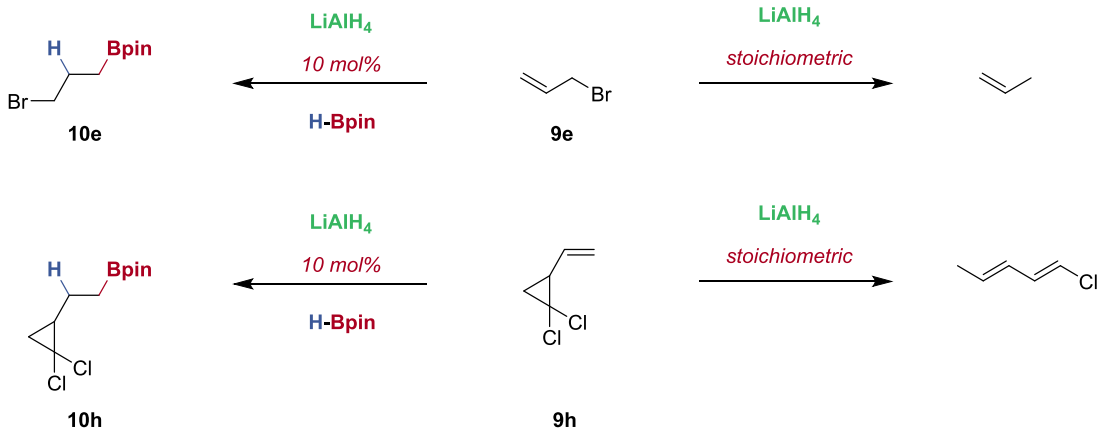

Scheme 3.3. Divergent reactivity of alkenes **9e** and **9h** with $LiAlH_4$.

Once the efficiency of the protocol was demonstrated on terminal alkyl alkenes, a series of substituted aryl alkenes were tested (Scheme 3.4). Styrene derivatives bearing both electron-withdrawing and electron-donating functionalities (**10j-10p**) all gave good yields and regioselectivities for the formation of alkyl boronic esters, demonstrating a negligible electronic effect on product formation. No protodeborylation was observed. Increasing the steric demands of the styrene derivatives (**10q-10s**) also showed a negligible effect on hydroboration yield, even with 2,4,6-trimethyl styrene (**10r**) undergoing successful hydroboration.

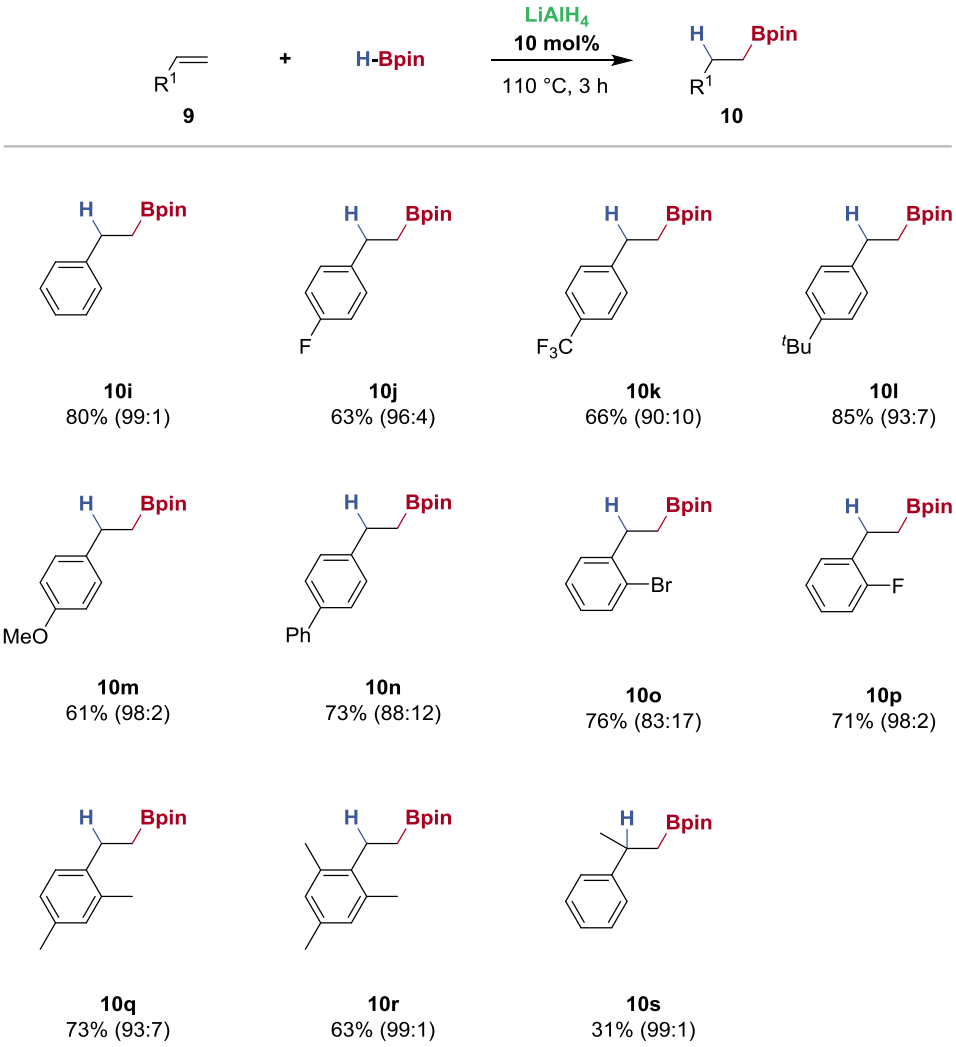

Scheme 3.4. Substrate scope. Isolated yield using $LiAlH_4$ (10 mol%), neat, 3 h, 110 °C; ratios in parentheses report the distribution of regioisomers (linear/branched).

This method is the first example reported of aluminium-catalysed hydroboration of alkenes. Notably, in comparison to previous method for aluminium-catalysed hydroboration of alkynes (see chapter 2),[22] a better group tolerance was observed which, in combination with simplicity of the protocol, give it broad interest for the synthesis of boronic esters.

Unfortunately, no internal alkene underwent successful hydroboration (Scheme 3.5). As expected the hydroalumination of these substrates is more challenging and usually requires the addition of a transition-metal-catalyst such as zirconium or titanium.[23],[24] The selective hydroboration of alkenes in the presence of functional groups containing potentially reducible carbon-heteroatom multiple bonds such as ketone was not possible, with hydroboration leading to a complex mixture of products with no evidence of chemoselective hydroboration at either functionality (Scheme 3.5).

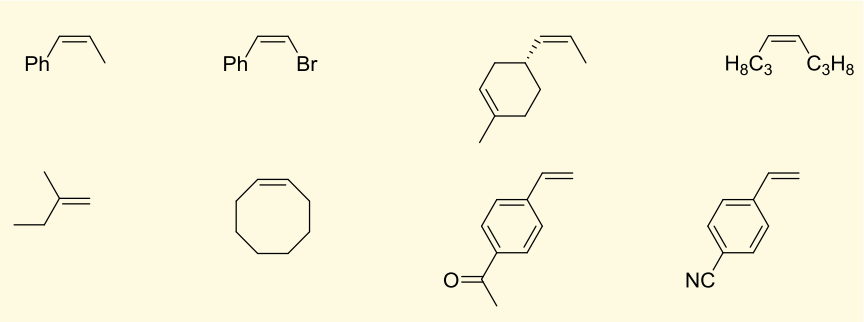

Scheme 3.5. Unsuccessful substrates.

3.4 Hydroboration of polar bonds

To further demonstrate the applicability of this hydroboration protocol, and given evidence of the hydroboration of polar bonds during substrate scope investigations, the aluminium-catalysed hydroboration protocol was applied to polar functionalities. This also provides a direct comparison to previously reported main-group systems. Here, the rate of hydroboration would need to significantly outcompete the background rate of the direct reduction of the polar bond. Hydroboration of acetophenone was successfully promoted by $LiAlH_4$ (0.5 mol%) at room temperature in only 30 minutes, with an 81% isolated yield of the alkoxy boronic ester (Scheme 3.6). This catalytic activity is, to the

best of our knowledge, the highest for the aluminum-catalysed hydroboration of a ketone[25],[26] with a TON >162.

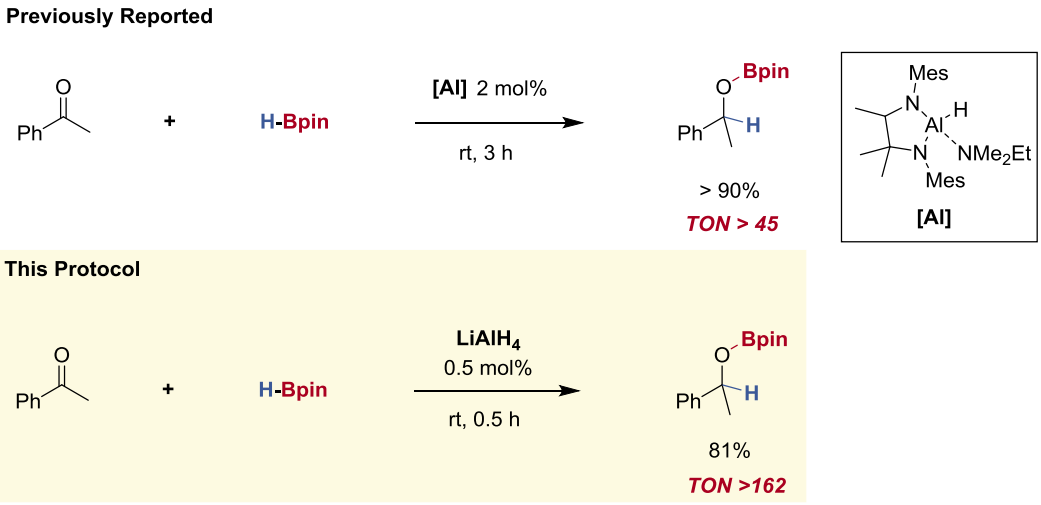

Scheme 3.6. Hydroboration of acetophenone.

The same protocol was then applied to the hydroboration of less electrophilic ester group. Again, using 0.5 mol% of $LiAlH_4$, ethyl acetate underwent successful hydroboration to the boronic ester in 79% yield in 8 hours at room temperature (Scheme 3.7).[27]

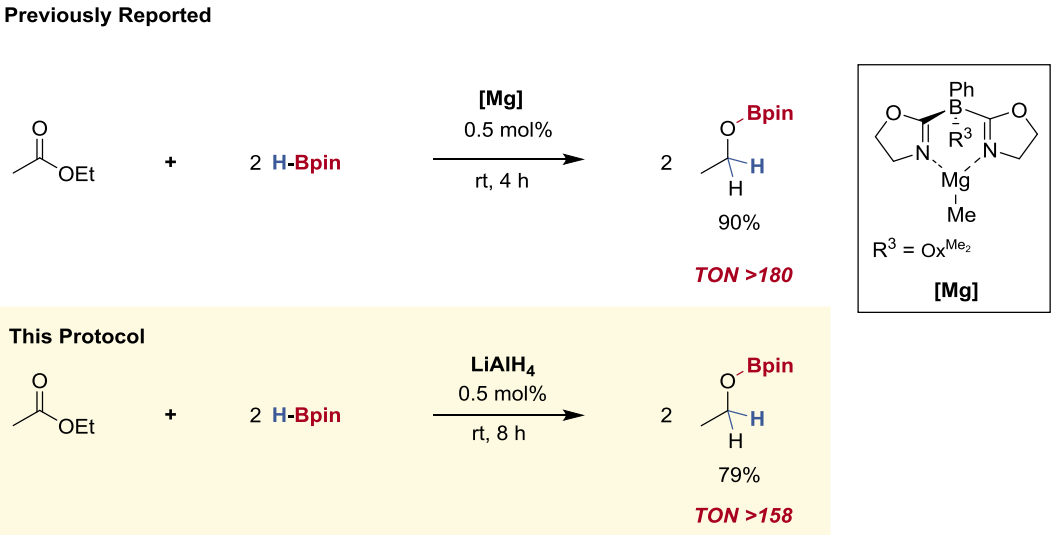

Scheme 3.7. Hydroboration of ethyl acetate.

With the hydroboration of C-O multiple bonds demonstrated, the nitrile motif was then investigated. Here a stronger triple bond would need to be reduced and the intermediate aluminium-nitrogen bond turned over. Using 4-trifluoromethylbenzonitrile as a model substrate, $LiAlH_4$ (1 mol%) succesfully catalysed the hydroboration of the nitrile in 6 hours at room temperature to give the amido boronic ester in 71% isolated yield (Scheme 3.8); showing catalyst activity comparable to transition metals[28] and exceeding the single example for main-group species previously reported.[29],[30] Hence, this protocol has potential for further reductive transformations of polar compounds.

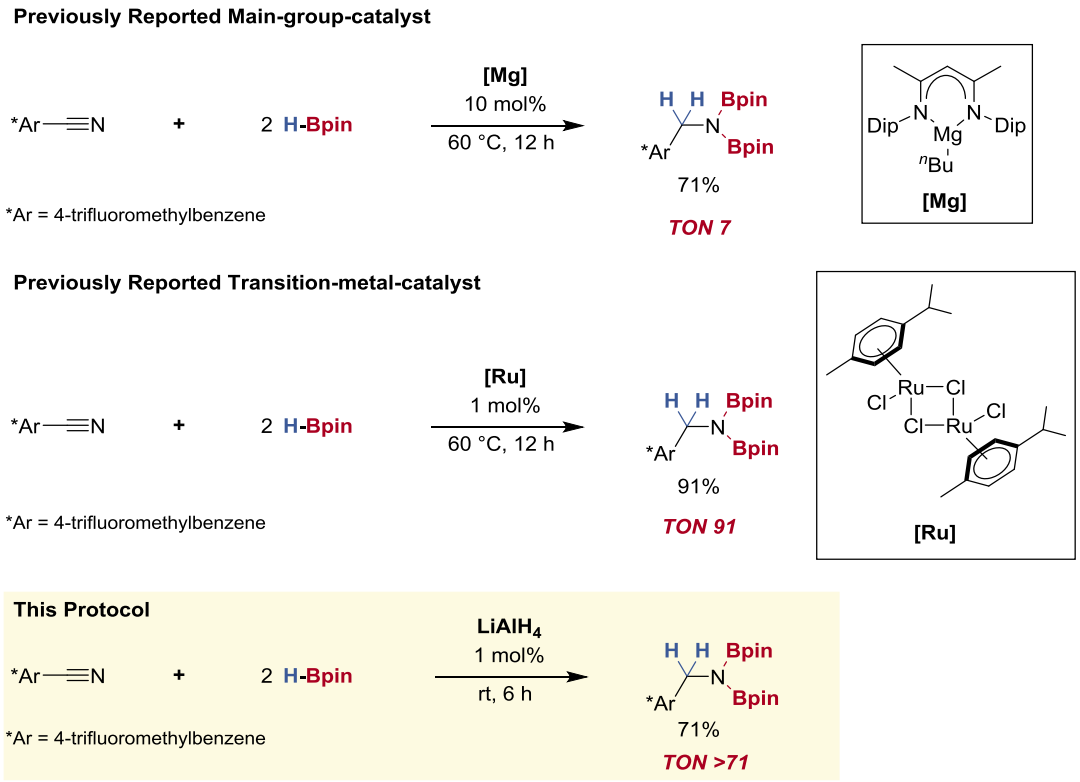

Scheme 3.8. Hydroboration of 4-(trifluorometyl)benzonitrile.

This protocol was also applied to chemoselective the hydroboration of a steroid, 16-dehydropregnenolone acetate, bearing an alkene, an ester and a ketone group (Scheme 3.9). In contrast to the reaction with stoichiometric $LiAlH_4$, which showed no selectivity among the unsaturated bonds, the catalytic hydroboration was chemoselective for

reaction at the ketone to give the secondary alcohol in 63% isolated yield, after SiO_2-mediated hydrolysis.

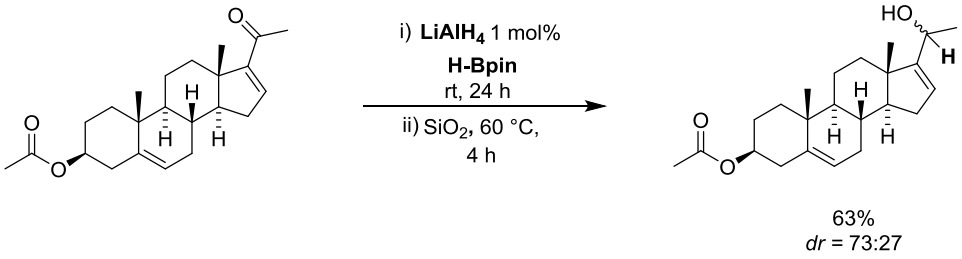

Scheme 3.9. Hydroboration of 16-pregnanolone-acetate.

3.5 Mechanistic studies

During our mechanistic investigation, a nucleophile-initiated hydroboration of unsaturated bonds was reported.[31] Zhao and co-workers used NaOH (5-10 mol%) to promote the hydroboration of aldehydes, ketones, imines, terminal alkynes, and terminal alkenes. Although this protocol is very efficient for the hydroboration of polar bonds, there were limited examples of alkene and alkyne substrates. Mechanistic investigations were attempted using stoichiometric sodium hydroxide and pinacol borane, however, the formation of an insoluble precipitate resulted in no significant information about the reaction mechanism. It was postulated that the reaction could lead to borohydride formation which could serve as an active hydride source. Carrying out the reaction using *B*-H-9-BBN dimer confirmed formation of a borohydride species which was isolated by addition of 15-crown-5 aid crystal grown. The latter was then used to further investigate the mechanism of the hydroboration of aldehydes, but without further analysis of the mechanism of hydroboration of carbon-carbon unsaturated bonds (see chapter 1, for further details). Inspired by this work, different main-group metal hydride species under our reaction conditions were investigated. LiH- and NaH-catalysed the hydroboration of styrene with moderate yields (41% and 45%, respectively, Scheme 3.10) with only a minor improvement observed upon increasing the catalyst loading to 20 mol% (43% and 48%, respectively). Although both LiH and NaH were active catalysts, the decreased yields using these hydride reagents together with the high activity demonstrated by

$Me_3N{\cdot}AlH_3$ (Scheme 3.10), suggests a catalytic role for aluminium beyond simple hydride delivery.

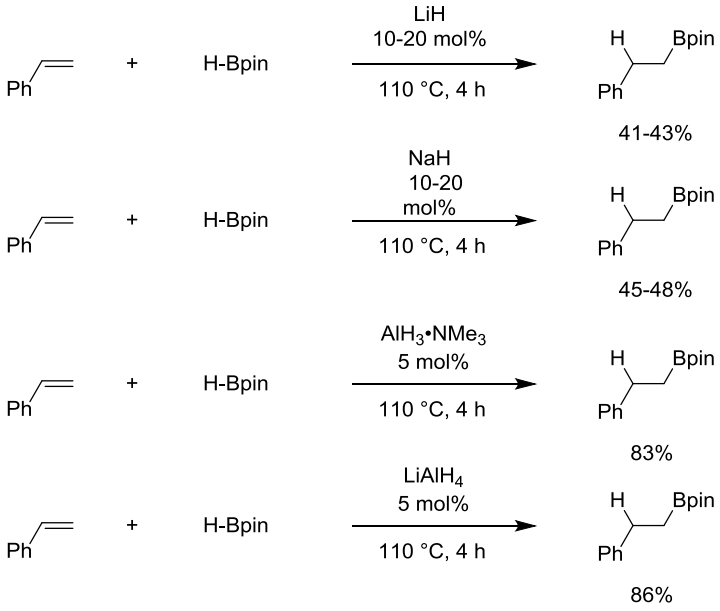

Scheme 3.10. Hydroboration of styrene using different metal-hydride species as catalysts.

Based on the precedent established for aluminium-catalysed hydroboration of alkynes, we hypothesised that this reaction may occur following a similar mechanism; alane generation, hydroalumination and σ-bond metathesis between the alkyl-aluminum and H-Bpin to form the boronic ester and regenerate the alane catalyst (see chapter 2, 2.4 Mechanistic Studies). However, the mechanistic investigation was made more challenging by the solvent-free conditions. In order to gain insight into the mechanism of the alkene hydroboration with HBpin a series of stoichiometric reaction were undertaken (Scheme 3.11). Initially, the reaction between $^{i}Bu_2Al$-H and HBpin was investigated. As with trialkyl aluminium species, the reaction showed formation of ^{i}BuBpin (δ ^{11}B = 33.3) confirming that substituent scrambling occurs, even in the presence of a hydride (Figure 3.2). The addition of pinacol borane to a solution of Red-Al displayed immediate formation of HBpin decomposition products such as B_2pin_3 (δ ^{11}B = 23.3, s) and $NaBH_4$ (δ ^{11}B = –42.3, q). This is not unexpected as metal-hydrides have been reported to reduce alkoxy borate species to the corresponding borane.[32],[33]

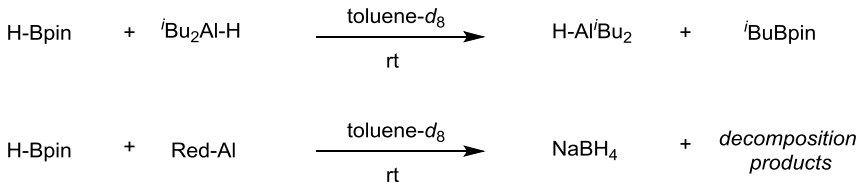

Scheme 3.11. Stoichiometric reaction of aluminium hydrides and HBpin.

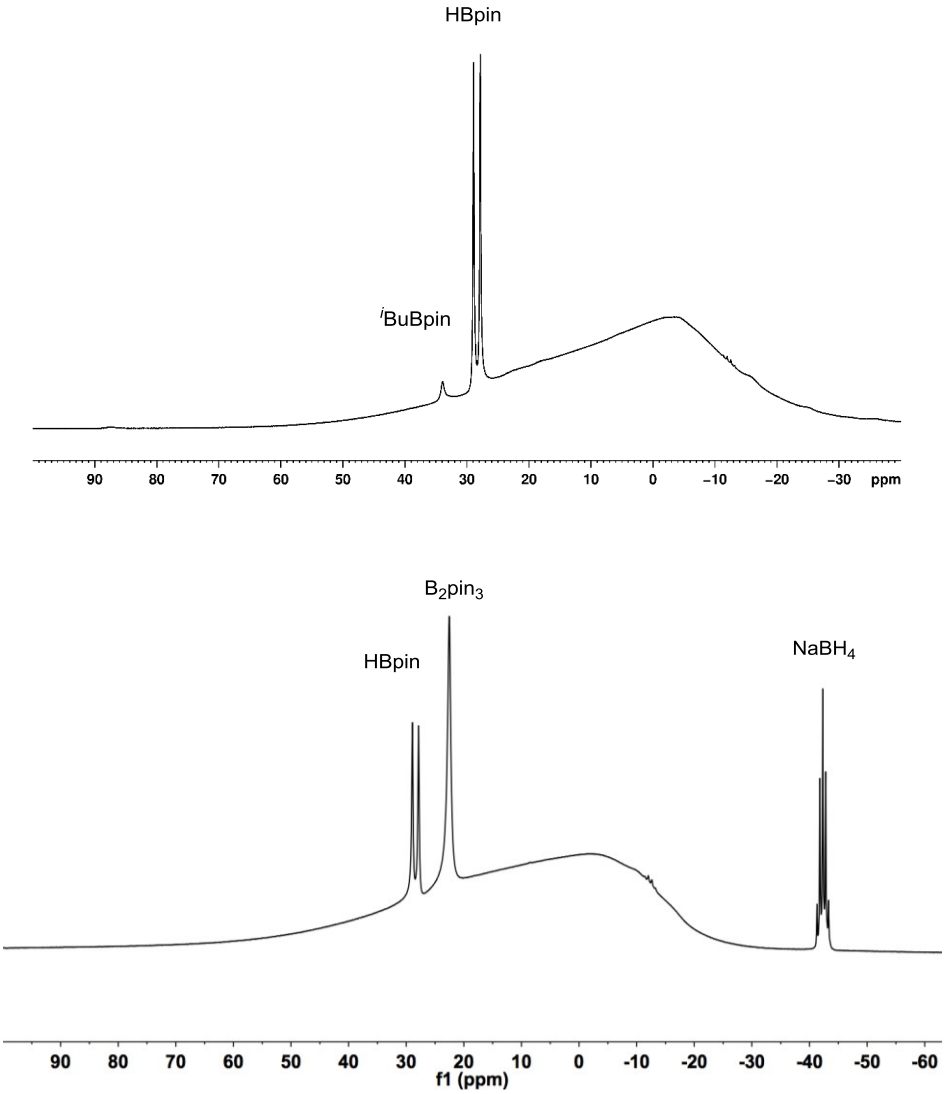

Figure 3.2. ^{11}B NMR spectra. *Top spectrum*: reaction of $^{i}Bu_2Al$-H and HBpin; *bottom spectrum*: reaction of Red-Al and HBpin of the reaction.

Once again, the most likely pathway to activate the substrate seemed to be through hydroalumination. In order to isolate the product of this reaction, different conditions were screened for the hydroalumintion of alkenes using Red-Al or $LiAlH_4$ as a model aluminium hydride species. Treating styrene with a stoichiometric amount of Red-Al or $LiAlH_4$ proved unsuccessful, with the reaction leading to a complex mixture of products regardless of the temperature or the aluminium species used (Scheme 3.12). Anionic aluminium species have been reported to promote styrene polymerisation which hampers the attempts to isolate any hydroalumination product. Therefore, $^{i}Bu_2Al$-H was used as a model aluminium species to seek mechanistic understanding. The hydroalumination of styrene by $^{i}Bu_2Al$-H gave in some product formation, but all attempts to isolate the product from the reaction mixture failed.

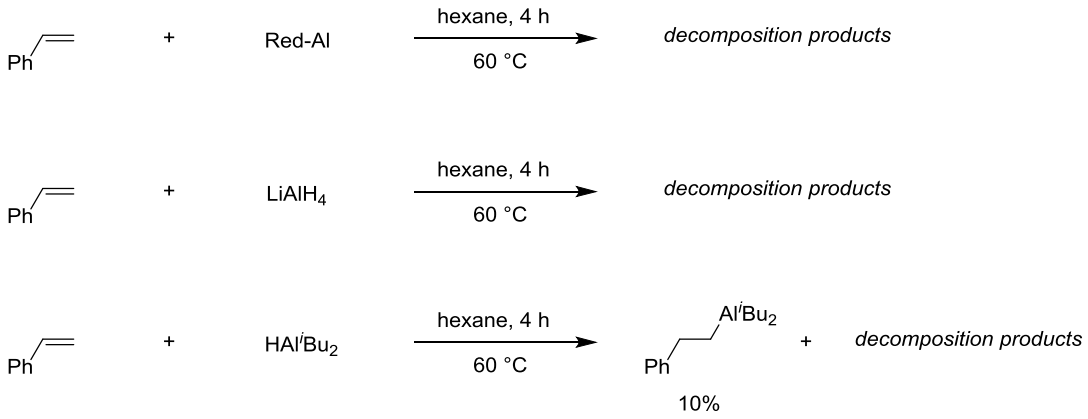

Scheme 3.12. Hydroalumination of styrene using Red-Al, $LiAlH_4$ and $^{i}Bu_2Al$-H.

Using $^{i}Bu_2Al$-H in a stoichiometric reaction with 3,3-dimethyl-1-butene gave the corresponding alkyl aluminium species (**11**) in 66% isolated yield within 4 hours at 60 °C (Scheme 3.13). Product formation was confirmed by ^{1}H NMR and $^{13}C\{H\}$ NMR showing diagnostic proton Al-CH_2R and carbon resonances Al-CH$_2$R (δ ^{1}H NMR = 0.48, m; 0.31, d); (δ ^{13}C NMR = 24.8, br s; 5.6, br s) (Figure 3.3). This species was isolated in 66% yield as a viscous liquid and was fully characterised by 1D and 2D NMR and high-resolution mass spectrometry.

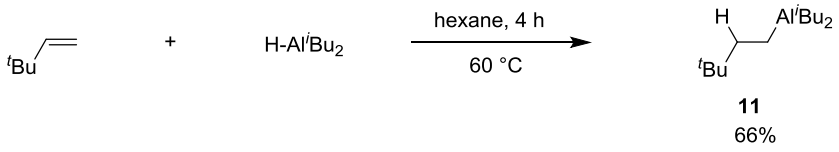

Scheme 3.13. Hydroalumination of 3,3-dimethyl-1-butene using $^{i}Bu_2Al$-H.

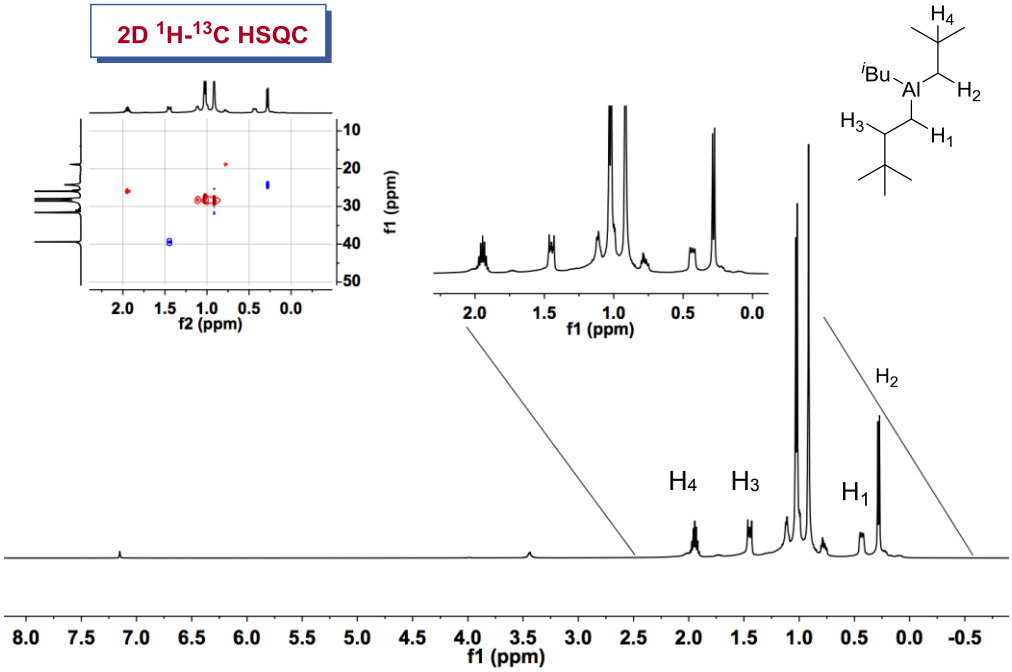

Figure 3.3. ^{1}H NMR (500 MHz, C_6D_6) of the alkyl aluminium (**11**) and HSQC ^{1}H-^{13}C NMR (C_6D_6) blue cross peak = CH_2, red cross peak = CH, CH_3.

Treatment of alkyl aluminium species (**11**) with HBpin immediately gave the alkyl boronic ester (**10b**) (Scheme 3.14), with concurrent formation of trialkyl borane species (i.e. $^{i}Bu_3B$). Although, under these conditions, the exchange behaviour of alanes (AlX_3) and boranes (BY_3) generates mixtures of the 'scrambled' alanes and boranes (e.g. AlX_nY_{3-n}, BY_nX_{3-n}),[34] this suggests that the crucial C-B bond-forming step occurs with concomitant Al-H regeneration (Figure 3.4).

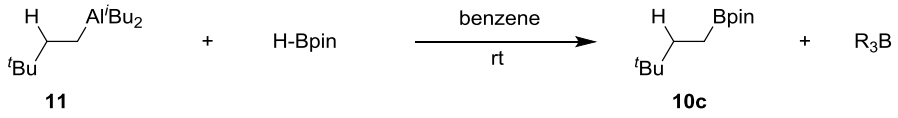

Scheme 3.14. Reaction of the alkenyl aluminium (**11**) and HBpin.

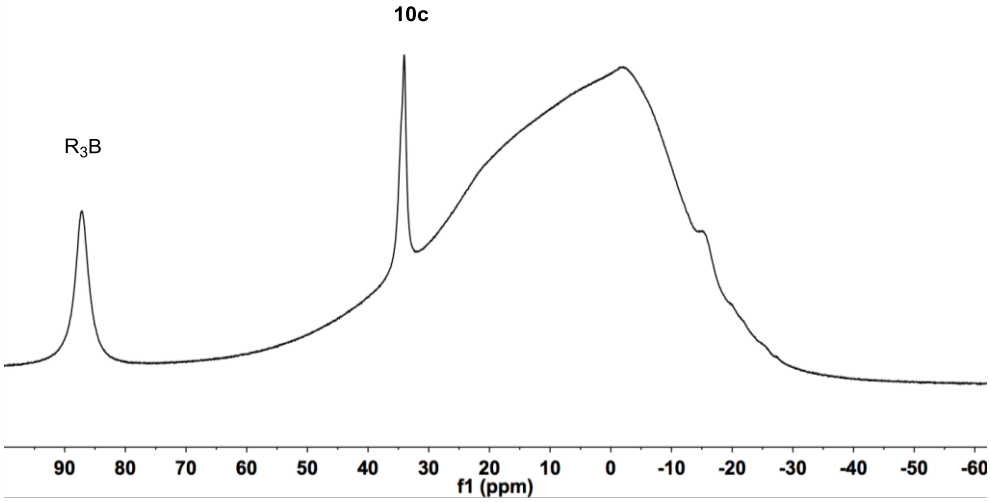

Figure 3.4. ^{11}B NMR spectrum of reaction of the alkenyl aluminium (**11**) and HBpin.

The catalytic activity of the trialkyl aluminium intermediate was also confirmed using $AlEt_3$ (10 mol%), as a surrogate of alane (**11**), under the optimised conditions to give the boronic ester (**10i**) in 75% yield (Scheme 3.15).

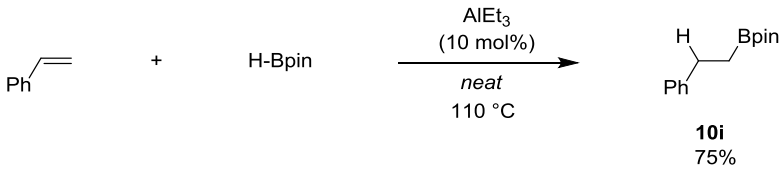

Scheme 3.15. Catalytic competence of $AlEt_3$.

Based on these experiments, the following catalytic cycle is proposed whereby the alkene undergoes hydroalumination followed by σ-bond metathesis of the alkyl aluminium species with pinacol borane (aluminium-boron exchange) (Scheme 3.16). This step releases the alkyl boronic ester product and regenerates the alane catalyst. However, these experiments do not account for reactivity using an aluminate precatalyst. Presumably here, reaction of the aluminate with HBpin generates a neutral aluminium species capable of entering the catalytic cycle.

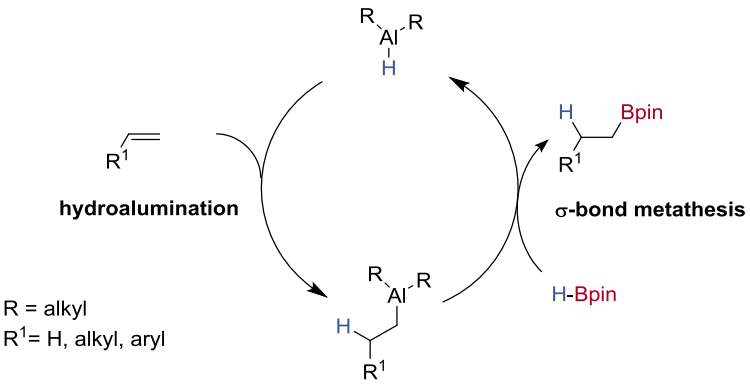

Scheme 3.16. Proposed catalytic cycle for aluminium-catalysed hydroboration of alkenes.

However, the stoichiometric reactions of pinacol borane and the aluminium species have often shown formation of borohydride or borane species. In order to clarify their catalytic activity $THF{\cdot}BH_3$ and $NaBH_4$ were tested for the hydroboration of styrene under our optimised conditions.[35] Surprisingly, both showed competence in this transformation with particularly good yield observed when borane was used as the catalyst (Scheme 3.17).

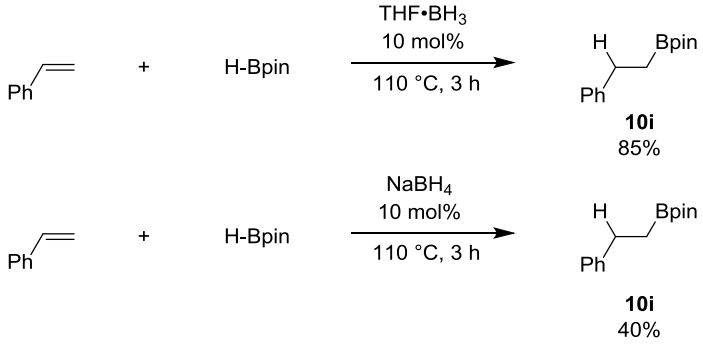

Scheme 3.17. Catalytic competence of $THF{\cdot}BH_3$ and $NaBH_4$ in the hydroboration of styrene.

In addition to its competence in catalysis, the formation of a borane species may have a further repercussion on the reaction mechanism. In fact, in 1995, Yamamoto reported that boranes and boronic acids are able to catalyse the hydroalumination of alkenes.[36] Several olefins underwent successful hydroalumination and further functionalised with different electrophiles using $LiAlH_4$ or $^{i}Bu_2Al$-H in the presence of either 10 mol% of $PhB(OH)_2$ acid or Et_3B (Scheme 3.18). In the absence of a borane catalyst, the rate of formation of hydroalumination product was much slower and, in some cases resulted in

only trace amounts of product. To this end the role of these species requires further investigations and thus any participation of borane or borohydride species in the catalysis cannot be ruled out.

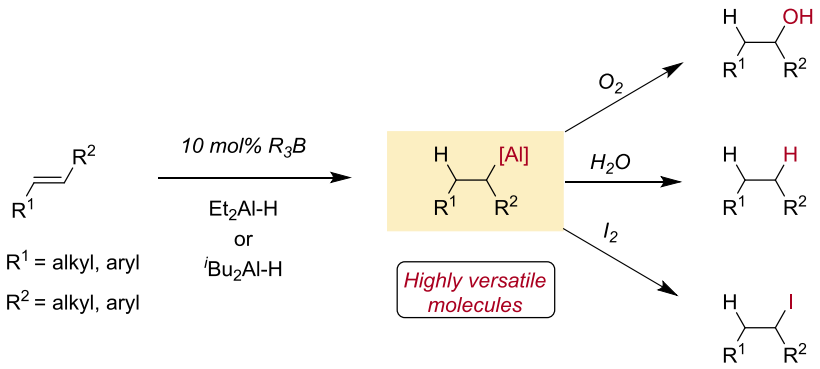

Scheme 3.18. Borane-catalysed hydroalumination.

In order to clarify whether this could be the case for the hydroboration of polar bonds THF·BH_3 and $NaBH_4$ were also tested as catalysts under the same reaction conditions. Attempting the hydroboration of acetophenone using 0.5 mol% of THF·BH_3 complex gave resulted in only a trace amount of product even when the catalyst loading was increased to 5 mol%. In contrast, sodium borohydride successfully promoted this transformation, but with significantly lower catalyst activity than the aluminium catalysts (Scheme 3.19).

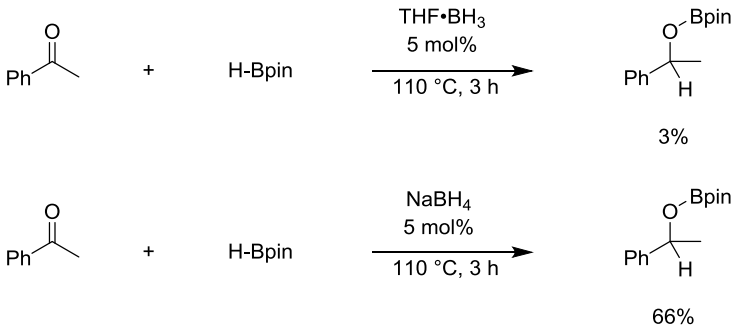

Scheme 3.19. Catalytic competence of THF·BH_3 and $NaBH_4$ in the hydroboration of acetophenone.

It was therefore possible to exclude any contribution of these species in the hydroboration of ketones. A possible mechanism for this transformation is reported

(Scheme 3.20). Once again substrate activation is provided by hydroalumination which upon treatment with pinacol borane releases the product and regenerates the catalyst. Notably, as computational investigation studies have supported, the activation energy barrier of hydroalumination and the σ-bond metathesis step are much lower (6.8 kcal mol^{-1}, 4.4 kcal mol^{-1}) compared to those for alkenes.[37] Additionally several experimental studies have reported the stoichiometric reduction of unsaturated polar bonds to be viable even at very low temperature allowing this transformation to be carried out in asymmetric fashion.[38],[39] All of this allowed the catalytic hydroboration of polar bonds to be carried out with a lower catalyst loading and at room temperature.

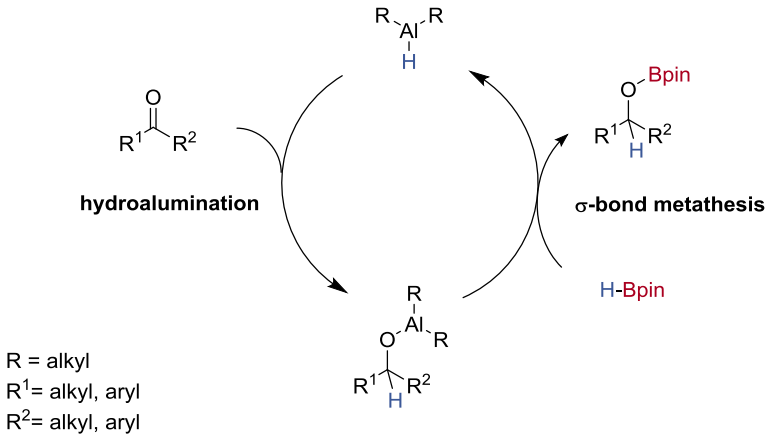

Scheme 3.20. Proposed mechanism for aluminium-catalysed hydroboration of ketones.

3.6 Conclusions and Future work

In conclusion, an operationally simple and environmentally benign formal hydroboration protocol has been developed (Scheme 3.21). This reaction has been successfully applied to the reduction of a variety of terminal alkenes bearing a range of functional groups. Both aryl and alkyl-olefins have been shown to undergo hydroboration under the developed reaction conditions in good yield and with good functional group tolerance. The same protocol was also successfully applied to the hydroboration of polar bonds including ketone, ester and nitrile functionalities and showed catalytic activity comparable to transition metal catalysts.

Hydroalumination and Al-B exchange reactions were used to provide a simple and economical synthesis of alkyl boronic esters using commercially available aluminate salts as catalysts. Mechanistic studies are consistent with an aluminium-hydride-catalysed hydroboration proceeding by initial hydroalumination, followed by σ-bond metathesis to exchange aluminum and boron, and regenerate the aluminium hydride.

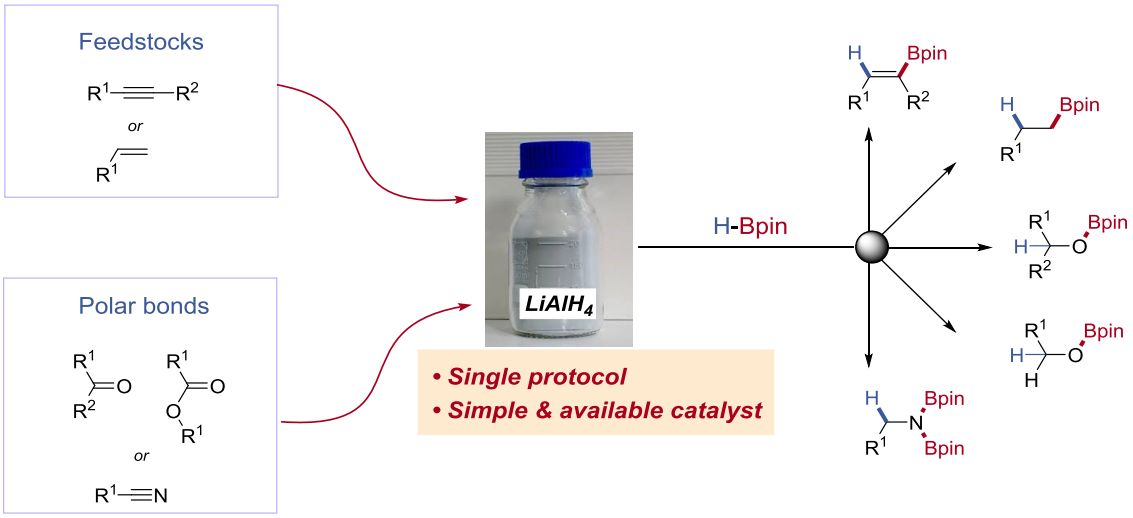

Scheme 3.21. Aluminium-catalysed hydroboration.

However, any mechanism involving borohydride or borane species as part of the catalysis for the hydroboration of alkenes cannot be ruled out.

Although this concept was demonstrated through catalytic hydroboration, we believe it will readily transfer to diverse hydrofunctionalisation chemistry, thus unleashing a wave of new, aluminium-catalysed processes.

This work has been published in ACS Catalysis (*ACS Catal*., 2018, **8**, 2001–2005, 10.1021/acscatal.7b04279, see Appendix 1).

3.7 References

[1] D. A. Evans and G. C. Fu, *J. Org. Chem.*, 1990, **55**, 2280–2282.

[2] K. Burgess and M. J. Ohlmeyer, *Chem. Rev.*, 1991, **91**, 1179–1191.

[3] J. Cipot, C. M. Vogels, R. McDonald, S. A. Westcott and M. Stradiotto, *Organometallics*, 2006, **25**, 5965–5968.

[4] J. V. Obligacion and P. J. Chirik, *Org. Lett.*, 2013, **15**, 2680–2683.

[5] J. V. Obligacion and P. J. Chirik, *Nat. Rev. Chem.*, 2018, **2**, 15–34.

[6] C. W. Liskey and J. F. Hartwig, *J. Am. Chem. Soc.*, 2012, **134**, 12422–12425.

[7] A. P. Pulis, D. J. Blair, E. Torres and V. K. Aggarwal, *J. Am. Chem. Soc.*, 2013, **135**, 16054–16057.

[8] Q. Li, C. W. Liskey and J. F. Hartwig, *J. Am. Chem. Soc.*, 2014, **136**, 8755–8765.

[9] C. Sandford and V. K. Aggarwal, *Chem. Commun.*, 2017, **53**, 5481–5494.

[10] A. Prokofjevs, A. Boussonnière, L. Li, H. Bonin, E. Lacôte, D. P. Curran and E. Vedejs, *J. Am. Chem. Soc.*, 2012, **134**, 12281–12288.

[11] Q. Yin, S. Kemper, H. F. T. Klare and M. Oestreich, *Chem. - A Eur. J.*, 2016, **22**, 13840–13844.

[12] K. Fagnou and M. Lautens, *Chem. Rev.*, 2003, **103**, 169–196.

[13] I. a I. Mkhalid, J. H. Barnard, T. B. Marder, J. M. Murphy and J. F. Hartwig, *Chem. Rev.*, 2009, **110**, 890–931.

[14] G. Cahiez and A. Moyeux, *Chem. Rev.*, 2010, **110**, 1435–1462.

[15] J. R. Dunetz, D. Fandrick and H.-J. Federsel, *Org. Process Res. Dev.*, 2015, **19**, 1325–1326.

[16] Z. Yang, M. Zhong, X. Ma, K. Nijesh, S. De, P. Parameswaran and H. W. Roesky, *J. Am. Chem. Soc.*, 2016, **138**, 2548–2551.

[17] A. Bismuto, S. P. Thomas and M. J. Cowley, *Angew. Chem. Int. Ed.*, 2016, **55**, 15356–15359.

[18] G. Zweifel and R. B. Steele, *J. Am. Chem. Soc.*, 1967, **89**, 5085–5086.

[19] E. V Gorobets, O. V Shitikova, S. L. Lomakina, G. A. Tolstikov and A. V Kuchin, *Russ. Chem. Bull.*, 1993, **42**, 1573–1578.

[20] C. W. Jefford, D. Kirkpatrick and F. Delay, *J. Am. Chem. Soc.*, 1972, **94**, 8905–8907.

[21] A. L. J. Beckwith and S. H. Goh, *J. Chem. Soc., Chem. Commun.*, 1983, **1**, 907.

[22] Z. Yang, M. Zhong, X. Ma, K. Nijesh, S. De, P. Parameswaran and H. W. Roesky, *J. Am. Chem. Soc.*, 2016, **138**, 2548–2551.

[23] S. Nagahara, K. Maruoka, H. Yamamoto, *Bull. Chem. Soc. Jpn.*, 1993, **66**, 3783–3789.

[24] R. I. Khusnutdinov, A. R. Bayguzina and U. M. Dzhemilev, *Russ. Chem. Rev.*, 2000, **69**, 134–149.

[25] Z. Yang, M. Zhong, X. Ma, S. De, C. Anusha, P. Parameswaran and H. W. Roesky, *Angew. Chem. Int. Ed.*, 2015, **54**, 10225–10229.

[26] V. K. Jakhar, M. K. Barman and S. Nembenna, *Org. Lett.*, 2016, **18**, 4710–4713.

[27] D. Mukherjee, A. Ellern and A. D. Sadow, *Chem. Sci.*, 2014, **5**, 959.

[28] A. Kaithal, B. Chatterjee and C. Gunanathan, *J. Org. Chem.*, 2016, **81**, 11153–11163.

[29] C. Weetman, M. D. Anker, M. Arrowsmith, M. S. Hill, G. Kociok-Köhn, D. J. Liptrot and M. F. Mahon, *Chem. Sci.*, 2016, **7**, 628–641.

[30] C. C. Chong and R. Kinjo, *ACS Catal.*, 2015, **5**, 3238–3259.

[31] Y. Wu, C. Shan, J. Ying, J. Su, J. Zhu, L. L. Liu and Y. Zhao, *Green Chem.*, 2017, **19**, 4169–4175.

[32] H. I. Schlesinger, H. C. Brown and A. E. Finholt, *J. Am. Chem. Soc.*, 1953, **75**, 205–209.

[33] H. I. Schlesinger, H. C. Brown and E. K. Hyde, *J. Am. Chem. Soc.*, 1953, **75**, 209–213.

[34] J. Klosin, G. R. Roof, E. Y. X. Chen and K. A. Abboud, *Organometallics*, 2000, **19**, 4684–4686.

[35] N. W. J. Ang, C. S. Buettner, S. Docherty, A. Bismuto, J. R. Carney, J. H. Docherty, M. J. Cowley and S. P. Thomas, *Synth.*, 2018, **50**, 803–808.

[36] K. Maruoka, H. Sano, K. Shinoda, S. Nakai and H. Yamamoto, *J. Am. Chem. Soc.*, 1986, **108**, 6036–6038.

[37] J. W. Bundens and M. M. Francl, *Organometallics*, 1993, **12**, 1608–1615.

[38] R. Noyori, I. Tomino, M. Yamada and M. Nishizawa, *J. Am. Chem. Soc.*, 1984, **106**, 6717–6725.

[39] R. Noyori, I. Tomino, Y. Tanimoto and M. Nishizawa, *J. Am. Chem. Soc.*, 1984, **106**, 6709–6716.

Chapter 4− Lewis acidic boron compounds

The Lewis acidity of boron trihalides BX_3 (X = F, Cl, Br) is well-known in both inorganic and organic chemistry. However, the low boiling point of these compounds and moisture sensitivity of the B-X bond have limited their use. In order to increase the stability of these compounds a change in the substituents was required. Perfluoro organo-substituents offer a similar electron-withdrawing nature to that of the parent halo compounds, but the presence of a carbon atom generates a less moisture sensitive and a boron compound $B(RF)_3$ with a higher boiling point. In 1963 Massey and co-workers reported the synthesis and the characterisation of tris(pentafluorophenyl)borane $B(C_6F_5)_3$[1] and analysed its electrophilic nature in the presence of phospino- or amino-donor. Despite the strong Lewis acidic properties, the peculiar steric hindrance, and the great potential of this compound it took almost twenty years to be widely exploited.[2]
The versatility of $B(C_6F_5)_3$ and its parent compounds has been widely demonstrated in organic synthesis, in catalysis and with the activation of small molecules through the development of Frustrated Lewis Pairs (FLPs) (Scheme 4.1).[2]–[6]

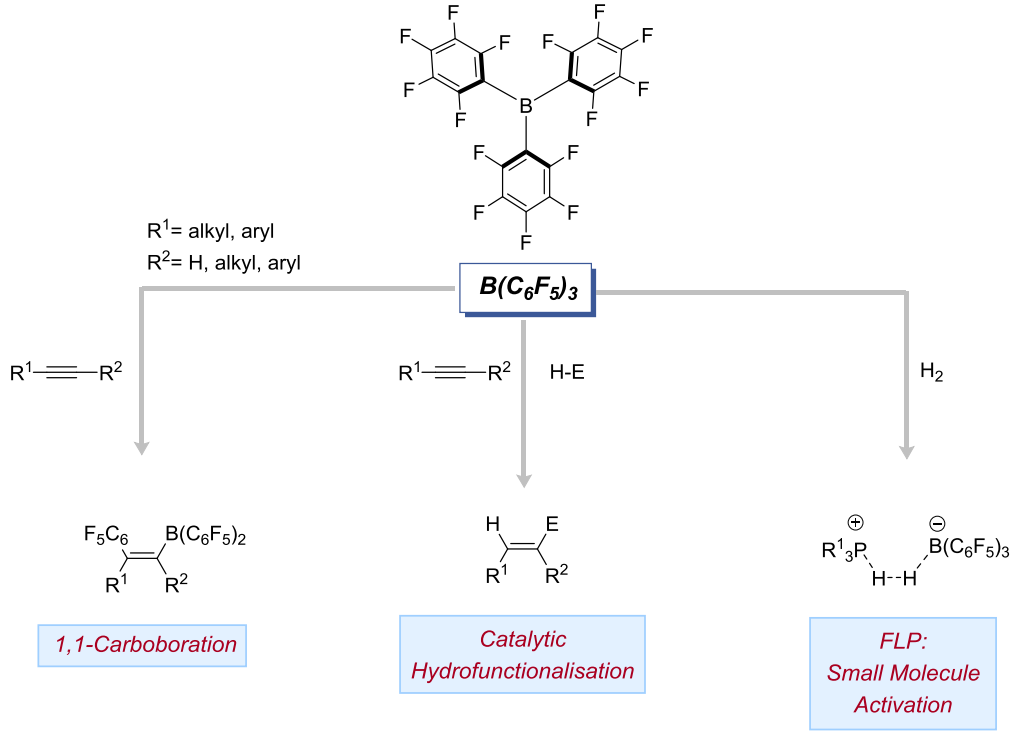

Scheme 4.1 The versatility of $B(C_6F_5)_3$.

4.1 1,1-Carboboration using $B(C_6F_5)_3$

The ligand exchange behaviour of Group 13 elements has been widely described in the previous chapter (Chapter 2, 2.4 Mechanistic studies). One of the first applications of tris(pentafluorophenyl)borane was, in fact, as a C_6F_5-transfer agent for the synthesis of the first Xenon-carbon bond, $[XeC_6F_5]^+$. During the following years, the reactivity was further explored, with the use of this reagent in the 1,1-carboboration of alkynes.

The 1,1-Carboboration of alkynes is a well-established method for the preparation of alkenyl boronic esters.[7] Pioneering work was reported by Wrackmeyer and co-workers who found that trimethylstannyl acetylenes react rapidly with triethylborane to give the tetra-substituted alkenylboranes (Scheme 4.2).[8] The reaction is proposed to proceed by formation of an alkenyl borate (**12**) through abstraction of the trimethyltin-substituent and subsequent rearrangement to give the 1,1-carboboration product (**13**). Initially, it was thought that the presence of metal substituents at the alkyne was required to favour 1,2-migration of the boron substituent.

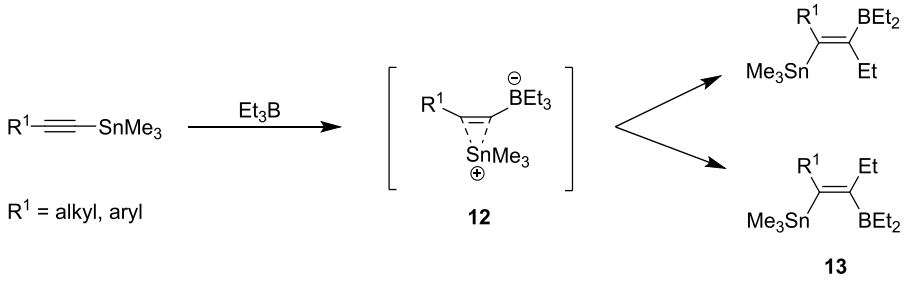

Scheme 4.2. 1,1-Carboboration of alkynyl stannate.

Further investigation revealed that the group transfer could be facilitated by increasing the Lewis acidity of the borane species. To this end, trispentafluorophenyl borane and related R-$B(C_6F_5)_2$ were explored. Erker and co-workers extended the scope of this transformation to internal and terminal unactivated alkynes.[9]–[11] Reacting phenyl acetylene and $B(C_6F_5)_3$ at room temperature in pentane the 1,1-carboboration product as a mixture ((*E*)-and (*Z*)-alkenyl borane 10:1) in 2 hours by 1,2-hydrogen migration and C_6F_5 transfer from boron to carbon to give the 1,1-carboboration product (Scheme 4.3).

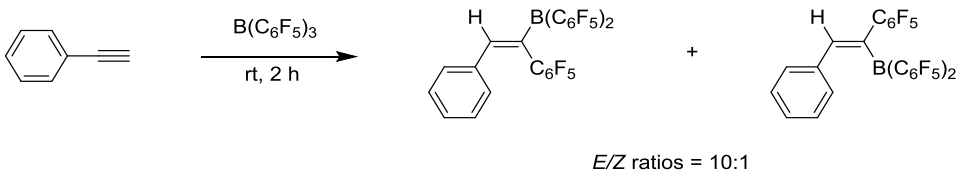

Scheme 4.3. 1,1-Carboboration of phenylacetylene.

Stoichiometric investigations were hampered by the fast rate of reaction of $B(C_6F_5)_3$ with PhC≡CH, which made isolation or observation of trace intermediates very challenging. The 1,1-carboboration reaction of alkynes was analysed using DFT calculations by Berke and Erker.[12],[13] All the studies were performed at the RI-TPPS-D/def2-TZVP level using the COSMO solvation model for CH_2Cl_2 as no minimum or stable species was found in the gas phase. The reaction was proposed to occur *via* initial activation of the alkyne (**14**) (π-adduct) which evolves to a transient zwitterion (**15**) (σ-adduct). The formation of the σ-type adduct (**15**) is slightly endothermic (7.1 kcal/mol) compared to the starting materials (Scheme 4.4). This is proposed to rearrange by a hydrogen-bridged transition state (**16**) to form a vinylidene fragment (**17**) which was proposed to be the rate-determining step. Migration of the C_6F_5 group leads to the formation of the alkenyl borane product. In both of the analysed cases (R^1 = H, ^{n}Bu) the DFT optimisation processes to establish vinylidene adducts (**17**) did not converge to a definite local minimum structure, but a very flat potential-energy surface (PES) was encountered. Formation of the vinylidene species is still considered the most likely pathway to the 1,1-(*E*)- and 1,1-(*Z*) carboboration products. Formation of these species is thermodynamically favoured due to the low energies (−42.5 *vs* −41.1 kcal/mol, respectively) compared to the energy of free $B(C_6F_5)_3$ and acetylene.

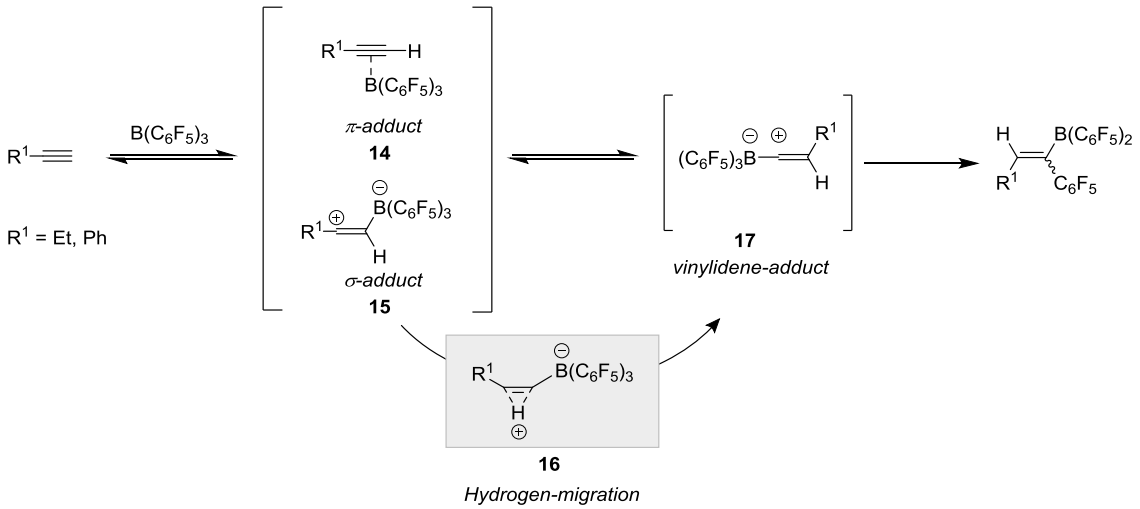

Scheme 4.4. Mechanism of 1,1-carboboration of alkynes.

As no experimental evidence of the zwitterion was reported, the reaction was further investigated in the presence of a phosphine or an amine donor to trap any potential intermediate. Pioneering work by Stephan and co-workers described the reactivity of a tris(pentafluorophenyl)borane/phosphine FLP system towards terminal alkynes.[14] It was found that the presence of the base hampers the 1,1-carboboration process leading instead to either a 1,2-addition to form the zwitterionic alkenyl phosphonium borate (**18**) or to form the alkynyl borate salt (**19**) (Scheme 4.5). In all cases, the addition of phenyl acetylene to a solution of phospine-$B(C_6F_5)_3$ adduct led to a colour change and to negative boron NMR resonances (δ ^{11}B = −15.1 to −20.1). Products identity was confirmed in most cases by single crystal X-ray analysis.

Reacting phenylacetylene with tris(pentafluorophenyl)borane in combination triphenyl phosphine, led to the preferential formation of the zwitterion (**18**). Using instead, the less sterically hindered and more basic tri-*tert*-butylphosphine, resulted in the formation of the alkynyl borate salt (**19**) (Scheme 4.5). In both case it was postulated that some degree of dissociation in the Lewis-acid-base adduct was necessary to determine the alkyne activation.

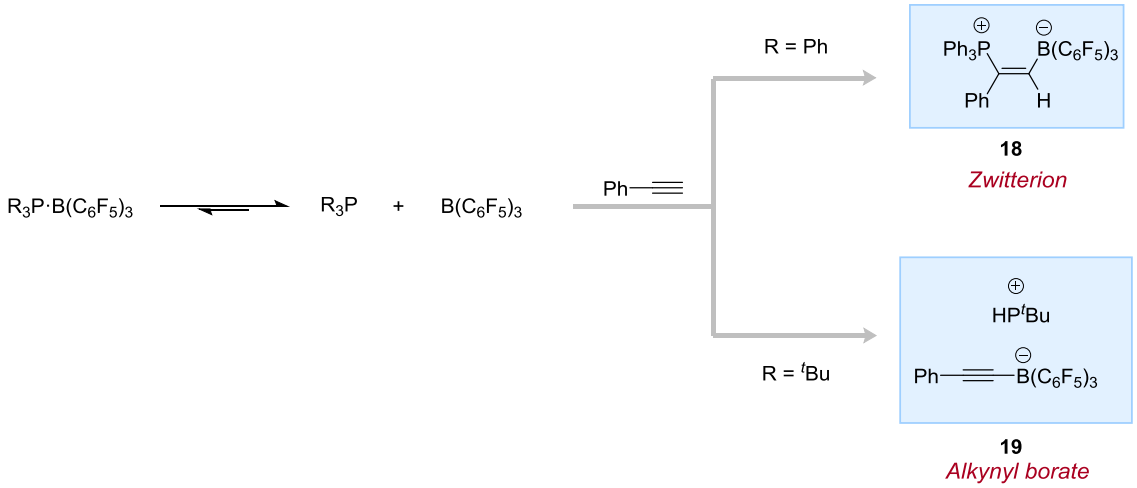

Scheme 4.5. Divergent reactivity of $B(C_6F_5)_3$ and phenylacetylene in the presence of different phosphine ligands.

A proposed mechanism was based on the initial dissociation of the $R_3P{\cdot}B(C_6F_5)_3$ adduct which allows an initial π-interaction to the alkyne with tris(pentafluorophenyl)borane. Coordination of the alkyne to $B(C_6F_5)_3$ can either activate the alkyne towards nucleophilic attack, generating the alkenyl zwitterion (**18**), or enhance the acidity of the alkyne C-H bond triggering deprotonation and subsequent alkynyl borate (**19**) formation. Thus, the nature of the phosphine determines the subsequent reactivity. A mechanism where the borane polarises the alkyne prompting nucleophilic addition to the more stable carbocation is consistent with this regiochemistry.

Few months later Berke and co-workers investigated the reaction of $B(C_6F_5)_3$ with the less sterically hindered alkyne, acetylene, in the presence of amine, phosphine and thiol donors.[12] Interestingly, reacting this less hindered alkyne with tetramethylpiperidine (TMP)·$B(C_6F_5)_3$ system led not only to the formation of the 1,2-borate/ammonium zwitterion (**20**), but also to a C_6F_5 group transfer to form the four-substituted alkenyl zwitterion (**21**) (Scheme 4.6). All the products of this transformation were characterised by single crystal X-ray and NMR analysis.

A possible reaction mechanism was proposed to involve preliminary coordination of the acetylene to $B(C_6F_5)_3$, which upon coordination, facilitated deprotonation by tetramethylpiperidine to form the σ-acetylide adduct $[B(C_6F_5)_3C{\equiv}CH]^-$ (**20**). Coordination of a further equivalent of $B(C_6F_5)_3$ molecule led to the formation of the vinylidene borane

adduct which, due to the strongly electrophilic α-carbon centre, triggered a 1,2-shift of the perfluoroaryl group to the more stable 1-(*E)* alkenyl borane (**21**).

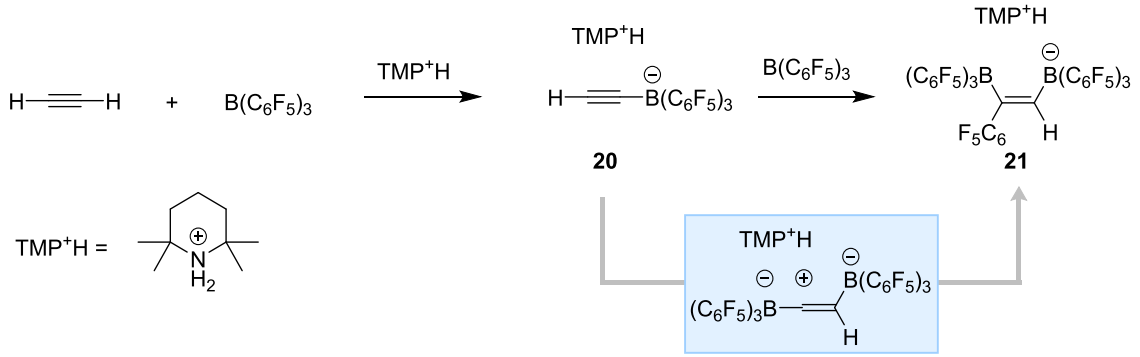

Scheme 4.6. Reaction of phenylacetylene, $B(C_6F_5)_3$ and TMP.

The role of the base and the mechanism of reaction with was further elucidated by Erker and co-workers.[15] The reaction of different tris(pentafluorophenyl)borane/phosphine systems with 1,2-diethynylbenzene was investigated. Upon changing of the phosphine component of the $R_3P{\cdot}B(C_6F_5)_3$ pair, different reaction products were obtained. Moving from $^tBu_3P$ to $Tol_3P{\cdot}B(C_6F_5)_3$ in the reaction with 1,2-diethynylbenzene, gave a modification of the reaction pathway, from a pure deprotonation route to give the borate (**22**) to a cooperative 1,2-addition reaction to give the alkenyl zwitterion (**23**) (Scheme 4.7). Using a less nucleophilic phosphine $(C_6F_5)_3P$ led to the formation of the 1,1-carboboration zwitterion (**24**) presumably through a combination of 1,1-carboboration and 1,2-addition.

Understanding and characterising this zwitterionic intermediate is of fundamental importance to improve the efficiency and the selectivity of 1,1-carboboration.

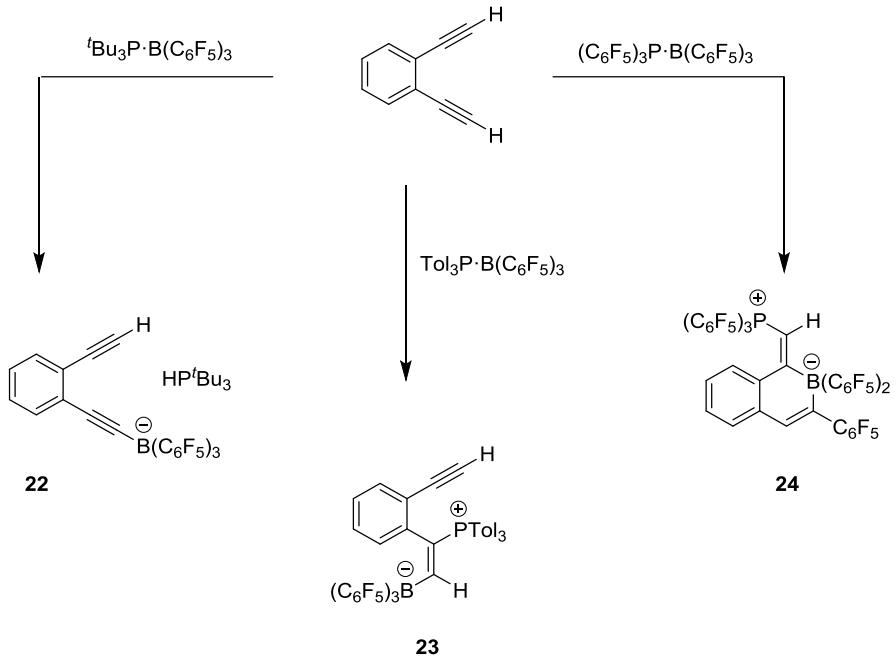

Scheme 4.7. Reaction of 1,2-diethynylbenzene and $R_3P{\cdot}B(C_6F_5)_3$.

4.2 Borane-catalysed hydroboration

During the last twenty years these electrophilic perfluoroboranes have been widely used in a variety of organic transformations.[2] Among these, borane-catalysed hydroboration is an emerging field. Pioneering work was reported by Crudden and co-workers who developed a metal-free catalytic method for the reduction of imines using a $DABCO{\cdot}B(C_6F_5)_3$ system (Scheme 4.8).[16] Various aryl- and aliphatic-imines underwent successful hydroboration with pinacol borane using 5 mol% of the catalyst. The mechanism of the reaction was investigated through a series of stoichiometric reactions. Treating $DABCO{\cdot}B(C_6F_5)_3$ adduct with stoichiometric amount of HBpin resulted in the formation of a DABCO-stabilised borenium ion (**25**). The addition of a base (DABCO) promotes the hydride shift from pinacol borane to $B(C_6F_5)_3$ with subsequent formation of a borohydride borenium salt (**25**). The generation of this species was fully assigned by ^1H and ^{11}B NMR, however, no crystal suitable for X-ray analysis was isolated. Treating the borohydride borenium salt (**25**) with a stoichiometric amount of imine in the absence of pinacol borane did not result in the imine reduction suggesting an external hydride

delivery. Kinetic investigations were consistent with this finding, suggesting that pinacol borane may be crucial for the hydride delivery. The reaction was therefore proposed to occur by *in situ* DABCO-stabilised borenium ion formation, which upon reaction with the imine undergoes a group exchange to generate an imino borenium species (Scheme 4.8). The latter is then reduced by pinacol borane releasing the borylated amine and regenerating the borenium catalyst.

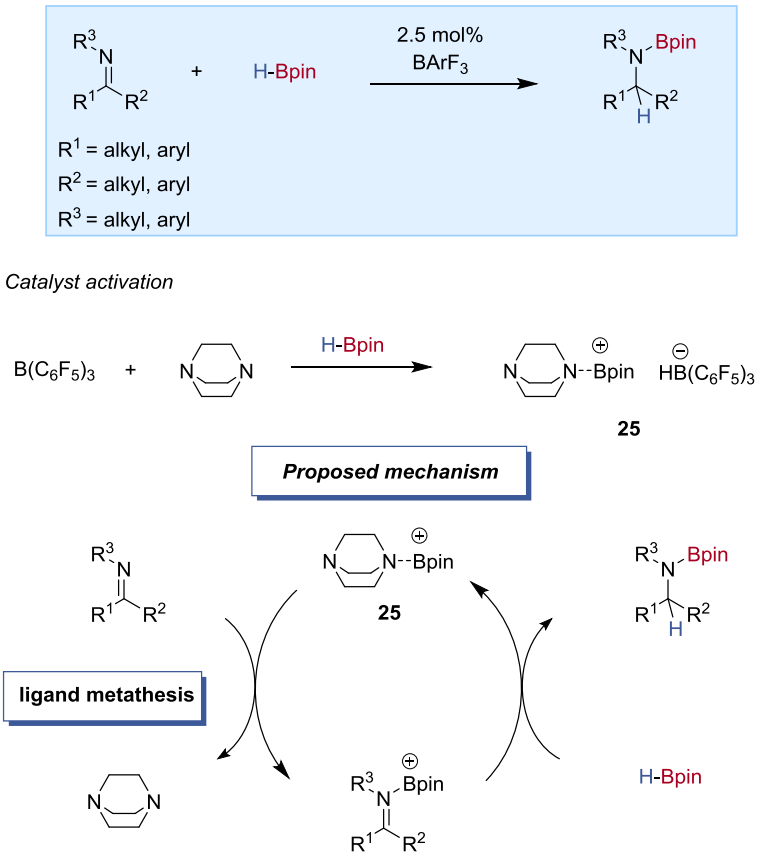

Scheme 4.8. DABCO·B(C_6F_5)$_3$-catalysed hydroboration of imines.

Oestreich, Melen and co-workers reported the more Lewis acid tris[3,5-bis(trifluoromethyl)phenyl]borane ($BArF_3$) as a catalyst for the hydroboration of imines without the use of an external base.[17] The role of borenium cations was further investigated by Ingleson and co-workers who reported the synthesis, characterisation of base-stabilised borenium cations, and investigated their role in hydroboration reactions.[18],[19]

Despite encouraging results, only limited examples were reported using commercially-available borane species as catalysts for the hydroboration of alkenes and alkynes. During the course of this PhD project, two important developments were reported.

Piers' borane and parent compounds successfully promoted the hydroboration of terminal and internal alkynes in good yield and good group functional tolerance.[20] Using $B(C_6F_5)_3$ as the catalyst also successfully promoted the hydroboration, albeit in lower yield. A preliminary mechanistic investigation, monitoring the reaction mixture by ^{19}F NMR spectroscopy, revealed a complex mixture of compounds. A potential cross-over between 1,1-carboboration and borane-catalysed hydroboration was envisaged with a similar zwitterionic intermediate. It is worth noting that the mode of activation is entirely different to previously reported borane-catalysed hydroboration protocol, in which a hydride shift and a formation of a borohydride/borenium species was fundamental to triggering catalyst activation. Stoichiometric reactions between $HB(C_6F_5)_2$, phenylacetylene and pinacol borane led to undetermined side products even at elevated temperature. Reacting stoichiometric amounts of phenylacetylene with $HB(C_6F_5)_2$ resulted in the 1,2-hydroboration product (**26**) which upon treatment with pinacol borane gave the 1,1-di-borylated alkane (**27**). Further addition of an equivalent of alkyne led to the formation of the alkenyl boronic ester with formation of Piers' borane (Scheme 4.9).

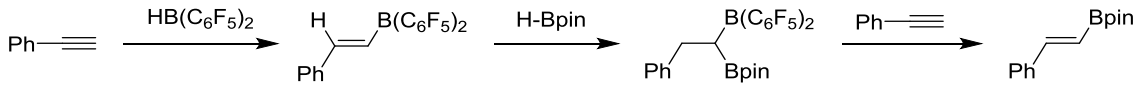

26 **27**

Scheme 4.9. Stoichiometric reactions of phenylacetylene, $HB(C_6F_5)_2$, and HBpin.

Based on these observations two possible mechanisms for the hydroboration of phenyl acetylene were proposed (Scheme 4.10). The first is based on the preliminary reaction of the alkyne and $HB(C_6F_5)_2$ to generate the 1,2-hydroboration product (**26**). This could then react with pinacol borane to undergo retro-hydroboration forming the 1,1-di-borylated alkane (**27**), which upon reaction with a further molecule of alkyne release the product and regenerates Piers borane. Alternatively, Piers' borane was proposed to be a pre-catalyst of this reaction which upon reaction with the alkyne and pinacol borane generates the active catalyst: the 1,1-di-borylated alkane (**27**). Once formed, this species can activate an alkyne to form a highly reactive zwitterion (**28**), which reacts with HBpin

to undergo 1,2-syn-concerted hydroboration. No isolation or spectroscopic observation of this zwitterion was reported. This procedure was highly efficient for the hydroboration of alkynes, but not for alkenes.

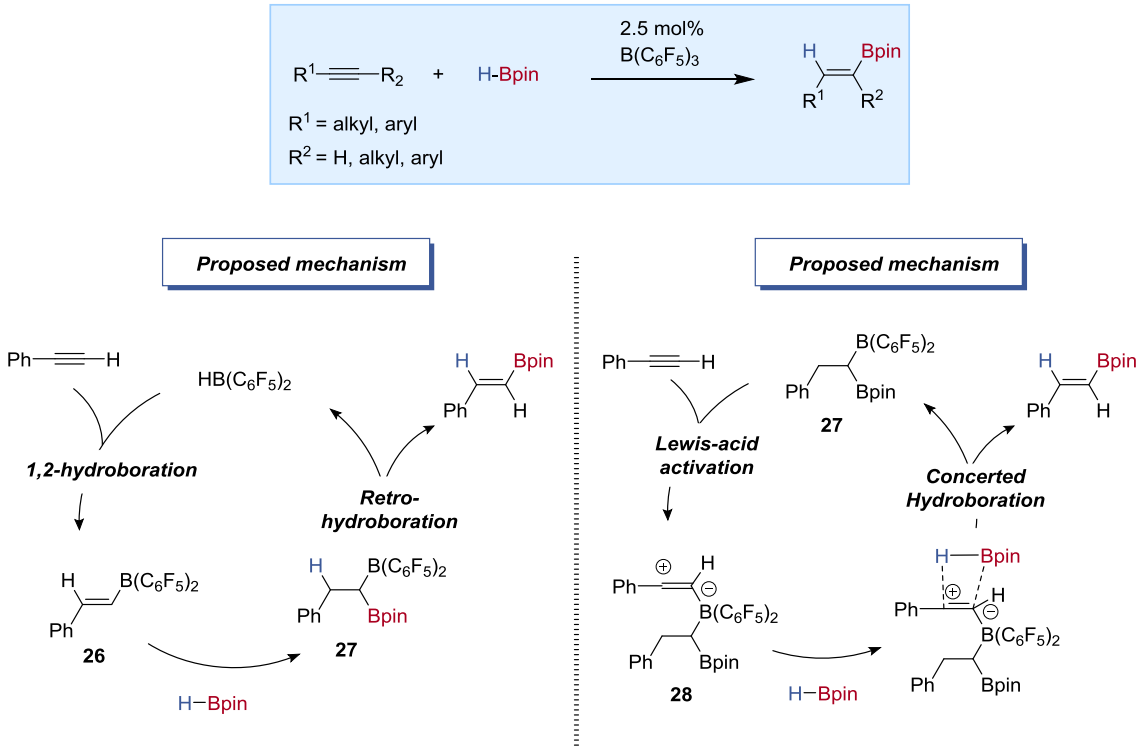

Scheme 4.10. Piers' borane-catalysed hydroboration of alkynes.

Oestreich and co-workers reported, for the first time, the hydroboration of alkenes with pinacol borane using ($BArF_3$) (Scheme 4.11).[21] The protocol gave excellent selectivity across a wide variety of substrates including substituted styrenes and aliphatic alkenes, with excellent *anti*-Markovnikov regioselectivity. Notably, $B(C_6F_5)_3$ did not promote the transformation under the reaction conditions.

Monitoring the reaction of ($BArF_3$) with pinacol borane at elevated temperature by NMR spectroscopy revealed clean formation of ArFBpin and diborane, showing that ligand redistribution was occurring. As diborane is known to readily undergo addition to olefins,[22],[23] styrene was added to the reaction mixture, but no hydroboration product was observed ruling out any role in catalysis.

Variation of the stoichiometry of HBpin in the reaction with ($BArF_3$) showed that two new boron compounds were formed, $[H_2BArF]_2$ and $[(ArF)(H)B(\mu\text{-}H)_2BArF_2]$. This mixture or one of these boranes, were proposed to be the active catalyst for this transformation. Notably, VT NMR spectroscopy showed that the reaction of $B(C_6F_5)_3$ and HBpin gave only B_2pin_3 and other unidentified compounds.[21] Following this, the reaction is proposed to occur *via* ligand redistribution between $BArF_3$ and pinacol borane, forming electron-deficient hydroboranes (**29**) (Scheme 4.11). These undergo 1,2-hydroboration of the alkene, followed by ligand exchange with HBpin, generating the pinacolboronate ester product and thus regenerating the catalyst.

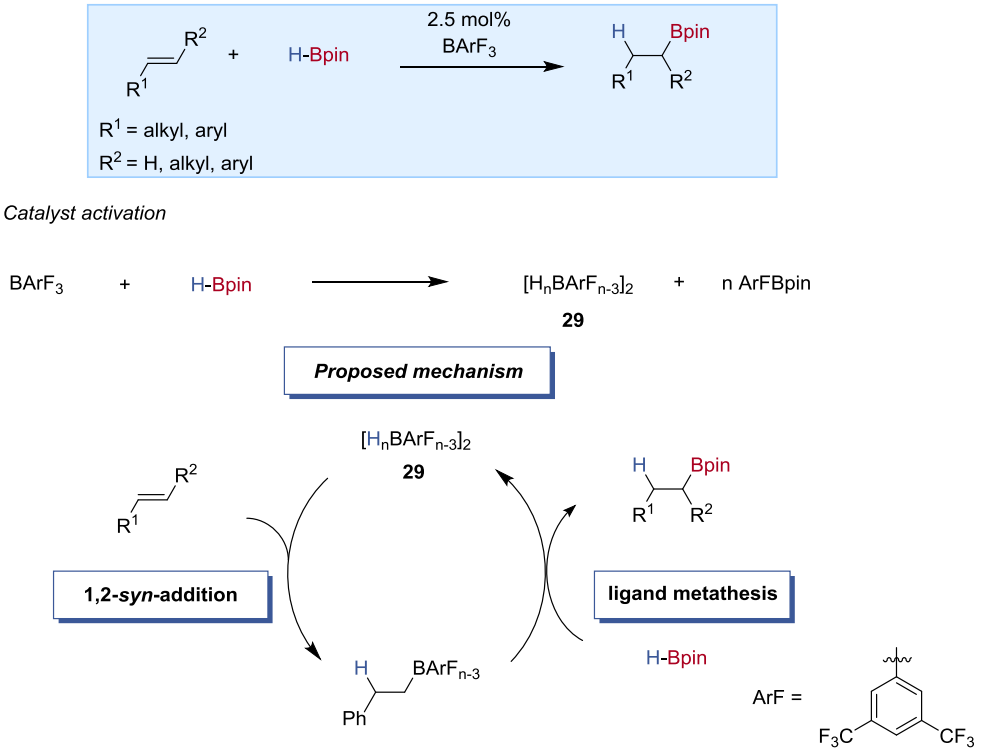

Scheme 4.11. $BArF_3$-catalysed hydroboration of alkenes.

4.3 Aims

As previously was highlighted, the reaction of alkynes and tris(pentafluorophenyl)borane leads to the formation of a transient zwitterionic intermediate which then evolves into the 1,1-carboboration product. The existence of this species has been supported by computational analysis, however, a comprehensive study with product isolation or experimental spectroscopic observation is still lacking.

The cross-over between 1,1-carboboration and Stephan's H-B(C_6F_5)$_2$-initiated hydroboration, along with wider frustrated Lewis-pair chemistries,[5],[24] rests on the stability of the proposed zwitterionic intermediate, and its reactivity with nucleophiles (i.e. H-Bpin for hydroboration) and propensity for rearrangement (1,1-carboboration). Understanding the stability and analysing the reactivity of this species is fundamental for the understanding of existing processes and to the development of new ones. However, no experimental evidence of this species has ever been reported.

The potential for divergent reactivity of the proposed, yet unobserved, alkenyl zwitterionic (**30**) intermediate led us to attempt to trap this intermediate and direct its reactivity. Significantly, we wished to access the key alkenyl zwitterion using B(C_6F_5)$_3$, rather than Piers borane, and study its reactivity (Scheme 4.12).

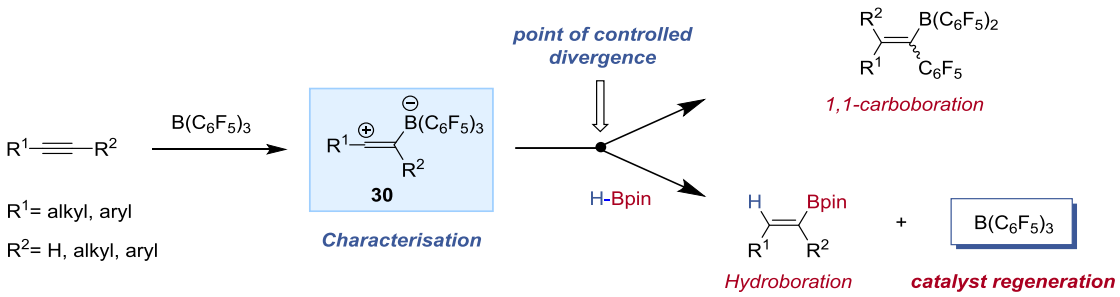

Scheme 4.12. Aims of the project.

4.4 Zwitterion intermediate

It was notice that the addition of phenylacetylene to a solution of $B(C_6F_5)_3$ resulted in a colour change, from colourless to red, which has often been indicative of a zwitterionic species. This red solution was short-lived and changed to orange within 10 minutes at room temperature with the formation of the 1,1-carboboration product. Therefore, it was decided to perform the reaction at lower temperature and study the reaction mixture by NMR spectroscopy (Scheme 4.13). Reacting $B(C_6F_5)_3$ and phenylacetylene at 233 K resulted in the immediate formation of the zwitterion (**32i**) identified by both ^{1}H and ^{13}C NMR spectroscopy with diagnostic resonances for the two-coordinate carbon (δ ^{13}C = 199.3) and the four-coordinate boron (δ ^{11}B = −12.1) (Figure 4.1). Also present in solution were unreacted phenylactylene (δ ^{13}C = 83.6, 77.6) and $B(C_6F_5)_3$(δ ^{11}B = 55.40), suggesting that (**32i**) exists in equilibrium with these precursors. The connectivity of the zwitterion was confirmed by 2D ^{1}H-^{11}B HMBC spectra in which a ^{1}H-^{11}B long-range correlation was observed between the boron resonance (δ ^{11}B = −12.1) and alkenyl proton (δ ^{1}H = 5.41) resonance. No short-range correlations were observed. The alkenyl proton also showed a long-range correlation in 2D ^{1}H-^{13}C HMBC spectra with the two-coordinate carbon resonance (δ ^{13}C = 199.3). The ^{13}C chemical shift of the two-coordinate carbon center is typical for alkenyl-cations.[25],[26] The quaternary nature of zwitterion carbon resonance was confirmed by DEPT 135 ^{13}C NMR spectrum and the PhC=**C**$^{+}$H−$^{-}$B$(C_6F_5)_3$ was identified as a broad multiplet (δ ^{13}C = 51.2) by 2D ^{1}H-^{13}C HSQC spectra by correlation with the alkenyl proton (δ^{1} H = 5.41).

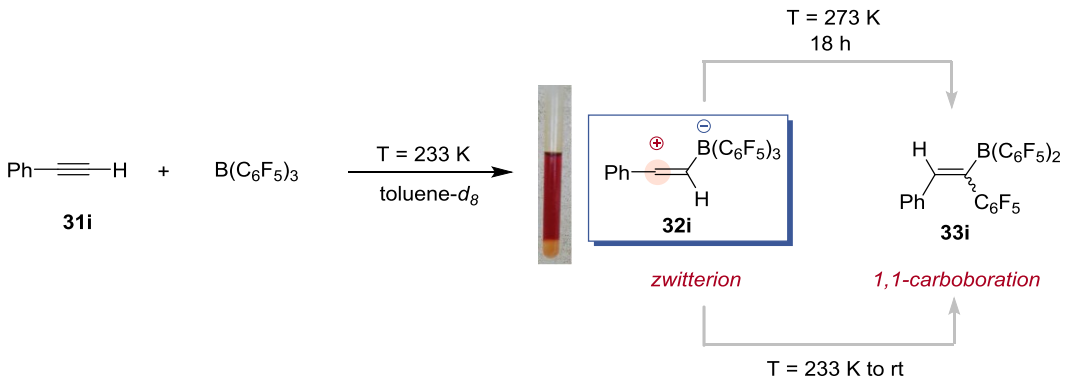

Scheme 4.13. Reaction of phenyl acetylene and $B(C_6F_5)_3$ at 233 K.

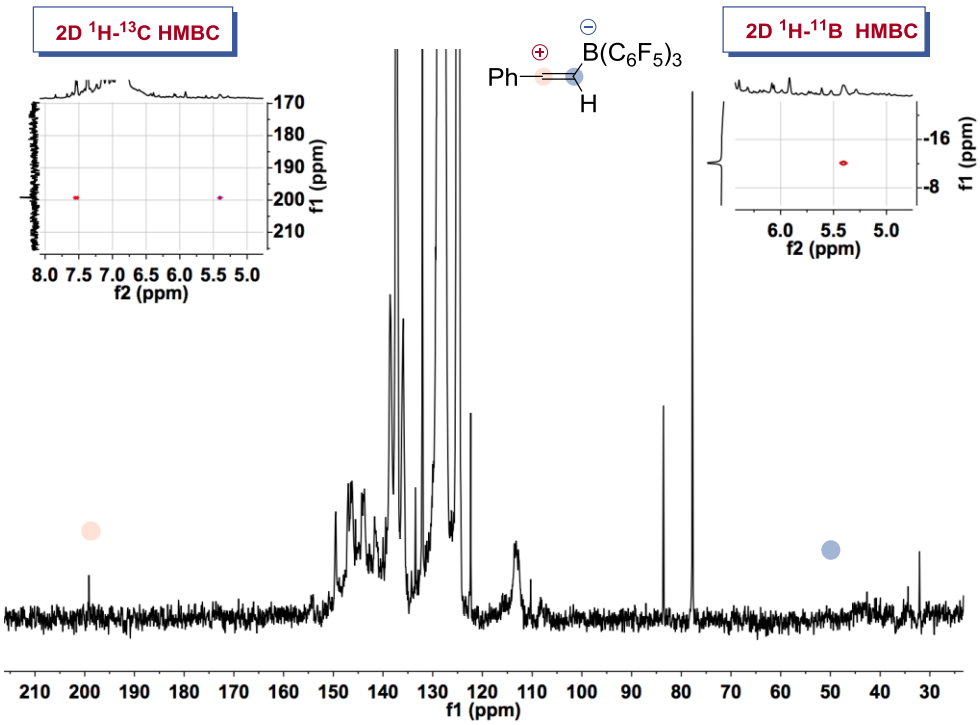

Figure 4.1. ^{13}C{H} NMR (400 MHz, toluene-d_8, T = 233 K) of the reaction of phenylacetylene and $B(C_6F_5)_3$. *Left spectrum* 2D ^{1}H,^{13}C HMBC. *Right spectrum* 2D ^{1}H-^{11}B HMBC.

As the nature of the quaternary carbon (C-B) was only supported by 2D NMR spectroscopy, to further confirm the connectivity between $B(C_6F_5)_3$ and phenylacetylene the same transformation was performed using carbon phenylacetylene-2-^{13}C, PhC≡^{13}CH. This time it was possible to observe the PhC^{+}=^{13}**C**H−$^{-}$B$(C_6F_5)_3$ resonance which appeared to be a quartet (δ ^{13}C = 51.2) due to the coupling with boron ($J_{C\text{-}B}$ = 44.4 Hz) (Figure 4.2). The same ^{11}B-^{13}C coupling was also confirmed through ^{11}B NMR spectroscopy, the four-coordinate boron this time gives rise to a doublet (δ ^{11}B = −12.1) characterised by the same coupling constant ($J_{C\text{-}B}$ = 44.4 Hz). Unfortunately, this time no evidence of the carbocation resonance was observed, most likely as the splitting caused by coupling to the ^{13}C decreases the intensity of the signal below the detectable limit.

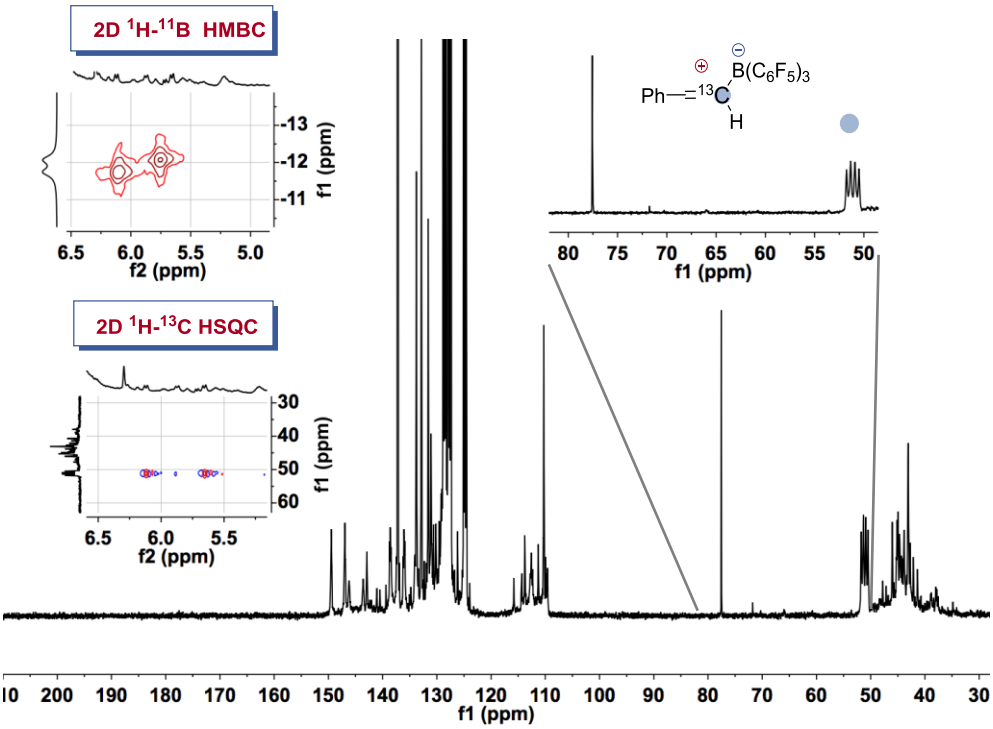

Figure 4.2. ^{13}C{H} NMR (100 MHz, toluene-d_8, T = 243 K) of the reaction of H^{13}C≡C-Ph and (**32i**) and *B*(C$_6$F$_5$)$_3$. *Top left spectrum* 2D ^{1}H-^{11}B HMBC. *Bottom left spectrum* 2D ^{1}H,^{13}C HSQC.

Despite extensive efforts, we were unable to isolate zwitterion (**32i**) due to rearrangement to the 1,1-carboboration product (**33i**) (δ ^{13}C = 162.7) above 243 K. However, we could follow the evolution of zwitterion (**32i**), generated from phenylacetylene and B(C$_6$F$_5$)$_3$, to the 1,1-carboboration product (**33i**) by ^{13}C{^{1}H} NMR spectroscopy at 273 K (Figure 4.3). After 18 hours, all of the alkyne was consumed, to give the 1,1-carboboration product, alongside unreacted B(C$_6$F$_5$)$_3$ and unidentified side products. Additionally, a temperature screening showed the prompt formation of the 1,1-carboboration product at room temperature.

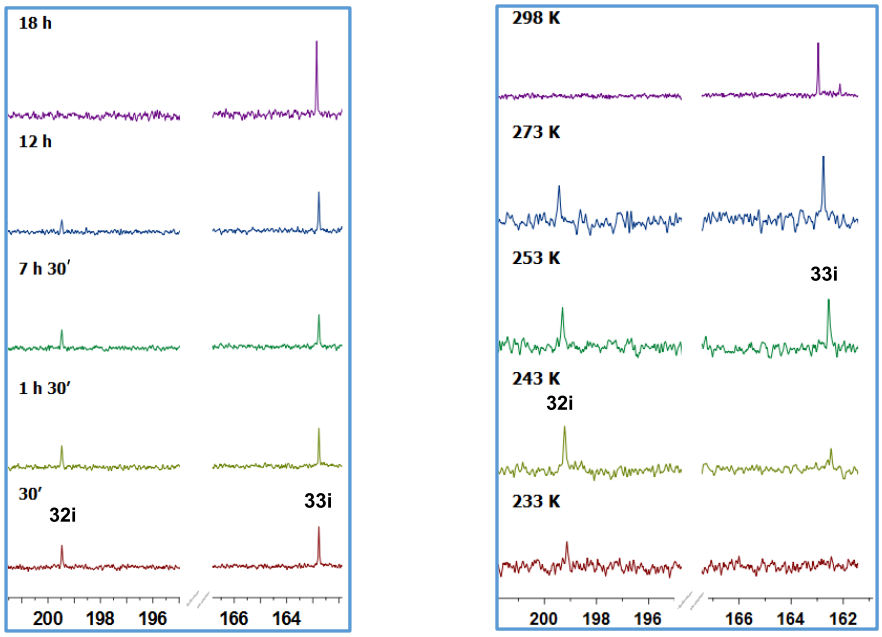

Figure 4.3. $^{13}C\{H\}$ NMR (100 MHz, 273 K, toluene-d_8) of the reaction of HC≡C-Ph and $B(C_6F_5)_3$. *Left spectrum* $^{13}C\{H\}$ NMR (100 MHz, toluene-d_8) evolution of reaction over time. *Right spectrum* $^{13}C\{H\}$ NMR (100 MHz, toluene-d_8) evolution of reaction at different temperatures.

To further confirm the presence of a zwitterionic intermediate, a different substituted alkyne, *p*-methoxy phenylacetylene, was tested (Scheme 4.14). Here the electron-donating substituent could potentially help to stabilise the zwitterion intermediate resulting in a longer half-life of the intermediate. Once again, the characteristic resonances of a zwitterion intermediate (**32k**) were immediately observed by ^{1}H, ^{11}B and ^{13}C NMR spectroscopy (Figure 4.4). In this case, no 1,1-carboboration product was observed below room temperature and no reaction was observed below 273 K. The reaction was therefore carried out at room temperature and monitored using NMR spectroscopy. Upon mixing of $B(C_6F_5)_3$ and *p*-methoxy phenylacetylene a purple colour was noted. Once again, formation of a zwitterion (**32k**) was observed, with particularly diagnostic resonances for the two-coordinate carbon (δ ^{13}C = 193.5) and the four-coordinate of the boron (δ ^{11}B = −11.9). Also present in solution were unreacted *p*-methoxy phenylacetylene (**31k**) (δ ^{13}C = 83.7, 75.8) and $B(C_6F_5)_3$ (δ ^{11}B = 60.40), suggesting that (**32k**) also exists in equilibrium. The connectivity of the zwitterion was confirmed by 2D ^{1}H-^{11}B HMBC in which a boron-proton long-range correlation was

observed between the boron (δ ^{11}B = −11.9) and alkenyl proton (δ ^{1}H = 5.47) resonances, no short-range correlations were observed. The latter also showed a long-range correlation in a 2D ^{1}H-^{13}C HMBC with the two-coordinate carbon (δ ^{13}C = 193.5) The quaternary nature of zwitterion carbon resonance was confirmed by DEPT 135 ^{13}C NMR spectrum and the PhC^{+}=**C**H−$^{-}$B(C$_6$F$_5$)$_3$ was identified as a broad multiplet by 2D ^{1}H-^{13}C HSQC (δ ^{13}C = 50.6)

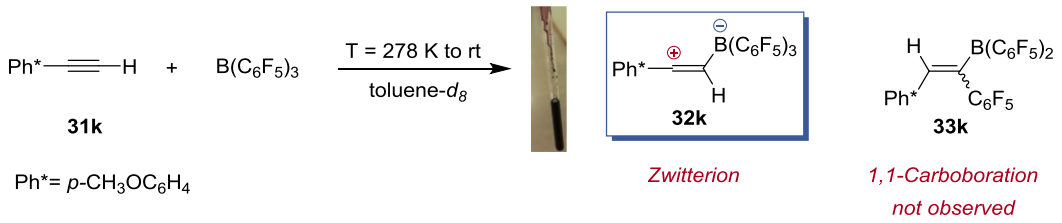

Scheme 4.14. Reaction of phenyl acetylene and B(C$_6$F$_5$)$_3$.

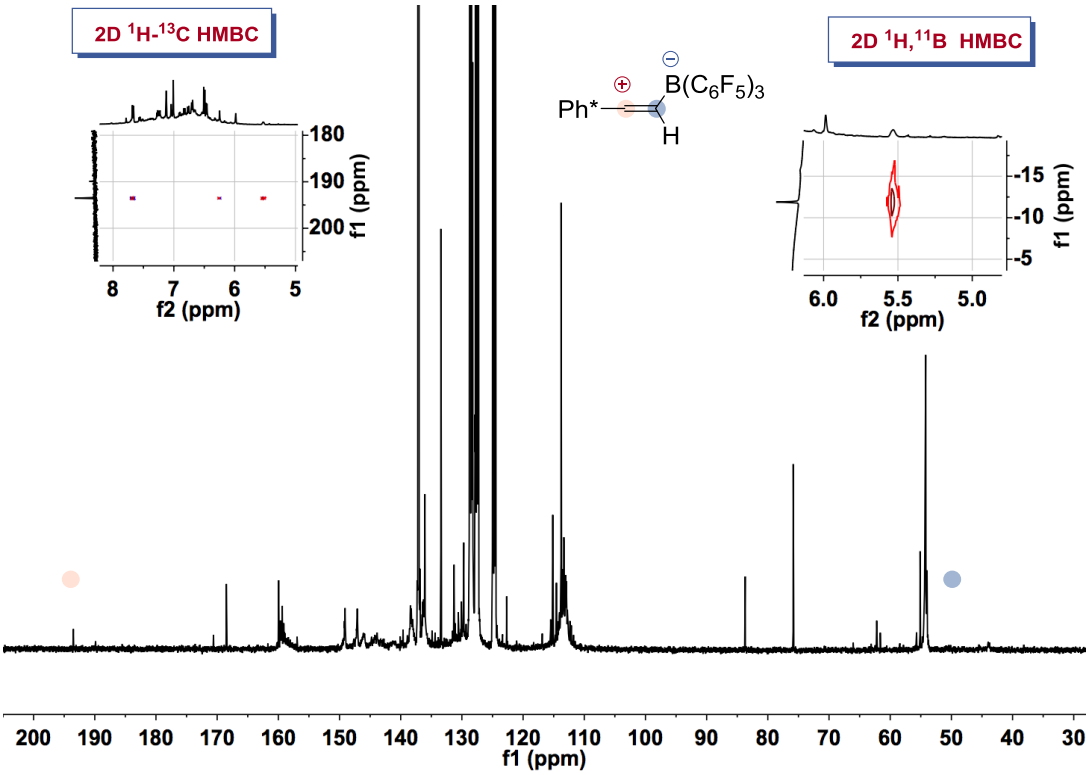

Figure 4.4. ^{13}C{H} NMR (126 MHz, toluene-d_8, 298 K) of the reaction of para-methoxy phenyl acetylene and *B*(C$_6$F$_5$)$_3$. *Left spectrum* 2D ^{1}H-^{13}C HMBC. *Right spectrum* 2D ^{1}H-^{11}B HMBC.

The zwitterion resonance disappeared after two days at room temperature compared to the zwitterion (**32i**). Presumably the *p*-methoxy substituent stabilises the species in comparison to phenyl group.

As we were unable to isolate the 'naked' zwitterion, we next attempted to trap the zwitterion with a suitable nucleophile. Generation of the zwitterion in the presence of 1,4-diazabicyclo[2.2.2]octane, DABCO, gave the adduct in 50% yield after 24 hours as a mixture of the DABCO adduct (**34a**) and alkynyl boronate $[(C_6F_5)_3B{-}C{\equiv}CPh]^-$ $[DABCO\text{-}H]^+$ (**34b**) (Scheme 4.15). Crystals suitable for single crystal X-ray analysis were grown from CH_2Cl_2 showing the DABCO trapped zwitterion (**34a**) (Figure 4.5). Solution phase characterization of (**34a**) and (**34b**) showed they exist in equilibrium. Consistent with this, isolated (**34b**) (precipitated from Et_2O), slowly converts to a mixture of (**34a**) and (**34b**) when dissolved in CD_2Cl_2.

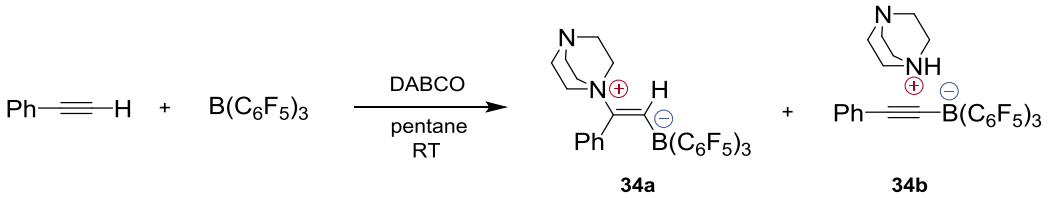

Scheme 4.15. Reaction of phenyl acetylene, $B(C_6F_5)_3$ and DABCO.

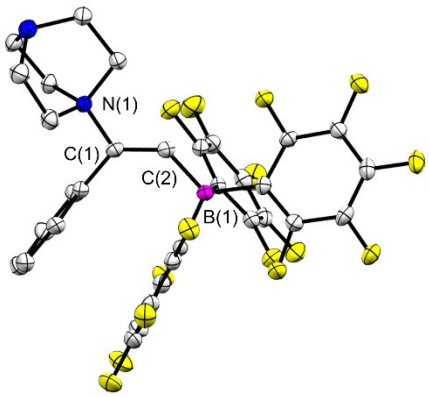

Figure 4.5. Crystal structure of zwitterion (**34a**). Ellipsoids are set to 50% probability; hydrogen atoms are omitted for clarity. Selected both lengths (Å) and angles [º]: B(1)–C(2) 1.630(4), C(2)–C(1) 1.324(4), N(1)–C(1) 1.534(3); B(1)–C(2)–C(1) 128.4(2), C(2)–C(1)–N(1) 121.1(2).

4.5 Ferrocene-substituted zwitterion

The transient nature of the zwitterionic species and the complicated mixture derived from the reaction of alkynes and $B(C_6F_5)_3$ rendered the analysis of the NMR spectra difficult and non-conclusive. A modification on the alkyne backbone was therefore required to stabilise the zwitterion and to drive its selective formation. Oestreich and co-workers have reported the use of ferrocene substituent to stabilise highly reactive species such as silyl cations.[27]–[30] The bonding interaction between the electron-rich Fe and the electron-poor silicon centre helps stabilising this transient species. The influence of the ferrocene motif is so significant that quantum calculation showed a 3-centre-2-electron bond structure with the charge delocalised on the upper ring. Inspired by those works, we envisaged the ferrocene backbone to stabilise the cationic nature of the zwitterion and potentially help product isolation.

Ethynylferrocene was allowed to react with $B(C_6F_5)_3$ at 243 K and the reaction progress was monitored by NMR spectroscopy (Scheme 4.16). Complete consumption of the starting alkyne was observed by ^{1}H NMR, and ^{13}C NMR spectroscopy. Once again, the resonances of a zwitterion intermediate (**32p**) were immediately observed by ^{1}H NMR, ^{11}B NMR and ^{13}C NMR spectroscopy (Figure 4.6). In contrast to the above-mentioned examples, where the zwitterion was formed in low yield, this time it is the major product, which allowed us to assign most of the NMR resonances.

The two-coordinate carbon, $R-\mathbf{C}^{+}=CH-^{-}B(C_6F_5)_3$, and the quaternary carbon resonance, $R-C^{+}=\mathbf{C}H-^{-}B(C_6F_5)_3$ were assigned to signals at δ ^{13}C = 186.7, δ ^{13}C = 107.8, respectively. These values are consistent with previously reported alkenyl ferrocene cations.[31],[32] The alkenyl proton resonance was observed at δ ^{1}H = 6.92. The connectivity of the alkenyl carbons as well as the resonances of the whole ferrocene motif were assigned through 2D ^{1}H-^{13}C HSQC and 2D ^{1}H-^{13}C HMBC NMR spectroscopy. Notably this time both the carbon and proton resonances of the zwitterion were shifted downfield compared to the resonances of the other zwitterions. Moreover, the connectivity of the quaternary carbon (C−B) was not confirmed by ^{13}C NMR and 2D ^{1}H-^{11}B HMBC NMR spectroscopy. ^{11}B NMR spectrum displayed two resonances ($\delta^{11}B$ = −12.7, −20.4) which confirmed a tetrahedral coordination motif. It is important to note, that after 6 hours at 243 K, despite the low temperature, the zwitterion resonances

disappeared with formation of unidentified side products, proving the transient nature of this species in solution.

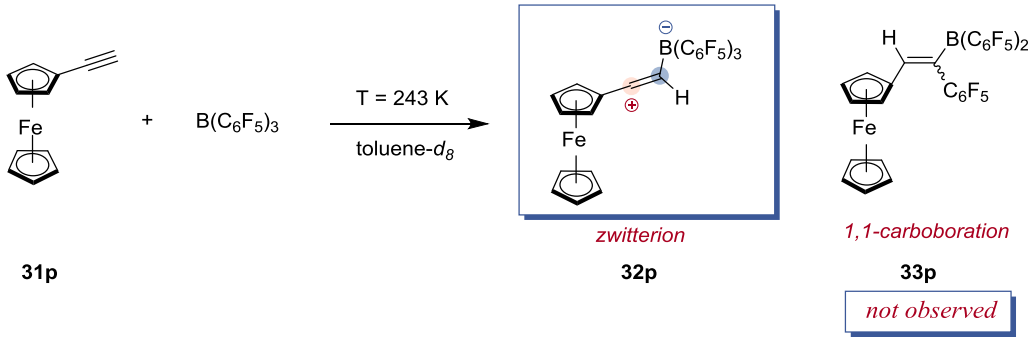

Scheme 4.16. Reaction of ethynylferrocene and $B(C_6F_5)_3$.

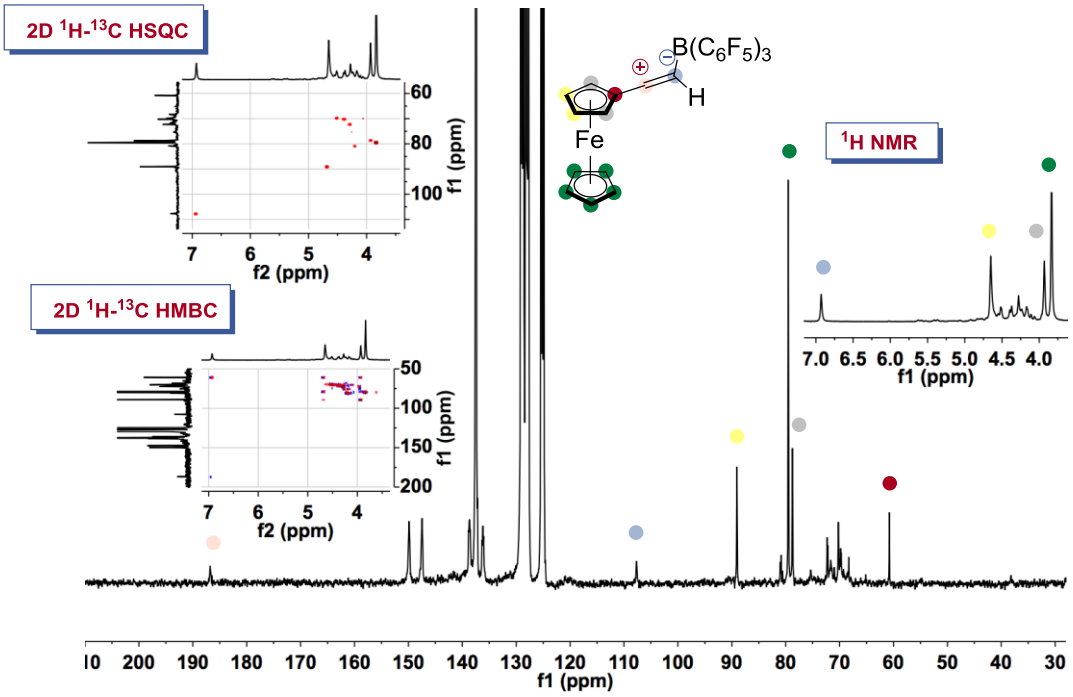

Figure 4.6. $^{13}C\{H\}$ NMR (100 MHz, toluene-d_8) of the reaction of ethynylferrocene and $B(C_6F_5)_3$. *Top left spectrum* 2D ^{1}H-^{13}C HSQC. *Bottom Left spectrum* 2D ^{1}H-^{13}C HMBC. *Right spectrum* ^{1}H NMR.

As the connectivity of ethynylferrocene zwitterion was suspicious, elucidation was attempted using ethynylferrocene-2-^{13}C. All of the above-mentioned data were confirmed, with some additional information on the nature of the carbon-carbon bond delivered through ^{1}H-^{13}C coupling constant. The enrichment of the ^{13}C labelled ethynylferrocene was confirmed by ^{1}H NMR, ^{13}C NMR with the diagnostic multiplicity of

the terminal proton (δ ^{1}H = 2.64, d, $J_{C\text{-}H}$ = 250.33 Hz) (Figure 4.7). A strong signal was observed for the labelled carbon (δ ^{13}C = 75.6) and the other alkynyl carbon (δ ^{13}C = 81.3, d, $J_{C\text{-}C}$ = 173 Hz) was observed as a doublet with diagnostic coupling constant for a triple bond, confirmed by ^{13}C INADEQUATE spectrum. Upon addition of $B(C_6F_5)_3$ at 243 K a shift of the starting alkynyl proton (from δ ^{1}H = 2.72, d, $J_{C\text{-}H}$ = 250.33 Hz, to δ ^{1}H = 6.92, d, $J_{C\text{-}H}$ = 165.33 Hz) and a net decrease of the coupling constant was observed confirming a possible change in the C-C bond order from triple to double. As before, the two-coordinate carbon, R−**C**$^{+}$=CH−$^{-}$$B(C_6F_5)_3$, and the R−C^{+}=**C**H alkenyl resonances were assigned at (δ ^{13}C = 186.7, d, $J_{C\text{-}C}$ = 99 Hz, δ ^{13}C = 107.8, s). Once again, a net change in the carbon-carbon coupling constant (from $J_{C\text{-}C}$ = 176.6 Hz, to $J_{C\text{-}C}$ = 99 Hz) indicates a change of the bond order which supports the formation of a zwitterion. Unfortunately, no splitting of the carbon resonance corresponding due to ^{11}B-^{13}C coupling was observed which left the carbon-boron connectivity still dubious.

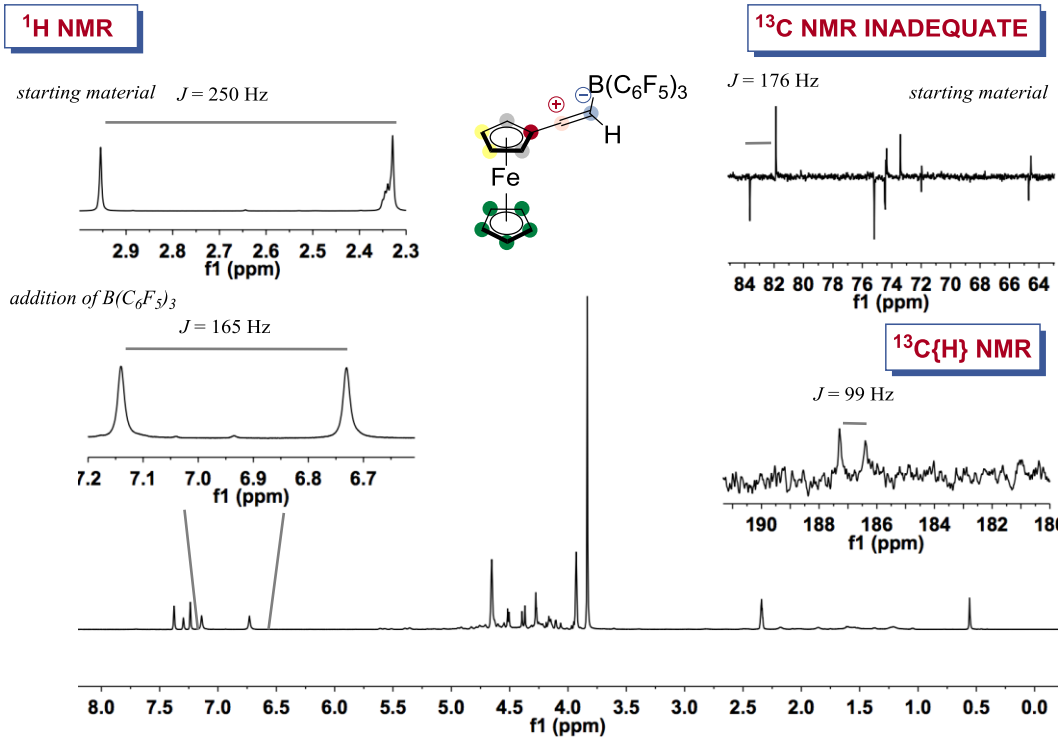

Figure 4.7. ^{1}H NMR (100 MHz, toluene-d_8) of the reaction of ethynylferrocene-2-^{13}C and $B(C_6F_5)_3$. *Top left spectrum* ^{1}H of the starting alkyne. *Bottom left spectrum* ^{1}H zoom of the reaction. *Top right* ^{13}*C INADEQUATE spectrum of the starting alkyne. Bottom right* ^{13}C NMR of the reaction.

Finally, after several attempts, X-ray diffraction quality crystals of the zwitterion (**32p**) were grown in 1:1 hexane/toluene mixture (Figure 4.8). X-ray analysis showed a significant longer C(1)–C(2) bond length (1.286 (5) (Å)) compared to those usually reported for alkynes (1.19-1.21 Å). This is indicative of a change in the bond order of the alkynyl fragment. The latter showed a bond length comparable to that of the alkenyl DABCO-trapped zwitterion (**34a**) (C−C = 1.286 (5) (Å) *vs* 1.324(4) (Å)). This was also supported by the B(1)–C(1)–C(2) bond angle (122.8(3)º) indicating a trigonal geometry around C(1) with a sum of angles 360 °C which is consistent with a sp^2–hybridised bond. The relatively short C(3)–C(2) bond length (1.379(5) Å) and the Fe(1)–C(2) bond length (2.379(4) (Å)) indicate a charge delocalisation on the ferrocene motif.

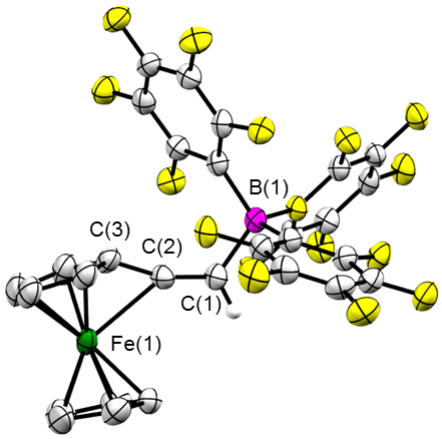

Figure 4.8. Crystal Structure of the alkenyl ferrocene zwitterion (**32p**). Ellipsoids are set to 50% probability; hydrogen atoms are omitted for clarity with the exception of the alkenyl C-H bond. Selected both lengths (Å) and angles [º]: B(1)–C(1) 1.654(5), C(2)–C(1) 1.286(5), C(3)–C(2) 1.379(5), Fe(1)–C(2) 2.379(4), Fe(1)–C(2) 1.990(4); B(1)–C(1)–C(2) 122.8(3), Fe(1)–C(2)–C(1)–140.47(2), C(3)–C(2)–C(1) 162.6(4).

4.6 Borane-catalysed hydroboration of alkynes

During the course of this PhD, Stephan and co-workers have demonstrated that $B(C_6F_5)_3$ could promote hydroboration of *p*-methyl phenylacetylene, we decide to focus on developing this reaction. An initial reaction with 1-octyne and with 1.5 equivalents of HBpin using commercially-available $B(C_6F_5)_3$ (20 mol%) at room temperature gave 30% conversion after 2 hours (Table 4.1, entry 1). Upon increasing the temperature to 60 °C a near full conversion to the (*E*)-alkenyl boronic ester species was observed by ^{1}H NMR spectroscopy in 2 hours with complete control of regio- and diastereoselectivity for the terminal (*E*)-alkenyl boronic ester (Entry 2). A number of boron compounds were tested as catalysts for the hydroboration of alkynes with alkyl or halo derivatives still promoting alkyne hydroboration, albeit to lower product yield (Entries 3-5). In order to test the activity of $B(C_6F_5)_3$ as a catalyst, further screening at lower catalyst loadings were then carried out with 2 mol% proved optimal (Entries 6-9).

Table 4.1. Catalyst Screening.

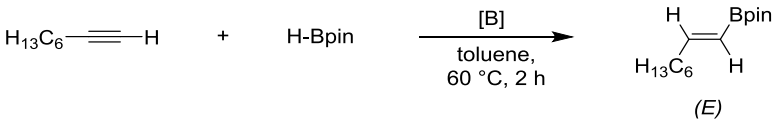

(E)

Entry	[B]	Catalyst loading	Yield (%)
1[a]	$B(C_6F_5)_3$	20 mol%	30
2	$B(C_6F_5)_3$	20 mol%	99
3[b]	BCl_3	20 mol%	43
4	BBr_3	20 mol%	43
5	BEt_3	20 mol%	31
6	$B(C_6F_5)_3$	10 mol%	99
7	$B(C_6F_5)_3$	5.0 mol%	99
8	$B(C_6F_5)_3$	2.5 mol%	99
9	$B(C_6F_5)_3$	2.0 mol%	83

Reaction conditions: (0.2-0.02 eq.) catalyst, 0.15 mmol (1 eq.) 1-octyne and 0.18 mmol (1.5 eq.) HBpin in 0.60 mL of the mL toluene-d_8, heated at 60 °C for 2 h. Yield determined by ^{1}H NMR of the crude reaction mixture using 1,3,5-trimethoxybenzene as an internal standard. [a] Reaction performed at room temperature for 2 h. [b] Product was obtained as 25:18 *E/Z* ratio.

Screening of all the other reaction parameters such as solvent, equvalents of HBpin and reaction concentration were then screened using $B(C_6F_5)_3$ (2.0 mol%) and 1-octyne as a model substrate. Performing the reaction in halogenated solvent or in coordinating polar solvents gave low yield (Table 4.2, entries 1-4). Toluene was selected as the solvent for the next optimisation. Decreasing the loading of HBpin from 1.5 to 1.1 equivalents did not show a significant difference in yield (Entries 5-8) while 1.0 equivalent gave a lower yield (Entry 8). Hence 1.1 equivalents was selected as the optimal condition. Furthermore, increasing the concentration of the reaction resulted in an improved yield of the alkeneyl boronic ester product (Entries 9-11) with the best result at a concertation of 1.0 M (Entry 10).

Table 4.2. Optimisation of reaction conditions.

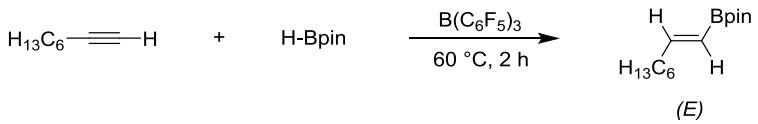

(E)

Entry	HBpin (eq.)	Solvent	Concentration	Yield (%)
1	1.5	dichloromethane	0.25 M	37
2	1.5	2-methyl-THF	0.25 M	5
3	1.5	THF	0.25 M	2
4	1.5	cyclopentylmethyl ether	0.25 M	2
5	1.5	toluene	0.25 M	83
6	1.2	toluene	0.25 M	82
7	1.1	toluene	0.25 M	82
8	1.0	toluene	0.25 M	73
9	1.1	toluene	0.50 M	88
10	1.1	toluene	1.00 M	88
11	1.1	toluene	2.00 M	82

Reaction conditions: (0.02 eq.) $B(C_6F_5)_3$, 1-octyne (1.0-1.5 eq.) and HBpin (1.0-1.5 eq.) heated at 60 °C in the indicated solvent for 2 h. Yield determined by ^1H NMR of the crude reaction mixture using 1,3,5-trimethoxybenzene as an internal standard.

4.7 Substrate Scope

Using these optimised conditions of alkyne (1 equivalent), HBpin (1.1 equivalents) and $B(C_6F_5)_3$ (2.5 mol%) at 60 °C for 2 hours, the substrate scope and functional group tolerance of this hydroboration protocol were explored (Scheme 4.17). In all reactions the stereoselectivity was determined by ^{1}H NMR $^3J_{H\text{-}H}$ coupling constants and by comparison to reported literature data. Terminal aliphatic alkynes bearing primary (**35a**), secondary (**35b**), and tertiary alkyl groups (**35c**) were successfully converted to the (*E*)-alkenyl boronic esters in good yield and stereoselectivity. No significant change in catalyst activity was observed with the increase of steric hindrance. The chemoselective hydroboration of alkyne was achieved in the presence of an alkene (**35d**). Good functional group tolerance was observed for halide- (**35e**), and silyl- (**35f**) groups tolerated without catalyst inhibition or deactivation. Internal alkyl alkynes gave the (*Z*)-boronic esters in good yield for both symmetrical (**35g**) and unsymmetrical examples (**35h**), with particularly good regioselectivity observed in the case of 4-methyl-2-pentenyl boronic ester (**35f**) (9:1), presumably due to different steric hindrance between methyl and *iso*propryl group.

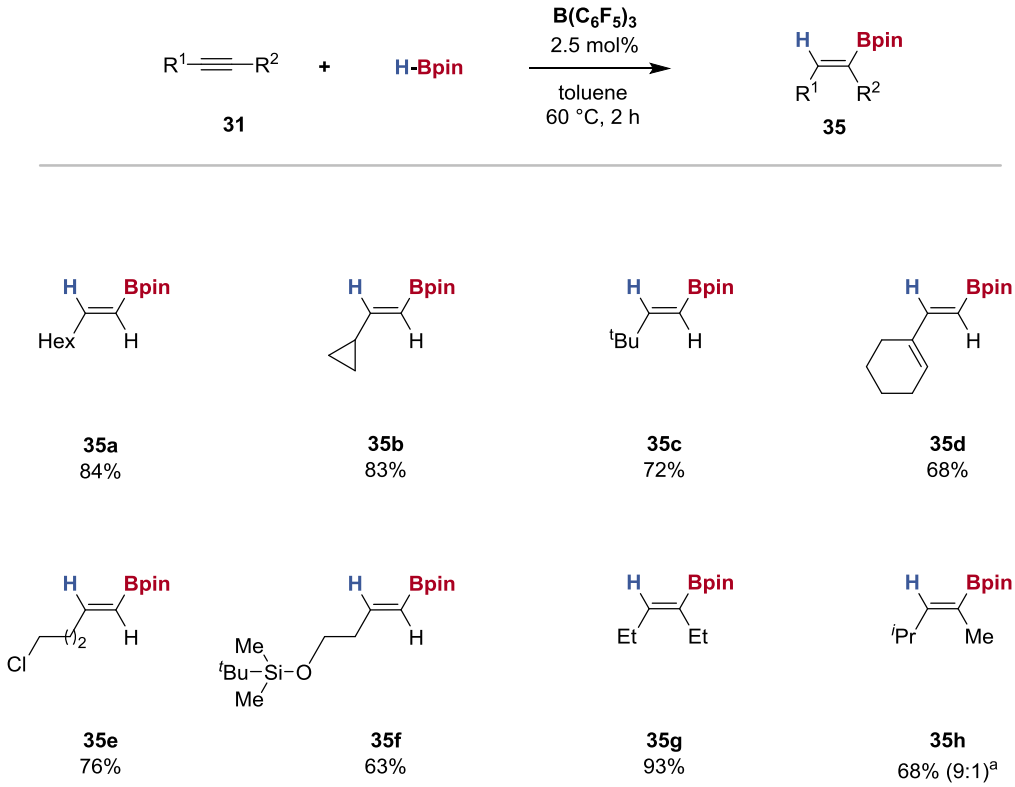

Scheme 4.17. Substrate scope. Isolated yield using $B(C_6F_5)_3$ (2.5 mol%), toluene, 2 h, 60 °C.[a] **35h** was obtained as mixture of regioisomers in the ratios indicated.

Terminal aryl alkynes all underwent successful hydroboration to the (*E*)-alkenyl boronic ester (**35i**-**35m**). Variation of the electronic character of the alkyne aryl substituent showed that equal catalyst activity was achieved across arenes bearing both electron-withdrawing (**35j** and **35l**) and electron-donating (**35k** and **35m**) substituents, and without exhibiting protodeborylation (Scheme 4.18). Groups susceptible to reduction such as an ester (**35l**) were tolerated. Diphenylacetylene (**35n**) gave the (*Z*)-alkenyl boronic ester (**35k**) in moderate yield, presumably caused by the steric hindrance. A disubstituted unsymmetrical alkyne could also be converted to the alkenyl boronic ester (**35o**) with good regioselectivity (9:1).

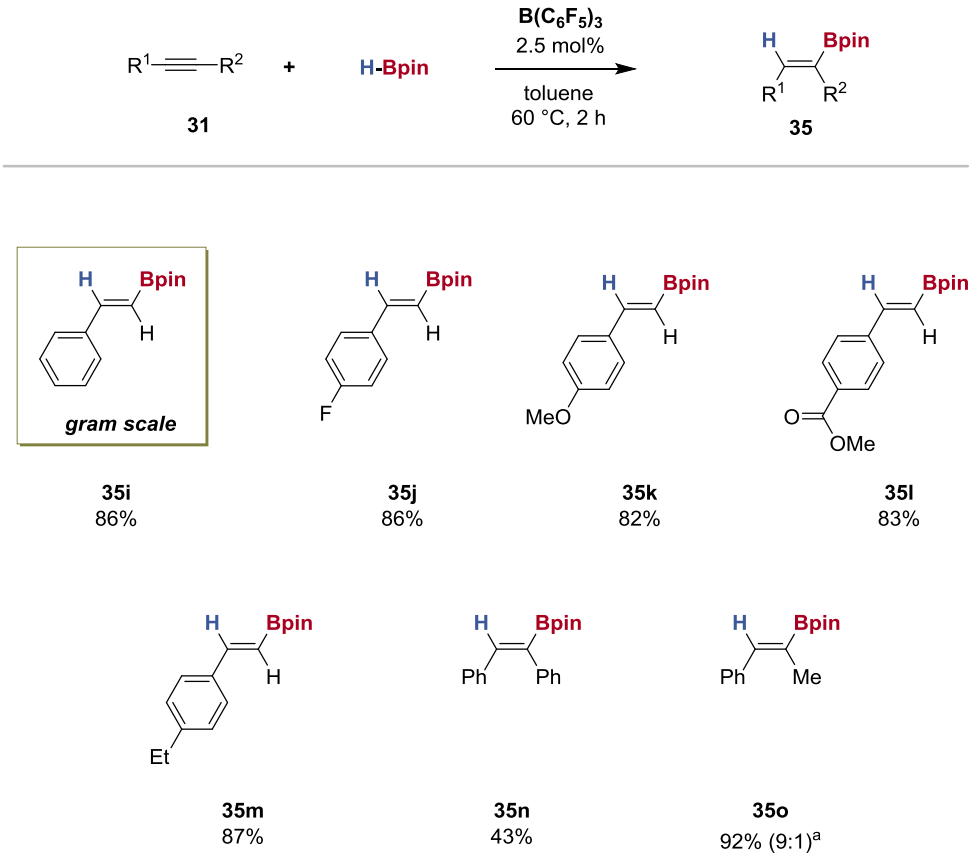

Scheme 4.18. Substrate scope. Isolated yield using $B(C_6F_5)_3$ (2.5 mol%), toluene, 2 h, 60 °C.[a] **35o** was obtained as mixture of regioisomers in the ratios indicated.

Unfortunately, alcohol, aldehyde, and nitrile functionalities were not tolerated, presumably due to catalyst deactivation caused by the strongly coordination nature of these substrates to $B(C_6F_5)_3$ (Scheme 4.19).

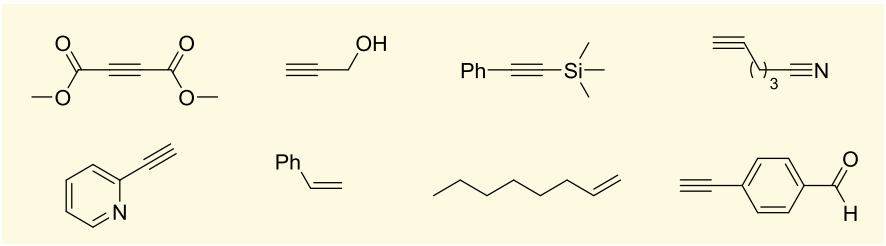

Scheme 4.19. Unsuccessful substrates.

Having established the competence of $B(C_6F_5)_3$ for initiating catalysis with zwitterion for the hydroboration of alkynes, we began to explore its potential in further applications. Recently, Oestreich and co-workers reported a detailed analysis of the difference in catalytic behavior of $B(C_6F_5)_3$ and $BArF_3$. While the stronger Lewis acid $BArF_3$ was able to promote the hydroboration of alkenes the parent compound $B(C_6F_5)_3$ was not a competent catalyst for this transformation. Hence, we wondered whether the Lewis acid zwitterion, formed by interaction between phenylacetylene and $B(C_6F_5)_3$, could be an effective catalyst for this transformation. Formation of catalytic amount of the zwitterion (**35i**) (5 mol%), *in situ*, in the presence of styrene and pinacol borane led to complete conversion of the starting material to give the alkyl boronic ester in excellent yield, and with complete control of regioselecivity (Scheme 4.20). Performing the reaction without any alkyne resulted only in trace amount of the product, in accordance with Oestreich and co-workers, confirming the pivotal role of the alkyne.

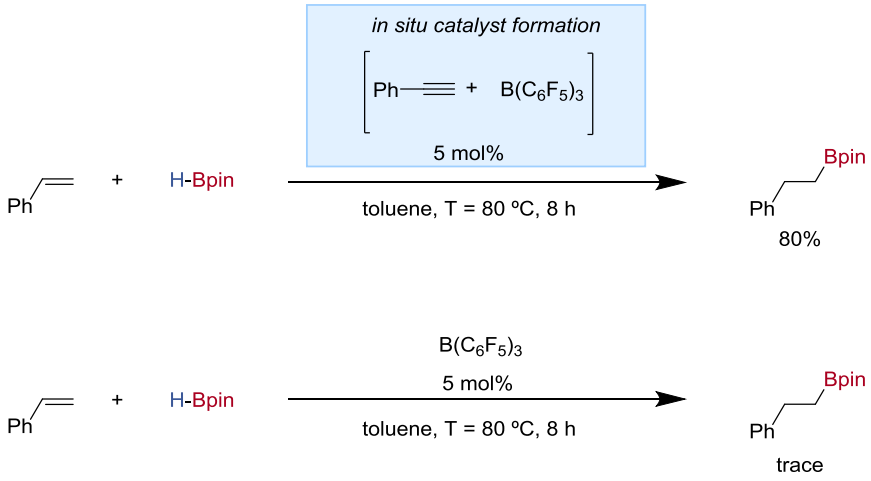

Scheme 4.20. Zwitterion- and $B(C_6F_5)_3$-catalysed hydroboration of styrene.

This result may pave the way for new tris(pentafluorophenyl)borane catalysis. Understanding the mode of operation of this catalytic system is challenging and will be the focus of future work.

4.8 Mechanistic Studies

Having characterised the zwitterion intermediate (**30**), and having established that $B(C_6F_5)_3$ could initiate hydroboration of alkynes, we wondered whether the zwitterion could be a common intermediate for 1,1-carboboration and $B(C_6F_5)_3$-catalysed hydroboration of alkynes. First, a stoichiometric reaction between $B(C_6F_5)_3$ with HBpin was carried out (Scheme 4.21). Monitoring the reaction by ^{11}B and ^{1}H NMR spectroscopy showed no formation of Piers' borane or any borohydride but decomposition products such as B_2pin_3 and other undefined boron oxygen species, along with concurrent H_2 generation. This siggested that a different mechanism compared to that reported by Stephan and co-workers may be operating.

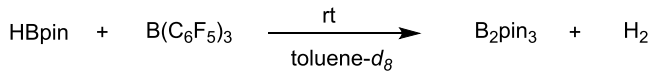

Scheme 4.21. Stoichiometric reaction of $B(C_6F_5)_3$ and HBpin.

The catalytic activity of the DABCO-trapped zwitterion (**34**) was then tested. Interestingly, lower reactivity (no conversion at 2.5 mol% loading and 15% conversion at 10 mol% loading) was observed when using the zwitterion (**34b**) as the catalyst, presumably due to the strong binding of DABCO and decreased Lewis acidity of Lewis acid-base complex. To clarify the role of the Lewis base we tested DABCO·$B(C_6F_5)_3$ for catalytic activity under our optimised reaction conditions (Scheme 4.22). No catalysis was observed under standard reaction conditions and only when the catalyst loading was increased could catalytic activity be observed, albeit with much reduced activity (Scheme 4.22). The addition of DABCO thus inhibits catalysis both by coordination to any free $B(C_6F_5)_3$, but also by promoting the formation of alkynyl borate (**34b**). Furthermore, the addition of base was observed to promote hydride transfer between HBpin and $B(C_6F_5)_3$[33] which decreases the amount of the active $B(C_6F_5)_3$ and increased deleterious side reactions.

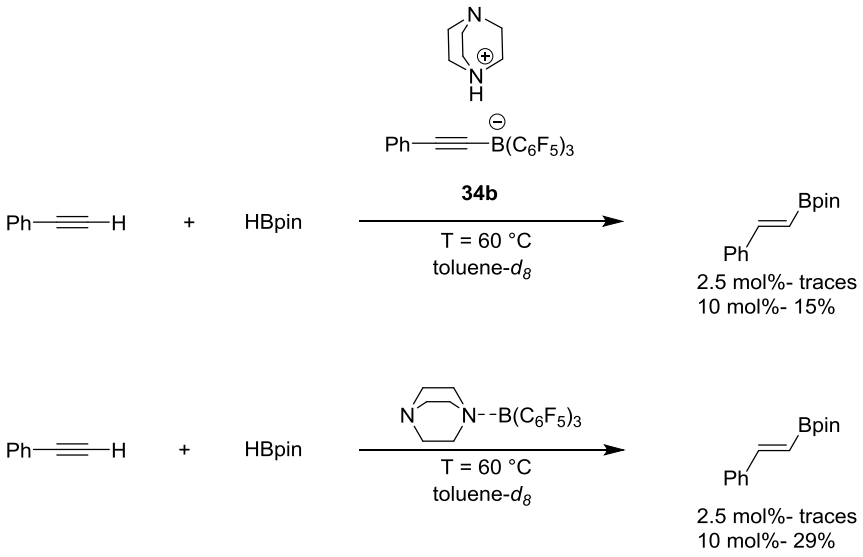

Scheme 4.22. Catalysis using zwitterion (**34b**); catalysis using DABCO·$B(C_6F_5)_3$.

As the *p*-methoxy phenylacetylene zwitterion exhibited increased thermal stability compared to the unsubstituted parent compound, we next investigated catalyst turnover. Unfortunately, forming the zwitterion (**32k**) *in situ* and treating it with a stoichiometric amount of pinacol borane did not result in catalyst turnover. $^{13}C\{H\}$ NMR spectrum of the reaction mixture showed a new resonance (δ ^{13}C = 240.1) which was assigned to *tert*-butyl methyl ketone by 2D NMR and by comparison with previously reported data. This is not surprising as strong Lewis acid have been reported to promote pinacol rearrangement.[34] However, when substoichiometric loading of zwitterion (**32k**) was used no pinacol rearrangement was observed. Generating the zwitterion (**32k**) *in situ* and using as the catalyst (<2.5 mol%) for the hydroboration of *p*-methoxy phenylacetylene, successfully promoted hydroboration formation of the *(E)*-alkenyl borane (**35k**) within 2 hours (Scheme 4.23).

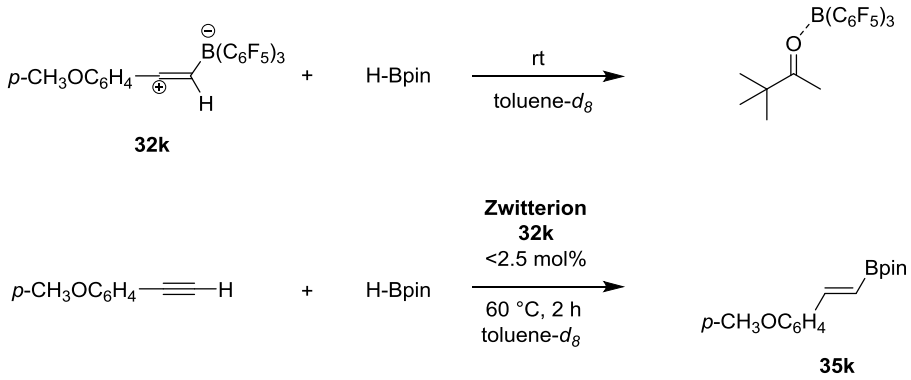

Scheme 4.23. Stoichiometric reactivity of zwitterion (**32k**) and HBpin; Catalytic competence of the zwitterion (**32k**) in the hydroboration of *p*-methoxy phenylacetylene.

Based on these observations a mechanism consistent with that reported by Stephan is presumably operating. However mechanistic investigation are still ongoing to determine if the zwitterion is an intermediate or is acting as strong Lewis acid and to determine the rate-limiting step of this hydroboration protocol.

4.9 Conclusions and Future work

A potential cross-over between 1,1-carboboration and $B(C_6F_5)_3$-catalysed hydroboration has been investigated and its divergent reactivity identified (Scheme 4.24). This has led to the characterisation of highly reactive zwitterionic intermediates. The thermal stability of these species in solution has been widely characterised by NMR spectroscopy and the tuning of the alkynyl substituent has allowed, for the first time, the characterisation by single crystal X-ray spectroscopy. This has led to the development of a $B(C_6F_5)_3$-catalysed hydroboration of alkynes using HBpin. The reaction is proposed to occur by Lewis acid activation of the alkynes to form a highly reactive zwitterionic species, which then undergoes concerted hydroboration with HBpin to give the alkenyl borane.

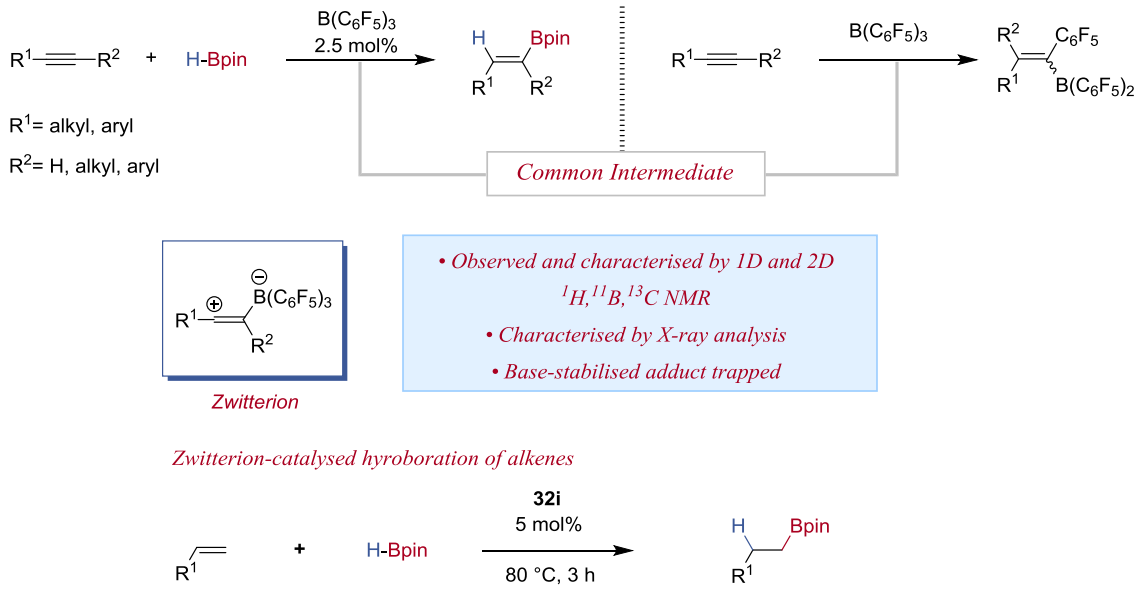

Scheme 4.24. Zwitterion-catalysed hydroboration.

Future work should focus on further analysis of the zwitterion reactivity. Its catalytic use as a Lewis acid in cycloaddition reaction and in catalytic hydrofunctionalisation will be investigated.

4.10 References

[1] A. G. Massey, A. S. Park, F. G. Stone, *Proc. Chem. Soc.*, 1964, **0**, 212–212.

[2] J. R. Lawson and R. L. Melen, *Inorg. Chem.*, 2017, **56**, 8627–8643.

[3] W. E. Piers and T. Chivers, *Chem. Soc. Rev.*, 1997, **26**, 345–354.

[4] W. E. Piers, T. Chivers and W. Piers, *Chem. Soc. Rev.*, 1998, **26**, 345–354.

[5] D. W. Stephan, *J. Am. Chem. Soc.*, 2015, **137**, 10018–10032.

[6] G. C. Welch and D. W. Stephan, *J. Am. Chem. Soc.*, 2007, **129**, 1880–1881.

[7] G. Kehr and G. Erker, *Chem. Commun.*, 2012, **48**, 1839–1850.

[8] B. Wrackmeyer, *Coord. Chem. Rev.*, 1995, **145**, 125–156.

[9] C. Chen, T. Voss, R. Frö, G. Kehr and G. Erker, *Org. Lett.*, 2011, **13**, 250–253.

[10] G. Kehr and G. Erker, *Chem. Sci.*, 2016, **7**, 56–65.

[11] C. Chen, G. Kehr, R. Fröhlich and G. Erker, *J. Am. Chem. Soc.*, 2010, **132**, 13594–13595.

[12] C. Jiang, O. Blacque and H. Berke, *Organometallics*, 2010, **29**, 125–133.

[13] C. Chen, F. Eweiner, B. Wibbeling, R. Fröhlich, S. Senda, Y. Ohki, K. Tatsumi, S. Grimme, G. Kehr and G. Erker, *Chem. - An Asian J.*, 2010, **5**, 2199–2208.

[14] M. A. Dureen and D. W. Stephan, *J. Am. Chem. Soc.*, 2009, **131**, 8396–8397.

[15] R. Liedtke, R. Fröhlich, G. Kehr and G. Erker, *Organometallics*, 2011, **30**, 5222–5232.

[16] P. Eisenberger, A. M. Bailey and C. M. Crudden, *J. Am. Chem. Soc.*, 2012, **134**, 17384–17387.

[17] Q. Yin, Y. Soltani, R. L. Melen and M. Oestreich, *Organometallics*, 2017, **36**, 2381–2384.

[18] J. S. McGough, S. M. Butler, I. a Cade and M. J. Ingleson, *Chem. Sci.*, 2016, **7**, 3384–3389.

[19] J. R. Lawson, L. C. Wilkins and R. L. Melen, *Chem. Eur. J.*, 2017, **23**, 10997–11000.

[20] M. Fleige, J. Möbus, T. vom Stein, F. Glorius and D. W. Stephan, *Chem. Commun.*, 2016, **52**, 10830–10833.

[21] Q. Yin, S. Kemper, H. F. T. Klare and M. Oestreich, *Chem. Eur. J.*, 2016, **22**, 13840–13844.

[22] C. Villiers and M. Ephritikhine, *Tetrahedron Lett.*, 2003, **44**, 8077–8079.

[23] S. Harder and J. Spielmann, *J. Organomet. Chem.*, 2012, **698**, 7–14.

[24] D. W. Stephan and G. Erker, *Chem. Sci.*, 2014, **5**, 2625.

[25] T. Müller, M. Juhasz and C. A. Reed, *Angew. Chem. Int. Ed.*, 2004, **43**, 1543–1546.

[26] P. A. Byrne, S. Kobayashi, E.-U. Würthwein, J. Ammer and H. Mayr, *J. Am. Chem. Soc.*, 2017, **139**, 1499–1511.

[27] K. Müther, R. Fröhlich, C. Mück-Lichtenfeld, S. Grimme and M. Oestreich, *J. Am. Chem. Soc.*, 2011, **133**, 12442–12444.

[28] A. R. Nödling, K. Müther, V. H. G. Rohde, G. Hilt and M. Oestreich, *Organometallics*, 2014, **33**, 302–308.

[29] K. Müther, P. Hrobárik, V. Hrobáriková, M. Kaupp and M. Oestreich, *Chem. - A Eur. J.*, 2013, **19**, 16579–16594.

[30] R. K. Schmidt, H. F. T. Klare, R. Fröhlich and M. Oestreich, *Chem. Eur. J.*, 2016, **22**, 5376–5383.

[31] E. Koch, H. Siehl, M. Hanack, *Tetrahedron*, 1985, **26**, 1493–1496.

[32] T. S. Abram and W. E. Watts, *J. Chem. Soc. Perkin Trans. 1*, 1977, **7**, 1522.

[33] C. J. Lata and C. M. Crudden, *J. Am. Chem. Soc.*, 2010, **132**, 131–137.

[34] C. Pavlik, M. Morton and M. Smith, *Synlett*, 2011, **2011**, 2191–2194.

Chapter 5−Experimental Methods

5.1 General Information

All manipulations were carried out under an argon atmosphere using standard Schlenk or glove box techniques, $Et_3Al{\cdot}DABCO$ and $B(C_6F_5)_3$ were stored and handled in glovebox. Solvents were dried over Na/benzophenone and distilled under an atmosphere of argon. C_6D_6 and toluene-d_8 were dried over potassium and then distilled under argon. NMR spectra were recorded on Bruker PRO 500 MHz (^{1}H 500.2 MHz, ^{11}B 160.5 MHz ^{13}C 125.8 MHz) AVA 500 (^{1}H 500.1 MHz, ^{2}H 500.2 MHz, ^{13}C 125.8 MHz MHz) or AVA 600 (^{1}H 600.8 MHz, ^{13}C 151.1 MHz) spectrometers. ^{1}H and ^{13}C were referenced to residual solvent signals ^{1}H NMR: δ (ppm) = 7.26 ($CDCl_3$), 7.15 (C_6D_6), (7.09) toluene-d_8 ^{13}C NMR: δ (ppm) = 77.16 ($CDCl_3$), 128.06 (C_6D_6), 137.48 (toluene-d_8).
Mass spectra were recorded on Thermo/Finngan MAT 900 Sector instrument (EI).
Infra-red (IR) spectra were recorded using Perkin-Elmer Spectrum One FT-IR (serial no. 10823). Melting points (mp) were determined on a Stuart Scientific SMP10 melting point apparatus in capillary tubes. Flash column chromatography was performed on silica gel (Merck Kielselgel 60, 40-63 μm) and product spots were visualised by UV light at 254 nm and $KMnO_4$. All the flash column were performed on a 10 mL syringe (outside diameter 17.30 mm).
Deuterated 3,3-dimethyl-1-butyne and deuterated pinacolborane (DBpin) were prepared according to modified literature procedures.[1,2] Di*iso*butylaluminium hydride (1 M, hexane) cat N 190306, triethylaluminium (1 M, hexane) cat N 252662 and 1,4-diazabicyclo[2.2.2]octane (DABCO) were purchased from Sigma Aldrich and used without further purification. Red-Al (sodium bis(2-methoxyethoxy)aluminum hydride, 70% weight in toluene) cat N 196193 were purchased from Sigma Aldrich, stored in a Young's flask and used without further purification. Pinacolborane (HBpin) Cat N 010818 was purchased from Fluorochem stored in a Young's flask. Phenylacetylene-2-^{13}C was purchased from Sigma Aldrich and used without further purification. Ethynylferrocene-2-^{13}C was generously donated by Prof. G. Lloyd-Jones.
All other reagents were purchased from Sigma Aldrich, Alfa Aesar, Acros organics, Tokyo Chemical Industries UK, and Fluorochem and used without further purification.

5.2 Experimental Details for Chapter 2

Synthesis of *$AlEt_3$·DABCO*

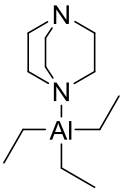

$AlEt_3$ (1 M in hexane, 6.0 mmol, 6.0 mL) was added to a solution of 1,4-diazabicyclo[2.2.2]octane (6.6 mmol, 740 mg) in diethyl ether (15.0 mL) at 0 °C and stirred for 1 hour.

The solution was then concentrated to 5.0 mL leading to product precipitation and solid was isolated by cannula filtration. The crude solid was recrystallised by dissolution in hot 1/1 benzene/hexane solution followed by slow cooling to 4 °C for 24 hours to give $Et_3Al{\cdot}$DABCO complex (1080 mg, 70%) as colourless needles. Melting point (argon sealed capillary) 87.2-87.9 °C.

HRMS (EI) = mass calc'd for $C_{12}H_{27}AlN_2$ 226.19842; found: 226.19824.

^{1}H NMR (500 MHz, C_6D_6) δ 2.15 (s, N−C**H$_2$**, 12H), δ 1.47 (t, CH_2−C**H$_3$** $J_{H\text{-}H}$ = 8.1 Hz, 9H), 0.10 (q, Al−C**H$_2$** $J_{H\text{-}H}$ = 8.1 Hz, 6H).

^{13}C{H} NMR (126 MHz, C_6D_6) δ 45.2, 10.4, −1.2.

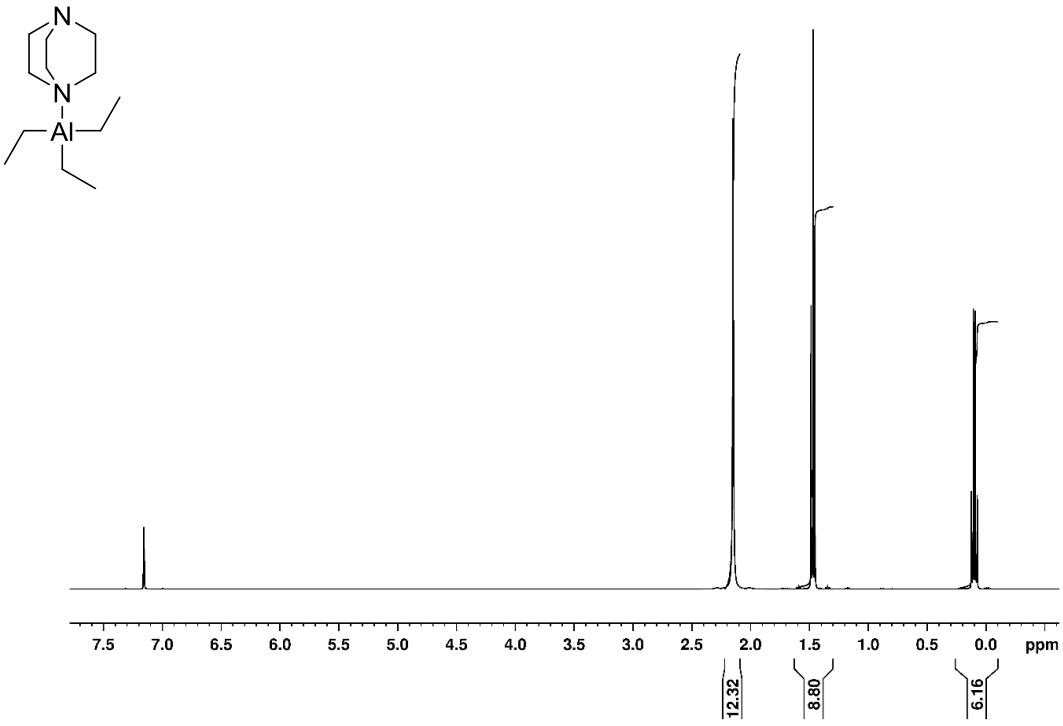

^{1}H NMR (500 MHz, C_6D_6) of Et_3Al·DABCO

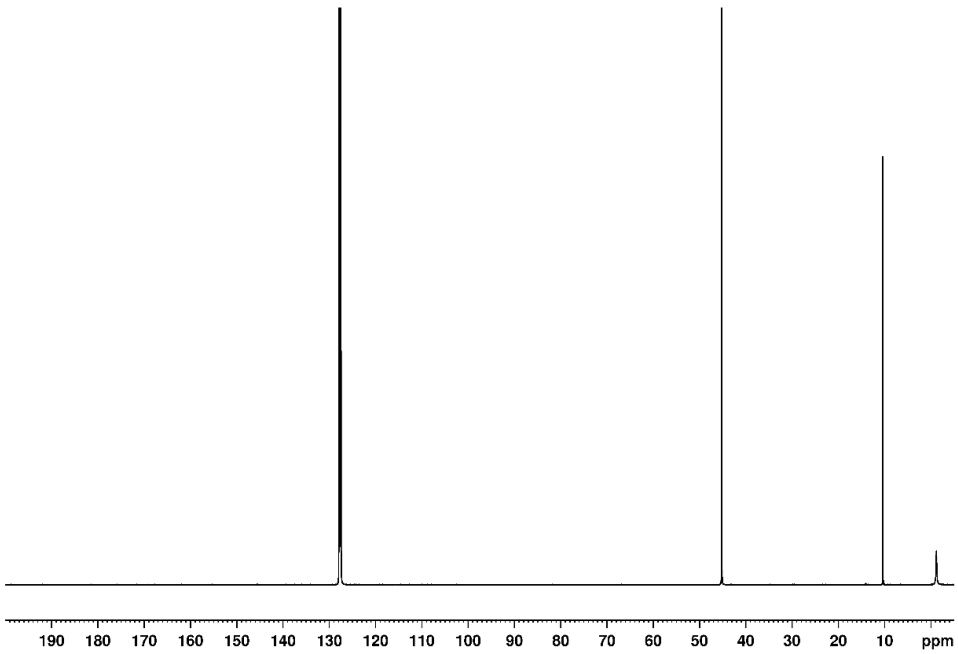

^{13}C{H} NMR (126 MHz, C_6D_6) of $AlEt_3$·DABCO

Synthesis of $^{i}Bu_2Al\,H{\cdot}DABCO$

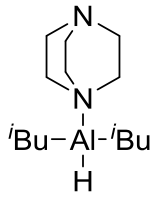

^{i}BuAl-H (1 M in hexane, 6.0 mmol, 6.0 mL) was added to a solution of 1,4-diazabicyclo[2.2.2]octane (6.6 mmol, 740 mg) in diethyl ether (15.0 mL) at 0 °C and stirred for 1 hour.

The solution was then concentrated to 5.0 mL leading to product precipitation and solid was isolated by cannula filtration. The crude solid was recrystallised from hexane at −20 to give $^{i}Bu_2AlH{\cdot}DABCO$ complex (837 mg, 45%) as colourless needles.

^{1}H NMR (500 MHz, C_6D_6) δ 4.0 (br s, Al−**H** 1H) 2.20 (s, 12H), 2.17 (m, CH_2−C**H**− $(CH_3)_2$, 2H) δ 1.33 (d, CH_2−CH−(C**H$_3$**)$_2$ *J* = 6.7 Hz, 4H), 0.12 (s, Al−C**H$_2$** *J* = 6.7 Hz, 4H).

^{13}C{H} NMR (126 MHz, C_6D_6) δ 45.3, 28.4, 27.1, 21.2 (br s).

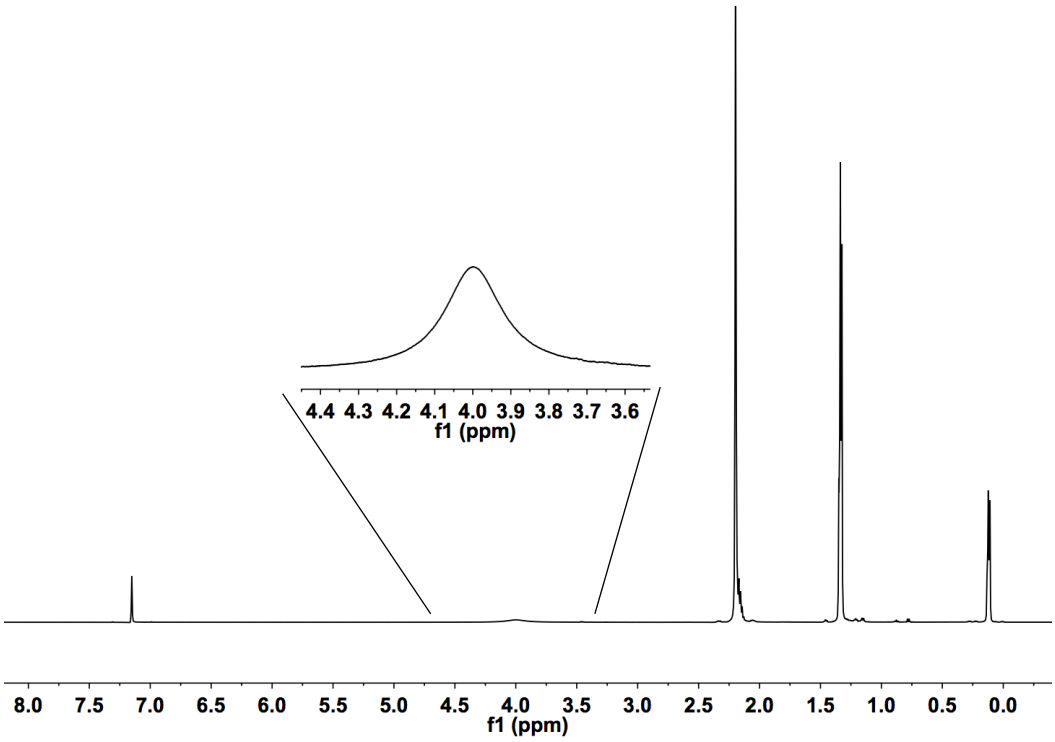

^{1}H NMR (500 MHz, C_6D_6) of $^{i}Bu_2Al$·DABCO

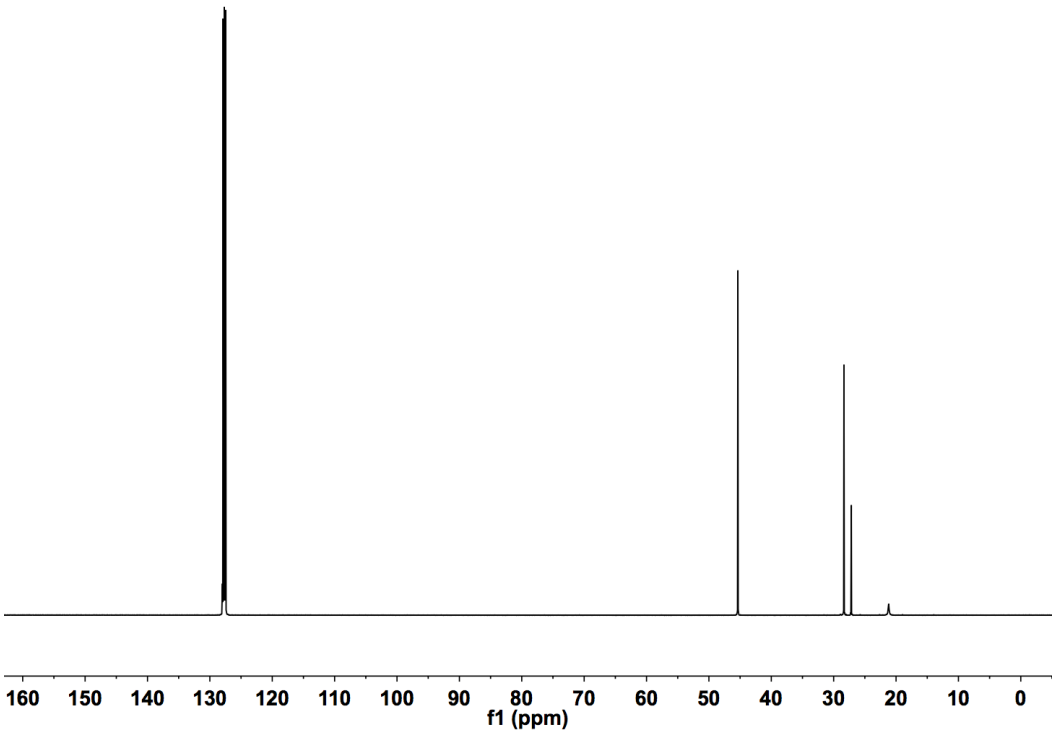

$^{13}C\{H\}$NMR (126 MHz, C_6D_6) of $^{i}Bu_2Al$·DABCO

5.3 Optimisation of catalysis conditions: hydroboration of alkynes

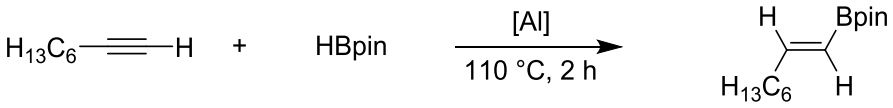

1-Octyne (0.15 mmol, 0.022 mL) was added to a solution of catalyst (10% or 5%), 1,3,5-trimethoxybenzene (0.03 mmol, 5.0 mg) and HBpin (0.032 mL, 0.22 mmol) in toluene-d_8 (0.60 mL) at room temperature and then heated at 110 °C for 2 h. The yield was determined by ^{1}H NMR of crude reaction mixture using 1,3,5-trimethoxybenzene as internal standard.

Entry	Catalyst (10 mol%)	Yield (%)
1	$AlMe_3$	23
2	$AlEt_3$	59
3	$^iBu_2Al$-H	73
4	$AlEt_3$·DABCO	72
5	$(AlMe_3)_2$·DABCO	36

Entry	Catalyst (5 mol%)	Yield
1	$AlEt_3$	34
2	$^iBu_2Al$-H	43
3	$AlEt_3$·DABCO	42

Solvent screening

1-Octyne (0.15 mmol, 0.022 mL) was added to a solution of Et_3Al·DABCO (0.015 mmol, 3.4 mg), 1,3,5-trimethoxybenzene (0.03 mmol, 5.0 mg) and HBpin (0.032 mL, 0.22 mmol) in the appropriate solvent (0.60 mL) at room temperature and then heated at 110 °C for 2 h. The mixture was filtered through a short pad of silica and solvent removed *in vacuo*. The mixture was dissolved in toluene-d_8 and the yield was determined by ^{1}H NMR using 1,3,5-trimethoxybenzene as internal standard.

Entry	Solvent	Yield (%)
1	dichloromethane	10
2	2-methyl-THF	12
3	Cyclopentyl methyl ether	4

HBpin equivalents

1-Octyne (0.15 mmol, 0.022 mL) was added to a solution of Et_3Al·DABCO (0.015 mmol, 3.4 mg), 1,3,5-trimethoxybenzene (0.03 mmol, 5.0 mg) and the corresponding amount of HBpin (1.2, 1.5, 2.0 eq.) in toluene-d_8 (0.60 mL) at room temperature and then heated at 110 °C for 2 h. The yield was determined by ^{1}H NMR of crude reaction mixture using 1,3,5-trimethoxybenzene as internal standard.

Entry	HBpin (eq.)	Yield (%)
1	1.2	70
2	1.5	72
3	3.0	84

Reaction concentration

1-Octyne (1 eq.) was added to a solution of Et_3Al·DABCO (0.1 eq), 1,3,5-trimethoxybenzene (0.03 mmol, 5.0 mg) and HBpin (1.2 eq.) in toluene-d_8 (0.60 mL) at room temperature and then heated at 110 °C for 2 h. The yield was determined by ^1H NMR of crude reaction mixture using 1,3,5-trimethoxybenzene as internal standard.

Entry	Concentration	Yield (%)
1	0.25 M	72
2	0.50 M	65
3	1.00 M	60

Temperature screening

1-Octyne (0.15 mmol, 0.022 mL) was added to a solution of Et_3Al·DABCO (0.015 mmol, 3.4 mg), 1,3,5-trimethoxybenzene (0.03 mmol, 5.0 mg) and HBpin (0.18 mmol, 0.024 mL) in toluene-d_8 (0.60 mL) at room temperature and the catalysis was then performed for 2 h at the indicated temperature.

Entry	T (°C)	Yield (%)
1	110	72
2	60	28
3	25	trace

Reaction Time screening

1-Octyne (0.15 mmol, 0.022 mL) was added to a solution of $Et_3Al{\cdot}DABCO$ (0.015 mmol, 3.4 mg), 1,3,5-trimethoxybenzene (0.03 mmol, 5.0 mg) and HBpin (0.18 mmol, 0.024 mL) in toluene-d_8 (0.60 mL) at room temperature and the catalysis was then performed at 110 °C for the time indicated.

Entry	t (h)	Yield (%)
1	1	50
2	2	72
3	3	81

Base screening

1-Octyne (0.15 mmol, 0.022 mL) was added to a solution of catalyst (0.015 mmol), 1,3,5-trimethoxybenzene (0.03 mmol, 5.0 mg), the base (0.015 mmol) and HBpin (0.18 mmol, 0.024 mL) in toluene-d_8 (0.60 mL) at room temperature and then heated at 110 °C for 2 h. The yield was determined by ^1H NMR of crude reaction mixture using 1,3,5-trimethoxybenzene as internal standard.

Entry	Catalyst (10 mol%)	Yield (%)
1	$^{i}Bu_2Al\text{-}H \cdot DABCO$	74
2	$AlEt_3{\cdot}DABCO$	72
3	$AlEt_3{\cdot}DABCO^*$	38
4	$AlEt_3{\cdot}DMAP$	40
5	$AlEt_3{\cdot}P(Ph)_3$	65
6	$AlEt_3{\cdot}$lutidine	71
7	$AlEt_3{\cdot}$pyrazine	56

* Catalysis was performed weighting the species in air (2 min)

General procedure A: Hydroboration using $^{i}Bu_2Al$-H

The alkyne (0.75 mmol) was added to a solution of $^{i}Bu_2Al$-H (1 M in hexane, 0.075 mL) in toluene (3.0 mL) and HBpin (0.130 mL, 0.90 mmol) was then added at room temperature.
The reaction mixture was stirred for 2 h at 110 °C. The mixture was filtred through a short pad of silica, and the product was purified by flash chromatography.

General procedure B: Hydroboration using Et_3Al·DABCO

The alkyne (0.75 mmol) was added to a solution of Et_3Al·DABCO (0.075 mmol, 17.0 mg) and HBpin (0.130 mL, 0.90 mmol) in toluene (3 mL) at room temperature.
The reaction mixture was stirred for 2 h at 110 °C. The mixture was filtred through a short pad of silica, and the product was purified by flash chromatography.

5.4 Characterisation of the alkenyl boronic esters

***(E)*-4,4,5,5-Tetramethyl-2-(oct-1-enyl)-1,3,2-dioxaborolane**

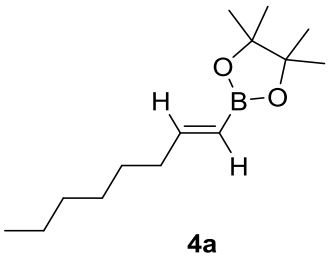

4a

According to general procedure A, 1-octyne (0.75 mmol, 0.110 mL), HBpin (0.9 mmol, 0.130 mL), $^{i}Bu_2Al$-H (1 M in hexane, 0.075 mL) were allowed to react. The residue was purified by flash chromatography (eluent: hexane/ethyl acetate 98:2), to give the boronic ester **4a** (0.127 g, 0.53 mmol, 71%) as a colourless oil.

According to general procedure B, 1-octyne (0.75 mmol, 0.110 mL), HBpin (0.9 mmol, 0.130 mL), $Et_3Al{\cdot}DABCO$ (0.075 mmol, 17.0 mg,) were allowed to react to give the boronic ester **4a** (112 mg, 0.50 mmol, 64%) as a colourless oil.

^{1}H NMR (500 MHz, $CDCl_3$) δ 6.63 (dt, *J* = 17.9, 6.4 Hz, 1H), 5.41 (dt, *J* = 17.9, 1.5 Hz, 1H), 2.14 (td, *J* = 7.9, 1.5 Hz, 2H), 1.45 – 1.34 (m, 3H), 1.34 – 1.19 (m, 14H), 0.92 – 0.81 (m, 6H).

^{11}B NMR (160 MHz, $CDCl_3$) δ 29.73.

^{13}C{H} NMR (126 MHz, $CDCl_3$) δ 154.9, 118.6 (br, *C-B*), 83.0, 35.9, 31.7, 28.9, 28.2, 24.8, 22.6, 14.1.

Data were in accordance with those previously reported.[3]

***(E)*-4,4,5,5-Tetramethyl-2-(cyclopropyl-1-enyl)-1,3,2-dioxaborolane**

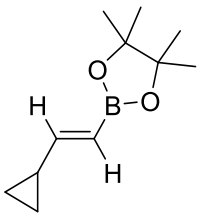

4b

According to general procedure A, cyclopropylacetylene (0.75 mmol, 0.063 mL), HBpin (0.9 mmol, 0.130 mL), $^i Bu_2Al$-H (1 M in hexane, 0.075 mL) were allowed to react. The residue was purified by flash chromatography (eluent: hexane/ethyl acetate 98:2), to give the boronic ester **4b** (112 mg, 0.58 mmol, 75%) as a colourless oil.

According to general procedure B, cyclopropylacetylene (0.75 mmol, 0.063 mL), HBpin (0.9 mmol, 0.130 mL), $Et_3Al{\cdot}DABCO$ (0.075 mmol, 17.0 mg) were allowed to react to give the boronic ester **4b** (104 mg, 0.54 mmol, 72%) as a colourless oil.

^{1}H NMR (500 MHz, CDCl3) δ 6.07 (ddd, *J* = 17.8, 9.3, 1.4 Hz, 1H), 5.49 (d, *J* = 17.8 Hz, 1H), 1.55 – 1.46 (m, 1H), 1.25 (s, 12H), 0.82 – 0.76 (m, 2H), 0.55 – 0.50 (m, 2H).

^{11}B NMR (160 MHz, $CDCl_3$) δ 29.65.

^{13}C{H} NMR (126 MHz, $CDCl_3$) δ 158.7, 115.4 (br, *C-B*), 83.0, 24.9, 17.1, 8.0.

Data were in accordance with those previously reported.[3]

***(E)*-2-4,4,5,5-Tetramethyl-2-(3,3-dimethylbut-1-enyl) 1,3,2-dioxaborolane**

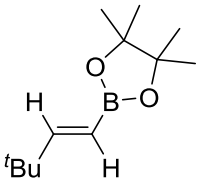

4c

According to general procedure A, 3,3-dimethyl-1-butyne (0.75 mmol, 0092 mL), HBpin (0.9 mmol, 0.130 mL), $^{i}Bu_2Al$-H (1 M in hexane, 0.075 mL) were allowed to react. The residue was purified by flash chromatography (eluent: hexane/ethyl acetate 98:2), to give the boronic ester **4c** (121 mg, 0.57 mmol, 77%) as a colourless oil.

According to general procedure B, 3,3-dimethyl-1-butyne (0.75 mmol, 0092 mL), HBpin (0.9 mmol, 0.130 mL), $Et_3Al{\cdot}DABCO$ (0.075 mmol, 17.0 mg) were allowed to react to give the boronic ester **4c** (110 mg, 0.52 mmol, 70%) as a colourless oil.

^{1}H NMR (500 MHz, $CDCl_3$) δ 6.62 (d, *J* = 18.3 Hz, 1H), 5.34 (d, *J* = 18.3 Hz, 1H), 1.25 (s, 12H), 1.00 (s, 9H).

^{11}B NMR (160 MHz, $CDCl_3$) δ 30.18.

^{13}C{H} NMR (126 MHz, $CDCl_3$) δ 164.5, 112.5 (br, *C*-*B*), 83.1, 35.1, 28.9, 24.9.

Data were in accordance with those previously reported.[4]

***(Z)*-4,4,5,5-Tetramethyl-2-(ethyl-1-buten-1-yl)-1,3,2-dioxaborolane**

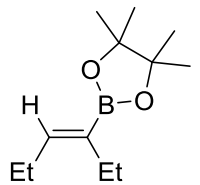

4d

According to general procedure A, 3-hexyne (0.75 mmol, 0.0.85 mL), HBpin (0.9 mmol, 0.130 mL), $^{i}Bu_2Al$-H (1 M in hexane, 0.075 mL) were allowed to react. The residue was

purified by flash chromatography (eluent: hexane/ethyl acetate 98:2), to give the boronic ester **4d** (96 mg, 0.45 mmol, 61%) as a colourless oil.

According to general procedure B, 3-hexyne (0.75 mmol, 0.085 mL), HBpin (0.9 mmol, 0.130 mL), $Et_3Al{\cdot}DABCO$ (0.075 mmol, 17.0 mg) were allowed to react to give the boronic ester **4d** (85 mg, 0.40 mmol, 54%) as a colourless oil.

^{1}H NMR (500 MHz, $CDCl_3$) δ 6.25 (t, *J* = 7.0 Hz, 1H), 2.18 – 2.09 (m, 4H), 1.25 (s, 12H), 0.99 (t, *J* = 7.6 Hz, 3H), 0.93 (t, *J* = 7.5 Hz, 3H).

^{11}B NMR (160 MHz, $CDCl_3$) δ 30.56.

^{13}C{H} NMR (126 MHz, $CDCl_3$) δ 147.1, 133.4 (br, *C-B*), 83.1, 24.9, 21.8, 21.6, 15.0, 14.0.

Data were in accordance with those previously reported.[5]

***(Z)*-4,4,5,5-Tetramethyl-2-(hex-2-en-3-yl)-1,3,2-dioxaborolane**

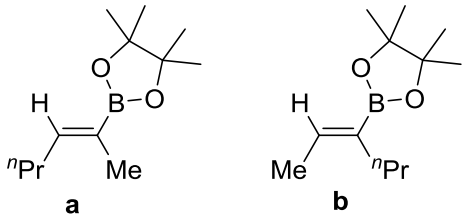

4e

According to general procedure A, 2-hexyne (0.75 mmol, 0.085 mL), HBpin (0.9 mmol, 0.130 mL), $^i Bu_2Al$-H (1 M in hexane, 0.075 mL) were allowed to react. The residue was purified by flash chromatography (eluent: hexane/ethyl acetate 98:2), to give the boronic ester **4e** as a colourless oil.

Overall yield 74% (70[a] +30[b]), compound **a** (81 mg, 0.38 mmol), compound **b** (0.17 mmol, 35 mg). According to general procedure B, 2-hexyne (0.75 mmol, 0.85 mL), HBpin (0.9 mmol, 0.130 mL), $Et_3Al{\cdot}DABCO$ (0.075 mmol, 17.0 mg) were allowed to react to give the boronic ester **4e** as a colourless oil.

Overall yield 66% (69[a]+31[b]) compound **a** (74 mg, 0.34 mmol), compound **b** (0.15 mmol, 25 mg).

^{1}H NMR 4e[a] isomer (500 MHz, $CDCl_3$) δ 6.31 (td, *J* = 7.0, 1.8 Hz, 1H) 2.10 (q, *J* = 7.1, 4H), 1.70 (d, *J* = 6.8 Hz, 3H), 1.67 (d, *J* = 1.6 Hz, 3H), 1.46-1.38 (m, 2H), 1.25 (s, 12H), 0.91 (t, *J* = 7.4 Hz, 3H).

^{1}H NMR 4e[b] isomer (500 MHz, $CDCl_3$) δ 6.41 (q, *J* = 6.8 Hz, 1H), 1.67 (d, *J* = 6.82 Hz, 3H), 1.42-1.34 (m, 2H) 1.24 (s, 12H), 0.87 (t, *J* = 7.37 Hz, 3H).

^{11}B NMR (160 MHz, $CDCl_3$) δ 30.37.

^{13}C{H} NMR 4e[a] isomer (126 MHz, $CDCl_3$) δ 146.5, 126.9 (br, *C-B*), 83.2, 30.9, 24.9, 22.2, 14.1, 14.0.

^{13}C{H} NMR 4e[b] isomer (126 MHz, $CDCl_3$) δ 140.4, 133.5 (br, *C-B*), 83.0, 30.2, 24.9, 23.1, 14.3, 14.2.

Data were in accordance with those previously reported.[6]

***(Z)*-4,4,5,5-Tetramethyl-2-(1,3 dimethyl-1-butenyl)-1,3,2-dioxaborolane**

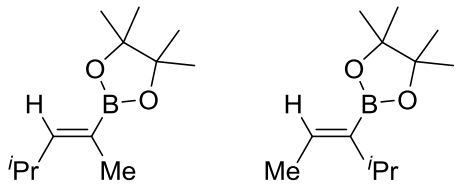

4f

According to general procedure A, 4-methyl-2-pentyne (0.75 mmol, 0.110 mL), HBpin (0.9 mmol, 0.130 mL), ^{i}Bu$_2$Al-H (1 M in hexane, 0.075 mL) were allowed to react. The residue was purified by flash chromatography (eluent: hexane/ethyl acetate 98:2), to give the boronic ester **4f** as a colourless oil.

Overall yield 85% (82+18[b]), compound **a** (109 mg, 0.52 mmol), and compound **b** (24 mg, 0.11 mmol). According to general procedure B, 4-methyl-2-pentyne (0.75 mmol, 0.110 mL), HBpin (0.9 mmol, 0.130 mL), $Et_3Al{\cdot}DABCO$ (0.075 mmol, 17.0 mg) were allowed to react to give the boronic ester **4f** as a colourless oil.

Overall yield 83% (88[a]+12[b]) compound **a** (115 mg, 0.55 mmol), compound **b** (0.07 mmol, 15 mg).

^{1}H NMR *4f* [a] (500 MHz, $CDCl_3$) δ 6.12 (dq, *J* = 9.1, 1.7 Hz, 1H), 2.68 (m, 1H), 1.68 (d, *J* = 1.8 Hz, 3H), 1.25 (s, 12H), 0.96 (d, *J* = 6.7 Hz, 6H). **^{1}H NMR** *4f* [b] (500 MHz, $CDCl_3$) δ

6.28 – 6.22 (q, 6.85, 1H), 2.79 – 2.73 (m, 1H), 1.70 (d, *J* = 6.8 Hz, 3H), 1.24 (s, 12H), 1.04 (d, *J* = 6.9 Hz, 6H).

^{11}B NMR (160 MHz, $CDCl_3$) δ 30.50.

^{13}C{H} NMR (126 MHz, $CDCl_3$) *4f* [a] δ 153.5, 124.3 (br, *C-B*), 83.1, 27.5, 24.9, 22.3, 13.8.

^{13}C{H} NMR (126 MHz, $CDCl_3$) *4f* [b] δ 137.4, 82.6, 27.9, 24.8, 21.9, 13.9.

Data were in accordance with those previously reported.[7]

***(E)*-4,4,5,5-Tetramethyl-2-(phenyl-1-enyl)-1,3,2-dioxaborolane**

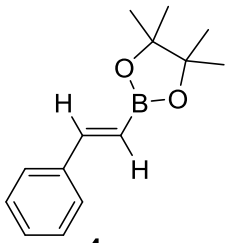

4g

According to general procedure A, phenylacetylene (0.75 mmol, 0.082 mL), HBpin (0.9 mmol, 0.130 mL), $^{i}Bu_2Al$-H (1 M in hexane, 0.075 mL) were allowed to react. The residue was purified by flash chromatography (eluent: hexane/ethyl acetate 98:2), to give the boronic ester **4g** (146 mg, 0.63 mmol, 85%) as a colourless oil.

According to general procedure B, phenylacetylene (0.75 mmol, 0.082 mL), HBpin (0.9 mmol, 0.130 mL), Et_3Al·DABCO (0.075 mmol, 17.0 mg) were allowed to react to give the boronic ester **4g** (129 mg, 0.56 mmol, 75%) as a colourless oil.

^{1}H NMR (500 MHz, $CDCl_3$) δ 7.51 – 7.48 (m, 2H), 7.41 (d, *J* = 18.4 Hz, 1H), 7.36 – 7.27 (m, 3H), 6.18 (d, *J* = 18.4 Hz, 1H), 1.32 (s, 12H).

^{11}B NMR (160 MHz, $CDCl_3$) δ 30.20.

^{13}C{H} NMR (126 MHz, $CDCl_3$) δ 149.6, 137.6, 129.0, 128.6, 127.2, 116.5 (br, *C-B*), 83.5, 24.9.

Data were in accordance with those previously reported.[3]

***(E)*-4,4,5,5-Tetramethyl-2-(4-methoxyphenyl-1-enyl)-1,3,2-dioxaborolane**

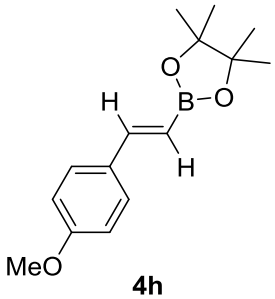

4h

According to general procedure A, 1-ethynyl-4-methoxybenzene (0.75 mmol, 99 mg), HBpin (0.9 mmol, 0.130 mL), $^{i}Bu_2Al$-H (1 M in hexane, 0.075 mL) were allowed to react. The residue was purified by flash chromatography (eluent: hexane/ethyl acetate 98:2), to give the boronic ester **4h** (156 mg, 0.60 mmol, 80%) as a yellow oil.

According to general procedure B, 1-ethynyl-4-methoxybenzene (0.75 mmol, 99 mg), HBpin (0.9 mmol, 0.130 mL), $Et_3Al{\cdot}DABCO$ (0.075 mmol, 17.0 mg) were allowed to react to give the boronic ester **4h** (138 mg, 0.53 mmol, 71%) as a yellow oil.

^{1}H NMR (500 MHz, $CDCl_3$) δ 7.45 – 7.42 (m, 2H), 7.36 (d, *J* = 18.4 Hz, 1H), 6.88 – 6.85 (m, 2H), 6.02 (d, *J* = 18.4 Hz, 1H), 3.80 (s, 3H), 1.31 (s, 12H).

^{11}B NMR (160 MHz, $CDCl_3$) δ 30.32.

^{13}C{H} NMR (126 MHz, $CDCl_3$) δ 160.4, 149.2, 130.5, 128.6, 114.1, 83.3, 55.4, 24.9.

Data were in accordance with those previously reported.[8]

***(E)*-4,4,5,5-Tetramethyl-2-(4-ethylphenyl-1-enyl)-1,3,2-dioxaborolane**

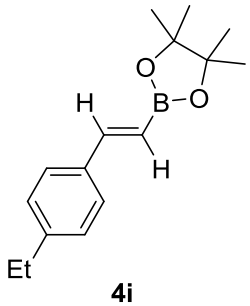

4i

According to general procedure A, 1-ethyl-4-ethynylbenzene (0.75 mmol, 0.105 mL), HBpin (0.9 mmol, 0.130 mL), $^{i}Bu_2Al$-H (1 M in hexane, 0.075 mL) were allowed to react. The residue was purified by flash chromatography (eluent: hexane/ethyl acetate 98:2), to give the boronic ester **4i** (172 mg, 0.66 mmol, 89%) as a colourless oil.

According to general procedure B, 1-ethyl-4-ethynylbenzene (0.75 mmol, 0.105 mL), HBpin (0.9 mmol, 0.130 mL), $AlEt_3$·DABCO (0.075 mmol, 17.0 mg) were allowed to react to give the boronic ester **4i** (162 mg, 0.63 mmol, 84%) as a colourless oil.

HRMS (E) mass calc'd for $C_{16}H_{23}BO_2$ 258.17856; found: 258.17991.

ATR-FTIR (υ, cm^{-1}) 2978, 2931, 2837, 1624, 1608, 1513, 1420, 1379, 1324, 1288, 1270, 1139, 1060, 969, 813.

^{1}H NMR (500 MHz, $CDCl_3$) δ 7.44-7.37 (m, 3H), 7.19 – 7.15 (m, 2H), 6.13 (d, *J* = 18.3 Hz, 1H) 2.65 (q, *J* = 7.6 Hz, 2H), 1.32 (s, 12H), 1.24 (t, *J* = 7.6 Hz, 3H).

^{11}B NMR (160 MHz, $CDCl_3$) δ 30.24.

^{13}C{H} NMR (126 MHz, $CDCl_3$) δ 149.6, 145.4, 135.2, 128.2, 127.2, 115.4 (br, *C*-*B*), 83.4, 28.8, 25.0, 15.5.

***(E)*-4,4,5,5-Tetramethyl-2-(4-fluorophenyl-1-enyl)-1,3,2-dioxaborolane**

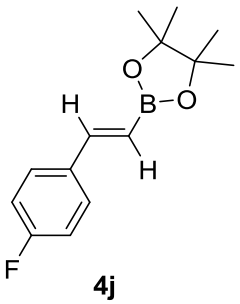

4j

According to general procedure A, 1-ethynyl-4-fluorobenzene (0.75 mmol, 90 mg), HBpin (0.9 mmol, 0.130 mL), $^{i}Bu_2Al$-H (1 M in hexane, 0.075 mL) were allowed to react. The residue was purified by flash chromatography (eluent: hexane/ethyl acetate 98:2), to give the boronic ester **4j** (135 mg, 0.55 mmol, 73%) as a colourless oil.

According to general procedure B, 1-ethynyl-4-fluorobenzene (0.75 mmol, 90 mg), HBpin (0.9 mmol, 0.130 mL), $Et_3Al{\cdot}DABCO$ (0.075 mmol, 17.0 mg) were allowed to react to give the boronic ester **4j** (128 mg, 0.52 mmol, 69%) as a colourless oil.

^{1}H NMR (500 MHz, $CDCl_3$) δ 7.48 – 7.43 (m, 2H), 7.35 (d, *J* = 18.4 Hz, 1H), 7.05 – 6.99 (m, 2H), 6.07 (d, *J* = 18.4 Hz, 1H), 1.31 (s, 12H).

^{11}B NMR (160 MHz, $CDCl_3$) δ 30.13.

^{13}C{H} NMR (126 MHz, $CDCl_3$) δ 163.10 (d, $J_{C\text{-}F}$ 247.9 Hz), 148.3, 133.9(d, *J* = 3.3 Hz), 128.9 (d, *J* = 8.7 Hz) 115.65 (d, *J* = 21.1 Hz), 83.5, 24.9.

^{19}F NMR (471 MHz, $CDCl_3$) δ −112.46 (m).

Data were in accordance with those previously reported.[3]

***(Z)*-4,4,5,5-Tetramethyl-2-(1,2 diphenyl-1-enyl)-1,3,2-dioxaborolane**

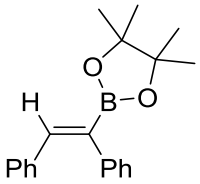

4k

According to general procedure A, diphenylacetylene (0.75 mmol, 133 mg), HBpin (0.9 mmol, 0.130 mL), $^i Bu_2Al$-H (1 M in hexane, 0.075 mL) were allowed to react. The residue was purified by flash chromatography (eluent: hexane/ethyl acetate 98:2), to give the boronic ester **4k** (91 mg, 0.30 mmol, 40%) as a colourless solid (melting point 89.5 °C).

According to general procedure B, diphenylacetylene (0.75 mmol, 133 mg), HBpin (0.9 mmol, 0.130 mL), $Et_3Al{\cdot}DABCO$ (0.075 mmol, 17.0 mg) were allowed to react to give the boronic ester **4k** (80 mg, 0.26 mmol, 35%) as a colourless solid.

^{1}H NMR (500 MHz, $CDCl_3$) δ 7.38 (s, 1H), 7.31 – 7.25 (m, 2H), 7.24 – 7.16 (m, 3H), 7.16-7.11 (m, 3H), 7.09 – 7.03 (m, 2H), 1.32 (s, 12H).

^{11}B NMR (160 MHz, $CDCl_3$) δ 30.72.

^{13}C{H} NMR (126 MHz, $CDCl_3$) δ 143.3, 140.6, 137.1, 130.1, 129.0, 128.4, 128.2, 127.7, 126.3, 83.9, 24.9.

Data were in accordance with those previously reported.[5]

***(E)*-4,4,5,5-Tetramethyl-2-(2-cyclohexenyl-1-enyl)-1,3,2-dioxaborolane**

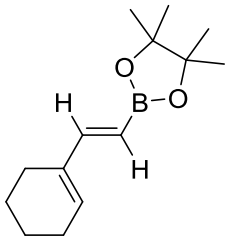

4l

According to general procedure A, 1-ethynylcyclohexene (0.75 mmol, 0.088 mL), HBpin (0.9 mmol, 0.130 mL), $^{i}Bu_2Al$-H (1 M in hexane, 0.075 mL) were allowed to react. The residue was purified by flash chromatography (eluent: hexane/ethyl acetate 98:2), to give the boronic ester **4l** (140 mg, 0.60 mmol, 80%) as a pale yellow oil.

According to general procedure B, 1-ethynylcyclohexene (0.75 mmol, 0.088 mL), HBpin (0.9 mmol, 0.130 mL), Et_3Al·DABCO (0.075 mmol, 17.0 mg) were allowed to react to give the boronic ester **4l** (131 mg, 0.56 mmol, 75%) as a pale yellow oil.

^{1}H NMR (500 MHz, $CDCl_3$) δ 7.01 (d, *J* = 18.3 Hz, 1H), 5.97-594 (m, 1H), 5.44-5.39 (m, 1H), 2.17 – 2.11 (m, 4H), 1.68 – 1.62 (m, 2H), 1.61 – 1.55 (m, 2H), 1.26 (s, 12H).

^{11}B NMR (160 MHz, $CDCl_3$) δ 30.34.

^{13}C{H} NMR (126 MHz, $CDCl_3$) δ 153.3, 137.3, 134.4, 112.1 (br, *C*-*B*), 83.1, 26.3, 24.9, 23.9, 22.6, 22.5.

Data were in accordance with those previously reported.[4]

5.5 Mechanistic Studies

HBpin (0.150 mmol, 0.021 mL) was added to a solution of the named aluminium compound (0.15 mmol) in 0.60 mL of toluene-d_8 in an NMR tube at room temperature.

Reaction of pinacolborane with $AlEt_3$

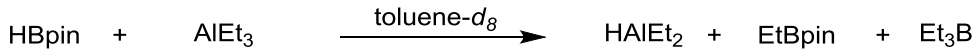

^{11}B NMR (160 MHz, toluene-d_8) δ 86.7 (br. s, *Et_3B*), 34.4 (s, *EtBpin*), 28.8 (d, J_{B-H} = 174.4 Hz, *HBpin*).

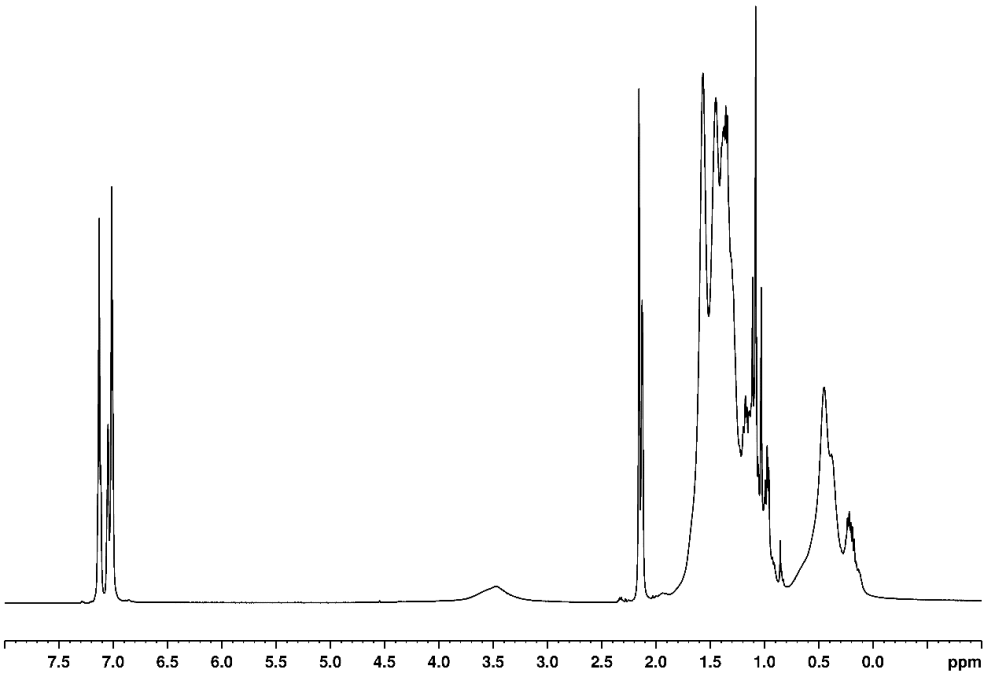

^{1}H NMR (500 MHz, toluene-d_8) spectrum of reaction of HBpin and $AlEt_3$.

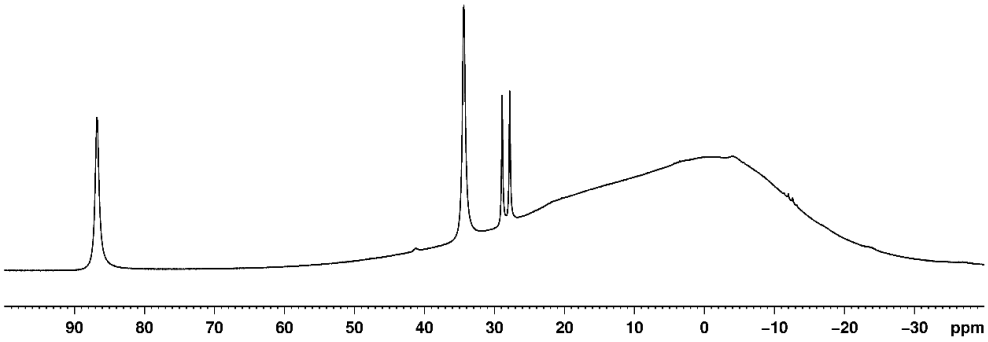

^{11}B NMR (160 MHz, toluene-d_8) spectrum of reaction of HBpin and $AlEt_3$.

Reaction of pinacolborane with Et_3Al·DABCO

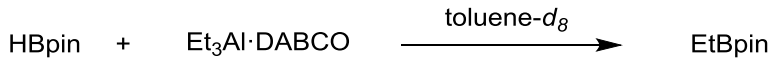

^{11}B NMR (160 MHz, toluene-d_8) δ 34.4 (s, *EtBpin*)[9], 28.8 (d, J_{B-H} = 174.4 Hz, *HBpin*),

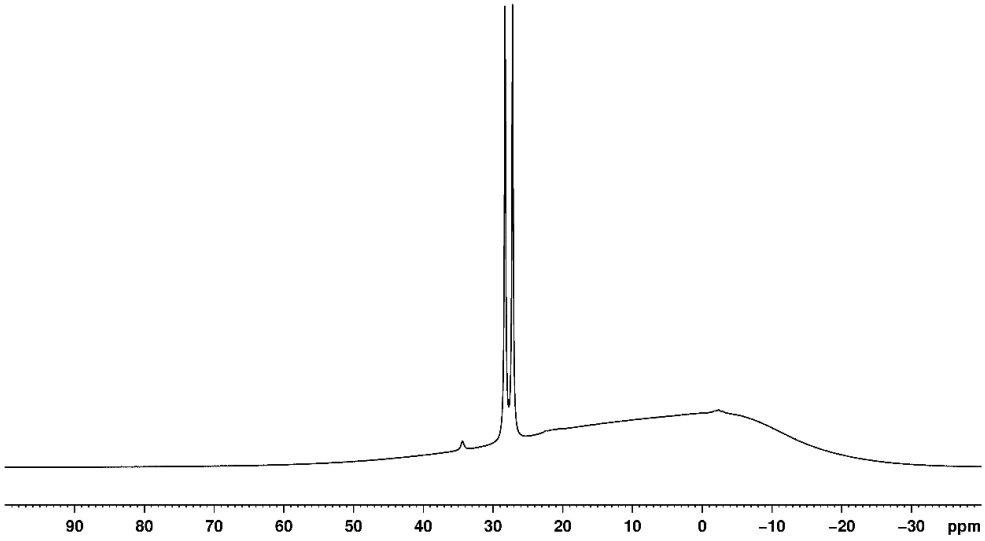

^{11}B NMR (160 MHz, toluene-d_8) spectrum of reaction of pinacolborane and Et_3Al· DABCO.

Reaction of pinacolborane with $AlMe_3$

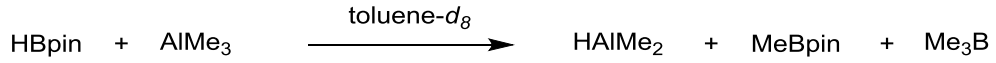

^{11}B NMR (160 MHz, toluene-d_8) δ 86.4 (s, *Me_3B*) [10], 33.9 (s, *MeBpin*), 28.8 (d, $J_{B\text{-}H}$ = 174.4 Hz, *HBpin*),

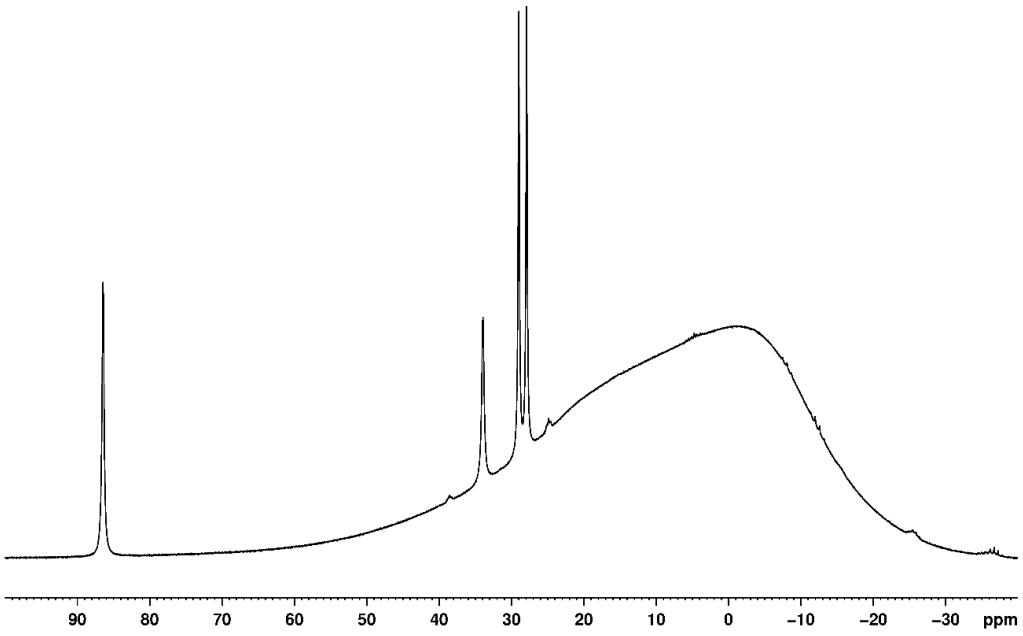

^{11}B NMR (160 MHz, toluene-d_8) spectrum of reaction of HBpin and $AlMe_3$.

Hydroalumination of 3,3-dimethyl-1-butyne

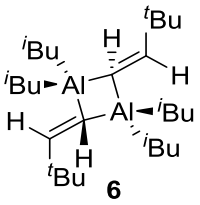

6

The compound was prepared according to modified literature procedure.[11]

A solution of di*iso*butylaluminium hydride (1 M in hexane, 2.6 mL, 2.6 mmol) was diluted with hexane (10 mL) and 3,3-dimethyl-1-butyne (0.37 mL, 3 mmol) was added dropwise. The solution was stirred for 30 minutes before concentrating *in vacuo*. Crystallisation from hexane at −20 °C gave a 95/5 mixture of the *cis/trans* alkenyl alane (**6**) as colourless cube crystals (386 mg, 60%).[11]

Melting point (argon sealed capillary) 49.5°C, lit. 127 °C.

^{1}H NMR (500 MHz, C_6D_6) *cis* isomer: δ 7.51 (d, Al-C**H**=CH, $J_{H\text{-}H}$ = 20.8 Hz, 1H), 5.89 (d, Al-CH=C**H**, $J_{H\text{-}H}$ = 20.8 Hz, 1H), 2.05 (*m*, C**H**$(CH_3)_2$, 2H), 1.13 (d, CH(**CH_3**)$_2$ $J_{H\text{-}H}$ = 6.6 Hz, 12H), 0.94 (s, C(**CH_3**)$_3$, 9H), 0.41 (d, Al−C**H_2**CH, $J_{H\text{-}H}$ = 7.2 Hz, 4H).

^{13}C{H} NMR (126 MHz, C_6D_6) δ 194.1, 118.5, 38.4, 28.2, 27.3, 26.6.

^{1}H NMR (500 MHz, C_6D_6) *trans* isomer: δ 7.50 (d, Al−C**H**=CH, $J_{H\text{-}H}$ = 20.8 Hz, 1H), 5.61 (d, Al−CH=C**H**, $J_{H\text{-}H}$ = 20.8 Hz, 1H), 2.05 (m, C**H**$(CH_3)_2$, 2H), 1.10 (d, CH(**CH_3**)$_2$, $J_{H\text{-}H}$ = 2.77 Hz, 12H), 0.82 (s, C(**CH_3**)$_3$, 9H), 0.41 (d, Al−C**H_2**CH, $J_{H\text{-}H}$ = 7.2 Hz, 4H).

^{13}C{H} NMR (126 MHz, C_6D_6) δ 198.6, 115.0, 38.7, 28.2, 27.3, 26.6.

MS (EI) = 391.3[$M^{\cdot+}$−Bu], 167.1 [1/2 M^{+}−Bu]

The NMR data were in accordance with previous reported.[11]

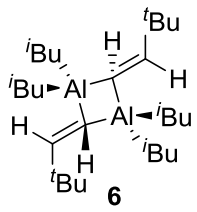

6

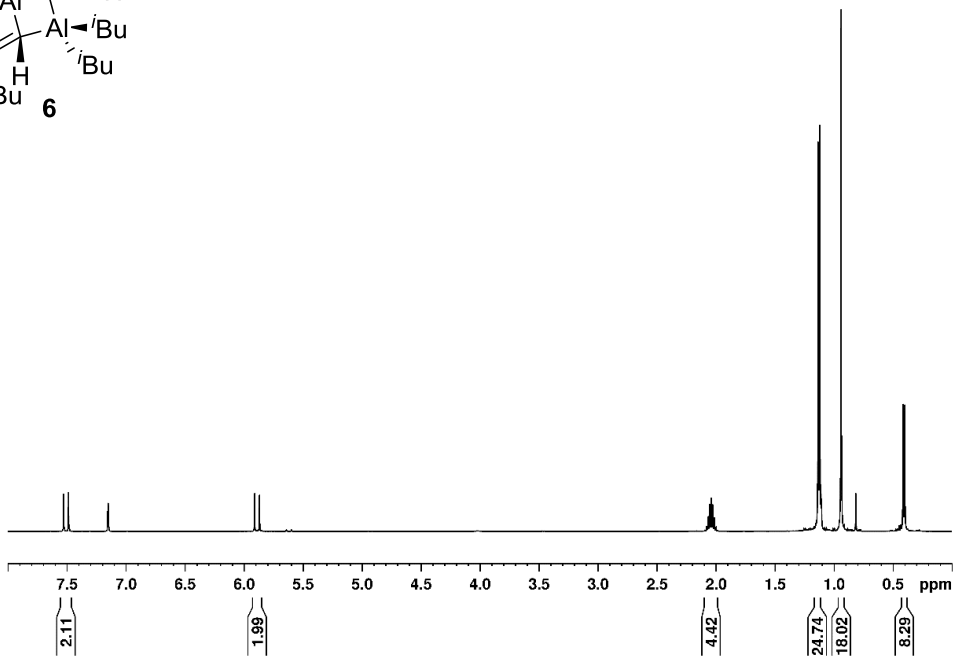

*^{1}H NMR (500 MHz, C_6D_6) of alkenylaluminium compound (**6**),(* = trans isomer).*

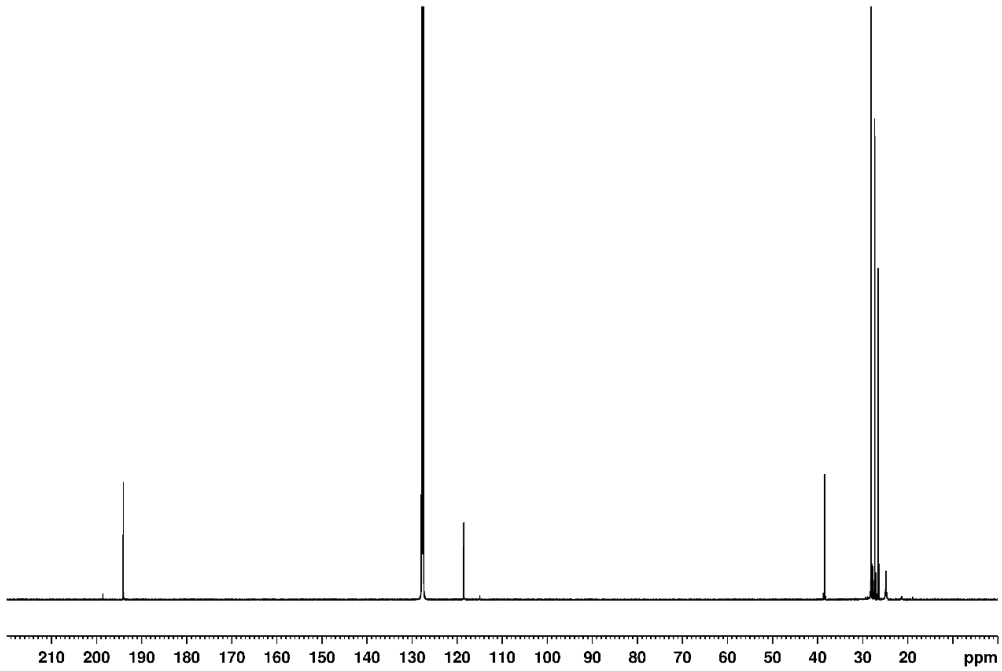

*^{13}C {H} NMR (126 MHz, C_6D_6) of alkenyl aluminium compound (**6**) (* = trans isomer).*

Reaction of alkenyl aluminium (6) with HBpin

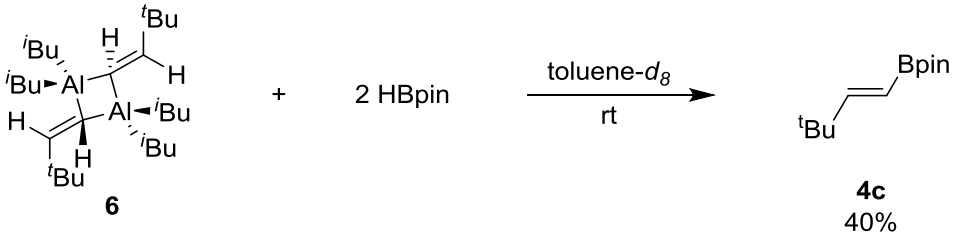

HBpin (0.150 mmol, 0.021 mL) and the alkenyl aluminium (**6**) (0.075 mmol) were added to an NMR tube charged with 0.60 mL of toluene-d_8 and the resulting mixture was left to stand for 30 minutes. Yield: 40%, determined by ^{1}H NMR of the crude reaction mixture using 1,3,5-trimethoxybenzene (25 mol%) as an internal standard.

Reaction of alkenyl aluminium (6) with HBpin and DABCO

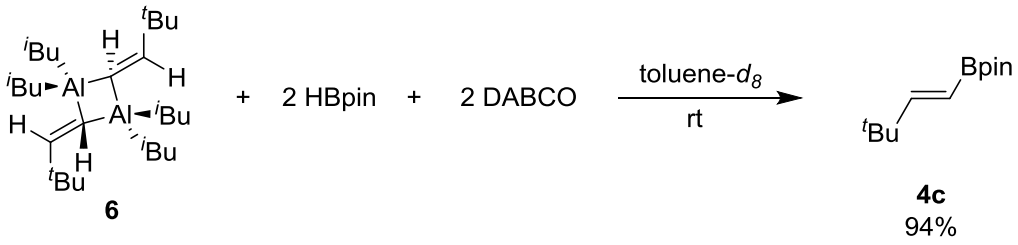

HBpin (0.150 mmol, 0.021 mL), **6** (0.075 mmol) and DABCO (0.15 mmol, 16.8 mg) were added to an NMR tube charged with toluene-d_8 and the resulting mixture was left to stand for 30 minutes. Yield: 94%, determined by ^{1}H NMR of the crude reaction mixture using 1,3,5-trimethoxybenzene (25 mol%) as an internal standard.

^{1}H NMR (500 MHz, toluene-d_8) δ 6.85 (d, C**H**=CHBpin, *J* = 18.2 Hz, 1H), 5.55 (d, CH=C**H**Bpin *J* = 18.2 Hz, 1H), 1.09 (s, 12H), 0.93 (s, 9H).

^{11}B NMR (160 MHz, toluene-d_8) δ 83.2 (s), 34.4 (s), 30.50 (s), 28.8 (d, *J* = 174.4 Hz), 0.49 (s), −12.3 (q, *J* = 100 MHz)[12], −15.81 (s).

Hydroboration of 3,3-dimethylbutyne using 2.5% alkenyl aluminium compound (6)

Catalysis with 2.5 mol% of alkenyl aluminium (6)

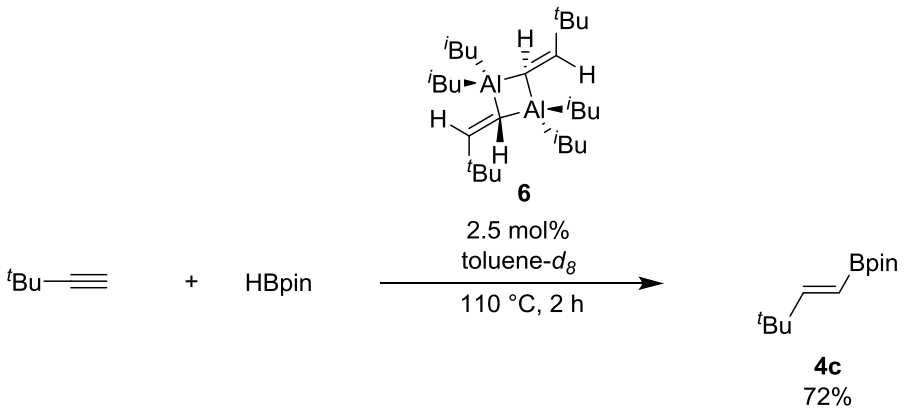

HBpin (0.180 mmol, 0.026 mL), alkenyl aluminium (**6**) (0.0037 mmol, 1.6 mg) and 3,3-dimethyl-1-butyne (0.15 mmol, 0.018 mL) were added to an NMR tube charged with 0.60 mL toluene-d_8. Yield (72%) determined by ^{1}H NMR of the crude reaction mixture using 1,3,5-trimethoxybenzene (20 mol%) as an internal standard.

Catalysis with 2.5 mol% of alkenyl aluminium (6) and DABCO

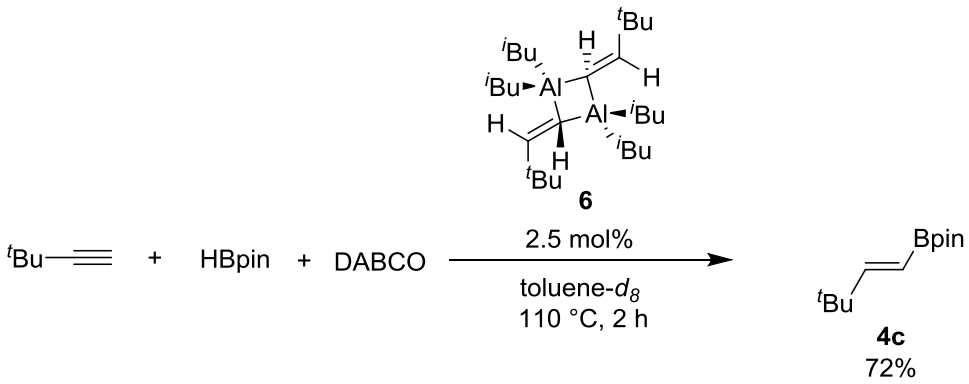

HBpin (0.180 mmol, 0.026 mL), (**6**) (0.0037 mmol, 1.6 mg), 3,3-dimethyl-1-butyne (0.15 mmol, 0.018 mL) and DABCO (0.015 mmol, 16.8 mg) were added to an NMR tube charged with 0.60 mL toluene-d_8. Yield (72%) determined by ^{1}H NMR of the crude reaction mixture using 1,3,5-trimethoxybenzene (20 mol%) as an internal standard.

Synthesis of d_1-3,3-dimethyl-1-butyne

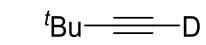

Prepared according to a modified procedure.[1]

3,3-dimethyl-1-butyne (1.1 mL, 9.9 mmol) was added to a solution of ^{n}BuLi (2.5 M in hexane, 3.0 mL,) at −100 °C. The mixture was allowed to warm slowly to 0 °C and stirred for 30 min. The solvent was removed in vacuo, the residue cooled to −80 °C, D_2O (0.32 mL, 16 mmol) added, and allowed to warm to room temperature and stirred overnight. The product was purified by distillation to give the deuterated alkyne as a colourless oil (380 mg, 61%).

^{1}H NMR (500 MHz, toluene-d_8) δ 1.16 (s, DC(**CH_3**)$_3$).

^{2}H NMR (77 MHz, toluene) NMR δ 1.83 (s, **D**C(CH_3)$_3$).

^{13}C {H} NMR (126 MHz, toluene-d_8) δ 91.7 (t, $J_{C\text{-}D}$ 7.31 Hz), 66.6 (t, $J_{C\text{-}D}$ 37.81 Hz), 30.5, 26.9.

Hydroboration of d_1-3,3-dimethyl-1-butyne

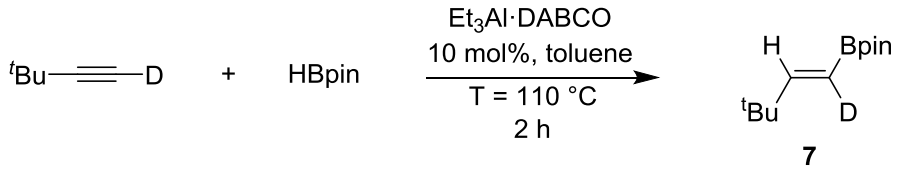

7

To a solution of $AlEt_3$·DABCO (0.075 mmol, 17.0 mg) in toluene (3.0 mL), HBpin (0.90 mmol, 0.130 mL) was added followed by d_1- 3,3-dimethyl-1-butyne (0.75 mmol, 0.087 mL). The reaction mixture was stirred for 2 h to 110 °C and quenched by filtration through a short pad of silica. The product was isolated by flash chromatography (SiO_2, hexane/ethyl acetate 98:2) to give **7** as a colourless oil (110 mg, 70%).

^{1}H NMR (500 MHz, toluene-d_8) δ 6.88 (t, C**H**=CD, $J_{H\text{-}D}$ = 2.75 Hz, 1H), 1.08 (s, C(C**H$_3$**)$_2$, 12H), 0.93 (s, C(**CH$_3$**)$_3$, 9H).

^{2}H NMR (77 MHz, toluene) δ 5.56 (d, CH=C**D**, $J_{H\text{-}D}$ = 2.75 Hz)

^{13}C{H} NMR (126 MHz, toluene-d_8) δ 164.3, 82.8, 34.8, 28.9, 24.9.

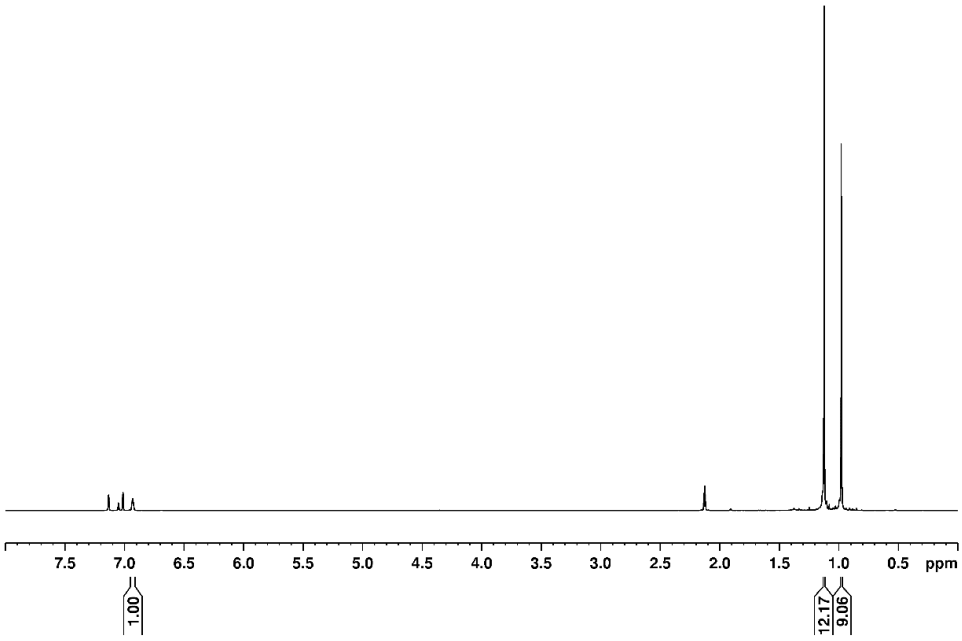

^{1}H NMR (500 MHz, toluene-d_8) of the hydroboration of d_1-3,3-dimethyl-1-butyne with 10 mol% of Et_3Al·DABCO.

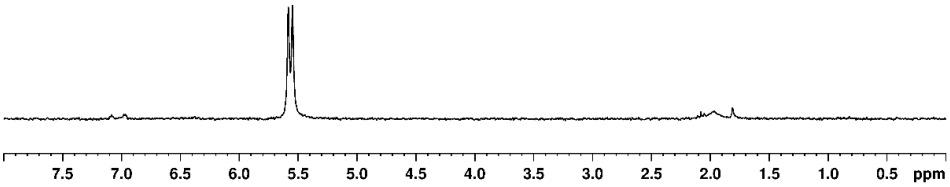

^{2}H NMR (77 MHz, toluene) of the hydroboration of d_1-3,3-dimethyl-1-butyne with 10 mol% of $Et_3Al{\cdot}DABCO$.

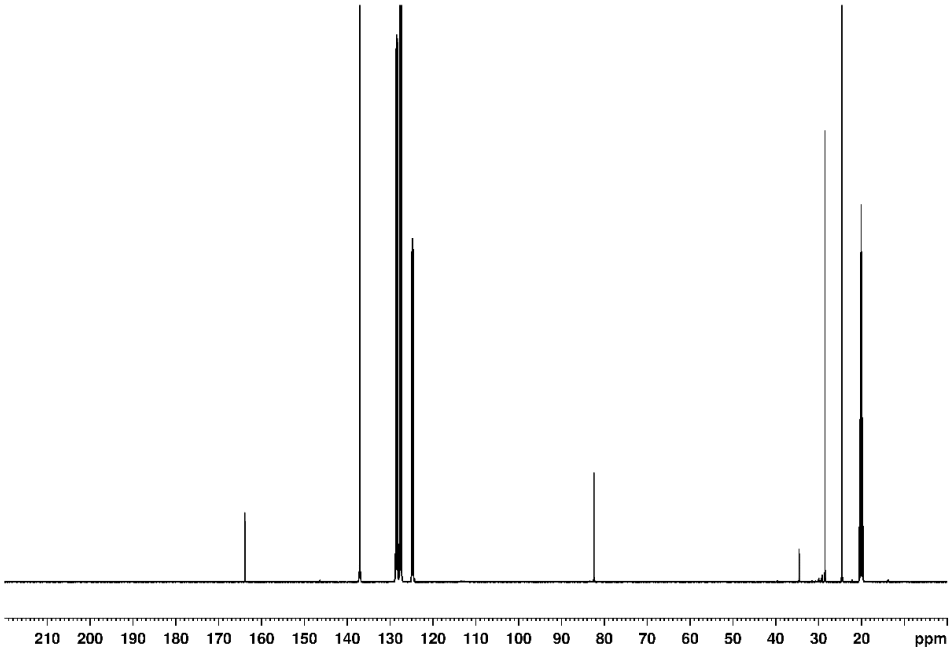

$^{13}C\{H\}$ NMR (126 MHz, toluene-d_8) of the hydroboration of d_1-3,3-dimethyl-1-butyne with 10 mol% of $Et_3Al{\cdot}DABCO$.

Hydroboration of 3,3-dimethyl-1-butyne with DBpin

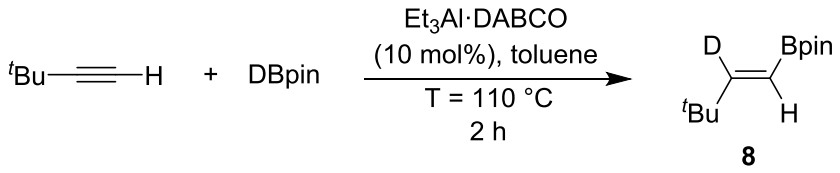

8

To a solution of Et_3Al·DABCO (0.075 mmol, 0.075 mmol, 17.0 mg) in toluene (3.0 mL), DBpin (0.90 mmol, 0.130 mL) was added followed by 3,3-dimethyl-1-butyne (0.75 mmol, 0.087 mL). The reaction mixture was stirred for 2 h to 110 °C and quenched by filtration through a short pad of silica. The product was isolated by flash chromatography (SiO_2, hexane/ethyl acetate 98:2) to give the boronic ester **8** as a colourless oil (0.110 g, 70%, 8 % of non-deuterated alkene was found).

^{1}H NMR (500 MHz, toluene-d_8) δ 5.56 (t, pinBC**H** =CD, $J_{H\text{-}D}$ = 2.75 Hz, 1H), 1.08 (s, C(C**H$_3$**)$_2$, 12H), 0.94 (s, C(**CH$_3$**)$_3$, 9H).

^{2}H NMR (77 MHz, toluene) δ 6.97 (d, pinBCH=C**D** $J_{H\text{-}D}$ = 2.75 Hz)

^{13}C NMR (126 MHz, toluene-d_8) δ 164.0, 82.8, 34.8, 28.9, 24.9.

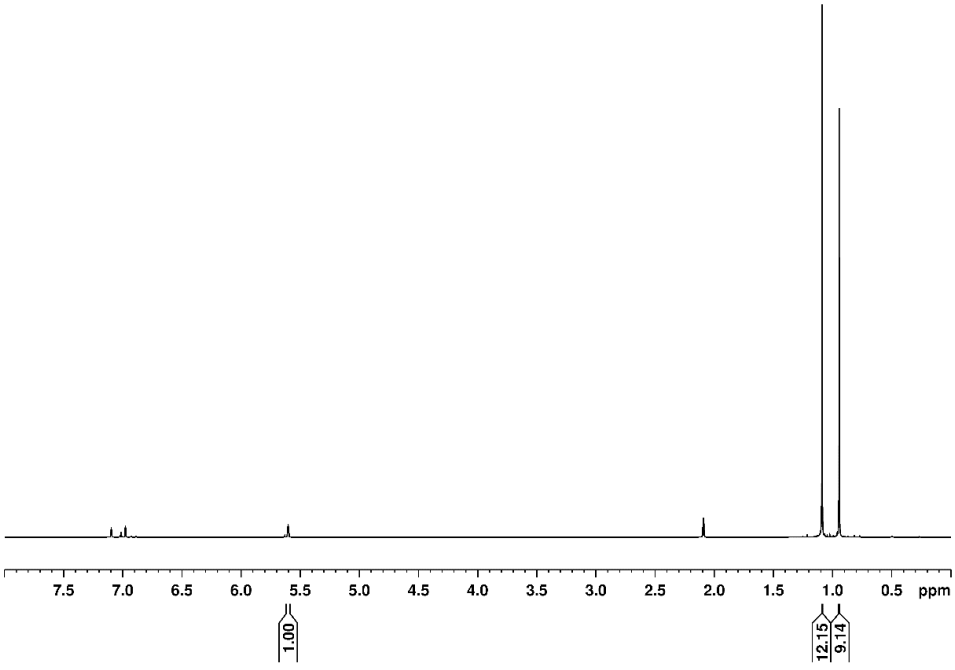

*^{1}H NMR (500 MHz, toluene-d_8) of the hydroboration of 3,3-dimethyl-1-butyne with DBpin using 10 mol% of Et_3Al·DABCO. * = 8% of non-deuterated alkene.*

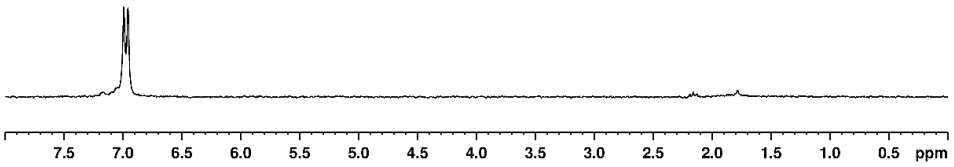

^{2}H NMR (77 MHz, toluene) of the hydroboration of 3,3-dimethyl-1-butyne with DBpin using 10 mol% of $Et_3Al{\cdot}DABCO$.

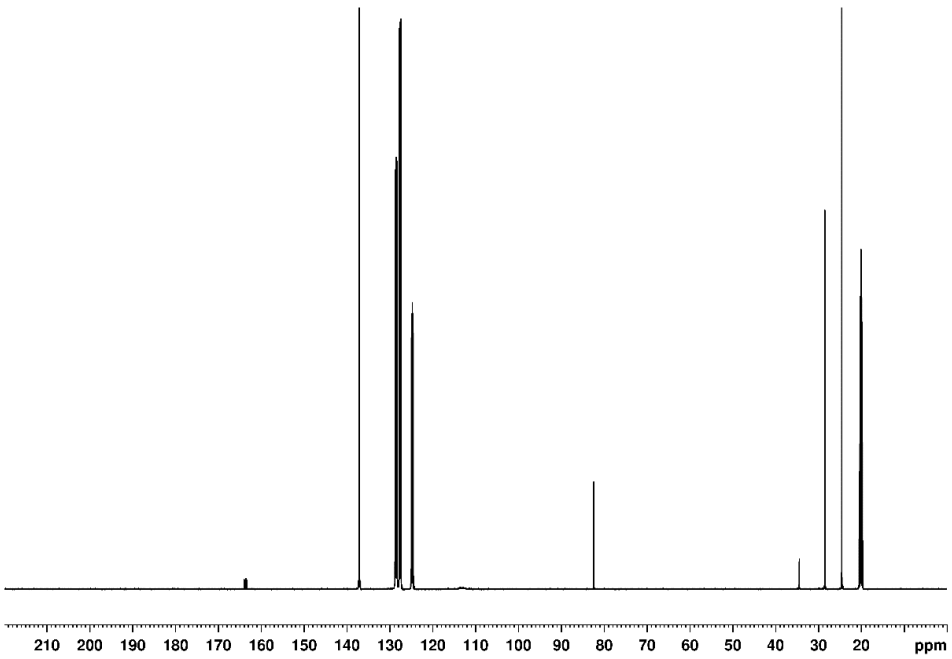

^{13}C{H} NMR (126 MHz, toluene-d_8) of the hydroboration of 3,3-dimethyl-1-butyne with DBpin using 10 mol% of $Et_3Al{\cdot}DABCO$.

5.6 Experimental Details for Chapter 3

5.7 Optimisation of catalysis conditions: hydroboration of alkenes

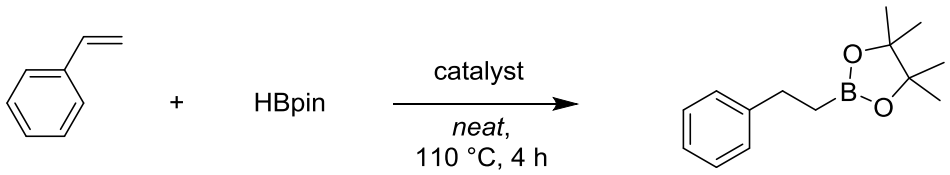

Styrene (0.45 mmol, 0.052 mL) and HBpin (0.54 mmol, 0.078 mL) were added neat to the catalyst (5-10 mol%), at room temperature and then heated at 110 °C for 4 h. The reaction was quenched using deuterated $CDCl_3$ and the yield was determined by ^1H NMR of the crude reaction mixture using 1,3,5-trimethoxybenzene as an internal standard.

Entry	Catalyst (10 mol%)	Yield (%)
1	-	trace
2	Red-Al	94
3	$AlEt_3$	75
4	$DABCO{\cdot}AlEt_3$	66
5	$AlEt_2Cl$	35
6	$^iBu_2AlH$	85
7	$Me_3N{\cdot}AlH_3$	94
8	$LiAlH_4$	95
9	$LiAlH_4$*	48
10	LiH[a]	43
11	NaH	48

*$LiAlH_4$ stored for 3 months under air

[a] the reaction was performed on 3 times the scale

Entry	Catalyst (5 mol%)	Yield (%)
1	Red-Al	86
2	DABCO·$AlEt_3$	40
4	$^{i}Bu_2AlH$	55
5	$Me_3N·AlH_3$	83
6	$LiAlH_4$[a]	86

[a]the reaction was performed on 3 times the scale.

Solvent screening

Styrene (0.45 mmol, 0.052 mL), HBpin (0.54 mmol, 0.078 mL) and Red-Al (10 mol%, 0.013 mL) were dissolved in the indicated solvent (1.0 mL) at room temperature and then heated at the boiling point for 4 h. The reaction was quenched using deuterated $CDCl_3$ and the yield was determined by ^1H NMR of the crude reaction mixture using 1,3,5-trimethoxybenzene as an internal standard.

Entry	Solvent	Yield (%)
1	CH_2Cl_2	2
2	THF	38
3	toluene	5

Temperature screening

Styrene (0.45 mmol, 0.052 mL) and HBpin (0.54 mmol, 0.078 mL) were added neat to $LiAlH_4$ (5 mol%), at room temperature and then heated at 110 °C for 4 h. The reaction was quenched using deuterated $CDCl_3$ and the yield was determined by ^1H NMR of the crude reaction mixture using 1,3,5-trimethoxybenzene as an internal standard.

Entry	T (°C)	Yield (%)
1	110	97
2	80	60
3	60	38

Equivalents of HBpin

Styrene (0.45 mmol, 0.052 mL) and HBpin (1.0-1.5 eq) were added neat to the catalyst (5 mol%), at room temperature and then heated at 110 °C for 4 h. The reaction was quenched using deuterated $CDCl_3$ and the yield was determined by ^1H NMR of the crude reaction mixture using 1,3,5-trimethoxybenzene as an internal standard.

Entry	HBpin (eq.)	Yield (%)
1	1.0	73
2	1.1	82
3	1.2	85
4	1.5	99

Kinetic analysis

Styrene (0.45 mmol, 0.052 mL) and HBpin (0.50 mmol, 0.072 mL) were added neat to the catalysts (Red-Al 5 mol% or DIBAL-H 10 mol%), at room temperature and then heated at 110 °C for 4 h. Different reactions were stopped at fixed intervals with the addition of $CDCl_3$ and the yield was determined by ^1H NMR of the crude reaction mixture using 1,3,5-trimethoxybenzene as an internal standard.

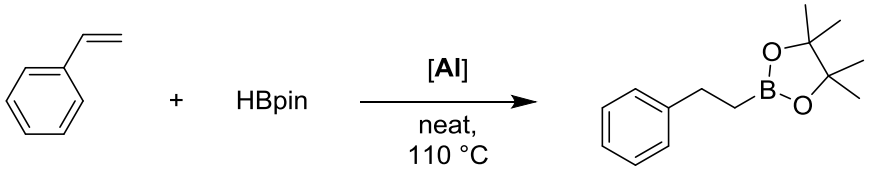

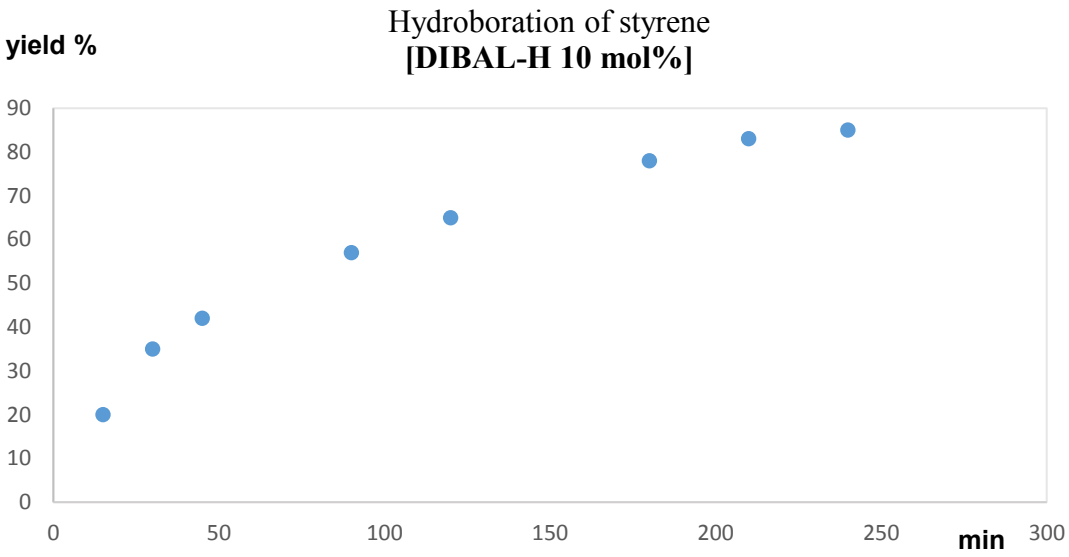

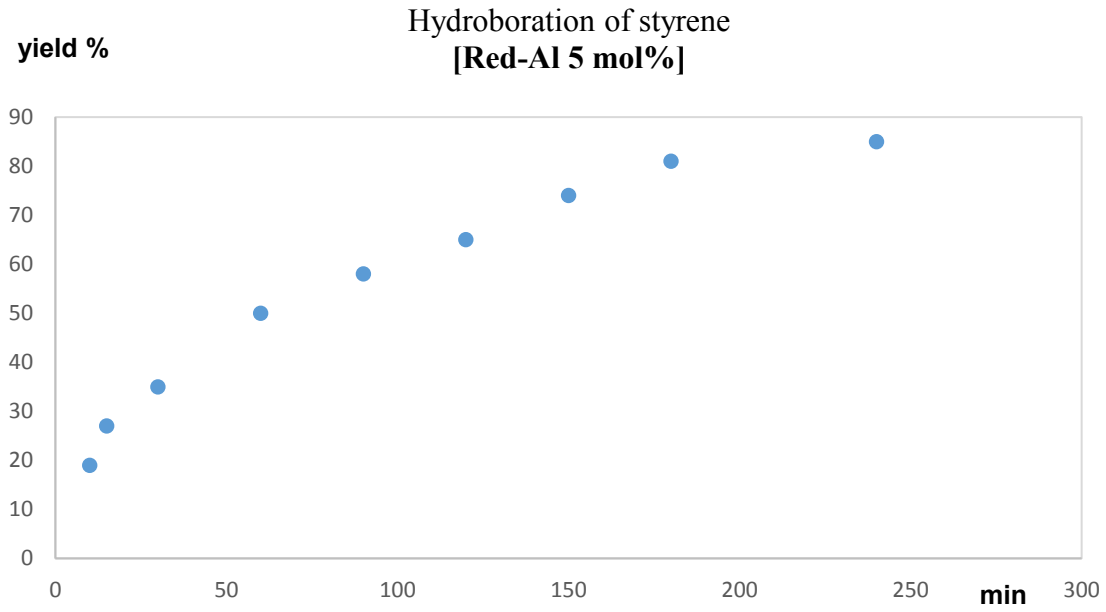
Hydroboration of styrene
[Red-Al 5 mol%]
yield %
90
80
70
60
50
40
30
20
10
0
0
50
100
150
200
250
300
min

Styrene (1.5 mmol, 0.173 mL) and HBpin (1.165 mmol, 0.240 mL) were added neat to the catalyst ($LiAlH_4$ 5 mol%), at room temperature and then heated at 110 °C for 4 h. Different reactions were stopped at fixed intervals with the addition of $CDCl_3$ and the yield was determined by ^1H NMR of crude reaction mixture using 1,3,5-trimethoxybenzene as an internal standard.

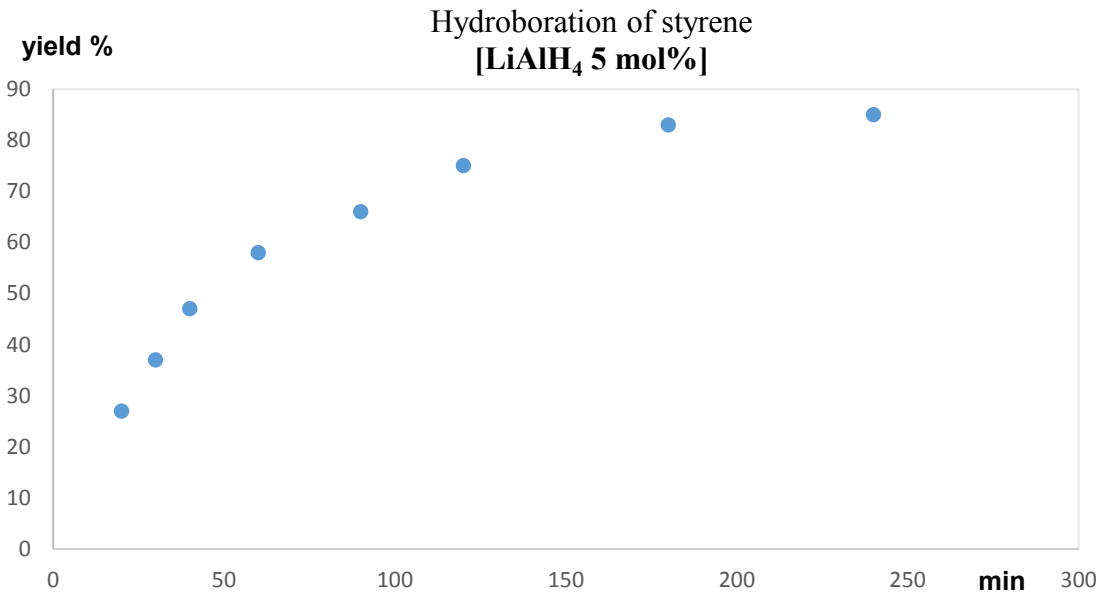

General procedure A: Hydroboration using $LiAlH_4$

The alkene (1.5 mmol) and HBpin (1.65 mmol) were added to a Young's flask containing $LiAlH_4$ (10 mol%, 0.15 mmol, 5.7 mg) at room temperature in this order. The reaction mixture was stirred for 3 h at 110 °C (oil bath temperature). The mixture was diluted with 5 mL of CH_2Cl_2 and filtered through a short pad of silica (4.0 cm in a pipette), and the product purified by flash chromatography.

Safety note: gas evolution may occur during reaction set-up.

5.8 Characterisation of the alkyl boronic esters

4,4,5,5-Tetramethyl-2-octyl-1,3,2dioxaborolane

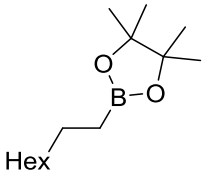

10a

According to general procedure A, 1-octene (1.5 mmol, 0.234 mL), HBpin (1.65 mmol, 0.240 mL), $LiAlH_4$ (0.15 mmol, 5.7 mg) were allowed to react. The residue was purified by flash chromatography (SiO_2, hexane to hexane/ethyl acetate 92:8, [UV/$KMnO_4$]), to give the boronic ester **10a** (360 mg, 0.1.27 mmol, 85%) as a colourless oil with a regioselectivity of 95:5 (Linear/Branched).

^{1}H NMR (500 MHz, $CDCl_3$) δ 1.39 (m, 2H), 1.32 – 1.20 (m, 22H), 0.87 (t, *J* = 8.0 Hz, 2H), 0.76 (t, *J* = 8.0 Hz, 3H).

^{11}B NMR (160 MHz, $CDCl_3$) δ 33.9.

^{13}C{H} NMR (126 MHz, $CDCl_3$) δ 83.0, 32.6, 32.0, 29.5, 29.4, 25.0, 24.2, 22.8, 14.3, 11.4 (br *C*-*B*).

Data were in accordance with those previously reported.[13]

4,4,5,5-Tetramethyl-2-(2-(cyclohexane)ethyl)-1,3,2-dioxaborolane

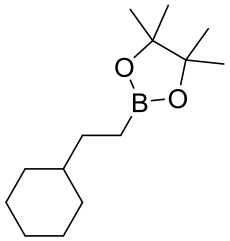

10b

According to general procedure A, vinyl cyclohexane (1.5 mmol, 0.202 mL), HBpin (1.65 mmol, 0.240 mL), $LiAlH_4$ (0.15 mmol, 5.7 mg) were allowed to react. The residue was purified by flash chromatography (SiO_2, hexane to hexane/ethyl acetate 92:8, [UV/$KMnO_4$]), to give the boronic ester **10b** (220 mg, 0.91 mmol, 61%) as a colourless oil with a regioselectivity of 95:5 (Linear/Branched).

^{1}H NMR (500 MHz, $CDCl_3$) δ 1.75 – 1.56 (m, 5H), 1.32 – 1.25 (m, 2H), 1.24 (s, 12H) 1.21-1.08 (m, 4H) 0.89 – 0.79 (m, 2H), 0.78 – 0.72 (m, 2H).

^{11}B NMR (160 MHz, $CDCl_3$) δ 34.27.

^{13}C{H} NMR (126 MHz, $CDCl_3$) δ 82.9, 40.0, 33.0, 31.4, 26.8, 26.5, 24.9.

Data were in accordance with those previously reported.[13]

4,4,5,5-Tetramethyl-2-(3,3-dimethyl butane)-1,3,2-dioxaborolane

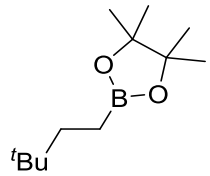

10c

According to general procedure A, 3 3-dimethyl-1-butene (1.5 mmol, 0.192 mL), HBpin (1.65 mmol, 0.240 mL), $LiAlH_4$ (0.15 mmol, 5.7 mg) were allowed to react. The residue was purified by flash (SiO_2, hexane to hexane/ethyl acetate 92:8, [UV/$KMnO_4$]), to give the boronic ester **10c** (254 mg, 1.2 mmol, 80%) as a colourless oil with a regioselectivity of 90:10 (Linear/Branched).

^{1}H NMR (500 MHz, CDCl3) δ 1.32 – 1.25 (m, 2H), 1.24 (s, 12H), 0.84 (d, 9H), 0.73 – 0.67 (m, 2H).

^{11}B NMR (160 MHz, $CDCl_3$) δ 34.3.

^{13}C{H} NMR (126 MHz, $CDCl_3$) δ 83.0, 37.9, 31.0, 29.0, 25.0.

Data were in accordance with those previously reported.[13]

4,4,5,5-Tetramethyl-2-(3-phenylpropyl)-1,3,2-dioxaborolane

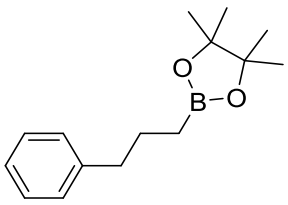

10d

According to general procedure A, allyl benzene (1.5 mmol, 198 mL), HBpin (1.65 mmol, 0.240 mL), $LiAlH_4$ (0.15 mmol, 5.7 mg) were allowed to react. The residue was purified by flash chromatography (SiO_2, hexane to hexane/ethyl acetate 92:8, [UV/$KMnO_4$]), to

give the boronic ester **10d** (270 mg, 1.1 mmol, 73%) as a colourless oil with a regioselectivity of 99:1 (Linear/Branched).

^{1}H NMR (500 MHz, $CDCl_3$) δ 7.31 – 7.26 (m, 4H), 7.22 – 7.16 (m, 1H), 2.66 – 2.60 (m, 2H), 1.80 – 1.72 (m, 2H), 1.27 (s, 12H), 0.85 (t, *J* = 8.0 Hz, 2H).

^{11}B NMR (160 MHz, $CDCl_3$) δ 33.8.

^{13}C{H} NMR (126 MHz, $CDCl_3$) δ 142.7, 128.5, 128.2, 125.6, 82.9, 38.6, 26.1, 24.8.

Data were in accordance with those previously reported.[14]

4,4,5,5-Tetramethyl-2-(3-bromopropyl)-1,3,2-dioxaborolane

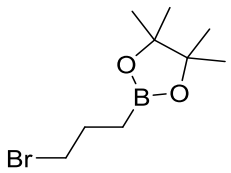

10e

According to general procedure A, allyl bromide (1.5 mmol, 128 mL), HBpin (1.65 mmol, 0.240 mL), $LiAlH_4$ (0.15 mmol, 5.7 mg) were allowed to react. The residue was purified by flash chromatography (SiO_2, hexane to hexane/ethyl acetate 92:8, [UV/$KMnO_4$]), to give the boronic ester **10e** (260 mg, 1.1 mmol, 73%) as a colourless oil with a regioselectivity of 99:1 (Linear/Branched).

^{1}H NMR (500 MHz, $CDCl_3$) δ 3.43 (t, *J* = 7.7 Hz, 2H), 2.02 – 1.95 (m, 2H), 1.26 (s, 12H), 0.93 (t, *J* = 7.7 Hz, 2H).

^{11}B NMR (160 MHz, $CDCl_3$) δ 33.57.

^{13}C{H} NMR (126 MHz, $CDCl_3$) δ 83.2, 36.2, 27.5, 24.8.

Data were in accordance with those previously reported.[15]

4,4,5,5-Tetramethyl-2-(pentyl 4-methylbenzenesulfonate)-1,3,2-dioxaborolane

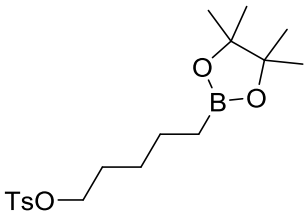

10f

According to general procedure A, 5-(4-methylbenzenesulfonate benzene)-1-pentene (1.5 mmol, 360 mg), HBpin (1.65 mmol, 0.240 mL), $LiAlH_4$ (0.15 mmol, 5.7 mg) were allowed to react. The residue was purified by flash chromatography (SiO_2, hexane to hexane/ethyl acetate 85:15, [UV/$KMnO_4$]), to give the boronic ester **10f** (378 mg, 1.1 mmol, 70%) as a colourless oil with a regioselectivity of 99:1 (Linear/Branched).

^{1}H NMR (500 MHz, $CDCl_3$) δ 7.80 (m, 2H), 7.36 (m, 2H), 4.04 (t, *J* = 6.6 Hz, 2H), 2.47 (s, 3H), 1.70 – 1.61 (m, 2H), 1.42 – 1.27 (m, 4H), 1.25 (s, 12H), 0.74 (t, *J* = 7.6 Hz, 2H).

^{11}B NMR (160 MHz, $CDCl_3$) δ 33.10.

^{13}C{H} NMR (126 MHz, $CDCl_3$) δ 144.70, 133.48, 129.92, 128.03, 83.11, 70.83, 28.76, 28.11, 24.96, 23.52, 21.78.

Data were in accordance with those previously reported.[16]

4,4,5,5-Tetramethyl-2-(3-triethoxysilylpropyl)-1,3,2-dioxaborolane

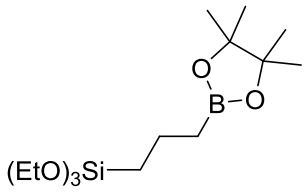

10g

According to general procedure A, allyl triethoxysilane (1.5 mmol, 0.252 mL), HBpin (1.65 mmol, 0.240 mL), $LiAlH_4$ (0.15 mmol, 5.7 mg) were allowed to react. The residue was

purified by flash chromatography (SiO_2, hexane to hexane/ethyl acetate 92:8, [UV/$KMnO_4$]), to give the boronic ester **10g** (428 mg, 1.1 mmol, 86%) as a colourless oil with a regioselectivity of 99:1 (Linear/Branched).

^{1}H NMR (500 MHz, $CDCl_3$) δ 3.80 (q, *J* = 7.0 Hz, 6H), 1.60 – 1.48 (m, 2H), 1.28 – 1.15 (m, 21H), 0.85 (t, *J* = 7.0 Hz, 2H), 0.71 – 0.61 (m, 2H).

^{11}B NMR (160 MHz, $CDCl_3$) δ 33.62.

^{13}C{H} NMR (126 MHz, $CDCl_3$) δ 82.8, 58.2, 24.8, 18.3, 17.5, 13.4.

^{29}Si NMR (126 MHz, $CDCl_3$) δ −45.02.

IR: *vmax* (neat): 2976, 1372, 1312, 1220, 1076, 956, 848, 781.

MS: HRMS (EI) mass calc'd for $C_{15}H_{33}BO_5Si$ 332.21848; found: 332.21639.

4,4,5,5-Tetramethyl-2-(2-dichlorocyclopropyl)-1,3,2-dioxaborolane

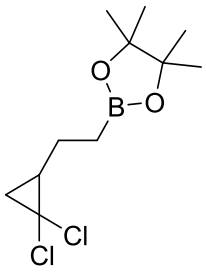

10h

According to general procedure A, 1,1-dichloro-2-vinylcyclopropane (1.5 mmol, 178 mL), HBpin (1.65 mmol, 0.240 mL), $LiAlH_4$ (0.15 mmol, 5.7 mg) were allowed to react. The residue was purified by flash chromatography (SiO_2, hexane to hexane/ethyl acetate 92:8, [UV/$KMnO_4$]), to give the boronic ester **10h** (273 mg, 1.0 mmol, 69%) as a colourless oil with a regioselectivity of 99:1 (Linear/Branched).

^{1}H NMR (500 MHz, $CDCl_3$) δ 1.82 – 1.68 (m, 1H), 1.66 – 1.50 (m, 3H), 1.27 (d, *J* = 1.8 Hz, 12H), 1.07 (t, *J* = 6.7 Hz, 1H), 1.02 – 0.94 (m, 2H).

^{11}B NMR (160 MHz, $CDCl_3$) δ 33.7.

^{13}C{H} NMR (126 MHz, $CDCl_3$) δ 83.1, 61.7, 32.7, 26.9, 25.0, 24.8.

IR: *vmax* (neat): 2984, 1368, 1325, 1251, 1143, 967, 847

HRMS (EI) mass calc'd for $C_{11}H_{19}BO_2Cl_2$ 264.08497; found: 264.08394.

4,4,5,5-Tetramethyl-2-(phenylethyl)-1,3,2-dioxaborolane

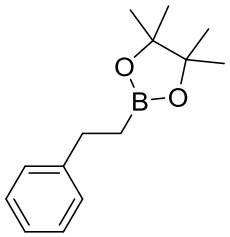

10i

According to general procedure A, styrene (1.5 mmol, 0.172 mL), HBpin (1.65 mmol, 0.240 mL), $LiAlH_4$ (0.15 mmol, 5.7 mg) were allowed to react. The residue was purified by flash chromatography (SiO_2, hexane to hexane/ethyl acetate 92:8, [UV/$KMnO_4$]), to give the boronic ester **10i** (278 mg, 1.2 mmol, 80%) as a colourless oil with a regioselectivity of 99:1 (Linear/Branched).

^{1}H NMR (500 MHz, $CDCl_3$) δ 7.32 – 7.21 (m, 4H), 7.17 (m, 1H), 2.75 (t, *J* = 8.0 Hz, 2H), 1.25 (s, 12H), 1.15 (t, *J* = 8.0 Hz, 2H).

^{11}B NMR (160 MHz, $CDCl_3$) δ 33.42.

^{13}C{H} NMR (126 MHz, $CDCl_3$) δ 144.4, 128.2, 128.0, 125.5, 83.1, 30.0, 24.8.

Data were in accordance with those previously reported.[13

4,4,5,5-Tetramethyl-2-(4-fluorophenethyl)-1,3,2-dioxaborolane

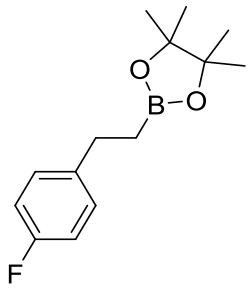

10j

According to general procedure A, 4-fluorostyrene (1.5 mmol, 0.178 mL), HBpin (1.65 mmol, 0.240 mL), $LiAlH_4$ (0.15 mmol, 5.7 mg) were reacted. The residue was purified by

flash chromatography (SiO_2, hexane to hexane/ethyl acetate 92:8, [UV/$KMnO_4$]), to give the boronic ester **10j** (236 mg, 0.93 mmol, 63%) as a colourless oil with a regioselectivity of 96:4 (Linear/Branched).

^{1}H NMR (500 MHz, $CDCl_3$) δ 7.19 – 7.12 (m, 2H), 6.96 – 6.90 (m, 2H), 2.72 (t, *J* = 8.1 Hz, 2H), 1.21 (s, 12H), 1.12 (t, *J* = 8.1 Hz, 2H).

^{11}B NMR (160 MHz, $CDCl_3$) δ 34.56.

^{13}C{H} NMR (126 MHz, $CDCl_3$) δ 161.1 (d, *J* = 242.6 Hz), 139.9 (d, *J* = 3.1 Hz), 129.3 (d, *J* = 7.8 Hz), 114.8 (d, *J* = 21.0 Hz), 83.1, 29.2, 24.8, 13.1 (br, C-B).

^{19}F NMR (471 MHz, $CDCl_3$) δ −118.40.

Data were in accordance with those previously reported.[1]

4,4,5,5-Tetramethyl-2-(4-trifluoromethyl)phenylethyl)-1,3,2-dioxaborolane

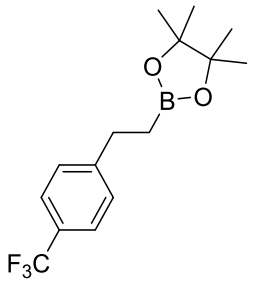

10k

According to general procedure A, 4-trifluoromethylstyrene (1.5 mmol, 221 mL), HBpin (1.65 mmol, 0.240 mL), $LiAlH_4$ (0.15 mmol, 5.7 mg) were allowed to react. The residue was purified by flash chromatography (SiO_2, hexane to hexane/ethyl acetate 92:8, [UV/$KMnO_4$]), to give the boronic ester **10k** (283 mg, 0.99 mmol, 66%) as a white amorphous solid with a regioselectivity of 90:10 (Linear/Branched).

^{1}H NMR (500 MHz, $CDCl_3$) δ 7.55 – 7.51 (m, 2H), 7.34-7.29 (m, 2H), 2.82 (t, *J* = 8.0 Hz, 2H), 1.24 (s, 12H), 1.18 (t, *J* = 8.0 Hz, 2H).

^{11}B NMR (160 MHz, $CDCl_3$) δ 33.42.

^{13}C{H} NMR (126 MHz, $CDCl_3$) δ 148.5, 128.3, 128.0, 125.1 (q, *J* = 3.8 Hz), 124.5, 83.2, 29.8, 24.8.

Melting point (hexane) 38.5-39.5 °C.

Data were in accordance with those previously reported. [17]

4,4,5,5-Tetramethyl-2-(4-(*tert*-butyl)phenylethyl)-1,3,2-dioxaborolane

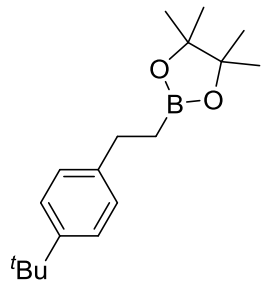

10l

According to general procedure A, 4-tertbutylstyrene (1.5 mmol, 0.274 mL), HBpin (1.65 mmol, 0.240 mL), $LiAlH_4$ (0.15 mmol, 5.7 mg) were allowed to react. The residue was purified by flash chromatography (SiO_2, hexane to hexane/ethyl acetate 92:8, [UV/$KMnO_4$]), to give the boronic ester **10l** (367 mg, 1.27 mmol, 85%) as a colourless oil with a regioselectivity of 93:7 (Linear/Branched).

^{1}H NMR (500 MHz, $CDCl_3$) 7.28 – 7.23 (m, 2H), 7.15 – 7.11 (m, 2H), 2.69 (t, *J* = 8.0 Hz, 2H), 1.28 (s, 9H), 1.20 (s, 12H), 1.12 (t, *J* = 8.0 Hz, 2H).

^{11}B NMR (160 MHz, $CDCl_3$) δ 33.50.

^{13}C{H} NMR (126 MHz, $CDCl_3$) δ 148.4, 141.5, 127.8, 125.2, 83.2, 34.5, 31.6, 29.5, 25.0.

Data were in accordance with those previously reported. [18]

4,4,5,5-Tetramethyl-2-(4-methoxy)phenylethyl)-1,3,2-dioxaborolane

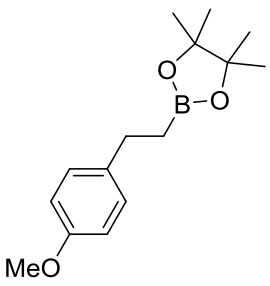

10m

According to general procedure A, 4-methoxystyrene (1.5 mmol, 0.202 mL), HBpin (1.65 mmol, 0.240 mL), $LiAlH_4$ (0.15 mmol, 5.7 mg) were allowed to react. The residue was purified by flash chromatography (SiO_2, hexane to hexane/ethyl acetate 92:8, [UV/$KMnO_4$]), to give the boronic ester **10m** (247 mg, 0.9 mmol, 61%) as a colourless oil with a regioselectivity of 98:2 (Linear/Branched).

^{1}H NMR (500 MHz, $CDCl_3$) δ 7.16 – 7.11 (m, 2H), 6.84 – 6.78 (m, 2H), 3.78 (s, 3H), 2.69 (t, *J* = 8.0 Hz, 2H), 1.22 (s, 12H), 1.12 (t, *J* = 8.0 Hz, 2H).

^{11}B NMR (160 MHz, $CDCl_3$) δ 33.56.

^{13}C{H} NMR (126 MHz, $CDCl_3$) δ 157.6, 136.6, 128.9, 113.6, 83.1, 55.3, 29.1, 24.8.

Data were in accordance with those previously reported.[18]

4,4,5,5-Tetramethyl-2-(4-phenyl)phenylethyl-1,3,2-dioxaborolane

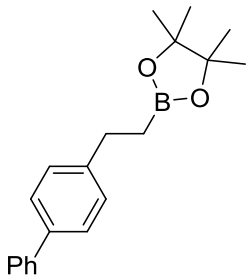

10n

According to general procedure A, 4-phenylstyrene (1.5 mmol, 308 mg), HBpin (1.65 mmol, 0.240 mL), $LiAlH_4$ (0.15 mmol, 5.7 mg) were allowed to react. The residue was purified by flash chromatography (SiO_2, hexane to hexane/ethyl acetate 92:8, [UV/$KMnO_4$]), to give the boronic ester **10n** (337 mg, 1.0 mmol, 73%) as an amorphous yellow solid with a regioselectivity of 88:12 (Linear/Branched).

^{1}H NMR (500 MHz, $CDCl_3$) δ 7.64 – 7.60 (m, 2H), 7.56 – 7.51 (m, 2H), 7.46 (m, 2H), 7.38 – 7.32 (m, 3H), 2.84 (t, *J* = 8.2, 3H), 1.27 (s, 12H), 1.23 (m, 2H).

^{11}B NMR (160 MHz, $CDCl_3$) δ 36.2.

^{13}C{H} NMR (126 MHz, $CDCl_3$) δ 143.6, 141.3, 138.5, 128.7, 128.5, 127.0, 127.0, 126.9, 83.2, 29.6, 24.9.

Melting point (hexane) 54.5−55.5 °C.

Data were in accordance with those previously reported.[19]

4,4,5,5-Tetramethyl-2-(2-bromophenylethyl)-1,3,2-dioxaborolane

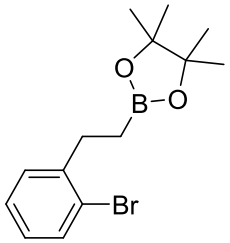

10o

According to general procedure A, 2-bromostyrene (1.5 mmol, 195 mL), HBpin (1.65 mmol, 0.240 mL), $LiAlH_4$ (0.15 mmol, 5.7 mg) were allowed to react. The residue was purified by flash chromatography (SiO_2, hexane to hexane/ethyl acetate 92:8, [UV/$KMnO_4$]), to give the boronic ester **10** (350 mg, 1.1 mmol, 76%) as a colourless oil with a regioselectivity of 83:17 (Linear/Branched).

^{1}H NMR (500 MHz, $CDCl_3$) δ 7.40 – 7.35 (m, 1H), 7.30 – 7.24 (m, 1H), 7.16 – 7.09 (m, 2H), 2.72 (t, *J* = 8.0 Hz, 2H), 1.22 (s, 12H), 1.12 (t, *J* = 8.0 Hz, 2H).

^{11}B NMR (160 MHz, $CDCl_3$) δ 33.74.

^{13}C{H} NMR (126 MHz, $CDCl_3$) δ 146.8, 131.2, 129.8, 128.6, 126.7, 122.2, 83.2, 29.7, 24.8.

IR: *vmax* (neat): 2980, 1568, 1472, 1317, 1272, 1142, 843

HRMS (EI) mass calc'd for $C_{14}H_{20}BO_2Br$ 310.07342; found: 310.07403.

4,4,5,5-Tetramethyl-2-(2-fluorophenylethyl)-1,3,2-dioxaborolane

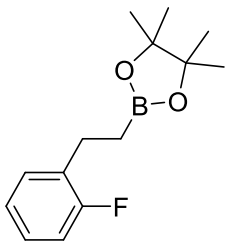

10p

According to general procedure A, 2-fluorostyrene (1.5 mmol, 180 mL), HBpin (1.65 mmol, 0.240 mL), $LiAlH_4$ (0.15 mmol, 5.7 mg) were allowed to react. The residue was purified by flash chromatography (SiO_2, hexane to hexane/ethyl acetate 92:8, [UV/$KMnO_4$]), to give the boronic ester **10p** (266 mg, 1.0 mmol, 71%) as a colourless oil with a regioselectivity of 98:2 (Linear/Branched).

^{1}H NMR (500 MHz, $CDCl_3$) δ 7.23 (m, 1H), 7.12 (m, 1H), 7.04 (m, 1H), 6.98 (m, 1H), 2.77 (t, *J* = 8.1 Hz, 2H), 1.23 (s, 12H), 1.17 – 1.12 (m, 2H).

^{11}B NMR (160 MHz, $CDCl_3$) δ 33.90.

^{13}C{H} NMR (126 MHz, $CDCl_3$) δ 161.0 (d, *J* = 15.7 Hz) 131.1 (d, *J* = 15.7 Hz), 130.0 (d, *J* = 5.1 Hz), 127.1 (d, *J* = 8.0 Hz), 123.7 (d, *J* = 3.5 Hz), 115.0 (d, *J* = 22.2 Hz), 83.1, 24.6 (d, *J* = 4.6 Hz), 23.2 (d, *J* = 3.5 Hz).

^{19}F NMR (471 MHz, $CDCl_3$) δ −118.78.

Data were in accordance with those previously reported.[18]

4,4,5,5-Tetramethyl-2-(2,4-dimethyl)phenylethyl-1,3,2-dioxaborolane

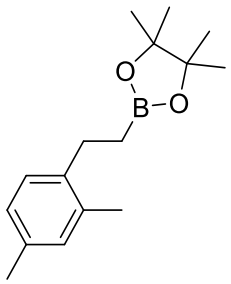

10q

According to general procedure A, 2,4-dimethylstyrene (1.5 mmol, 218 mL), HBpin (1.65 mmol, 0.240 mL), $LiAlH_4$ (0.15 mmol, 5.7 mg) were allowed to react. The residue was purified by flash chromatography (SiO_2, hexane to hexane/ethyl acetate 92:8, [UV/$KMnO_4$]), to give the boronic ester **10q** (284 mg, 1.1 mmol, 73%) as a colourless amorphous solid with a regioselectivity of 93:7 (Linear/Branched).

^{1}H NMR (500 MHz, $CDCl_3$) δ 7.09 (m, 1H), 6.95 (m, 2H), 2.70 – 2.66 (t, *J* = 8.3 Hz, 2H), 2.29 (s, 6H), 1.26 (s, 12H), 1.10 (t, *J* = 8.3 Hz, 2H).

^{11}B NMR (160 MHz, $CDCl_3$) δ 33.90.

^{13}C{H} NMR (126 MHz, $CDCl_3$) δ 139.5, 135.6, 134.9, 130.8, 128.0, 126.5, 83.1, 26.8, 24.9, 20.9, 19.2.

Melting point (hexane) 54.5-55.5 °C.

HRMS (EI) mass calc'd for $C_{16}H_{25}BO_2$ 260.19421; found: 260.19305.

IR: *vmax* (neat): 2976, 1453, 1375, 1313, 1140, 969, 884, 848.

4,4,5,5-Tetramethyl-2-(2,4,6-trimethyl)phenylethyl-1,3,2-dioxaborolane

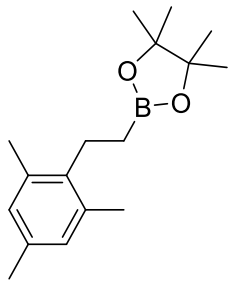

10r

According to general procedure A, 2,4,6-trimethylstyrene (1.5 mmol, 242 mL), HBpin (1.65 mmol, 0.240 mL), $LiAlH_4$ (0.15 mmol, 5.7 mg) were allowed to react. The residue was purified by flash chromatography (SiO_2, hexane to hexane/ethyl acetate 92:8, [UV/$KMnO_4$]), to give the boronic ester **10r** (260 mg, 1.0 mmol, 63%) a colourless amorphous solid with a regioselectivity of 99:1 (Linear/Branched).

^{1}H NMR (500 MHz, $CDCl_3$) 6.86 (s, 2H), 2.71(t, *J* = 8.3 Hz, 2H), 2.34 (s, 6H), 2.28 (s, 3H), 1.31 (s, 12H), 1.02 (t, *J* = 8.3 Hz, 2H).

^{11}B NMR (160 MHz, $CDCl_3$) δ 34.10.

^{13}C{H} NMR (126 MHz, $CDCl_3$) δ 138.5, 135.6, 134.6, 128.8, 83.1, 24.9, 23.3, 20.8, 19.7.

Melting point (hexane) 54.5−55.5 °C.

HRMS (EI) mass calc'd for $C_{17}H_{27}BO_2$ 274.20986; found: 274.20799.

IR: *vmax* (neat): 2975, 1448, 1369, 1310, 1141, 965, 885, 848.

4,4,5,5-Tetramethyl-2-(2-phenylpropyl)-1,3,2-dioxaborolane

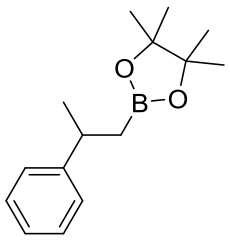

10s

According to general procedure A, α-methylstyrene (1.5 mmol, 194 mL), HBpin (1.65 mmol, 0.240 mL), $LiAlH_4$ (0.15 mmol, 5.7 mg) were allowed to react. The residue was purified by flash chromatography (SiO_2, hexane to hexane/ethyl acetate 92:8, [UV/$KMnO_4$]), to give the boronic ester **10s** (114 mg, 0.46 mmol, 31%) as a colourless oil with a regioselectivity of 99:1 (Linear/Branched).

^{1}H NMR (500 MHz, $CDCl_3$) δ 7.31 – 7.25 (m, 4H), 7.18 (m, 1H), 3.07 (h, *J* = 7.2 Hz, 1H), 1.32 (d, *J* = 6.9 Hz, 3H), 1.20 (s, 12H).

^{11}B NMR (160 MHz, $CDCl_3$) δ 33.7.

^{13}C{H} NMR (126 MHz, $CDCl_3$) δ 149.2, 128.2, 126.6, 125.7, 83.0, 35.8, 24.9, 24.8, 24.7.

Data were in accordance with those previously reported.[17]

5.9 Unsuccessful substrates

no reaction

mixture of unidentified products

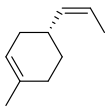

no reaction

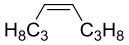

no reaction

low reactivity

low reactivity

no reaction

no reaction

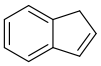

no reaction

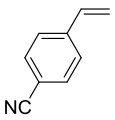

mixture of reduced species

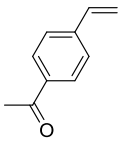

mixture of reduced species

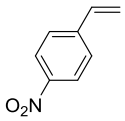

mixture of unidentified products

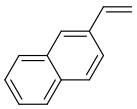

low reactivity

mixture of reduced species

no reaction probably due pyridine coordination

5.10 Hydroboration of polar bonds

Hydroboration of acetophenone

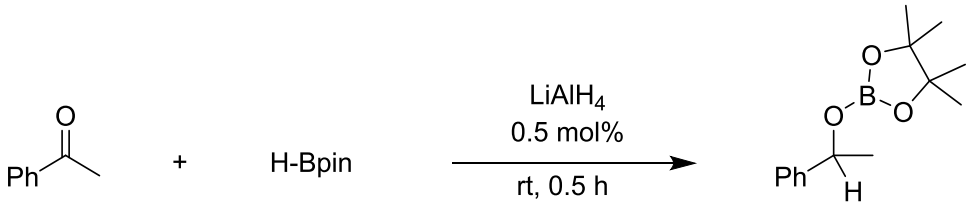

Safety note: gas evolution during reaction set-up may occur.

A solution of $LiAlH_4$ (3.7 mg, 0.1 mmol) in THF (1.0 mL) was prepared. Acetophenone (1.0 mmol) and HBpin (1.1 mmol) were added at room temperature to a Young's flask containing a solution of $LiAlH_4$ (0.05 mL, 0.1 M in THF) and stirred for 40 minutes. The mixture was dried under vacuum, dissolved in hexane and filtered over a celite plug to give the boronic ester (81%, 0.81 mmol) as a colourless oil.

^{1}H NMR (500 MHz, C_6D_6) δ 7.38 – 7.34 (m, Ar**H**, 2H), 7.17 – 7.10 (m, Ar**H**, 2H), 7.07 – 7.01 (m, Ar**H**, 1H), 5.41 (q, ArC**H**CH_3, *J* = 6.5 Hz, 1H), 1.45 (d, CHC**H$_3$**, *J* = 6.5 Hz, 3H), 1.00 (d, C(C**H$_3$**)$_2$, *J* = 12.8 Hz, 12H).

^{11}B NMR (160 MHz, C_6D_6) δ 22.57.

^{13}C{H} NMR (126 MHz, C_6D_6) δ 145.0, 128.2, 127.0, 125.3, 82.1, 72.6, 25.4, 24.3, 24.2.

Data were in accordance with those previously reported.[20]

Hydroboration of Ethyl acetate

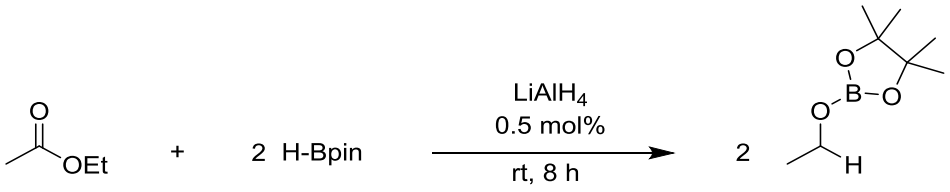

Safety note: gas evolution may occur during reaction set-up.

A solution of $LiAlH_4$ (3.7 mg, 0.1 mmol) in THF (1.0 mL) was prepared. Ethyl acetate (1.0 mmol) and HBpin (2.2 mmol) were added at room temperature to a Young's flask containing a solution of $LiAlH_4$ (0.05 mL, 0.1 M in THF) and stirred for 8 h. The mixture was dried under vacuum, dissolved in hexane and filtered over a celite plug to give the boronic ester (79%, 1.58 mmol) as a colourless oil.

^{1}H NMR (500 MHz, C_6D_6) 3.90 (q, C**H$_2$**CH_3, *J* = 7.0 Hz, 2H), 1.10 (t, CH_2C**H$_3$**, *J* = 7.0 Hz, 3H), 1.05 (s, C(C**H$_3$**)$_2$, 12H).

^{11}B NMR (160 MHz, C_6D_6) δ 22.67.

^{13}C{H} NMR (126 MHz, C_6D_6) δ 82.0, 60.3, 24.3, 17.1.

Data were in accordance with those previously reported.[21]

Hydroboration of 4-trifluoromethylbenzonitrile

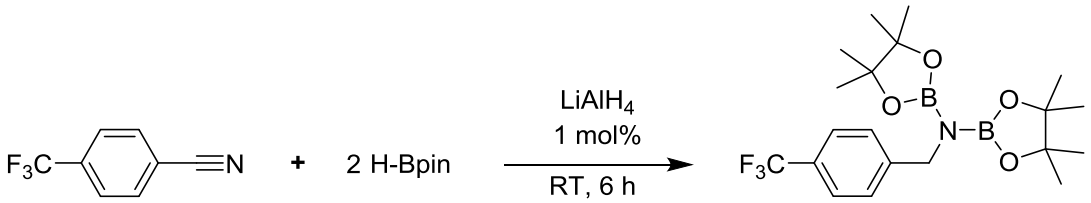

Safety note: gas evolution might occur during the reaction set-up.

A solution of $LiAlH_4$ (3.7 mg, 0.1 mmol) in THF (1.0 mL) was prepared. 4-Trifluoromethylbenzonitrile (1.0 mmol), HBpin (2.2 mmol) and THF (0.20 mL) were added at room temperature to a Young's flask containing a solution of $LiAlH_4$ (0.1 mL, 0.1 M in THF) and stirred for 6 h. The mixture was dried under vacuum and the boronic ester (71%, 0.71 mmol) recrystallised from hexane at −30 °C as colourless needles.

^{1}H NMR (500 MHz, C_6D_6) 7.41 (s, Ar**H,** 4H), 4.49 (s, ArC**H_2**, 2H), 1.01 (s, C(C**H_3**)$_2$, 24H).

^{11}B NMR (160 MHz, C_6D_6) δ 22.57.

^{13}C{H} NMR (126 MHz, C_6D_6) δ 147.7, 128.0, 125.3, (m) 82.8, 47.5, 24.7.

Melting point: decomposition.

Data were in accordance with those previously reported.[22]

Hydroboration of 16-dehydropregnenolone acetate

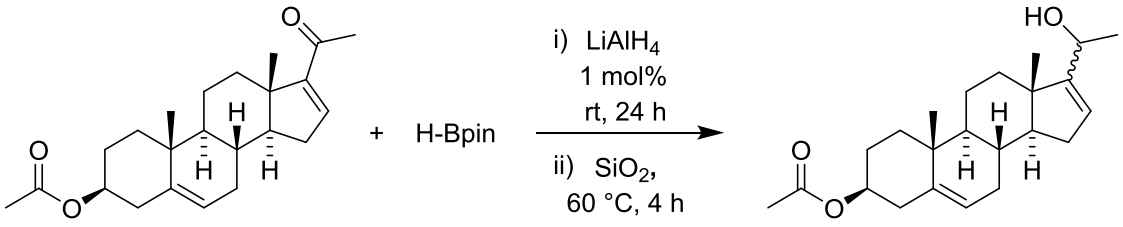

Safety note: gas evolution might occur during the reaction set up.

A solution of $LiAlH_4$ (3.7 mg, 0.1 mmol) in THF (1.0 mL) was prepared. 16-dehydropregnenolone acetate (1.0 mmol), HBpin (1.0 mmol) and THF (0.20 mL) were added at room temperature to a Young's flask containing a solution of $LiAlH_4$ (0.1 mL, 0.1 M in THF) and stirred for 24 h. The mixture was diluted with CH_2Cl_2 and hydrolised to the corresponding alcohol adding SiO_2 gel (500 mg) and stirring over 4 h at 60 °C. The residue was extracted with $HCl_{(aq)}$ (10% w/w) and purified by flash chromatography (SiO_2, hexane/ethyl acetate 9:1 to hexane/ethyl acetate 7:3, [UV/$KMnO_4$]), to give *the alcohol* (225 mg, 0.63 mmol, 63%) as a white amorphous solid with a diastereoisomeric ratio of 72:27.

^{1}H NMR (500 MHz, C_6D_6) δ 5.58 –5.51 (m, 1H), 5.35 –5.31 (m, 1H), 4.86 – 4.78 (m, 1H), 4.25 (q, *J* = 7.6 Hz, 1H), 2.52 –2.46 (m, 1H), 2.41– 2.33 (m, 1H) 2.00 –1.93 (m, 1H), 1.90 –1.81 (m, 3H), 1.78– 1.70 (m, 4H), 1.60 –1.44 (m, 4H), 1.44 –1.22 (m, 7H), 1.18 (s, 1H), 1.00 – 0.80 (m, 8H).

^{13}C{H} NMR (126 MHz, C_6D_6) δ 169.3, 159.6, 158.9, 139.9, 139.8, 123.0, 122.5, 122.3, 122.3, 73.6, 65.1, 65.0, 57.6, 57.4, 50.5, 46.0, 45.9, 38.3, 36.8, 36.7, 35.2, 35.0, 31.6, 30.9, 30.8, 30.3, 30.3, 27.9, 23.3, 23.0, 20.7, 20.7, 18.9, 16.6, 16.4.

Melting point (hexane/EtOAc) 128.5-129.5 °C.

HRMS (EI) mass calc'd for $C_{23}H_{33}O_3$ 357.243521; found: 357.24060.

IR: *vmax* (neat): 3336, 2929, 2851, 1731, 1440, 1371, 1249, 1233, 1196, 1121, 1074, 956, 903, 879, 812.

5.11 Mechanistic Studies

HBpin (0.150 mmol, 0.021 mL) was added to a solution of the named aluminium compound (0.15 mmol) in 0.60 mL of toluene-d_8 in an NMR tube at room temperature.

Stoichiometric reaction of DIBAL-H and HBpin

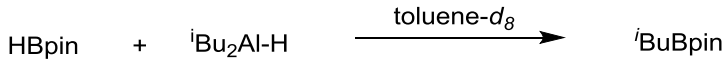

^{11}B NMR (160 MHz, toluene-d_8) δ 33.9 (s, *^{i}BuBpin*), 28.8 (d, $J_{B\text{-}H}$ = 174.4 Hz, *HBpin*).

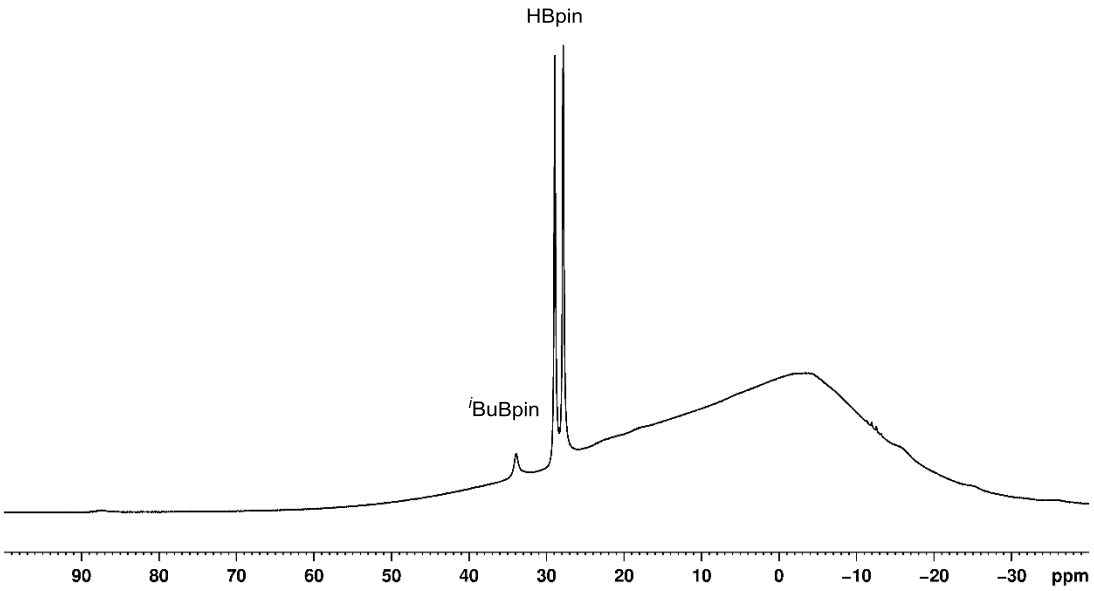

^{11}B NMR (160 MHz, toluene-d_8) spectrum of pinacolborane and ^{i}Bu$_2$Al-H.

Stoichiometric reaction of Red-Al and HBpin

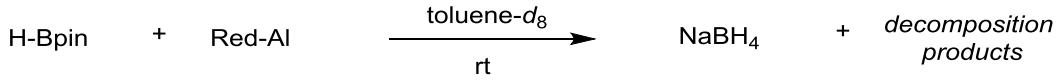

^{11}B NMR (160 MHz, toluene-d_8) δ 28.8 (d, J_{B-H} = 174.4 Hz, *HBpin*), 22.6 (s, B_2pin_3), −42.3 (q, J_{B-H} = 82.0 Hz, *$NaBH_4$*).

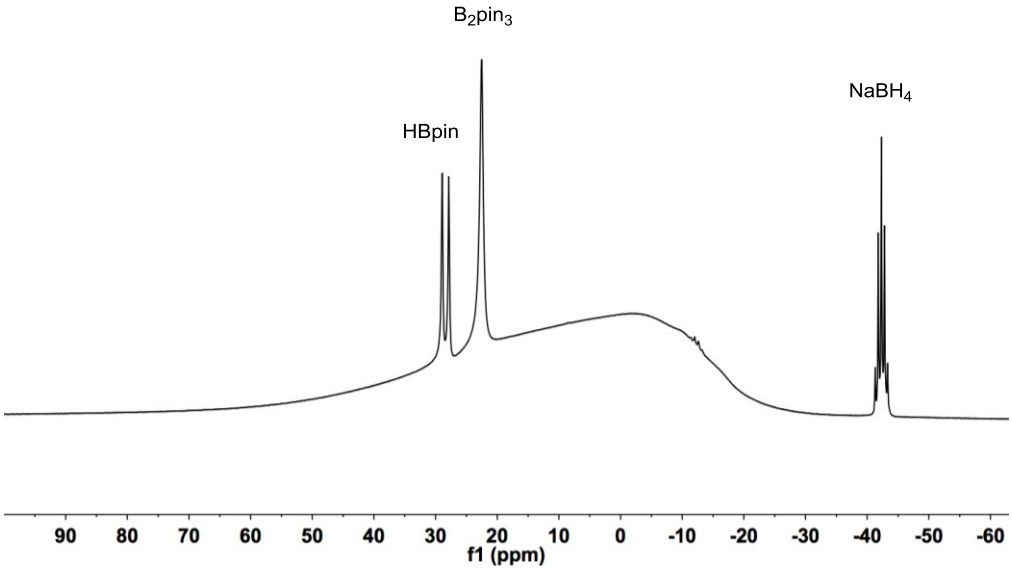

^{11}B NMR (160 MHz, toluene-d_8) spectrum of reaction of Red-Al and HBpin of the reaction.

Hydroalumination of 3,3-dimethyl-1-butene

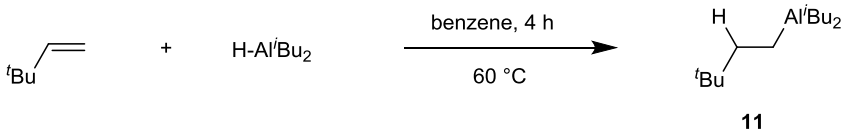

11

3,3-Dimethyl-1-butene (0.100 mL, 0.7 mmol) was added dropwise to di*iso*butylaluminum hydride (1 M in hexane, 0.30 mL, 0.5 mmol) and stirred for 4 h at 60 °C (oil bath temperature) before concentrating *in vacuo* to give the alane **11** (150 mg, 0.66 mmol, 66%) as a colourless oil.

^{1}H NMR (500 MHz, C_6D_6) δ 1.97 (h, *J* = 6.7 Hz, 2H), 1.48 (m, 2H), 1.13 (d, *J* = 6.7 Hz, 12H), 0.94 (s, 9H), 0.48 (m, 2H) 0.31 (d, *J* = 6.7 Hz, 4H).

^{13}C NMR (126 MHz, C_6D_6) δ 39.3, 31.3, 28.2, 28.0, 26.6, 24.8, 5.6.

HRMS (EI) mass calc'd for $C_{14}H_{31}Al$ 226.22467; found: 226.22444.

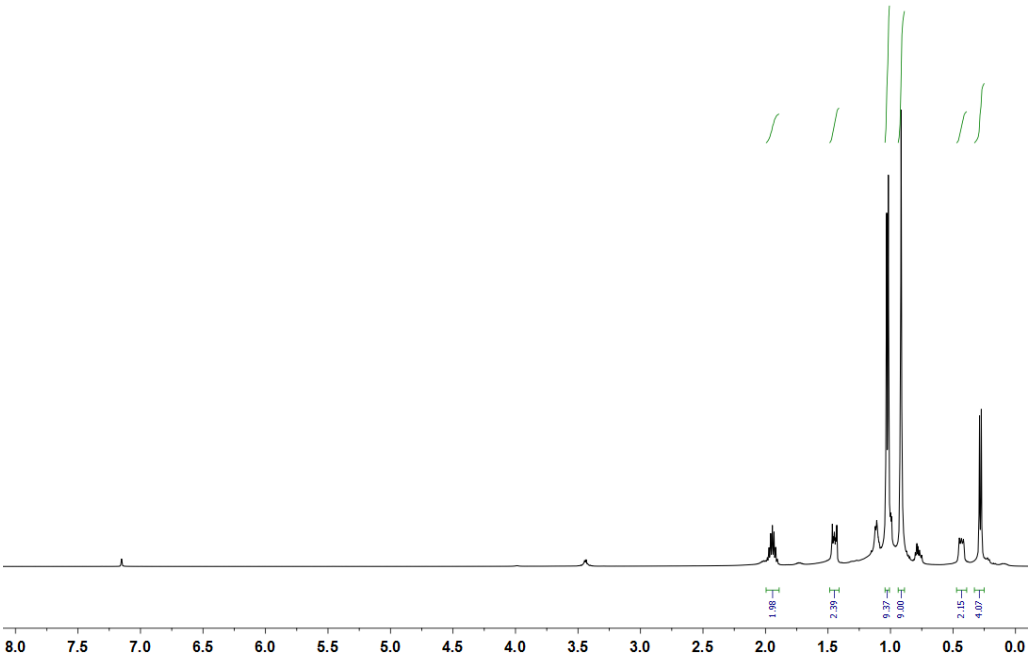

*^{1}H NMR (160 MHz, C_6D_6) spectrum of alane (**11**).*

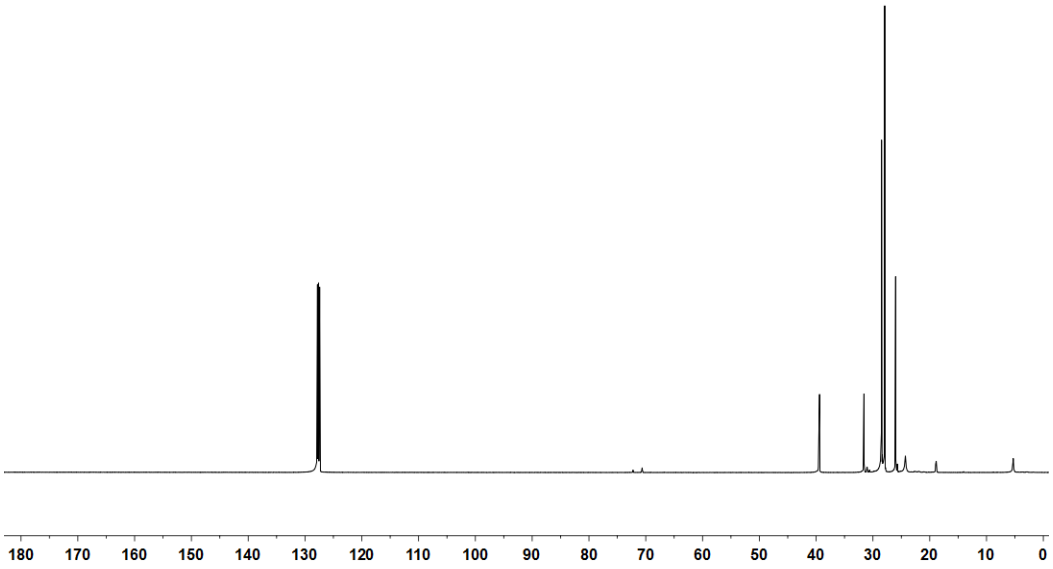

*^{13}C NMR (126 MHz, C_6D_6) spectrum of alane (**11**).*

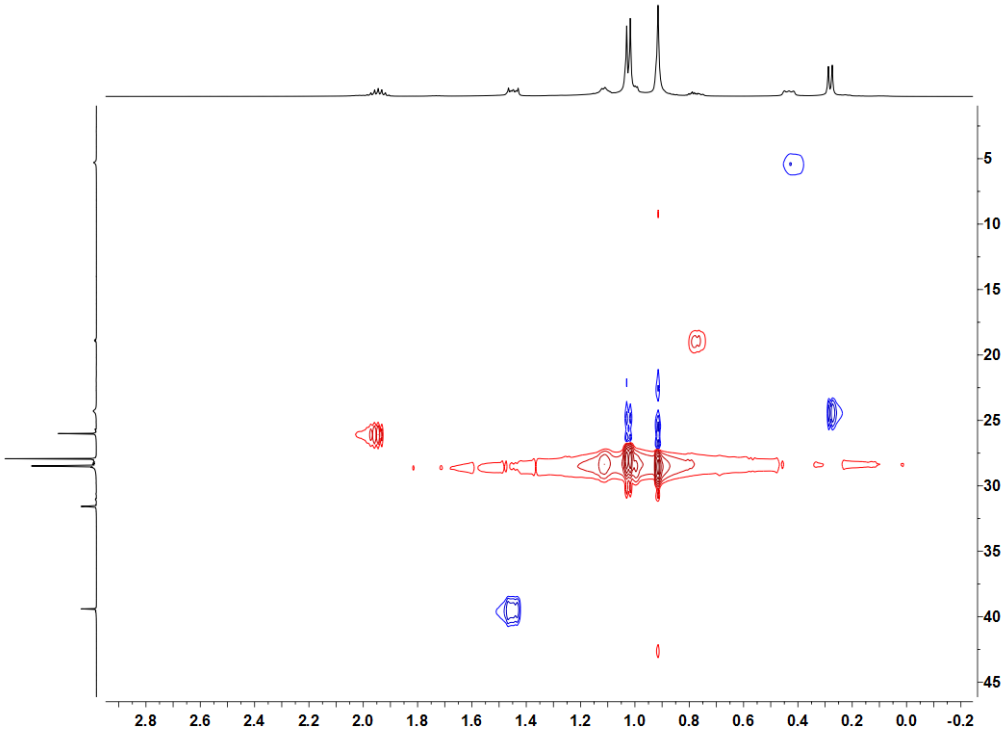

*HSQC ^{1}H-^{13}C NMR (C_6D_6) spectrum of alane (**11**).*

Stoichiometric reaction of alane (11) with HBpin

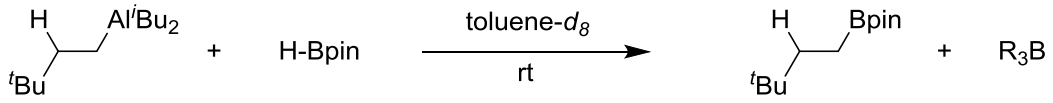

11 **10c**

HBpin (0.150 mmol, 0.021 mL) and alane **11** (0.150 mmol) were added to an NMR tube charged with 0.60 mL of toluene-d_8 and the resulting mixture was then analysed by NMR spectroscopy.

^{11}B NMR (160 MHz, toluene-d_8) 83.2 (s), 34.4 (s).

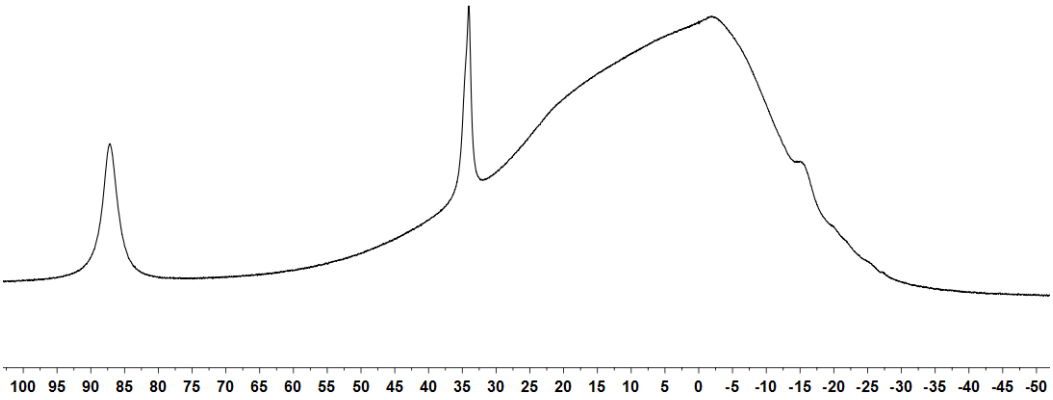

*^{11}B NMR (160 MHz, toluene-d_8) spectrum of reaction of alane (**11**) with HBpin.*

5.12 Experimental Details for Chapter 4

5.13 Synthesis of tris(pentafluorophenyl)borane

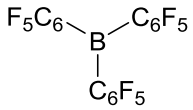

Magnesium turnings (75 mmol, 1.8 g) were suspended in diethyl ether (150 mL) at room temperature. BrC_6F_5 (75 mmol, 18.5 g) was added dropwise and the solution developed a grey turbid appearance followed by a net colour change to a dark brown when the reaction is completed.

$BF_3 \cdot Et_2O$ (25 mmol, 3.5 g) were dissolved in toluene (30 mL) and cool to 0 ºC. The Grignard reagent solution was added by cannula resulting solution was allowed to warm to room temperature and then stirred for 1 h.

The solution was concentrated to 30 mL and refluxed for 1 h at 100 °C. All volatiles were removed under vacuum until a dry brown cake is obtained. The precipitate was extracted twice with warm (45 ºC) hexanes (2×100 mL). The solution was concentrated and Et_2O (7.5 mL) were added and the product recrystallised at −20 °C to give $B(C_6F_5)_3 \cdot Et_2O$ (14.5 mmol, 10 g, 58%) as yellow needles.

Pure product (13.7 mmol, 7.15 g, 95%) was obtained by sublimation as white powder.

^{11}B NMR (160 MHz, toluene-d_8) δ 55.0.

^{13}C{H} NMR (126 MHz, toluene-d_8) δ 150.5 – 148.8 (m), 148.0 – 147.0 (m), 146.6 – 145.9 (m), 144.3 (m), 138.8 (m), 136.8 (m), 113.3 (s).

^{19}F NMR (471 MHz, toluene-d_8) δ −133.87, −147.3, −165.48.

NMR data were in accordance with those previously reported.[23]

5.14 Stoichiometric reaction of phenylacetylene and $B(C_6F_5)_3$

Phenyl acetylene (0.12 mmol, 0.014 mL) was added to a solution of $B(C_6F_5)_3$ (0.12 mmol, 61.4 mg) in toluene-d_8 (0.60 mL) at T =195 K in a NMR tube. NMR spectra were recorded at T = 233 K.

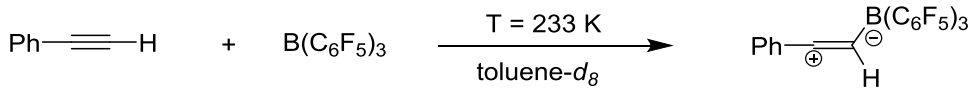

31i **32i**

^{1}H NMR (400 MHz, toluene-d_8) δ 7.48 (m, *ortho* Ar**H**, 1H), 5.41 (br s, C$^+$=C**H**−B, 1H).
^{11}B NMR (128 MHz, toluene-d_8) δ −12.1 (s).
^{13}C{H} NMR (100 MHz, toluene-d_8) δ 199.3 (**C**$^+$=C), 51.2 (C$^+$=**C**H−B).

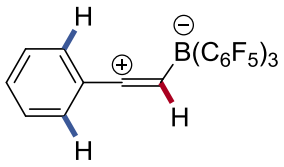

32i

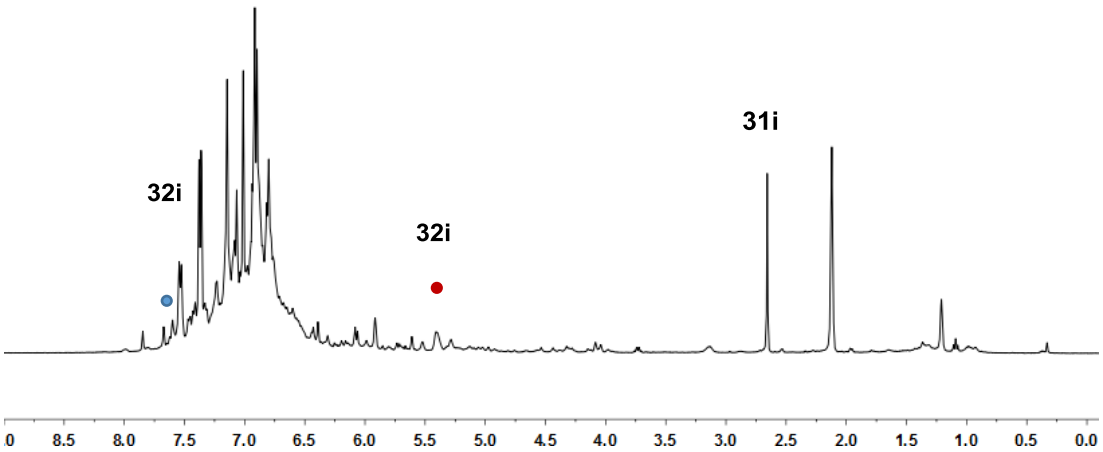

^{1}H NMR (400MHz, 233 K, toluene-d_8) spectrum of phenyl acetylene and $B(C_6F_5)_3$.

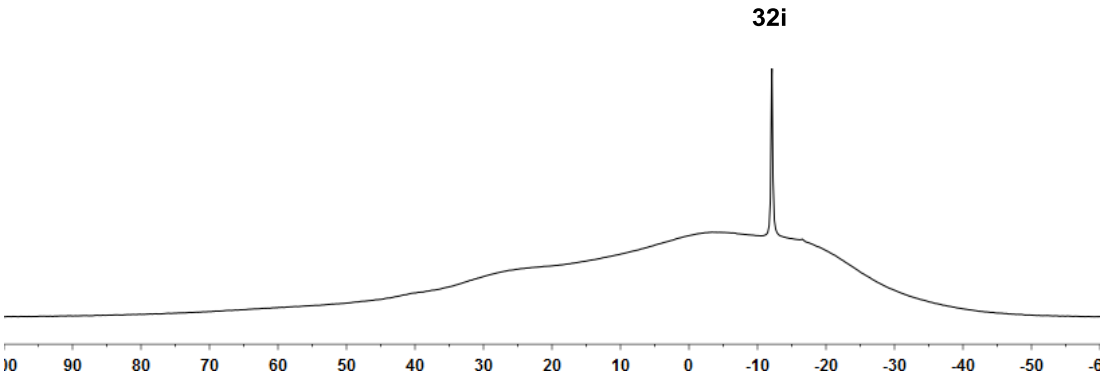

^{11}B NMR (128 MHz, 233 K, toluene-d_8) spectrum of phenyl acetylene and $B(C_6F_5)_3$

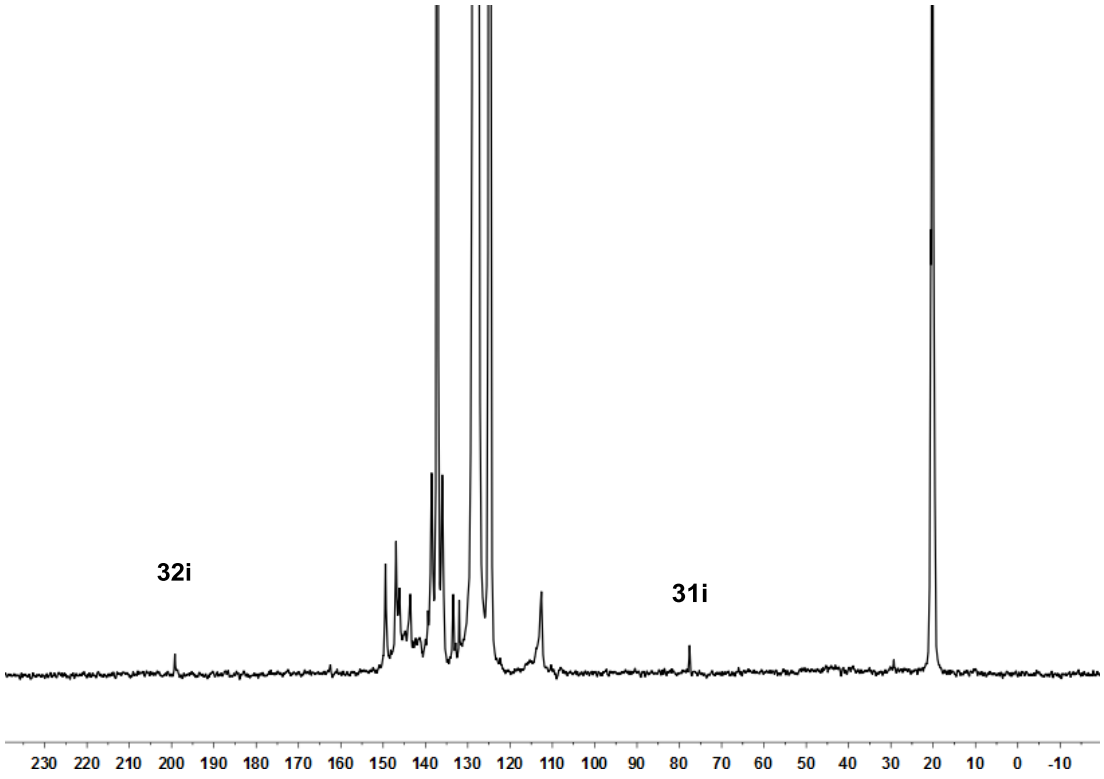

^{13}C{H} NMR (100 MHz, 233 K, toluene-d_8) spectrum of phenyl acetylene and $B(C_6F_5)_3$

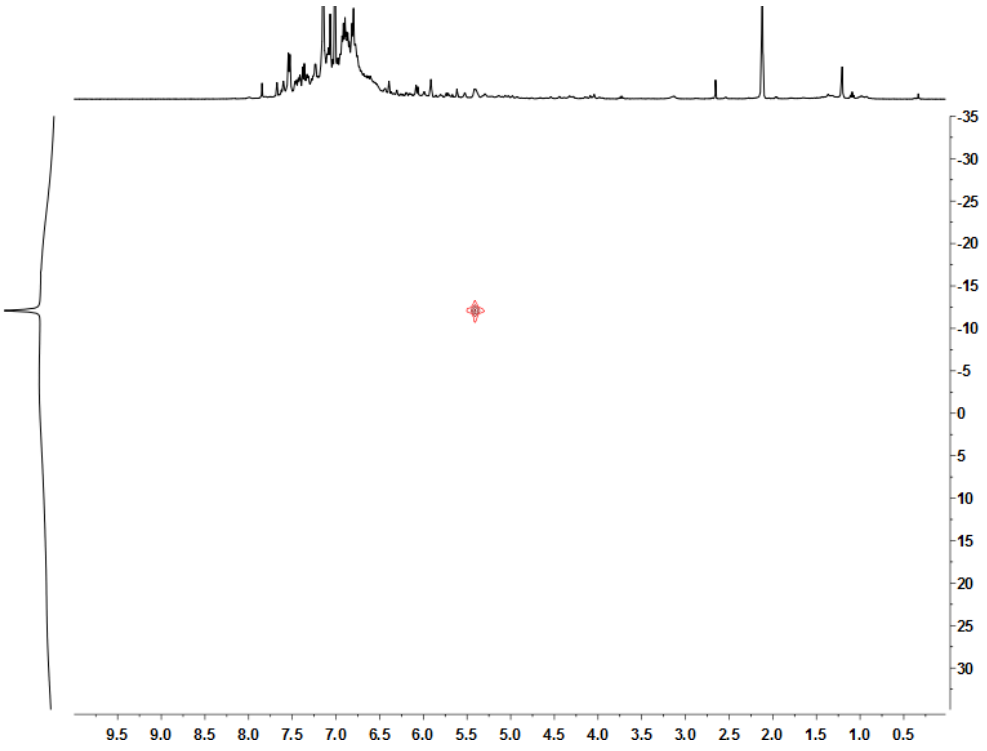

2D ^{1}H -^{11}B HMBC NMR spectra of phenyl acetylene and $B(C_6F_5)_3$.

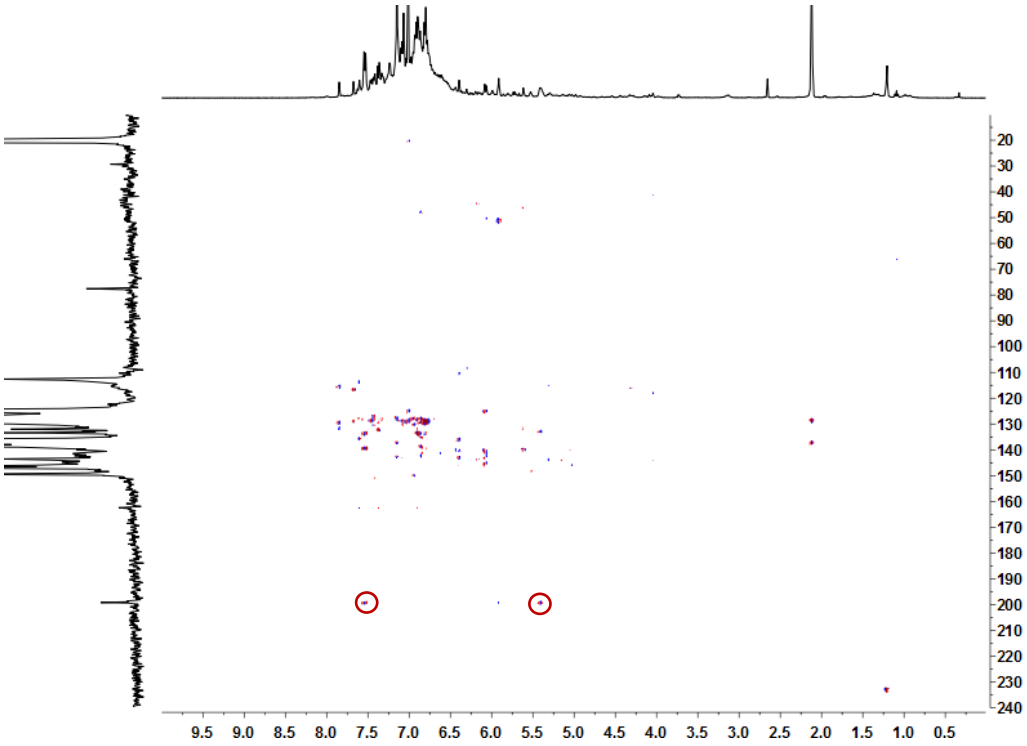

2D ^{1}H -^{13}C HMBC NMR spectra of phenyl acetylene and $B(C_6F_5)_3$.

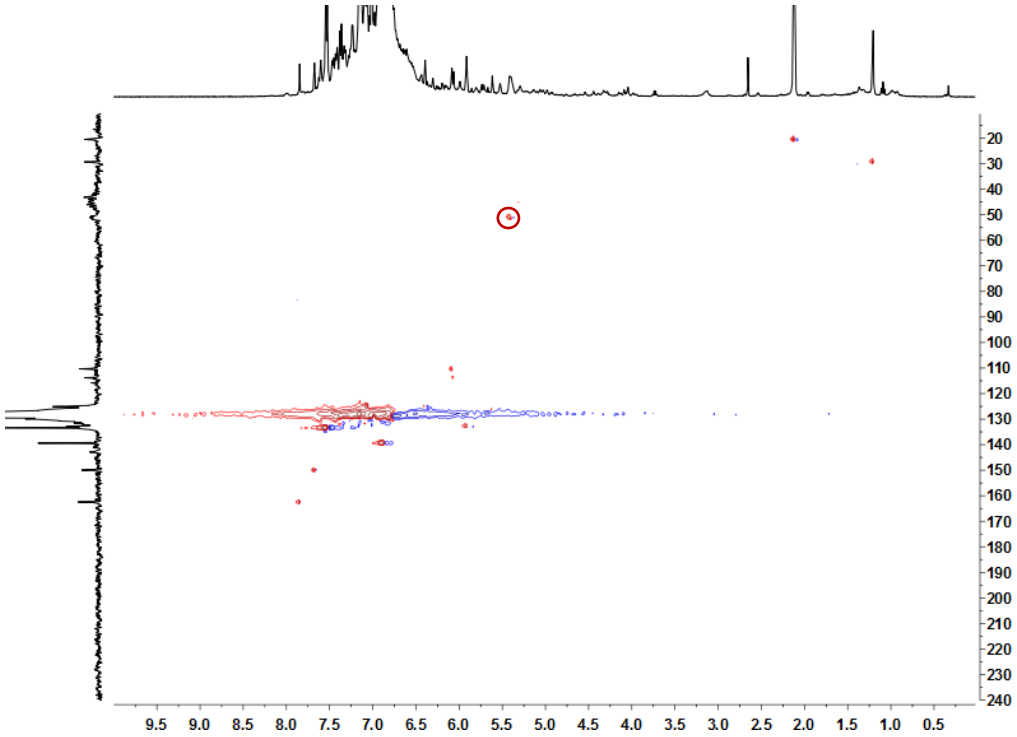

2D ^{1}H -^{13}C HSQC NMR spectra of phenyl acetylene and $B(C_6F_5)_3$

5.15 Stoichiometric reaction of phenylacetylene-2-^{13}C and $B(C_6F_5)_3$

Phenylacetylene-2-^{13}C (0.12 mmol, 0.014 mL) was added to a solution of $B(C_6F_5)_3$ (0.12 mmol, 61.4 mg) in toluene-d_8 (0.60 mL) at T =195 K in a NMR tube. NMR spectra were recorded at T = 233 K.

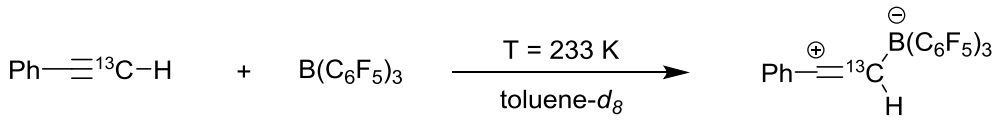

31i-2-^{13}C **32i-2-^{13}C**

^{11}B NMR (128 MHz, toluene-d_8) δ −12.1 (d, *J* = 44.4 Hz).

^{13}C{H} NMR (100 MHz, toluene-d_8) δ 51.2 (q, *J* = 44.4 Hz, C^+=**C**H−B).

Ph—≡^{13}C—H

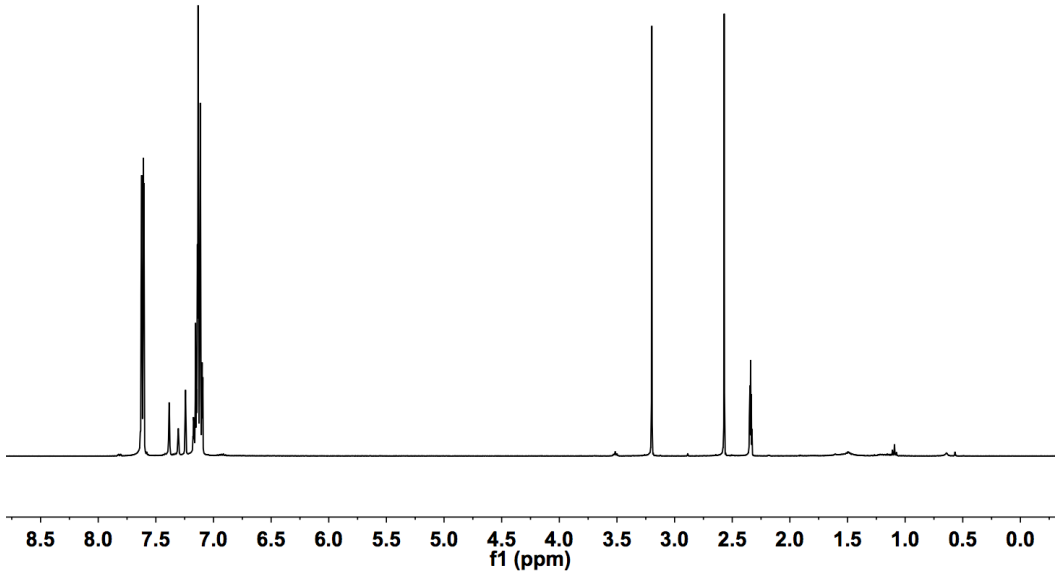

^{1}H NMR (400MHz, 233 K, toluene-d_8) spectrum of PhC≡^{13}C-H.

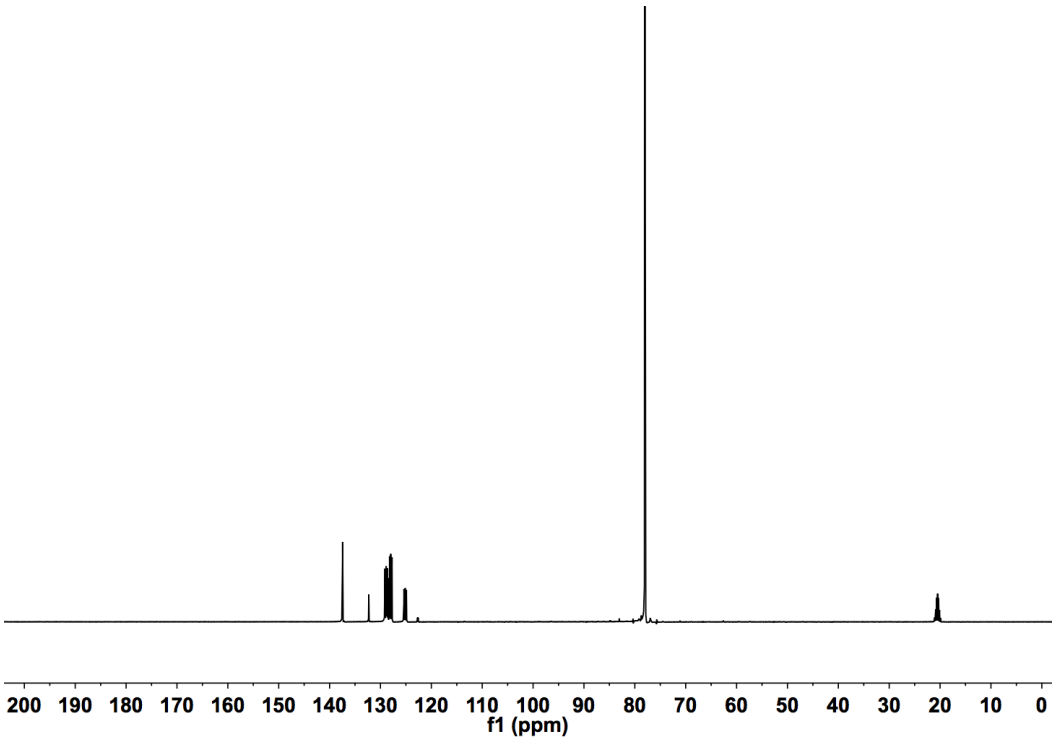

$^{13}C\{H\}$ NMR (100 MHz, 233 K, toluene-d_8) spectrum of PhC≡^{13}C-H.

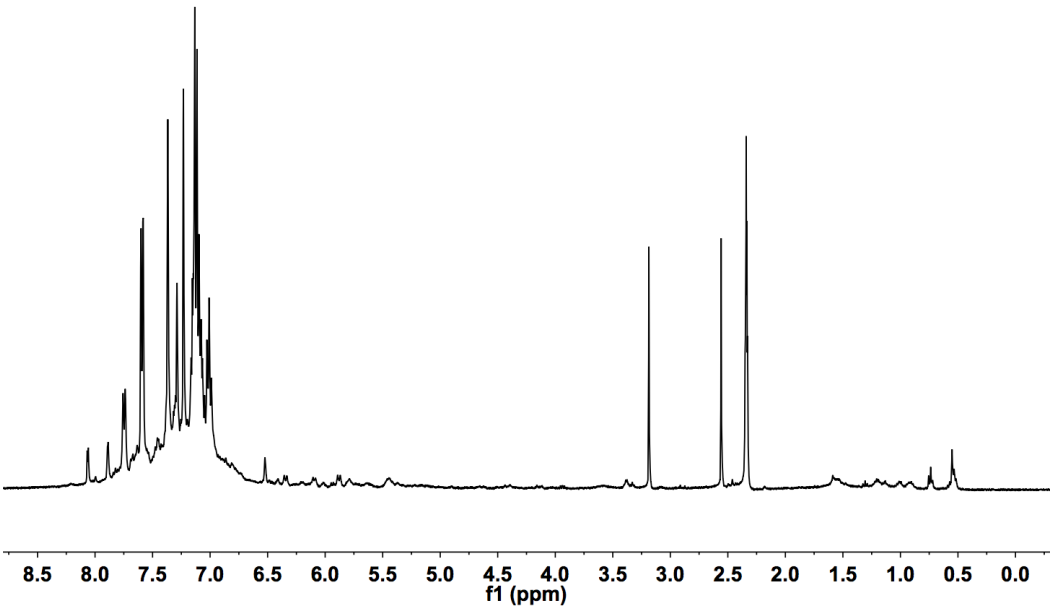

^{1}H NMR (400MHz, 233 K, toluene-d_8) spectrum of PhC≡^{13}C-H and $B(C_6F_5)_3$.

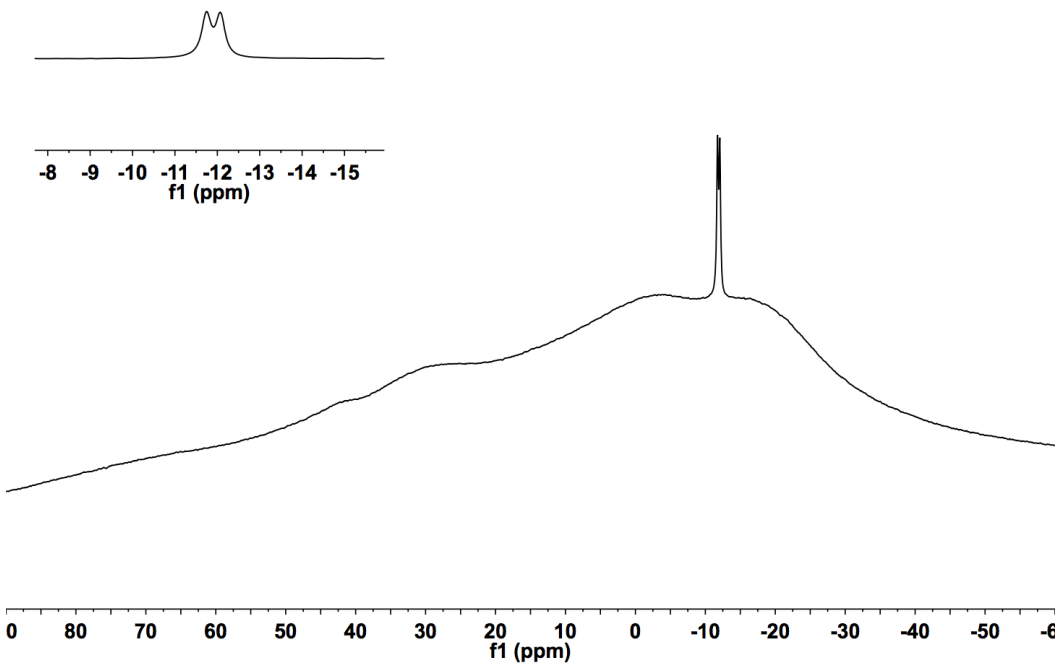

^{11}B NMR (128 MHz, 233 K, toluene-d_8) spectrum of PhC≡^{13}C-H and B(C_6F_5)$_3$.

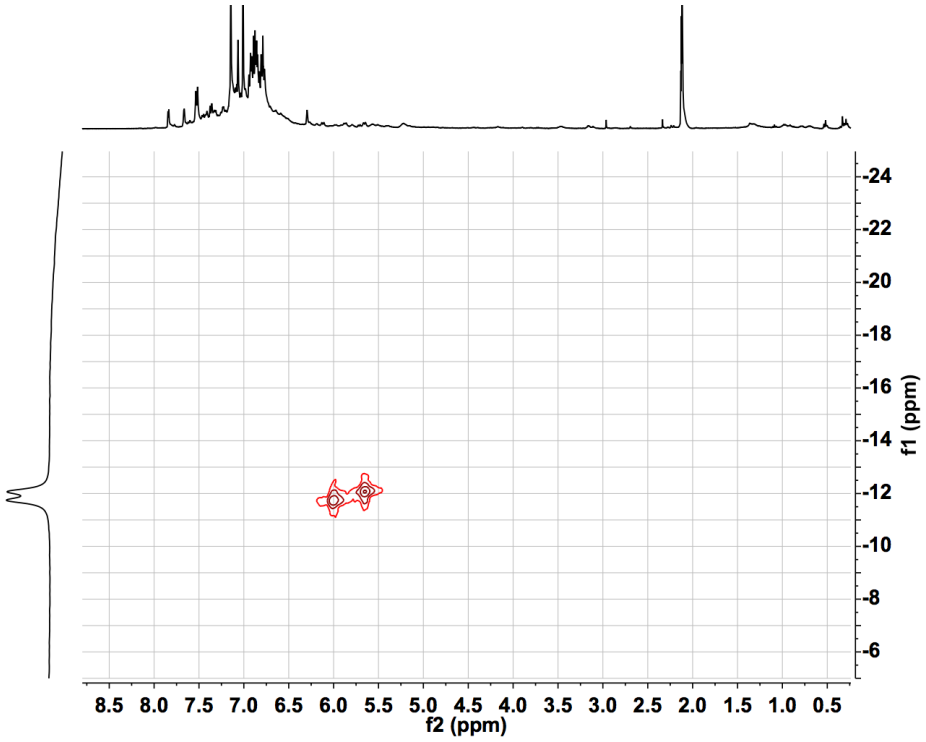

2D ^{1}H -^{11}B HMBC NMR spectra of PhC≡^{13}C-H and B(C_6F_5)$_3$.

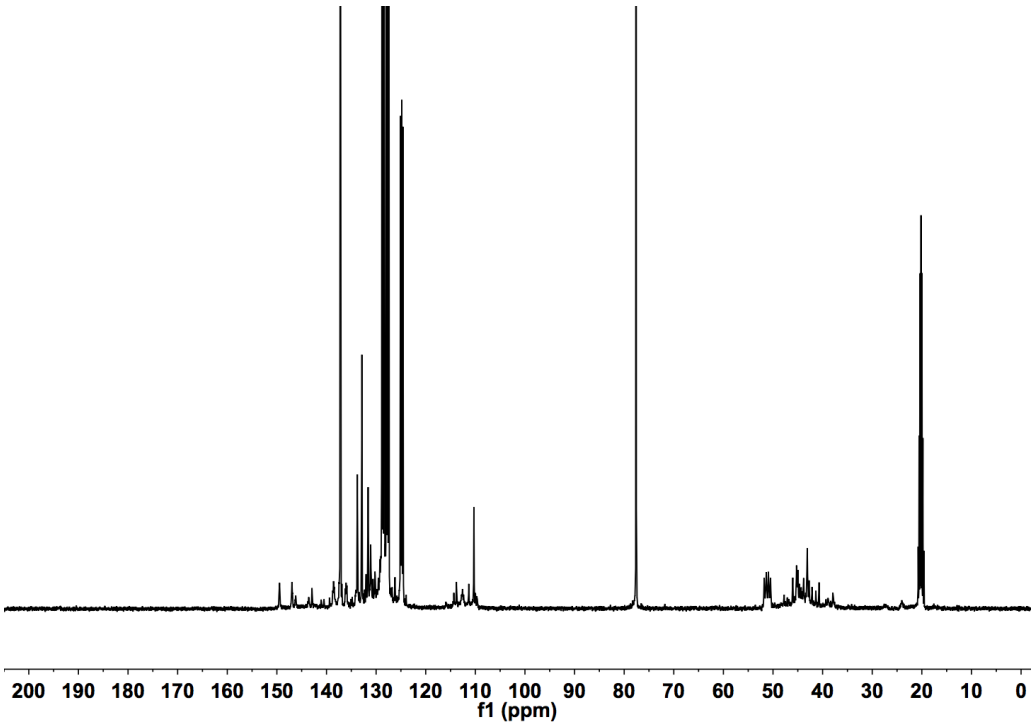

$^{13}C\{H\}$ NMR (100 MHz, 233 K, toluene-d_8) spectrum of PhC≡^{13}C-H and $B(C_6F_5)_3$.

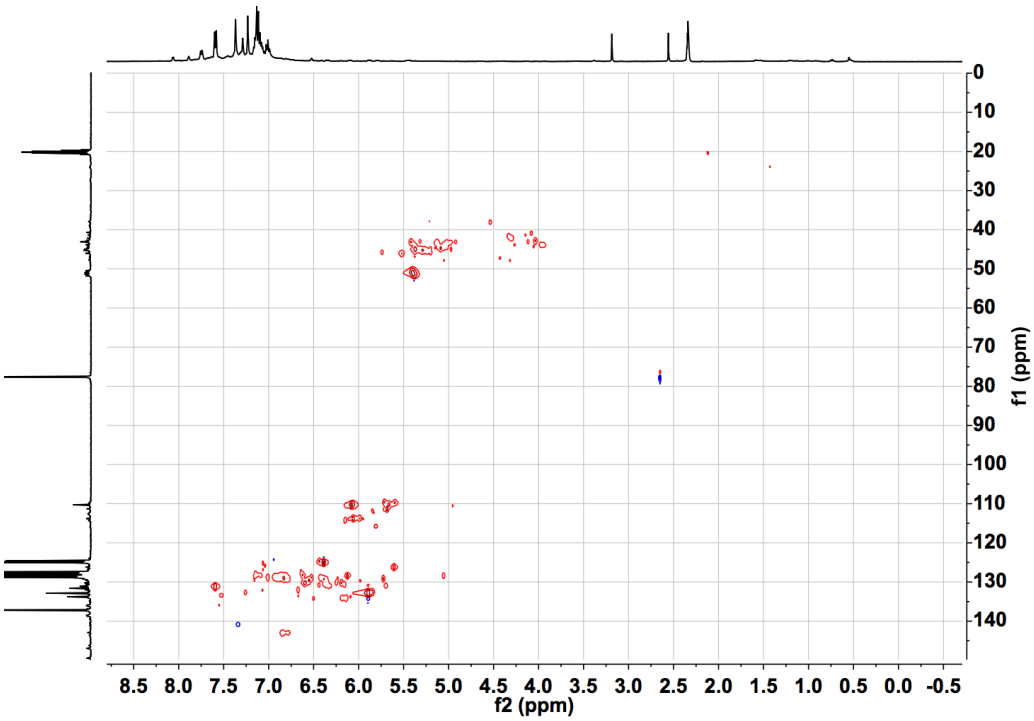

2D ^1H -^{13}C HSQC NMR spectra of PhC≡^{13}C-H and $B(C_6F_5)_3$.

5.16 VT NMR study of phenyl acetylene and $B(C_6F_5)_3$

Phenyl acetylene (0.12 mmol, 0.014 mL) was added to a solution of $B(C_6F_5)_3$ (0.12 mmol, 61.4 mg) in 0.60 mL of toluene-d_8 at T =195 K in an NMR tube. NMR spectra were recorded starting from T = 233 K to room temperature.

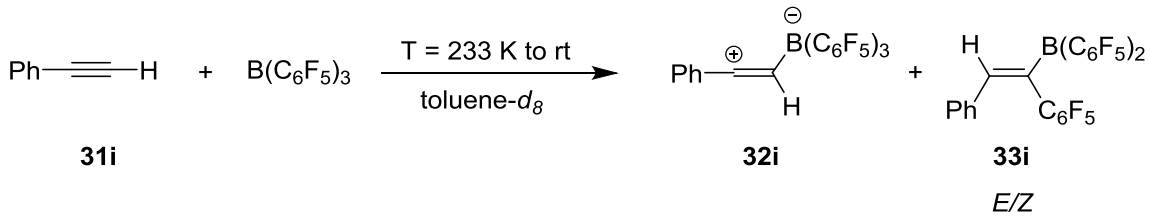

31i **32i** **33i** *E/Z*

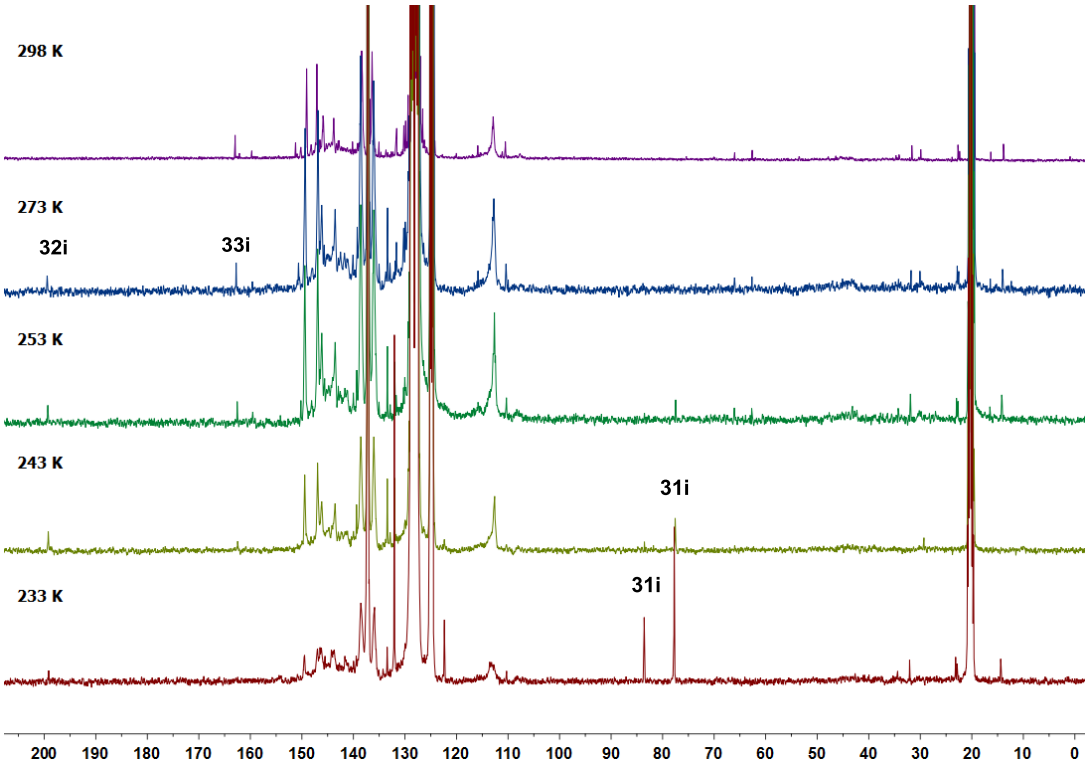

VT experiment of $^{13}C\{H\}$ NMR (100 MHz, toluene-d_8) spectra of phenylacetylene and $B(C_6F_5)_3$.

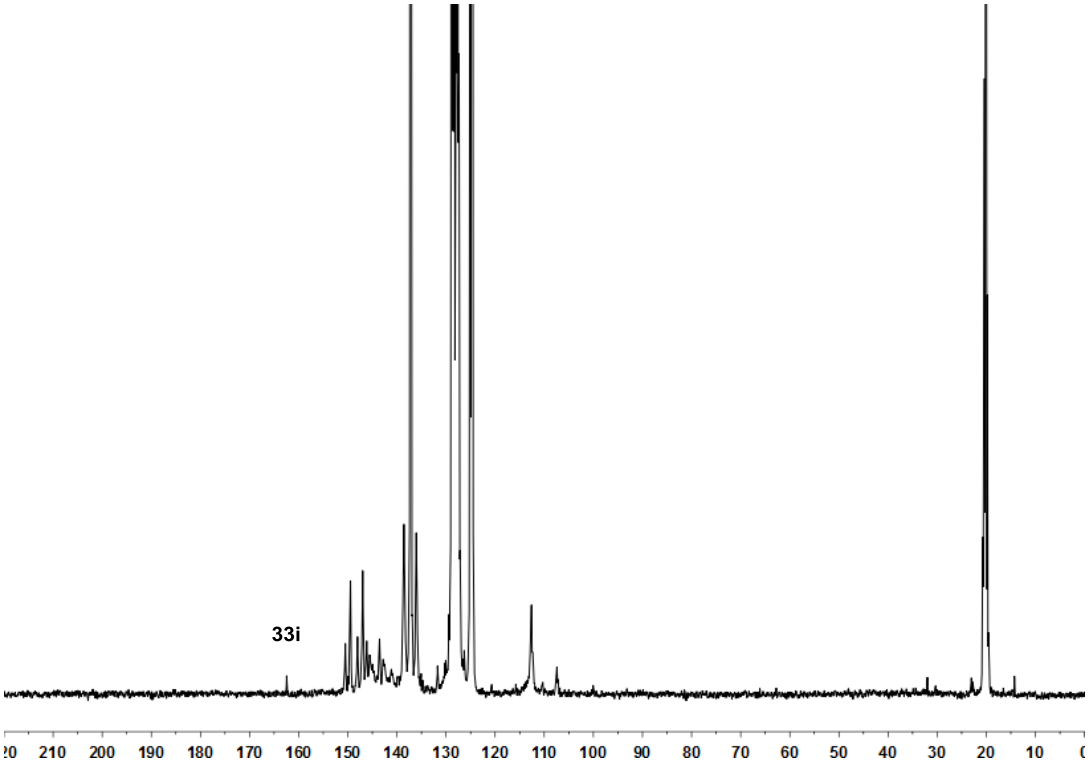

$^{13}C\{H\}$ NMR (125 MHz, 298 K, toluene-d_8) spectrum of phenylacetylene and $B(C_6F_5)_3$ after 48 h.

5.17 Time evolution of phenyl acetylene and $B(C_6F_5)_3$

Phenylacetylene (0.12 mmol, 0.014 mL) was added to a freeze solution of $B(C_6F_5)_3$ (0.12 mmol, 61.4 mg) in 0.60 mL of toluene-d_8 at T =195 K in an NMR tube. NMR spectra were recorded starting at T = 273 K at selected intervals of time.

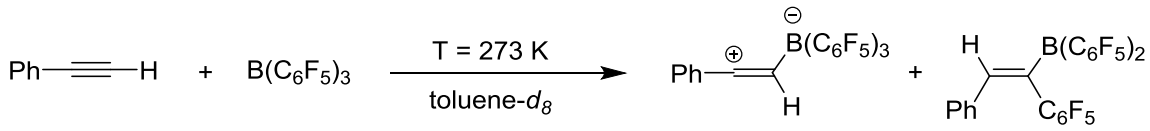

31i **32i** **33i** *E/Z*

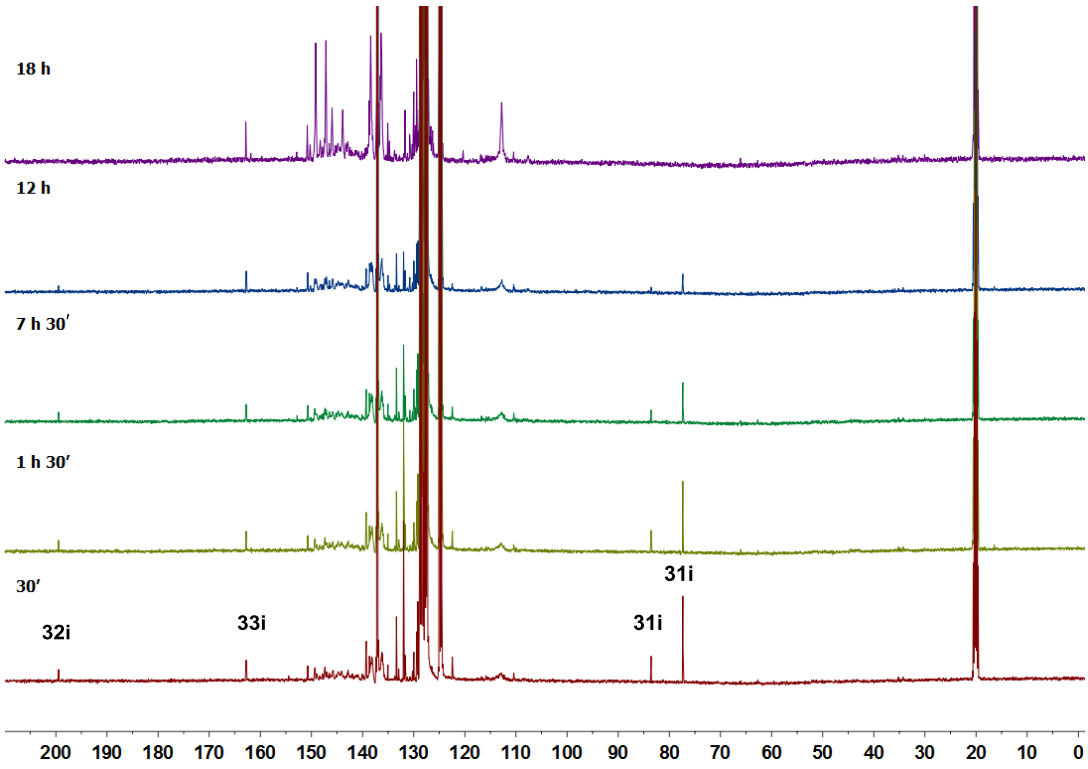

Time series experiment of $^{13}C\{H\}$ NMR (100 MHz, 273 K, toluene-d_8) spectra of phenylacetylene and $B(C_6F_5)_3$.

5.18 Stoichiometric reaction of *p*-methoxy phenylacetylene and $B(C_6F_5)_3$

A solution of *p*-methoxy phenylacetylene (0.12 mmol, 16.2 mg) in 0.60 mL of toluene-d_8 was added at 233 K to $B(C_6F_5)_3$ (0.12 mmol, 61.4 mg) in an NMR tube. The solution was allowed to warm up to room temperature and NMR spectra were recorded.

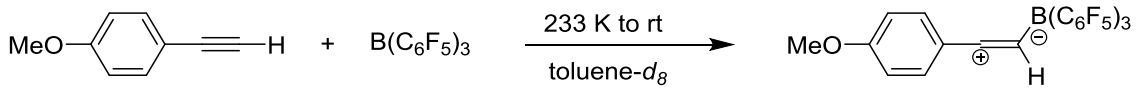

31k **32k**

^{1}H NMR (500 MHz, toluene-d_8) δ 5.53 (br s, C^{+}=C**H**−B, 1H).

^{11}B NMR (160 MHz, toluene-d_8) δ −11.9 (s).

^{13}C{H} NMR (126 MHz, toluene-d_8) δ 193.5 (**C^{+}**=CHB), 50.6 (C^{+}=H**C**−B).

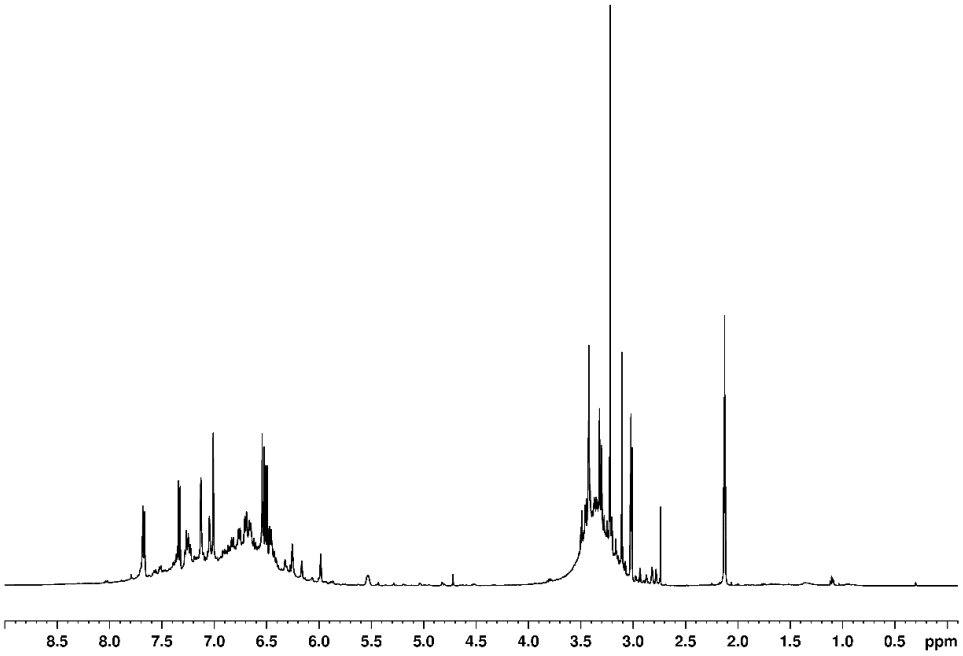

^{1}H NMR (500MHz, 298 K toluene-d_8) of p-methoxy phenylacetylene and $B(C_6F_5)_3$.

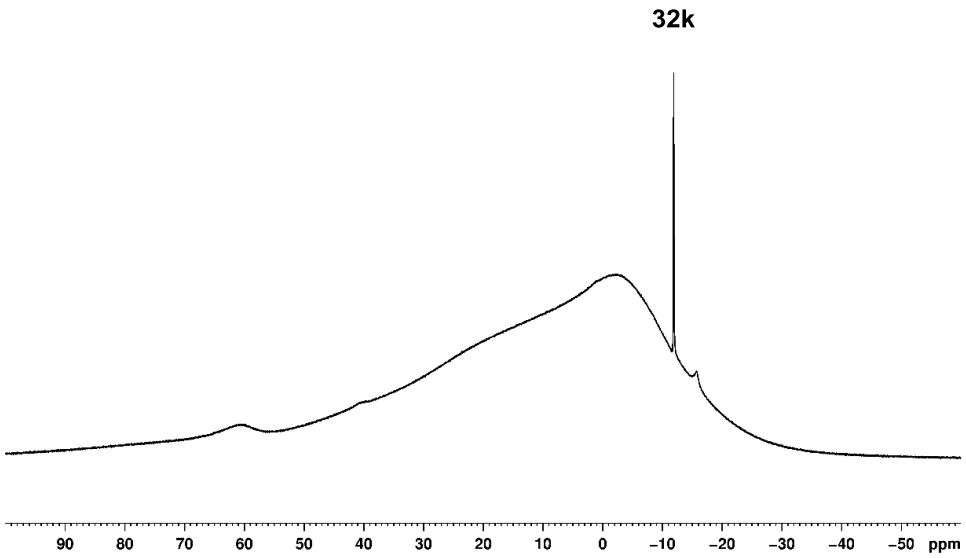

^{11}B NMR (160 MHz, 298 K toluene-d_8) spectrum of p-methoxy phenylacetylene and $B(C_6F_5)_3$.

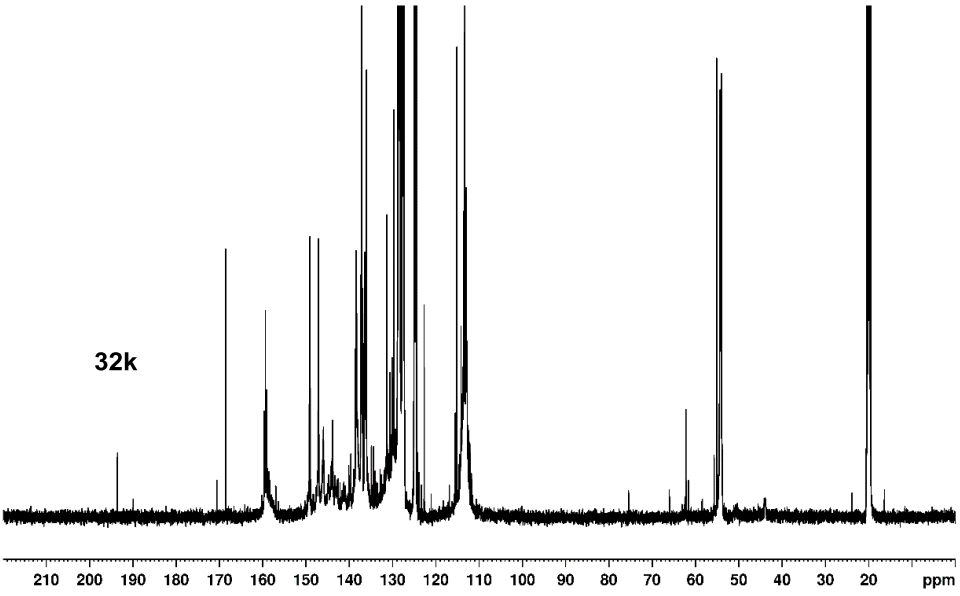

^{13}C{H} NMR (160 MHz, 298 K, toluene-d_8) spectrum of p-methoxy phenylacetylene and $B(C_6F_5)_3$.

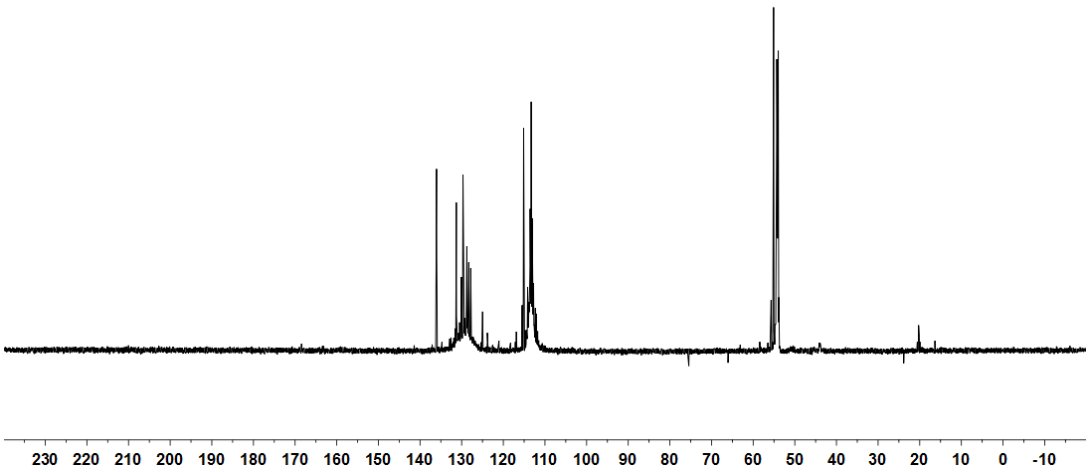

DEPT 135 ^{13}C NMR (160 MHz, 298 K, toluene-d_8) spectrum of p-methoxy phenylacetylene and $B(C_6F_5)_3$.

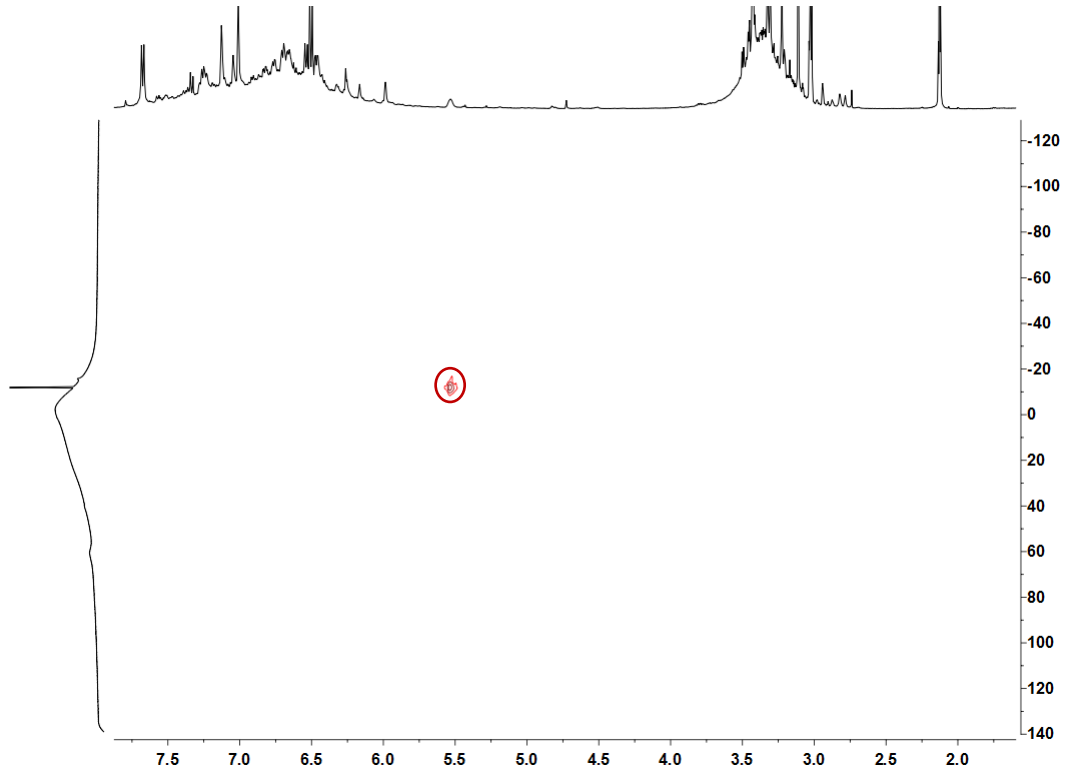

2D ^{1}H -^{11}B HMBC NMR spectra of p-methoxy phenylacetylene and $B(C_6F_5)_3$.

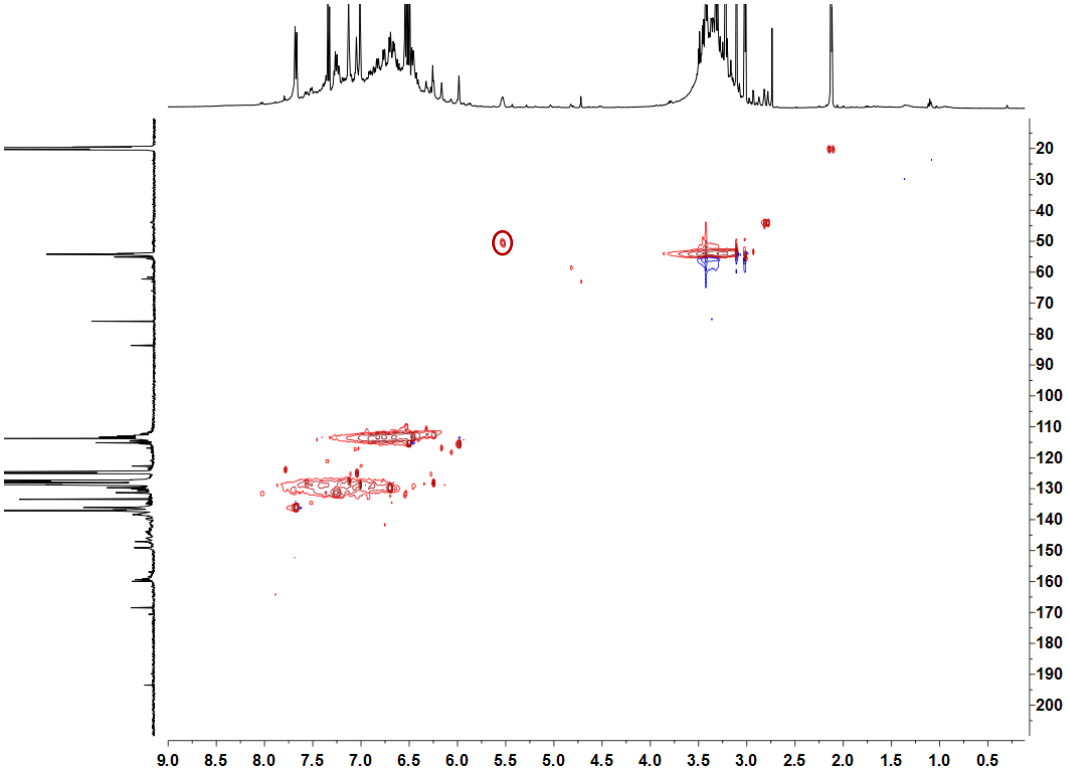

2D HSQC ^{1}H -^{13}C NMR of p-methoxy phenylacetylene and $B(C_6F_5)_3$.

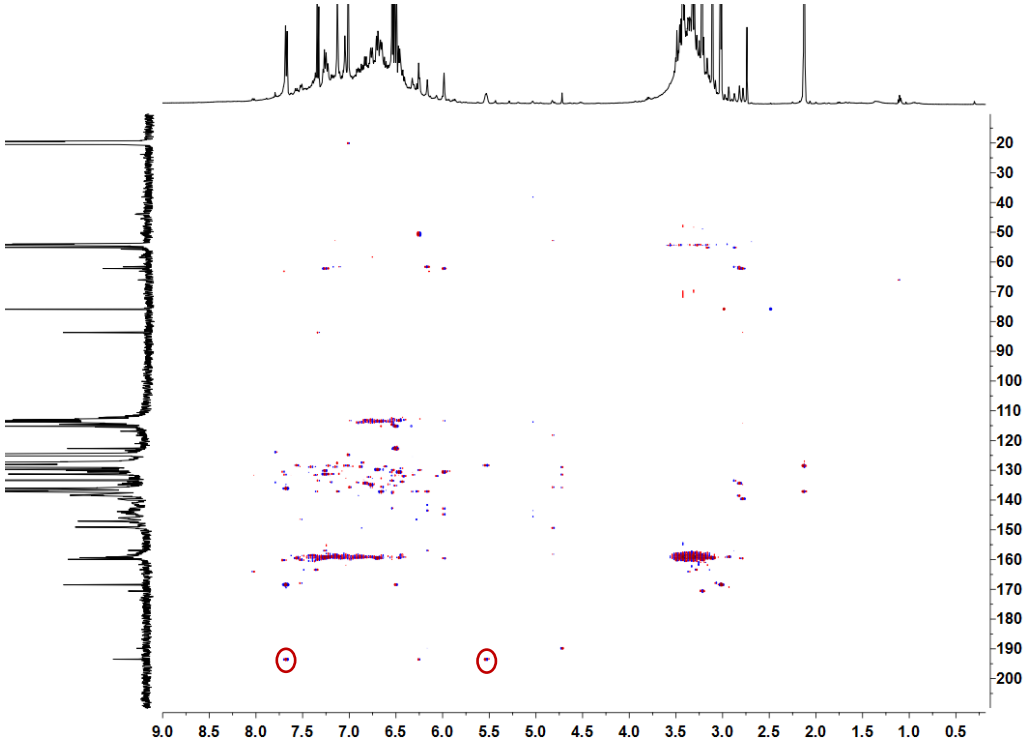

HMBC ^{1}H-^{13}C NMR of p-methoxy phenylacetylene and $B(C_6F_5)_3$.

5.19 Synthesis of the zwitterion (34)

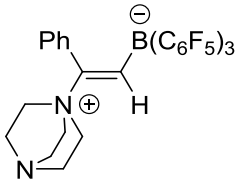

34a

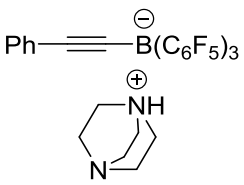

34b

$B(C_6F_5)_3$ (0.70 mmol, 360 mg) and 1,4-diazabicyclo[2.2.2]octane (0.70 mmol, 78 mg) were suspended in pentane (10 mL) and phenylacetylene (0.90 mmol, 91.2 mg) was added at room temperature and stirred overnight.

The solvent was removed by cannula filtration and the precipitate washed with hexane (2×10 mL) to give a mixture of **34a** and **34b** as (0.41 mmol, 300 mg, 59%) brown powder. The mixture was dissolved in cold Et_2O (10 mL) and **34b** (0.125 mmol, 100mg) was recrystallised as white needles**.** Compound **34a** was recrystallised from CH_2Cl_2 (2 mL) at −20 °C.

Compound 34a:

^{1}H NMR (500 MHz, CD_2Cl_2) δ 7.43 (s, C=C**H**, 1H), 7.25 (m, Ar**H**, 1H), 7.12 (m, Ar**H**, 2H), 6.80 (m, Ar**H**, 2H), 3.37 (m, N−(C**H₂**)$_3$, 6H), 3.15 (m, N−(C**H₂**)$_3$, 6H).

^{13}C{H} NMR (126 MHz, CD_2Cl_2) δ 148.47 (d, *J* = 236.3 Hz), 145.18 (m), 144.21 (q, *J* = 53.6 Hz), 139.81 (s), 137.96 (s), 136.07 (d, *J* = 11.7 Hz), 132.45 (s), 124.42 (s), 54.04, 46.45 (s).

^{11}B NMR (160 MHz, CD_2Cl_2) δ −16.57.

^{19}F NMR (471 MHz, CD_2Cl_2) δ −132.16 (d, *J* = 23.4 Hz), −162.83 (t, *J* = 20.5 Hz), −167.00 (t, *J* = 19.7 Hz).

HRMS (EI) = mass calc'd for $C_{32}H_{18}BN_2F_{15}$ 726.13258; found: 726.13180.

Compound 34b:

^{1}H NMR (500 MHz, CD_2Cl_2) δ 7.40 – 7.36 (m, Ar**H**, 2H), 7.32 (m, Ar**H**, 2H), 7.29 – 7.25 (m, Ar**H**, 1H), 7.20 – 7.05 (br s, N**H**, 2H), 2.93 (m, N−(C**H₂**)$_6$, 12H).

^{13}C{H} NMR (126 MHz, CD_2Cl_2) δ 148.6 (d, *C*−F *J* = 244.1 Hz), 138.1 (t, *C*−F *J* = 238.6 Hz), 131.8 (s), 129.3 (s), 128.0 (s), 126.0 (s), 123.6 (*C*−B, m), 110.8 (*C*−B, q, *J* = 71.3 Hz), 94.9 (m), 66.12 (CH_3CH_2O, s), 45.6 (d, *J* = 258.0 Hz), 15.5 (CH_3CH_2O, s).

^{11}B NMR (160 MHz, CD_2Cl_2) δ −20.90

^{19}F NMR (471 MHz, CD_2Cl_2) δ −133.26 (d, *J* = 22.0 Hz), −162.11 (t, *J* = 20.5 Hz), −166.30 (t, *J* = 19.7 Hz).

HRMS (EI) = mass calc'd for $C_{36}H_{28}BON_2F_{15}$ 800.20497; found: 800.20689.

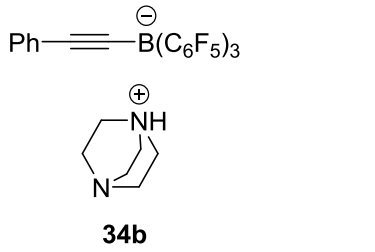

34b

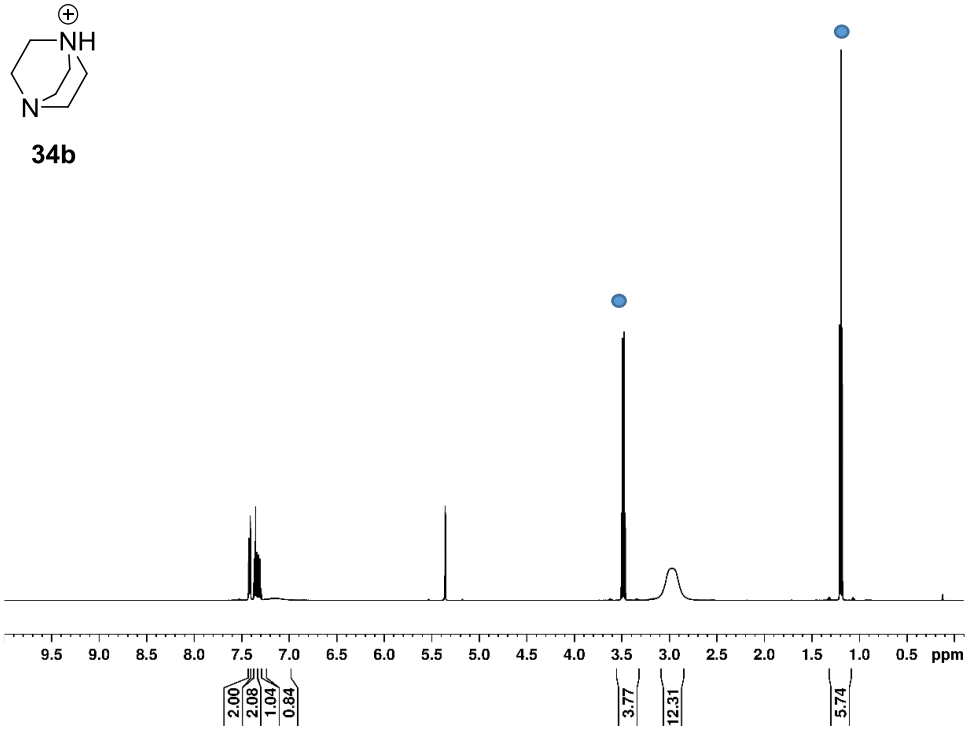

*^{1}H NMR (500 MHz, CD_2Cl_2) of zwitterion (**34b**), ● =Et_2O*

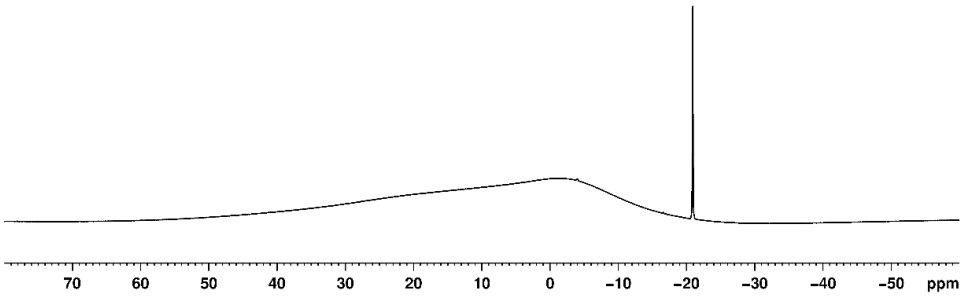

*^{11}B NMR (160 MHz, CD_2Cl_2) of zwitterion (**34b**)*

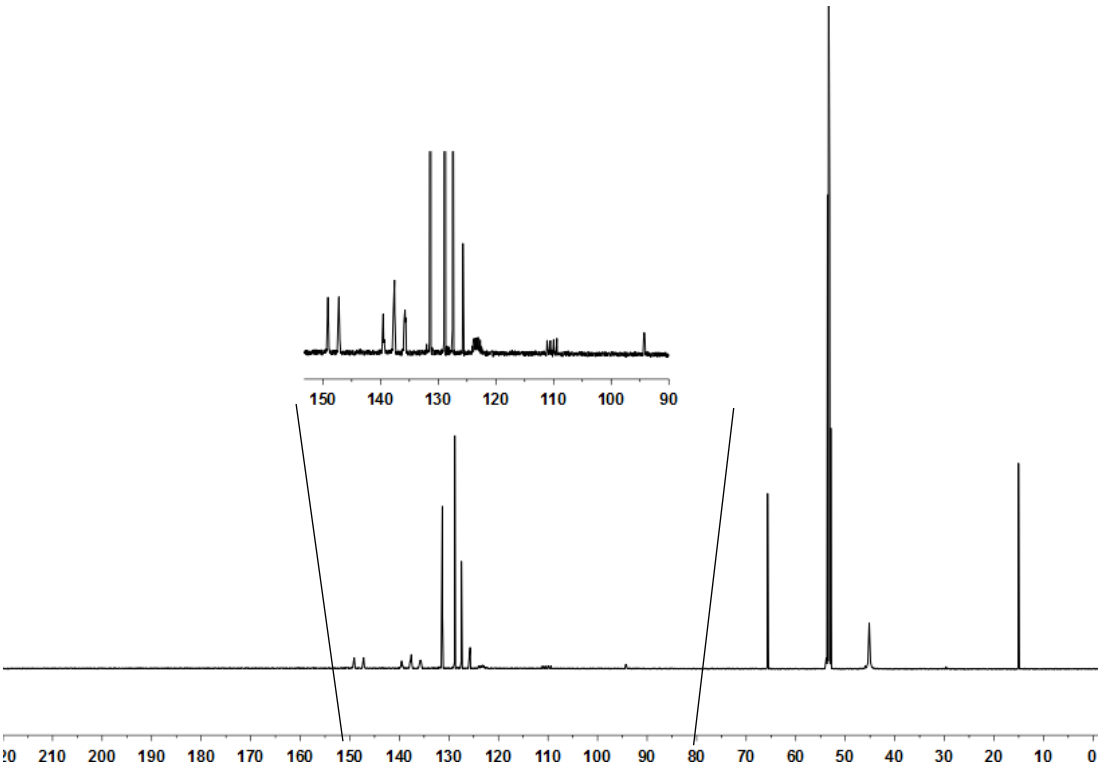

*$^{13}C\{H\}$ NMR (126 MHz, toluene-d_8) of zwitterion (**34b**)*

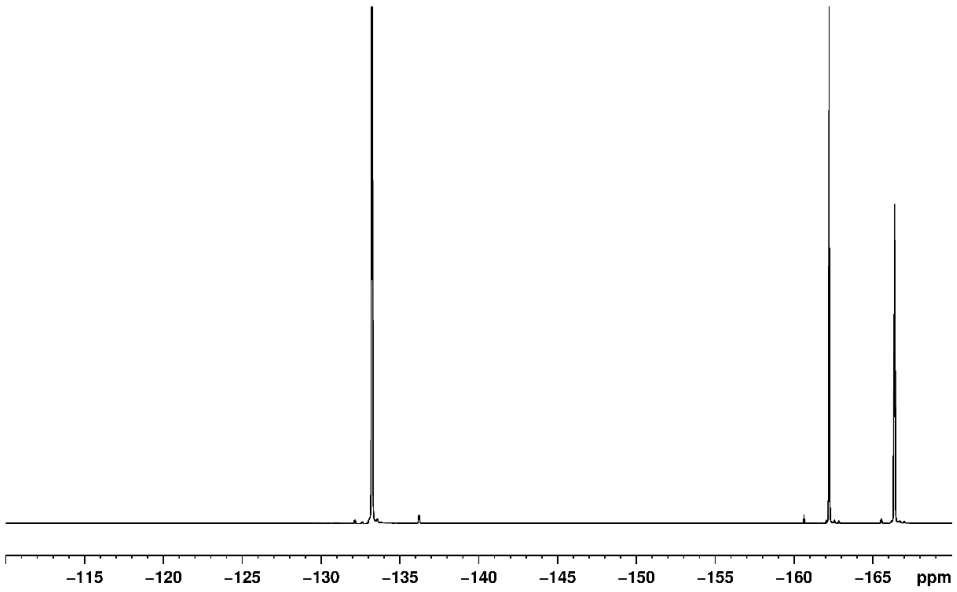

*^{19}F NMR (471 MHz, toluene-d_8) of zwitterion (**34b**)*

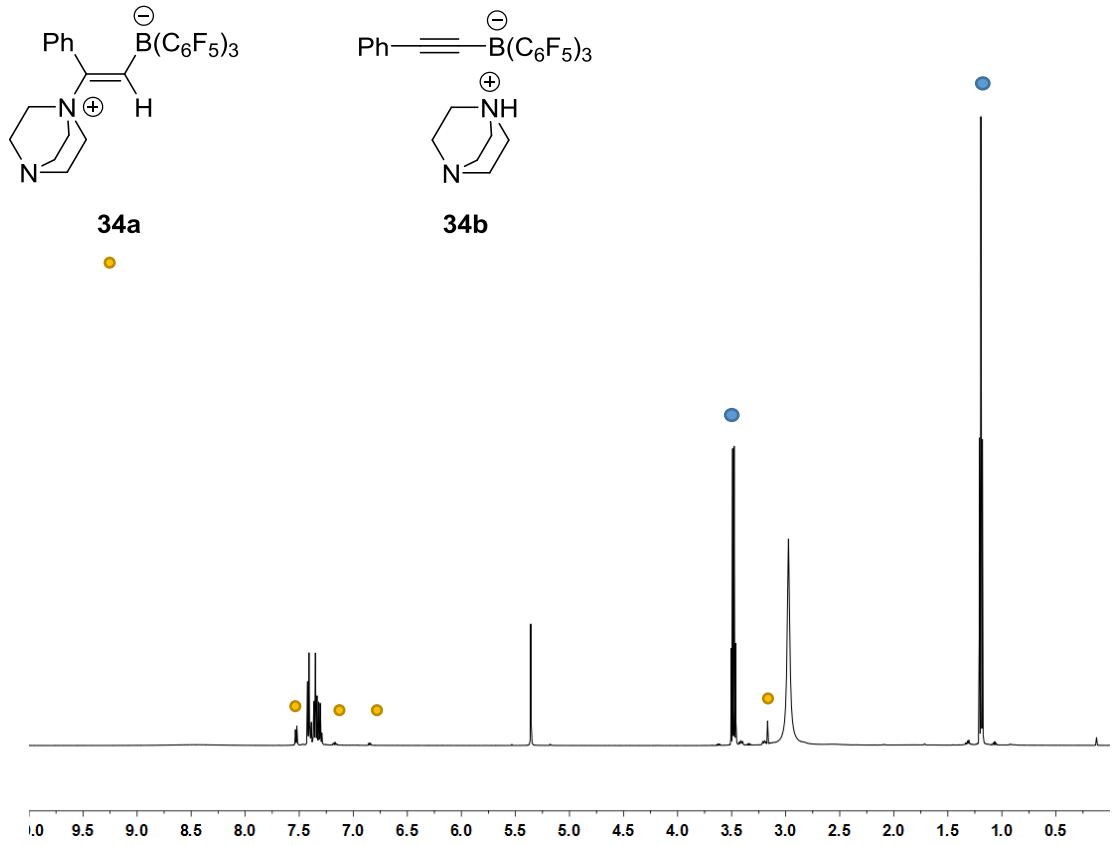

*^{1}H NMR (500 MHz, CD_2Cl_2) of **34b** after 2 days ● =Et_2O,*

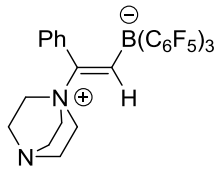

34a

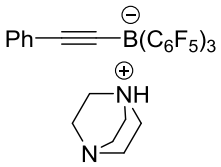

35b

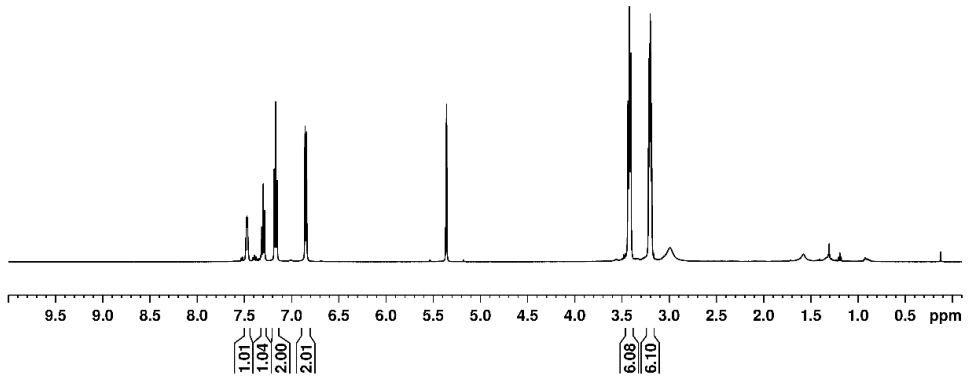

*^{1}H NMR (500 MHz, CD_2Cl_2) of zwitterion (**34a**) (major product) and zwitterion (**34b**)*

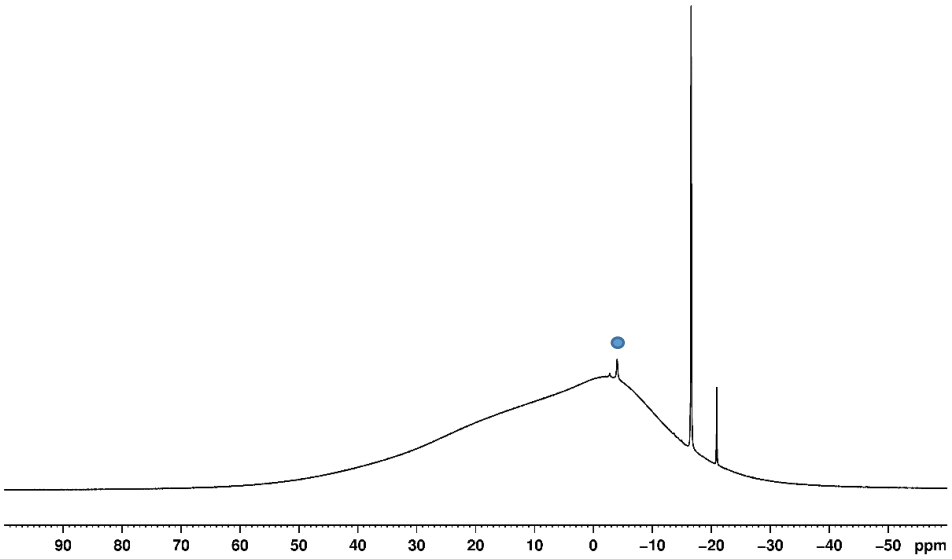

*^{11}B NMR (160 MHz, CD_2Cl_2) of zwitterion (**34a**) and zwitterion (**34b**)*

● = *DABCO·B(C_6F_5)$_3$*

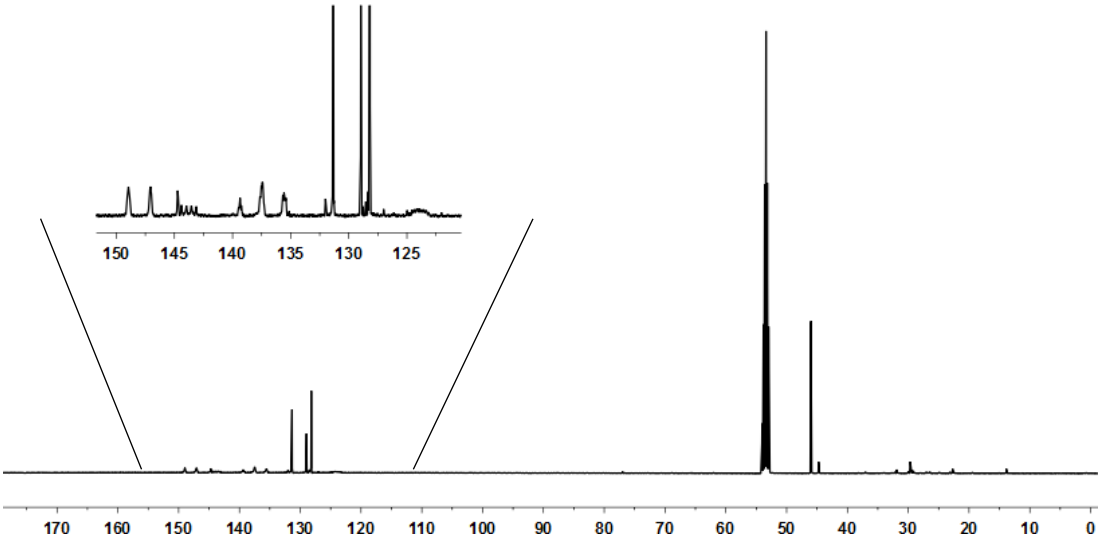

*$^{13}C\{H\}$ NMR (126 MHz, toluene-d_8) of zwitterion (**34a**) and zwitterion (**34b**)*

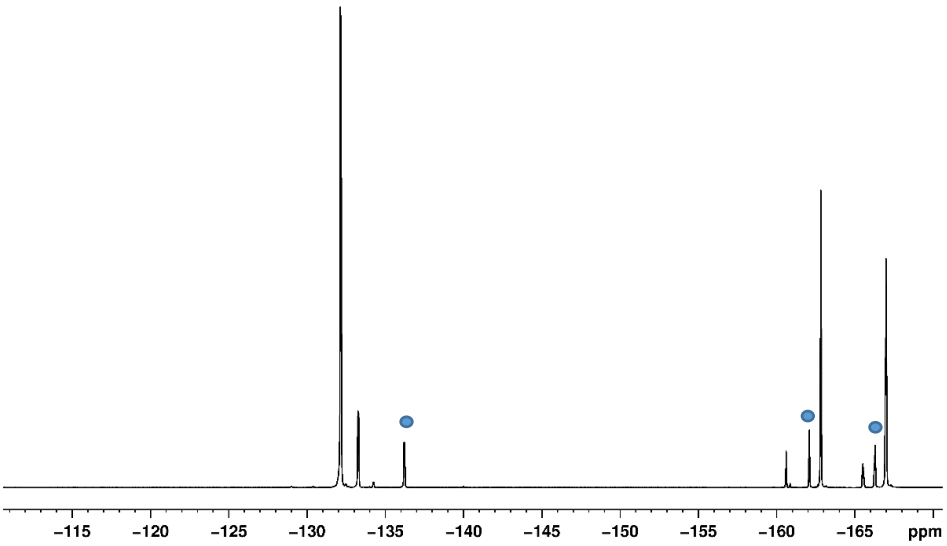

*^{19}F NMR (471 MHz, CD_2Cl_2) of zwitterion (**34a**) and zwitterion (**34b**)*

● = *DABCO·B(C_6F_5)$_3$*

5.20 Stoichiometric reaction of ethynylferrocene and $B(C_6F_5)_3$

Ethynylferrocene(0.10 mmol, 21.0 mg) was added to a solution of $B(C_6F_5)_3$ (0.12 mmol, 61.4 mg) in toluene-d_8 (0.60 mL) at T =195 K in a NMR tube. NMR spectra were recorded at T = 243 K.

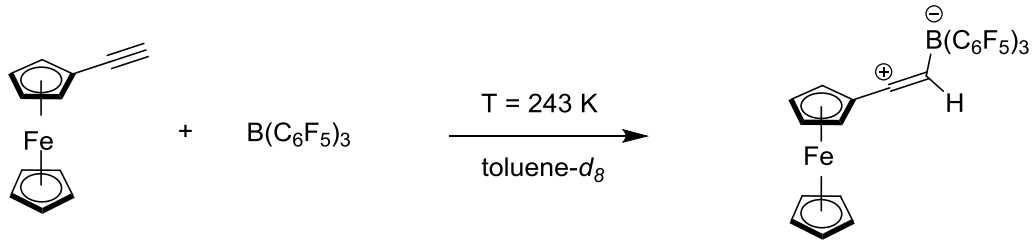

zwitterion

31p **32p**

^{1}H NMR (400 MHz, toluene-d_8) δ 6.93 (s, C^+=C**H**, 1H), 4.65 (s, cp**H**, 2H). 3.93 (s, cp**H**, 2H), 3.83 (s, cp**H**, 5H).

^{11}B NMR (128 MHz, toluene-d_8) δ −12.74 (s), −20.30.

^{13}C{H} NMR (100 MHz, toluene-d_8) δ 186.7 (**C$^+$**=CH−B), 107.7 (C^+=**C**H−B), 89.1, 79.5, 78.7, 60.8.

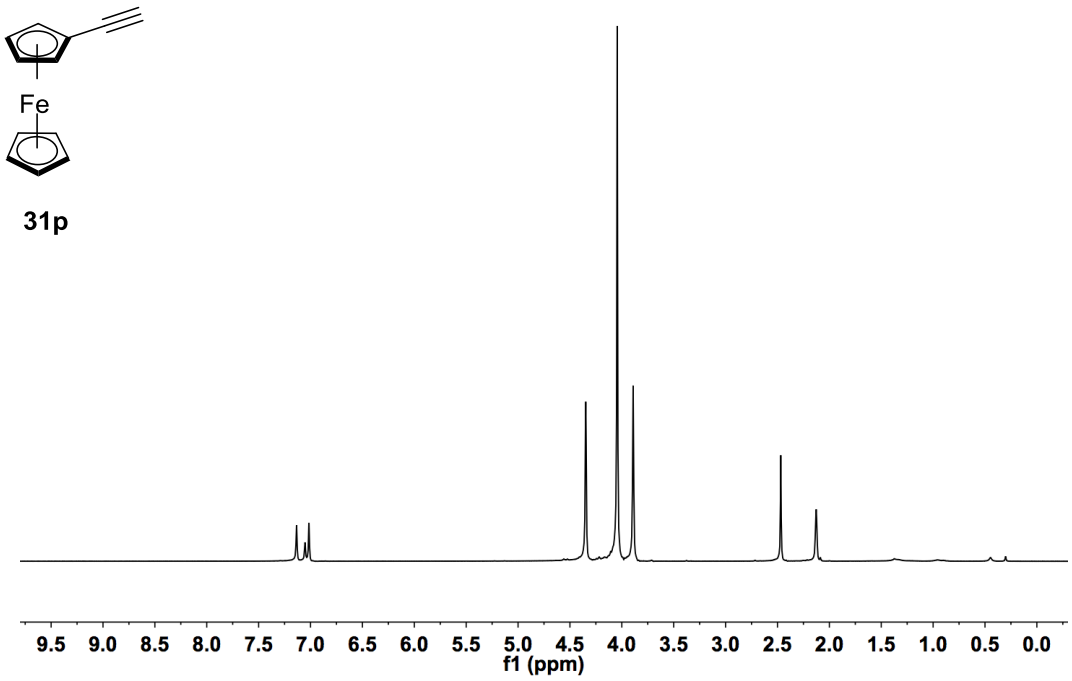

*^{1}H NMR (400 MHz, 243 K, toluene-d_8) of ethynylferrocene (**31p**).*

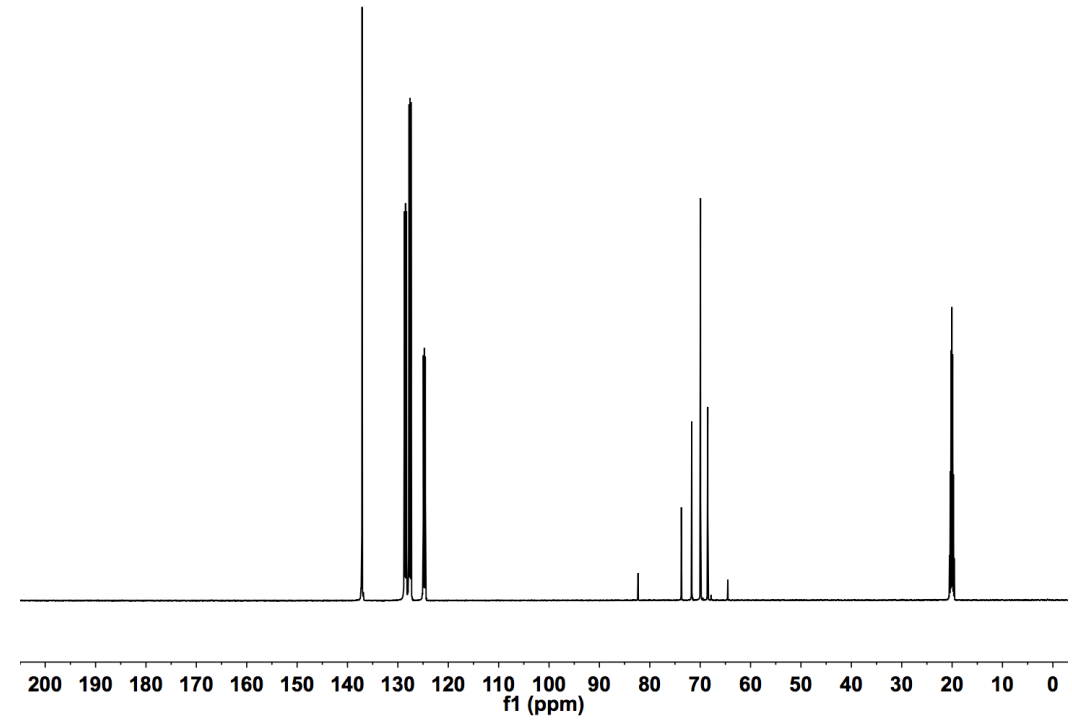

*^{13}C{H} NMR (100 MHz, 243 K, toluene-d_8) of ethynylferrocene (**31p**).*

After the addition of $B(C_6F_5)_3$

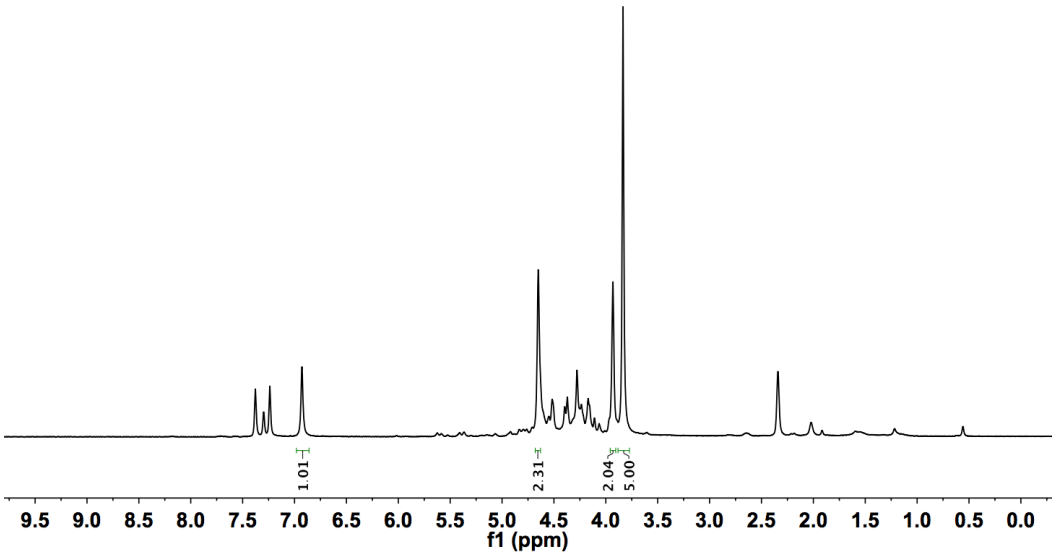

*^{1}H NMR (400 MHz, 243 K, toluene-d_8) of reaction of ethynylferrocene (**31p**) and $B(C_6F_5)_3$.*

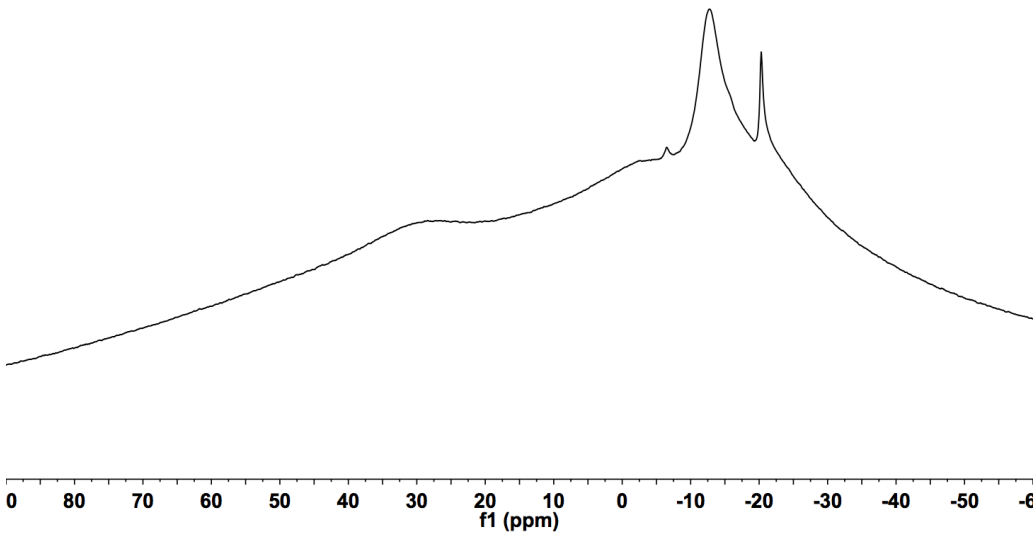

*^{11}BNMR (128 MHz, 243 K, toluene-d_8) of reaction of ethynylferrocene (**31p**) and $B(C_6F_5)_3$.*

.

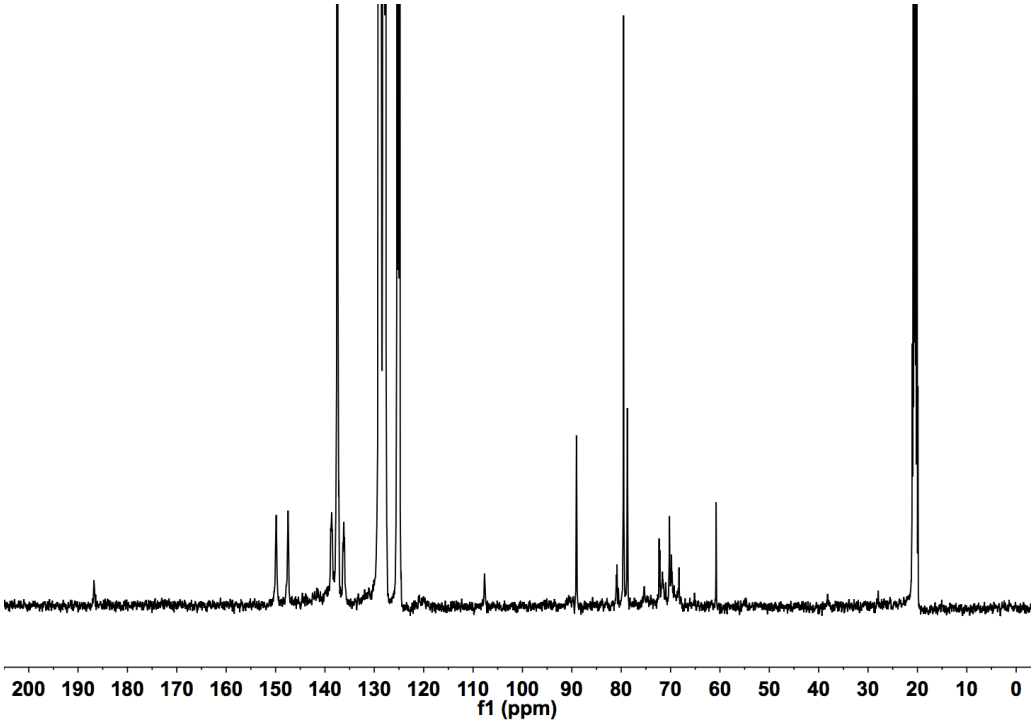

*$^{13}C\{H\}$ NMR (100 MHz, 243 K, toluene-d_8) of reaction of ethynylferrocene (**31p**) and $B(C_6F_5)_3$.*

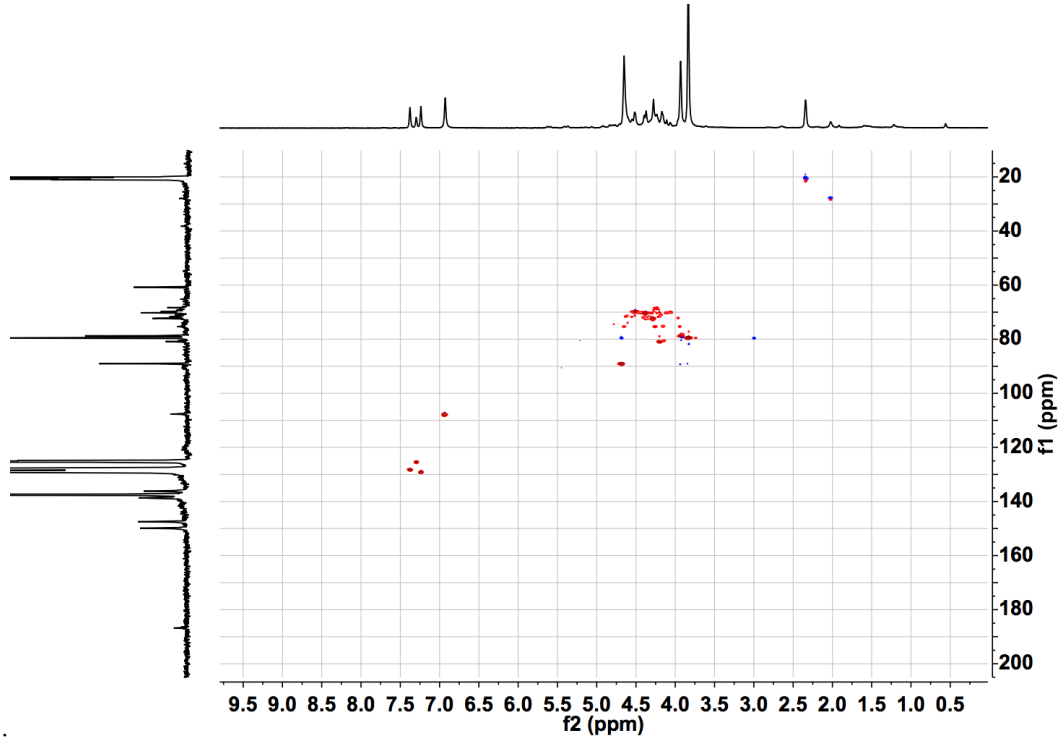

*2D ^{1}H -^{13}C HSQC of reaction of ethynylferrocene (**31p**) and $B(C_6F_5)_3$.*

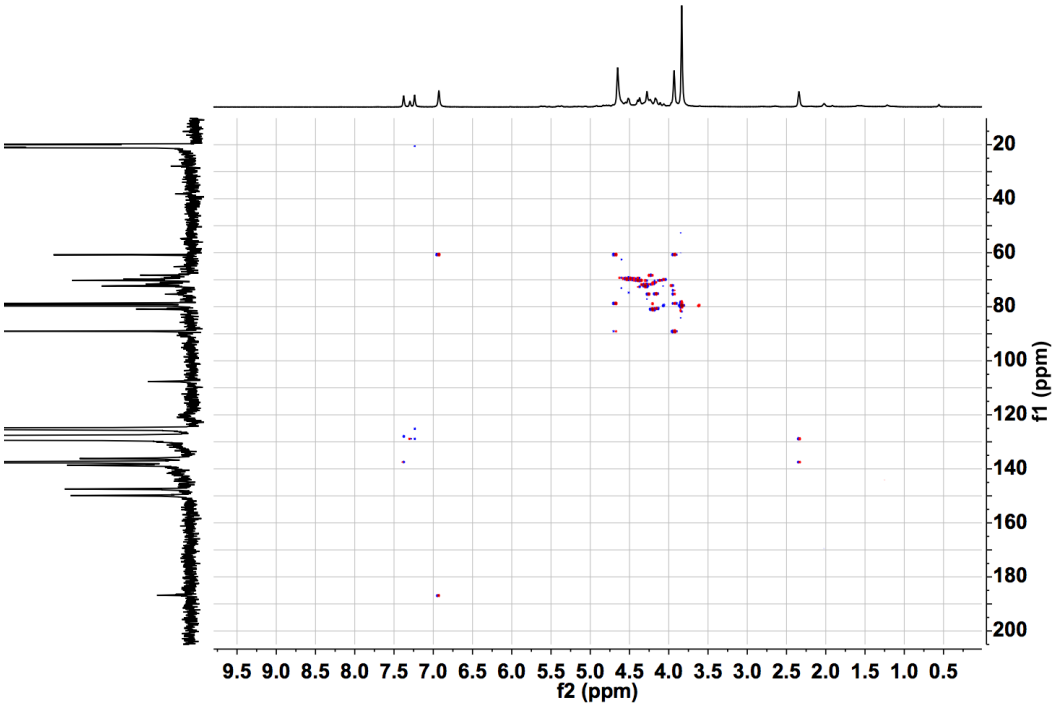

*2D ^{1}H -^{13}C HMBC of reaction of ethynylferrocene (**31p**) and $B(C_6F_5)_3$.*

5.21 Stoichiometric reaction of ethynylferrocene-2-^{13}C and $B(C_6F_5)_3$

Ethynylferrocene-2-^{13}C (0.10 mmol, 21.0 mg) was added to a solution of $B(C_6F_5)_3$ (0.12 mmol, 61.4 mg) in toluene-d_8 (0.60 mL) at T =195 K in a NMR tube. NMR spectra were recorded at T = 243 K.

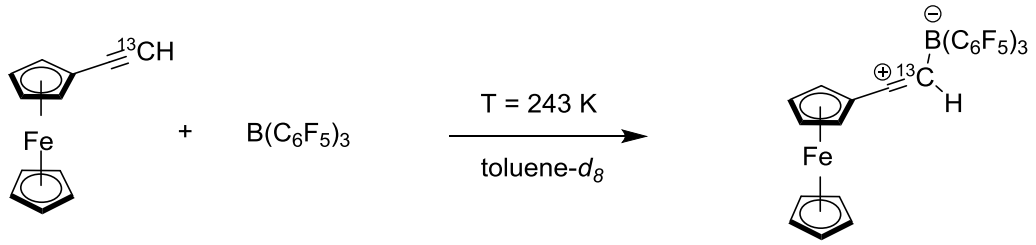

31p

zwitterion

32p

^{1}H NMR (400 MHz, toluene-d_8) δ 6.92 (d, J = 165.3 Hz, C$^+$=^{13}C**H**, 1H)

^{13}C{H} NMR (100 MHz, toluene-d_8) δ 186.7 (d, J = 99 Hz, **C$^+$**=HCB), 107.7 (C$^+$=**C**H-B),

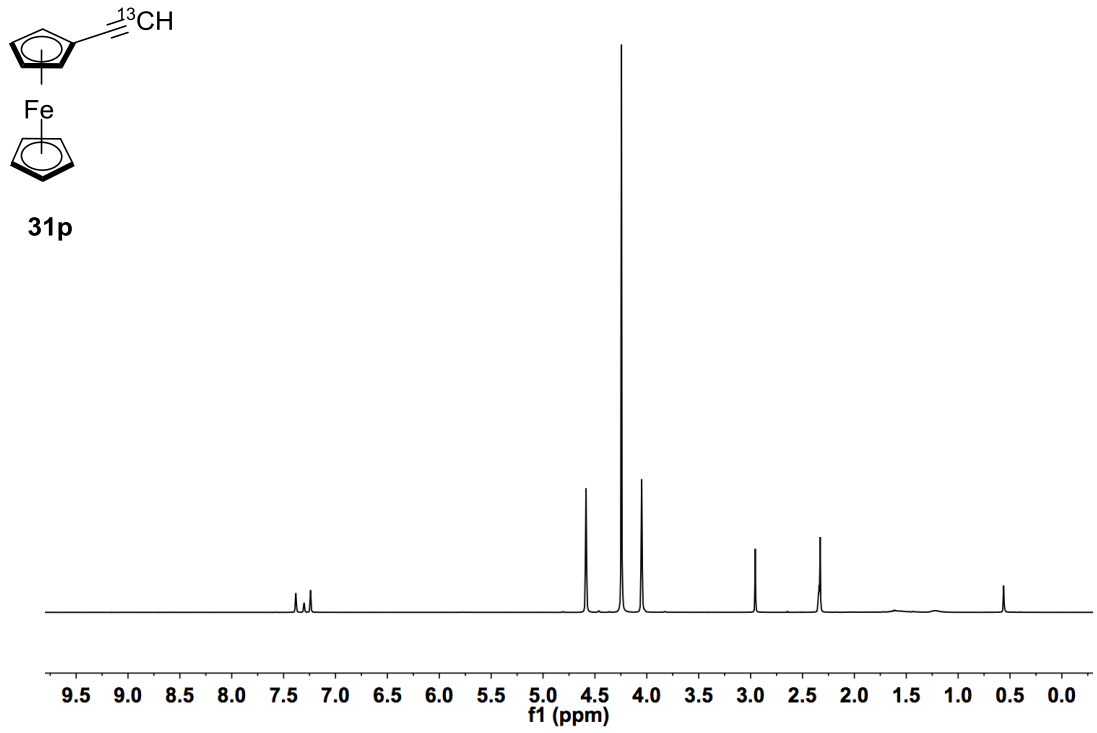

31p

^{1}H NMR (400 MHz, 243 K, toluene-d_8) spectrum of ethynylferrocene-2-^{13}C.

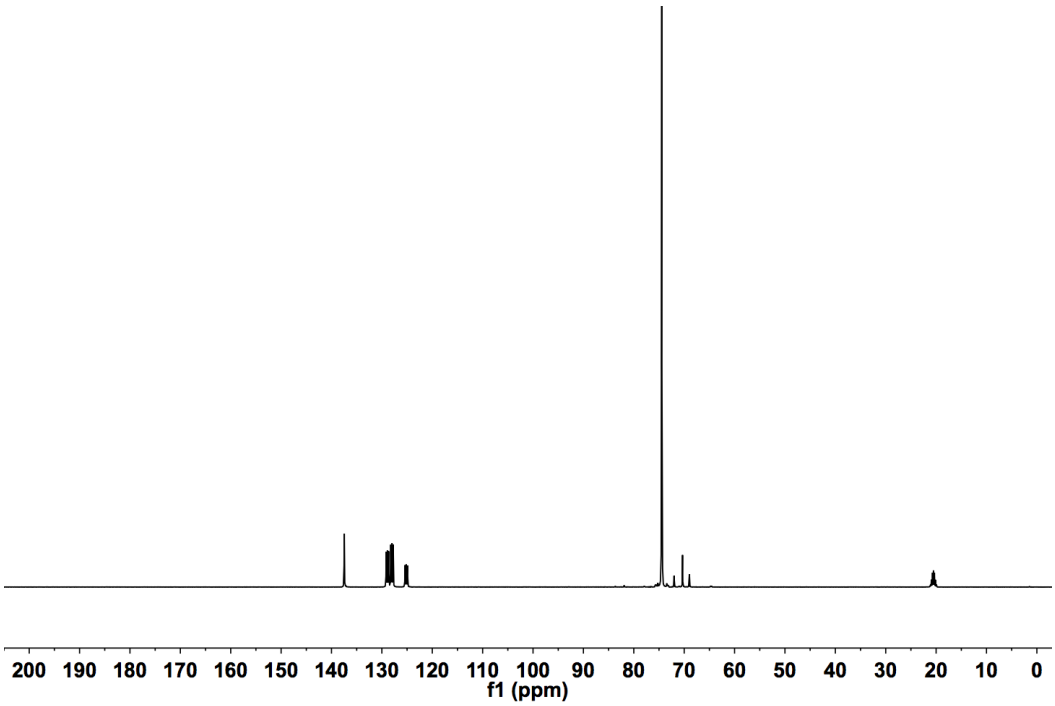

$^{13}C\{H\}$ NMR (100 MHz, 243 K, toluene-d_8) spectrum of ethynylferrocene-2-^{13}C.

After the addition of $B(C_6F_5)_3$

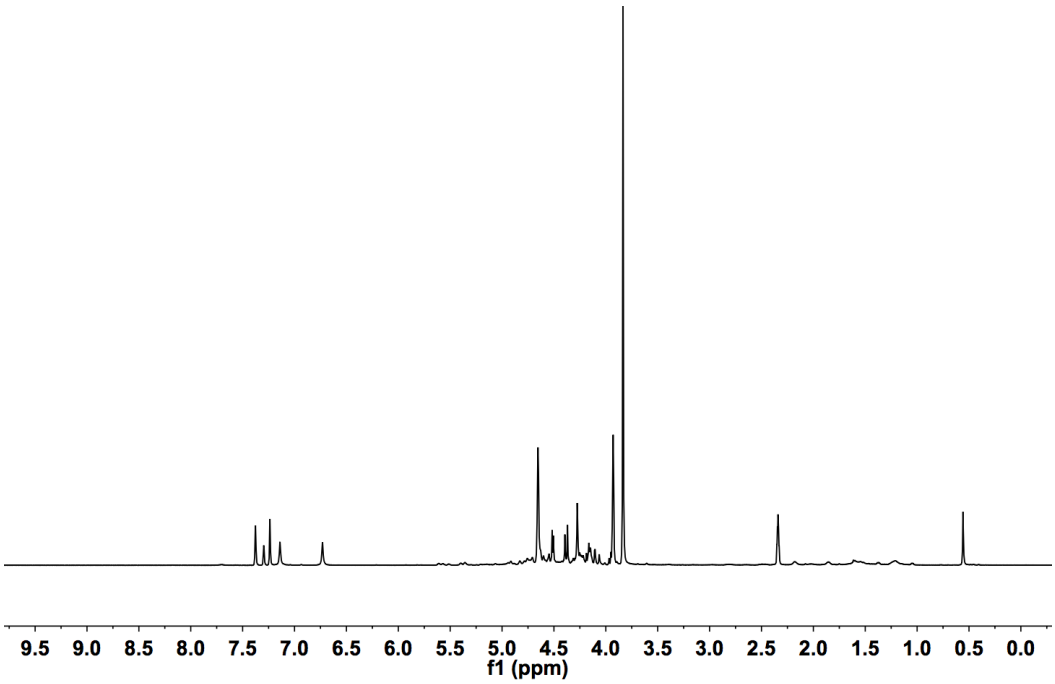

^{1}H NMR (400 MHz, 243 K, toluene-d_8) of reaction of ethynylferrocene-2-^{13}C and $B(C_6F_5)_3$.

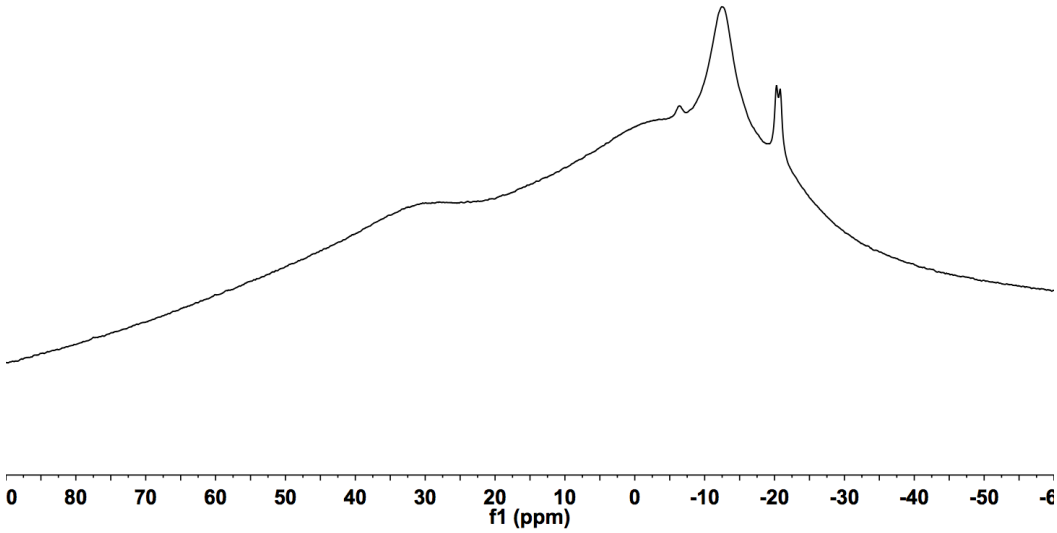

^{11}B NMR (128 MHz, 243 K, toluene-d_8) of reaction of ethynylferrocene-2-^{13}C and $B(C_6F_5)_3$.

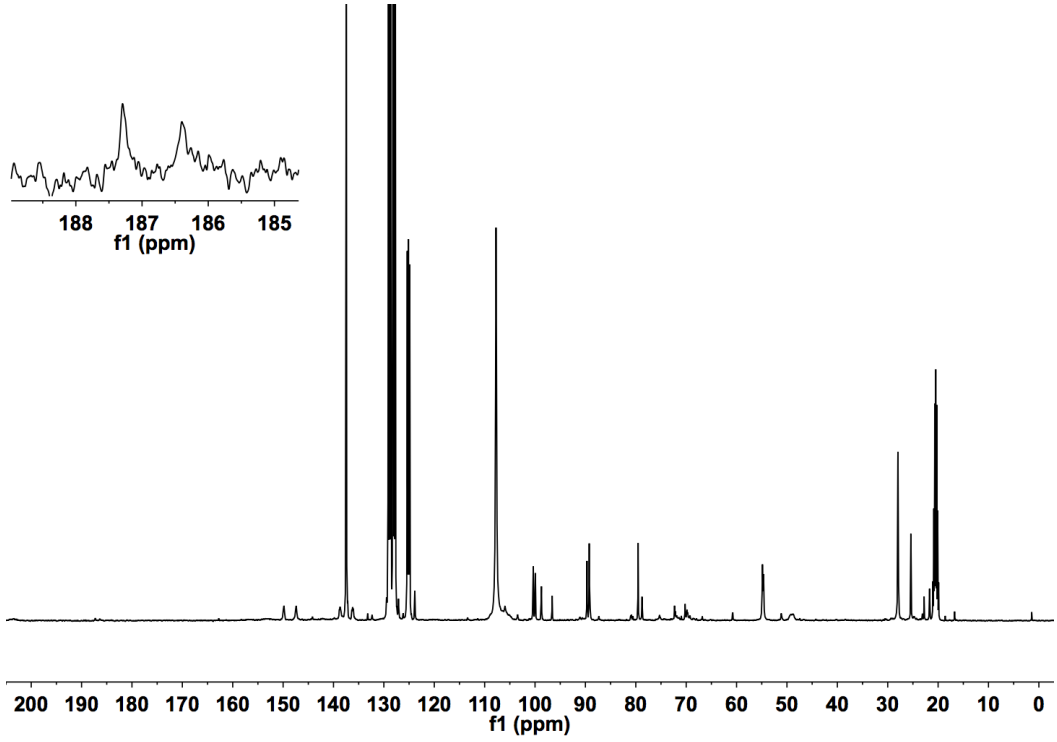

^{13}C{H} NMR (100 MHz, 243 K, toluene-d_8) of reaction of ethynylferrocene-2-^{13}C and $B(C_6F_5)_3$.

5.22 Optimisation of catalysis conditions: hydroboration of alkynes

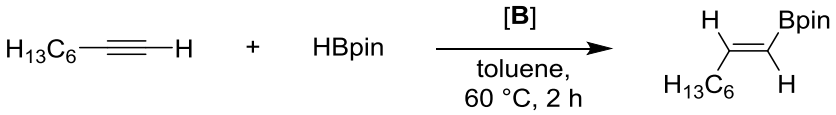

1-Octyne (0.15 mmol, 0.022 mL) was added to a solution of catalyst (20 mol%), 1,3,5-trimethoxybenzene (0.03 mmol, 5.0 mg) and HBpin (0.032 mL, 0.22 mmol) in toluene-d_8 (0.60 mL) at room temperature and then heated at 60 °C for 2h. The yield was determined by ^{1}H NMR of crude reaction mixture using 1,3,5-trimethoxybenzene as internal standard.

Entry	Catalyst (20 mol%)	Yield (%)	T (°C)	Time (h)
1	$B(C_6F_5)_3$	99	60	2
2	BCl_3	43 (25:18 *E/Z* ratio)	60	2
3	BF_3	20	60	2
4	BBr_3	43	60	2
5	BEt_3	31	60	2
6	BPh_3	35	60	2

Catalyst loading

Entry	Catalyst loading $B(C_6F_5)_3$	Yield(%)
1	10%	99
2	5.0%	99
3	2.5%	99
4	2.0%	83

Solvent screening

1-Octyne (0.15 mmol, 0.022 mL) was added to a solution of $B(C_6F_5)_3$(2.0 mol%, 0.003 mmol, 1.5 mg), 1,3,5-trimethoxybenzene (0.03 mmol, 5.0 mg) in the appropriate solvent (0.60 mL) and HBpin (0.22 mmol, 0.032 mL) was then added at room temperature. The solution was heated at 60 °C for 2h. The mixture was filtered through a short pad of silica and solvent removed *in vacuo*. The mixture was dissolved in toluene-d_8 and the yield was determined by ^{1}H NMR using 1,3,5-trimethoxybenzene as internal standard.

Entry	Solvent	Yield (%)
1	dichloromethane	37
2	2-methyl-THF	5
3	THF	2
4	cyclopentyl methyl ether	2

Equivalents of HBpin

1-Octyne (0.15 mmol, 0.022 mL) was added to a solution of $B(C_6F_5)_3$(2.0 mol%, 0.003 mmol, 1.5 mg), 1,3,5-trimethoxybenzene (0.03 mmol, 5.0 mg) in toluene-d_8 (0.60 mL) and HBpin was then added at room temperature. The solution was heated at 60 °C for 2 h. The yield was determined by ^{1}H NMR of crude reaction mixture using 1,3,5-trimethoxybenzene as internal standard.

Entry	HBpin (eq.)	Yield (%)
1	1.0	73
2	1.1	82
3	1.2	82
4	1.5	83

Reaction Concentration

1-Octyne (1.0 eq.) was added to a solution of $B(C_6F_5)_3$(0.02 eq.), 1,3,5-trimethoxybenzene (0.2 eq.) in toluene-d_8 (0.60 mL) and HBpin (1.1 eq.) was then added at room temperature. The solution was heated at 60 °C for 2h. The mixture was dissolved in toluene-d_8 and the yield was determined by ^{1}H NMR using 1,3,5-trimethoxybenzene as internal standard.

Entry	Reaction Concentration	Yield (%)
1	0.25 M	83
2	0.50 M	88
3	1.00 M	88
3	2.00 M	82

Time screening

1-Octyne (0.15 mmol, 0.022 mL) was added to a solution of $B(C_6F_5)_3$(2.0 mol%, 0.003 mmol, 1.5 mg), 1,3,5-trimethoxybenzene (0.03 mmol, 5.0 mg) and the corresponding amount of HBpin (0.165 mmol, 0.024 mL) in toluene-d_8 (0.60 mL) at room temperature and the catalysis was then performed for the time indicated at 60 ºC.

Entry	t (h)	Yield (%)
1	1	50
2	2	82

Temperature screening

1-Octyne (0.15 mmol, 0.022 mL) was added to a solution of of $B(C_6F_5)_3$(2.0 mol%, 10 mol% 1.5 mg), 1,3,5-trimethoxybenzene (0.03 mmol, 5.0 mg) and the corresponding amount of HBpin (0.165 mmol, 0.024 mL) in toluene-d_8 (0.60 mL) at room temperature and the catalysis was then performed for 2h at the indicated temperature.

Entry	T (°C)	Yield (%)
1	60	82
2	25	30

General procedure for hydroboration

The alkyne (0.75 mmol) was added to a solution of $B(C_6F_5)_3$(0.0187 mmol, 9.6 mg) in toluene (0.75 mL) and HBpin (0.82 mmol, 0.120 mL) was then added at room temperature.

The reaction mixture was stirred for 2 h at 60 °C. The mixture was filtered through a short pad of silica, and the product was purified by flash chromatography.

5.23 Characterisation of the alkenyl boronic esters

***(E)*-4,4,5,5-Tetramethyl-2-(oct-1-enyl)-1,3,2-dioxaborolane**

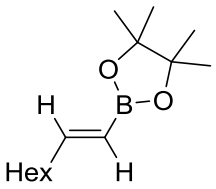

35a

According to general procedure, 1-octyne (0.75 mmol, 0.110 mL), HBpin (0.82 mmol, 0.120 mL), $B(C_6F_5)_3$ (0.0187 mmol, 9.6 mg) were reacted. The mixture was filtered through a short pad of silica to give the boronic ester **35a** (150 mg, 0.63 mmol, 84%) as colourless oil.

^{1}H NMR (500 MHz, $CDCl_3$) δ 6.63 (dt, *J* = 17.9, 6.4 Hz, 1H), 5.41 (dt, *J* = 17.9, 1.5 Hz, 1H), 2.14 (td, *J* = 7.9, 1.5 Hz, 2H), 1.45 – 1.34 (m, 3H), 1.34 – 1.19 (m, 14H), 0.92 – 0.81 (m, 6H).

^{11}B NMR (160 MHz, $CDCl_3$) δ 29.73.

^{13}C{H} NMR (126 MHz, $CDCl_3$) δ 154.9, 118.6 (br, *C*-*B*), 83.0, 35.9, 31.7, 28.9, 28.2, 24.8, 22.6, 14.1.

NMR data were in accordance with literature.[24]

(E)-4,4,5,5-Tetramethyl-2-(cyclopropyl-1-enyl)-1,3,2-dioxaborolane

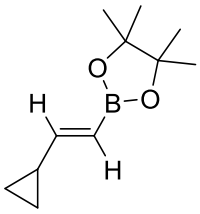

35b

According to general procedure, cyclopropylacetylene (0.75 mmol, 0.063 mL), HBpin (0.82 mmol, 0.120 mL), $B(C_6F_5)_3$ (0.0187 mmol, 9.6 mg) were reacted. The mixture was filtered through a short pad of silica to give the boronic ester **35b** (120 mg, 0.63 mmol, 83%) as a colourless oil.

^{1}H NMR (500 MHz, CDCl3) δ 6.07 (ddd, *J* = 17.8, 9.3, 1.4 Hz, 1H), 5.48 (d, *J* = 17.8 Hz, 1H), 1.55 – 1.46 (m, 1H), 1.24 (s, 12H), 0.82 – 0.76 (m, 2H), 0.55 – 0.50 (m, 2H).

^{11}B NMR (160 MHz, $CDCl_3$) δ 29.65.

^{13}C{H} NMR (126 MHz, $CDCl_3$) δ 158.7, 115.4 (br, *C-B*), 83.0, 24.9, 17.1, 8.0.

Data were in accordance with those previously reported.[24]

(E)-2-4,4,5,5-Tetramethyl-2-(3,3-dimethylbut-1-enyl) 1,3,2-dioxaborolane

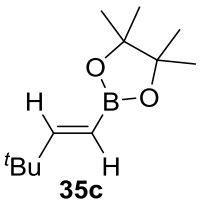

35c

According to general procedure, 3,3-dimethyl-1-butyne (0.75 mmol, 0092 mL), HBpin (0.82 mmol, 0.120 mL), $B(C_6F_5)_3$ (0.0187 mmol, 9.6 mg) were reacted. The mixture was filtered through a short pad of silica to give the boronic ester **35c** (113 mg, 0.53 mmol, 71%) as a colourless oil.

^{1}H NMR (500 MHz, $CDCl_3$) δ 6.62 (d, *J* = 18.3 Hz, 1H), 5.34 (d, *J* = 18.3 Hz, 1H), 1.26 (s, 12H), 1.01 (s, 9H).

^{11}B NMR (160 MHz, $CDCl_3$) δ 30.18.

^{13}C{H} NMR (126 MHz, $CDCl_3$) δ 164.5, 112.5 (br, *C-B*), 83.1, 35.1, 28.9, 24.9.

Data were in accordance with those previously reported.[24]

(E)-4,4,5,5-Tetramethyl-2-(2-cyclohexenyl-1-enyl)-1,3,2-dioxaborolane

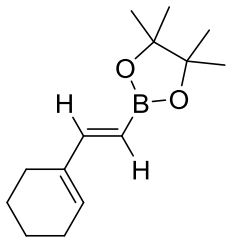

35d

According to general procedure A, 1-ethynylcyclohexene (0.75 mmol, 0.088 mL), HBpin (0.82 mmol, 0.120 mL), $B(C_6F_5)_3$ (0.0187 mmol, 9.6 mg). The residue was purified by flash chromatography (eluent: hexane/ethyl acetate 98:2), to give the boronic ester **35d** (119 mg, 0.51 mmol, 68%) as a pale yellow oil.

1H NMR (500 MHz, CDC_{l3}) δ 7.01 (dd, *J* = 18.3, 3.5 Hz, 1H), 5.97-5.94 (m, 1H), 5.44-539 (m, 1H), 2.17 – 2.11 (m, 4H), 1.68 – 1.62 (m, 2H), 1.61 – 1.55 (m, 2H), 1.26 (s, 12H).

^{11}B NMR (160 MHz, $CDCl_3$) δ 30.34.

^{13}C{H} NMR (126 MHz, $CDCl_3$) δ 153.3, 137.3, 134.4, 134.4, 112.1 (br, *C-B*), 83.1, 26.3, 24.9, 23.9, 22.6, 22.5.

Data were in accordance with those previously reported. [24]

(*E*) 4,4,5,5-Tetramethyl-2-(5-chloropent-1-en-1-yl)-1,3,2-dioxaborolane

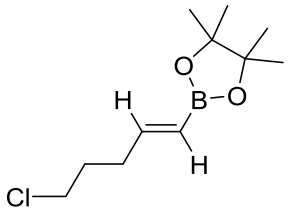

35e

According to general procedure, 5-chloro-1-pentyne (0.75 mmol, 0.110 mL), HBpin (0.82 mmol, 0.120 mL), $B(C_6F_5)_3$ (0.0187 mmol, 9.6 mg) were reacted. The mixture was filtered through a short pad of silica to give the boronic ester **35e** (130 mg, 0.57 mmol, 76%) as a colourless oil.

^{1}H NMR (500 MHz, $CDCl_3$) δ 6.57 (dt, *J* = 17.9, 6.4 Hz, 1H), 5.57 5.47 (dt, *J* = 18.0, 1.5 Hz, 1H), 3.52 (t, *J* = 6.7 Hz, 2H), 2.36 – 2.24 (m, 2H), 1.88 (p, *J* = 7.0 Hz, 2H), 1.25 (s, *J* = 1.7 Hz, 12H)

^{11}B NMR (160 MHz, $CDCl_3$) δ 29.53.

^{13}C{H} NMR (126 MHz, $CDCl_3$) δ 152.1, 120.4 (br, *C-B*), 83.1, 44.3, 32.7, 31.0, 24.8.

Data were in accordance with those previously reported.[25]

***(E)*-4,4,5,5-Tetramethyl-2-(cyclopropyl-1-enyl)-1,3,2-dioxaborolane**

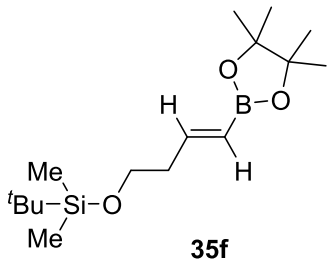

35f

According to general procedure, 4-(tert-butyldimethylsilyloxy)-1-butyne (0.75 mmol, 0.154 mL), HBpin (0.82 mmol, 0.120 mL), $B(C_6F_5)_3$ (0.0187 mmol, 9.6 mg). The residue was purified by flash chromatography (eluent: hexane/ethyl acetate 95:5), to give the boronic ester **35f** (140 mg, 0.60 mmol, 63%) as a colourless oil.

^{1}H NMR (500 MHz, $CDCl_3$) δ 6.58 (dt, *J* = 18.0, 6.7 Hz, 1H), 5.48 (dt, *J* = 18.0, 1.3 Hz, 1H), 3.68 (t, *J* = 7.0 Hz, 2H), 2.41 – 2.33 (m, 2H), 1.25 (s, 12H), 0.87 (s, 9H), 0.03 (s, 6H).

^{11}B NMR (160 MHz, $CDCl_3$) δ 30.1.

^{13}C{H} NMR (126 MHz, $CDCl_3$) δ 150.81, 83.18, 62.40, 39.59, 26.10, 24.91, 18.52, -5.11.

Data were in accordance with those previously reported.[26]

(Z)-4,4,5,5-Tetramethyl-2-(ethyl-1-buten-1-yl)-1,3,2-dioxaborolane

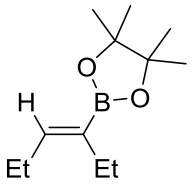

35g

According to general procedure, 3-hexyne (0.75 mmol, 0.085 mL), HBpin (0.82 mmol, 0.120 mL), $B(C_6F_5)_3$ (0.0187 mmol, 9.6 mg). The residue was purified by flash chromatography (eluent: hexane/ethyl acetate 98:2), to give the boronic ester **35g** (146 mg, 0.70 mmol, 93%) as a colourless oil.

^{1}H NMR (500 MHz, $CDCl_3$) δ 6.25 (t, *J* = 7.0 Hz, 1H), 2.18 – 2.09 (m, 4H), 1.25 (s, 12H), 0.99 (t, *J* = 7.6 Hz, 3H), 0.93 (t, *J* = 7.5 Hz, 3H).

^{11}B NMR (160 MHz, $CDCl_3$) δ 30.56.

^{13}C{H} NMR (126 MHz, $CDCl_3$) δ 147.1, 133.4 (br, *C-B*), 83.1, 24.9, 21.8, 21.6, 15.0, 14.0.

Data were in accordance with those previously reported.[24]

(Z)-4,4,5,5-Tetramethyl-2-(hex-2-en-3-yl)-1,3,2-dioxaborolane

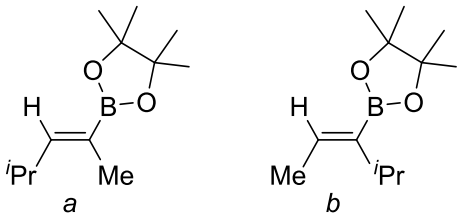

35h

According to general procedure, 4-methyl-2-pentyne (0.75 mmol, 0.110 mL), HBpin (0.82 mmol, 0.120 mL), $B(C_6F_5)_3$ (0.0187 mmol, 9.6 mg). The residue was purified by flash chromatography (eluent: hexane/ethyl acetate 98:2), to give the boronic ester **35h** as a colourless oil.

The product was found as an inseparable mixture of **35h** (*a*+*b*).

Overall yield 68% (82+18[b], 106 mg, 0.51 mmol).

^{1}H NMR 35h$_a$ (500 MHz, $CDCl_3$) 6.12 (dq, *J* = 9.1, 1.7 Hz, 1H), 2.68 (m, 1H), 1.68 (d, *J* = 1.8 Hz, 3H), 1.25 (s, 12H), 0.96 (d, *J* = 6.7 Hz, 6H).

^{11}B NMR (160 MHz, $CDCl_3$) δ 30.50.

^{13}C{H} NMR (126 MHz, $CDCl_3$) δ 153.3, 83.0, 27.4, 24.8, 22.2, 13.7.

Data were in accordance with those previously reported.[24]

(E)-4,4,5,5-Tetramethyl-2-(phenyl-1-enyl)-1,3,2-dioxaborolane

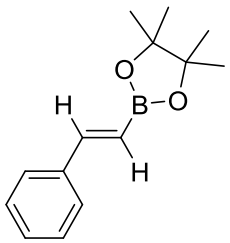

35i

According to general procedure, phenylacetylene (10 mmol, 1.10 mL), HBpin (12 mmol, 1.60 mL), $B(C_6F_5)_3$ (0.25 mmol, 0.128 g). The residue was purified by flash

chromatography (eluent: hexane/ethyl acetate 98:2), to give the boronic ester **35i** (2.0 g, 8.6 mmol, 86%) as a colourless oil.

^{1}H NMR (500 MHz, $CDCl_3$) δ 7.51 – 7.48 (m, 2H), 7.41 (d, *J* = 18.4 Hz, 1H), 7.36 – 7.27 (m, 3H), 6.19 (d, *J* = 18.4 Hz, 1H), 1.32 (s, 12H).

^{11}B NMR (160 MHz, $CDCl_3$) δ 30.20.

^{13}C{H} NMR (126 MHz, $CDCl_3$) δ 149.6, 137.6, 129.0, 128.6, 127.2, 116.5 (br, *C-B*), 83.5, 24.9.

Data were in accordance with those previously reported. [24]

(E)-4,4,5,5-Tetramethyl-2-(4-fluorophenyl-1-enyl)-1,3,2-dioxaborolane

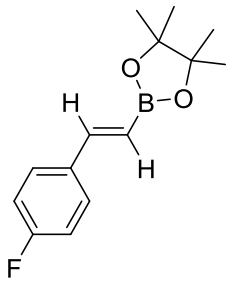

35j

According to general procedure, 1-ethynyl-4-fluorobenzene (0.75 mmol, 0.090 g), HBpin (0.82 mmol, 0.120 mL), $B(C_6F_5)_3$ (0.0187 mmol, 9.6 mg). The residue was purified by flash chromatography (eluent: hexane/ethyl acetate 98:2), to give the boronic ester **35j** (160 mg, 0.64 mmol, 86%) as a colourless oil.

^{1}H NMR (500 MHz, $CDCl_3$) δ 7.48 – 7.43 (m, 2H), 7.35 (d, *J* = 18.4 Hz, 1H), 7.05 – 6.99 (m, 2H), 6.07 (d, *J* = 18.4 Hz, 1H), 1.31 (s, 12H).

^{11}B NMR (160 MHz, $CDCl_3$) δ 30.13.

^{13}C{H} NMR (126 MHz, $CDCl_3$) δ 163.1 (d, $J_{C\text{-}F}$ 247.9 Hz), 148.3, 133.9 (d, *J* = 3.3 Hz), 128.9 (d, *J* = 8.7 Hz) 115.65 (d, *J* = 21.1 Hz), 83.5, 24.9.

^{19}F NMR (471 MHz, $CDCl_3$) δ -112.46 (m).

Data were in accordance with those previously reported. [24]

(E)-4,4,5,5-Tetramethyl-2-(4-methoxyphenyl-1-enyl)-1,3,2-dioxaborolane

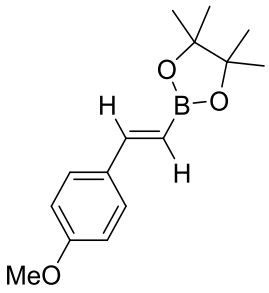

35k

According to general procedure, 1-ethynyl-4-methoxybenzene (0.75 mmol, 0.099 g), HBpin (0.82 mmol, 0.120 mL), $B(C_6F_5)_3$ (0.0187 mmol, 9.6 mg). The residue was purified by flash chromatography (eluent: hexane/ethyl acetate 98:2), to give the boronic ester **35k** (160 mg, 0.61 mmol, 82%) as a colourless oil.

^{1}H NMR (500 MHz, $CDCl_3$) δ 7.45 – 7.42 (m, 2H), 7.36 (d, *J* = 18.4 Hz, 1H), 6.88 – 6.85 (m, 2H), 6.02 (d, *J* = 18.4 Hz, 1H), 3.80 (s, 3H), 1.31 (s, 12H).

^{11}B NMR (160 MHz, $CDCl_3$) δ 30.32.

^{13}C{H} NMR (126 MHz, $CDCl_3$) δ 160.4, 149.2, 130.5, 128.6, 114.1, 83.3, 55.4, 24.9.

Data were in accordance with those previously reported.[24]

Methyl4-[(*E*)-2-(4,4,5,5-tetramethyl-2-yl)-ethenyl]benzoate-1,3,2-dioxaborolane

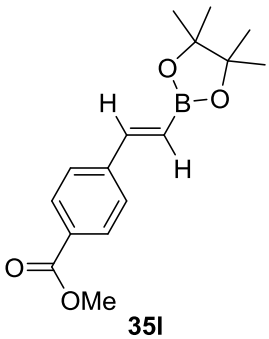

35l

According to general procedure, methyl 4-ethynylbenzoate (0.75 mmol, 120 mg), HBpin (0.82 mmol, 0.120 mL), $B(C_6F_5)_3$ (0.0187 mmol, 9.6 mg). The residue was purified by flash chromatography (eluent: hexane/ethyl acetate 98:2), to give the boronic ester **35l**

(180 mg, 0.62 mmol, 83%) as an amorphous pale yellow powder. Melting point (hexane/ethyl acetate) 97.4 °C, Lit. 90-91 °C.

^{1}H NMR (500 MHz, $CDCl_3$) δ 8.02 – 7.98 (m, 2H), 7.55 – 7.51 (m, 2H), 7.41 (d, *J* = 18.4 Hz, 1H), 3.91 (s, 3H), 1.31 (s, 12H).

^{11}B NMR (160 MHz, $CDCl_3$) δ 30.2.

^{13}C{H} NMR (126 MHz, $CDCl_3$) δ 166.9, 148.3, 141.8, 130.0, 129.7, 127.0, 119.7 (br, *C-B*), 83.7, 52.2, 24.9.

Data were in accordance with those previously reported.[25]

(E)-4,4,5,5-Tetramethyl-2-(4-ethylphenyl-1-enyl)-1,3,2-dioxaborolane

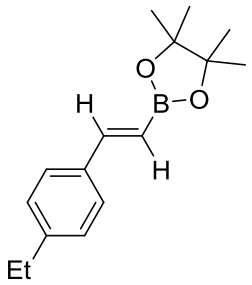

35m

According to general procedure, 1-ethyl-4-ethynylbenzene (0.75 mmol, 0.105 mL), HBpin (0.82 mmol, 0.120 mL), $B(C_6F_5)_3$ (0.0187 mmol, 9.6 mg). The residue was purified by flash chromatography (eluent: hexane/ethyl acetate 98:2), to give the boronic ester **35m** (169 mg, 0.65 mmol, 87%) as a colourless oil.

^{1}H NMR (500 MHz, $CDCl_3$) δ 7.44-7.37 (m, 3H), 7.19 – 7.15 (m, 2H), 6.13 (d, *J* = 18.3 Hz, 1H) 2.65 (q, *J* = 7.6 Hz, 2H), 1.32 (s, 12H), 1.24 (t, *J* = 7.6 Hz, 3H).

^{11}B NMR (160 MHz, $CDCl_3$) δ 30.24.

^{13}C{H} NMR (126 MHz, $CDCl_3$) δ 149.6, 145.4, 135.2, 128.2, 127.2, 115.4 (br, *C-B*), 83.4, 28.8, 25.0, 15.5.

Data were in accordance with those previously reported.[24]

(Z)-4,4,5,5-Tetramethyl-2-(1,2 diphenyl-1-enyl)-1,3,2-dioxaborolane

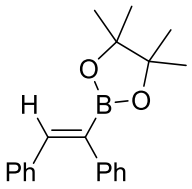

35n

According to general procedure, diphenylacetylene (0.75 mmol, 133 mg), HBpin (0.82 mmol, 0.120 mL), $B(C_6F_5)_3$ (0.0187 mmol, 9.6 mg). The residue was purified by flash chromatography (eluent: hexane/ethyl acetate 98:2), to give the boronic ester **35n** (99 mg, 0.32 mmol, 43%) as a white needles.

Melting point (hexane/ethyl acetate) 89.4 °C, Lit. 90-91 °C.

^{1}H NMR (500 MHz, $CDCl_3$) δ 7.38 (s, 1H), 7.31 – 7.25 (m, 2H), 7.24 – 7.16 (m, 3H), 7.16-7.11 (m, 3H), 7.09 – 7.03 (m, 2H), 1.32 (s, 12H).

^{11}B NMR (160 MHz, $CDCl_3$) δ 30.72.

^{13}C{H} NMR (126 MHz, $CDCl_3$) δ 143.3, 140.6, 137.1, 130.1, 129.0, 128.4, 128.2, 127.7, 126.3, 83.9, 24.9.

Data were in accordance with those previously reported.[24]

(*Z*)-4,4,5,5-Tetramethyl-2-(1-phenyl(prop-1-en)-2-yl)-1,3,2-dioxaborolane

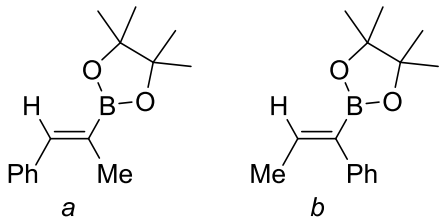

a *b*

35o

According to general procedure, 1-phenyl-1propyne (0.75 mmol, 0.094 mL), HBpin (0.82 mmol, 0.120 mL), $B(C_6F_5)_3$ (0.0187 mmol, 9.6 mg). The residue was purified by flash chromatography (eluent: hexane/ethyl acetate 98:2), to give the boronic ester **35o** as a colourless liquid.

The product was found as an inseparable mixture of **35o** (*a*+*b*).

Overall yield 92% (88[a]+12[b], 168 mg, 0.70 mmol).

Compound 35o[a] : **^{1}H NMR** (500 MHz, $CDCl_3$) δ 7.41-7.30 (m, 4H), 7.24 – 7.18 (m, 2H), 2.04 (d, *J* = 1.8 Hz, 3H), 1.85 – 1.77 (m, 3H), 1.35 (s, 12H), 1.31 (s, 9H).

^{11}B NMR (160 MHz, $CDCl_3$) δ 29.8.

^{13}C{H} NMR (126 MHz, $CDCl_3$) δ 142.8, 142.5, 139.9, 138.1, 129.5, 129.2, 128.2, 127.9, 127.2, 126.0, 83.6, 83.5, 25.0, 24.9, 16.1, 16.0.

Data were in accordance with those previously reported.[27]

5.24 Hydroboration of styrene catalysed by zwitterion (32i)

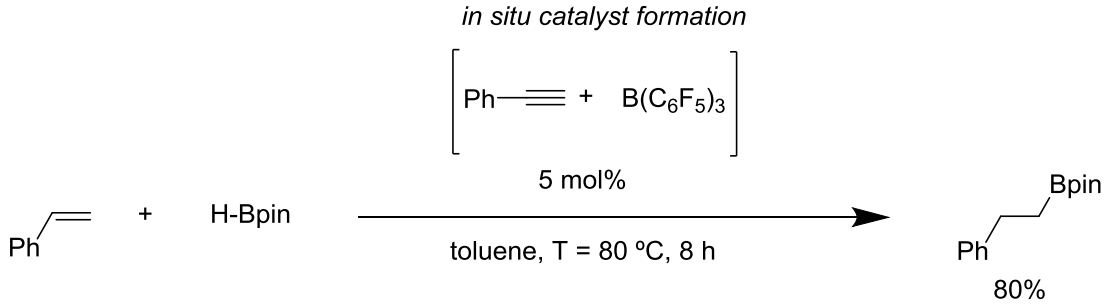

Phenylacetylene (0.0375 mmol, 4 μL) was added to a solution of $B(C_6F_5)_3$ (0.0375 mmol, 5 mol%) in toluene (0.5 mL) at room temperature. To this solution styrene (0.75 mmol, 0.088 mL), HBpin (0.9 mmol, 0.130 mL) were added and heated at 80 ºC for 18 h. The mixture was diluted with 5 mL of CH_2Cl_2 and filtered through a short pad of silica (4.0 cm in a pipette). The residue was purified by flash chromatography (SiO_2, hexane to hexane/ethyl acetate 92:8, [UV/$KMnO_4$]), to give the boronic ester (278 mg, 1.2 mmol, 80%) as a colourless oil with a regioselectivity of 99:1 (Linear/Branched).

^{1}H NMR (500 MHz, $CDCl_3$) δ 7.32 – 7.21 (m, 4H), 7.17 (m, 1H), 2.75 (t, *J* = 8.0 Hz, 2H), 1.25 (s, 12H), 1.15 (t, *J* = 8.0 Hz, 2H).

^{11}B NMR (160 MHz, $CDCl_3$) δ 33.42

^{13}C{H} NMR (126 MHz, $CDCl_3$) δ 144.4, 128.2, 128.0, 125.5, 83.1, 30.0, 24.8.

Data were in accordance with those previously reported.[13]

5.25 Mechanistic Studies

Catalysis with DABCO·B(C_6F_5)$_3$

DABCO and B(C_6F_5)$_3$ (0.015 mmol, 9.0 mg) were suspended in 0.60 mL of toluene-d_8 and let react for 2 h. Phenyl acetylene (0.15 mmol, 0.018 mL) and HBpin (0.165 mmol, 0.023 mL) were added to the suspension and heated for 2 h at 60 °C.

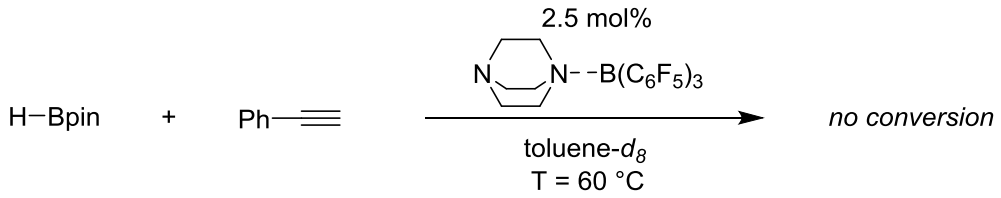

DABCO (0.015 mmol, 1.7 mg) and B(C_6F_5)$_3$ (0.015 mmol, 7.68 mg) were suspended in 0.60 mL of toluene-d_8 and let react for 2 h to allow complex formation. Phenyl acetylene (0.15 mmol, 0.018 mL) and HBpin (0.165 mmol, 0.023 mL) were added to the suspension and heated for 2 h at 60 °C.

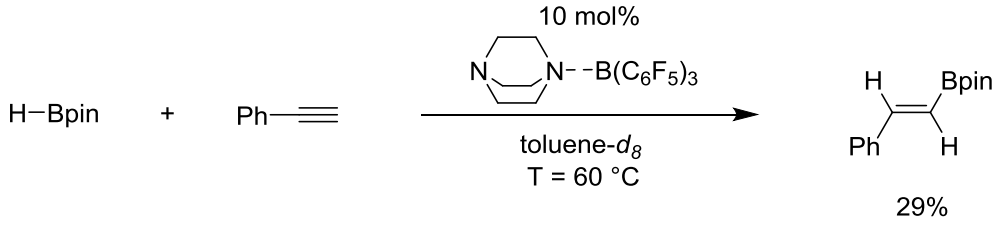

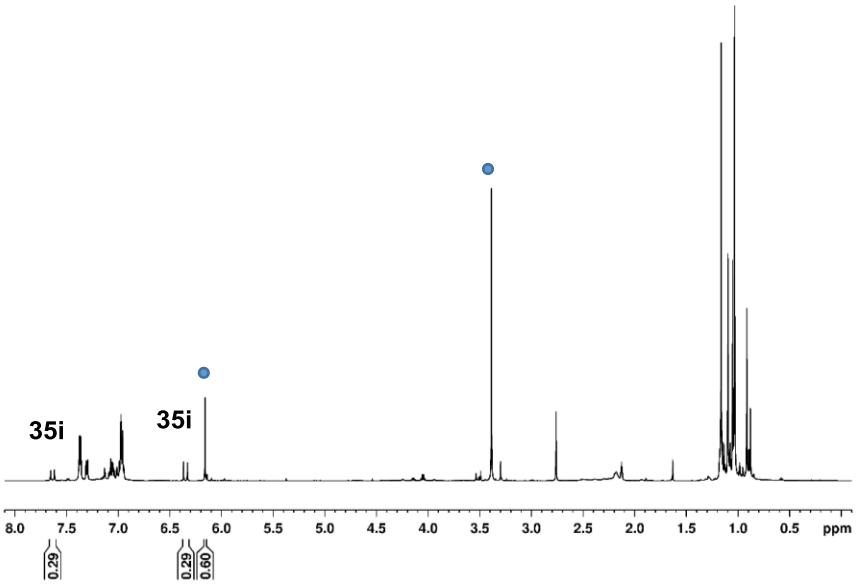

^{1}H NMR (500 MHz, toluene-d_8) of catalysis with DABCO·B(C_6F_5)$_3$

● **=** *1,3,5-trimethoxybenzene internal standard.*

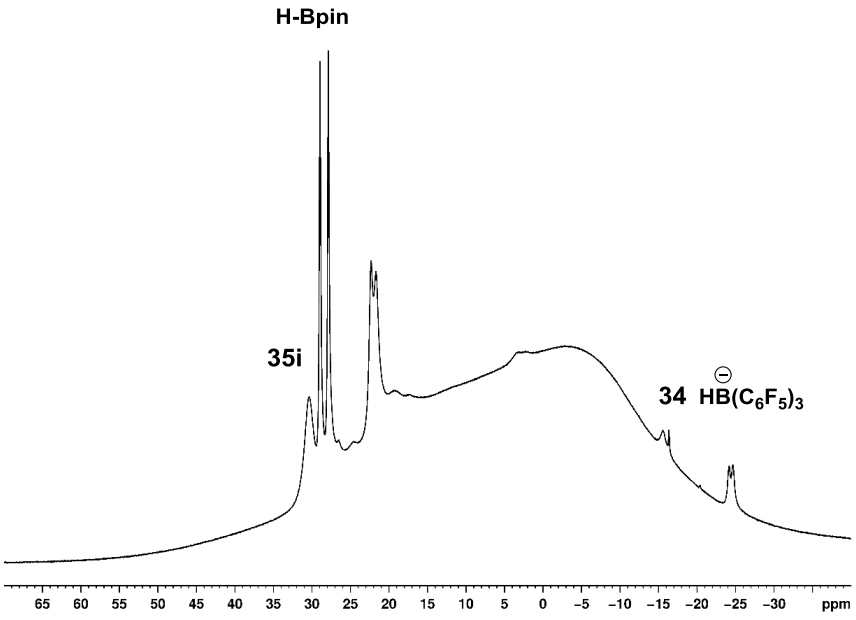

^{11}B NMR (160 MHz, toluene-d_8) spectra of catalysis with DABCO·B(C_6F_5)$_3$.

Catalysis with compound zwitterion 34b

Phenyl acetylene (0.15 mmol, 0.018 mL) and HBpin (0.165 mmol, 0.024 mL) were added to a solution of **34b** (0.003 mmol, 2.2 mg) in 0.60 mL of toluene-d_8 in an NMR tube.

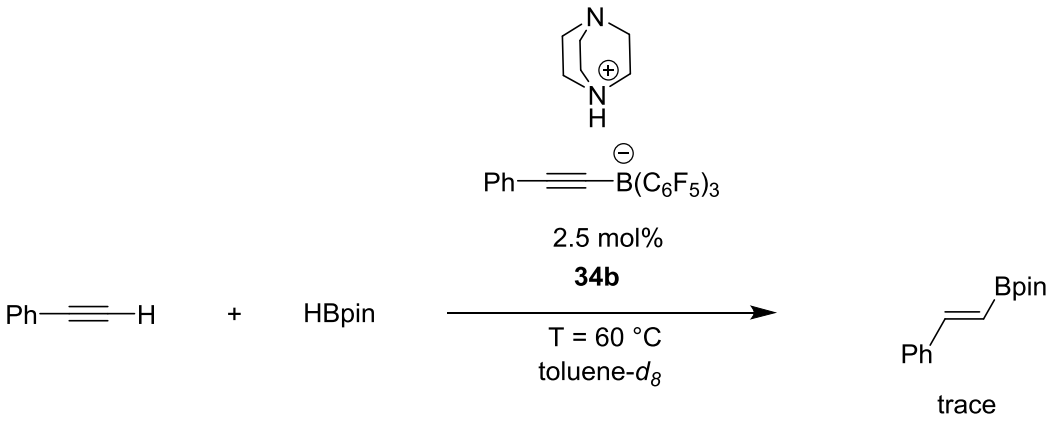

Phenyl acetylene (0.15 mmol, 0.018 mL) and HBpin (0.165 mmol, 0.024 mL) were added to a solution of **34b** (0.015 mmol, 10.8 mg) in 0.60 mL of toluene-d_8 in an NMR tube.

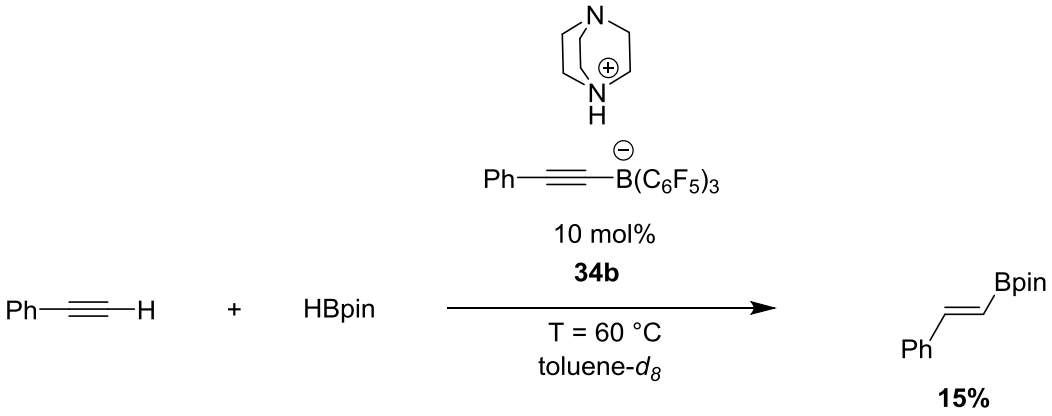

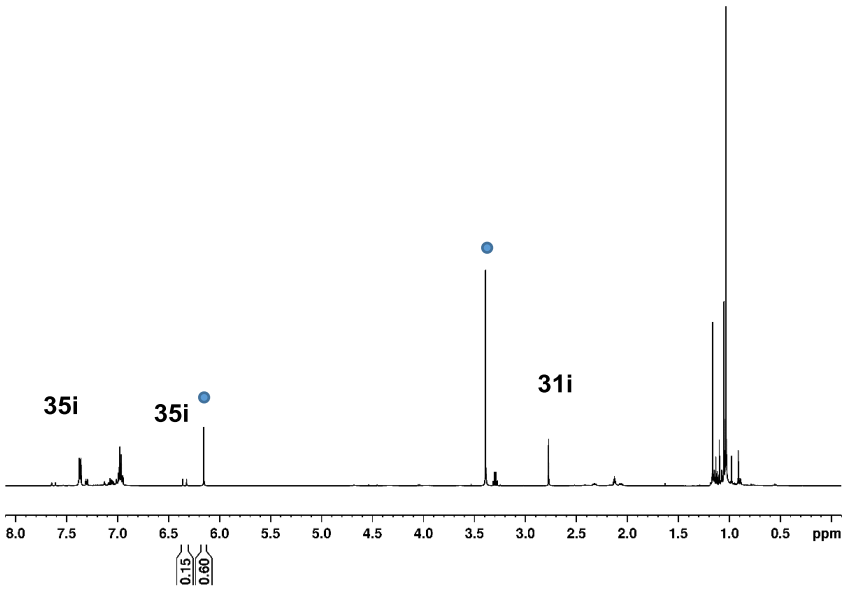

*^{1}H NMR (500 MHz, toluene-d_8) of catalysis using zwitterion (**34**), ● = 1,3,5-trimethoxybenzene internal standard.*

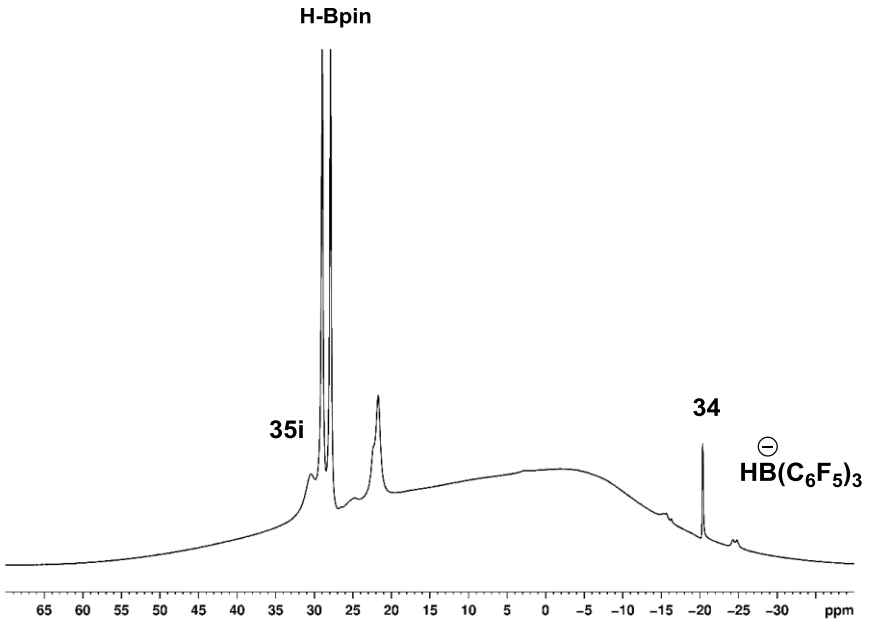

*^{11}B NMR (160 MHz, toluene-d_8) spectrum of of catalysis using zwitterion (**34**).*

Stoichiometric reaction of paramethoxy-phenyl acetylene and $B(C_6F_5)_3$ and HBpin

A solution of paramethoxy-phenyl acetylene (0.12 mmol, 16.2 mg) in 0.60 mL of toluene-d_8 was added at 233 K to $B(C_6F_5)_3$ (0.12 mmol, 61.4 mg) in an NMR tube. The solution was allowed to warm up to room temperaure and NMR spectra were recorded. After 1 h, 1 eq. of HBpin was added and the NMR spectra were recorded.

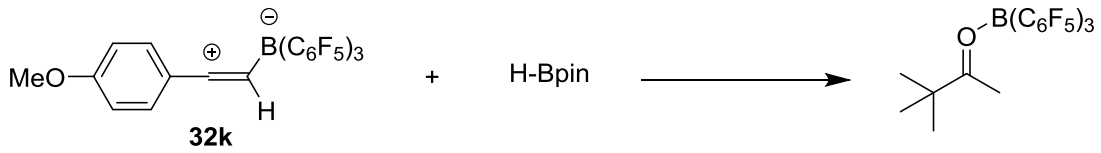

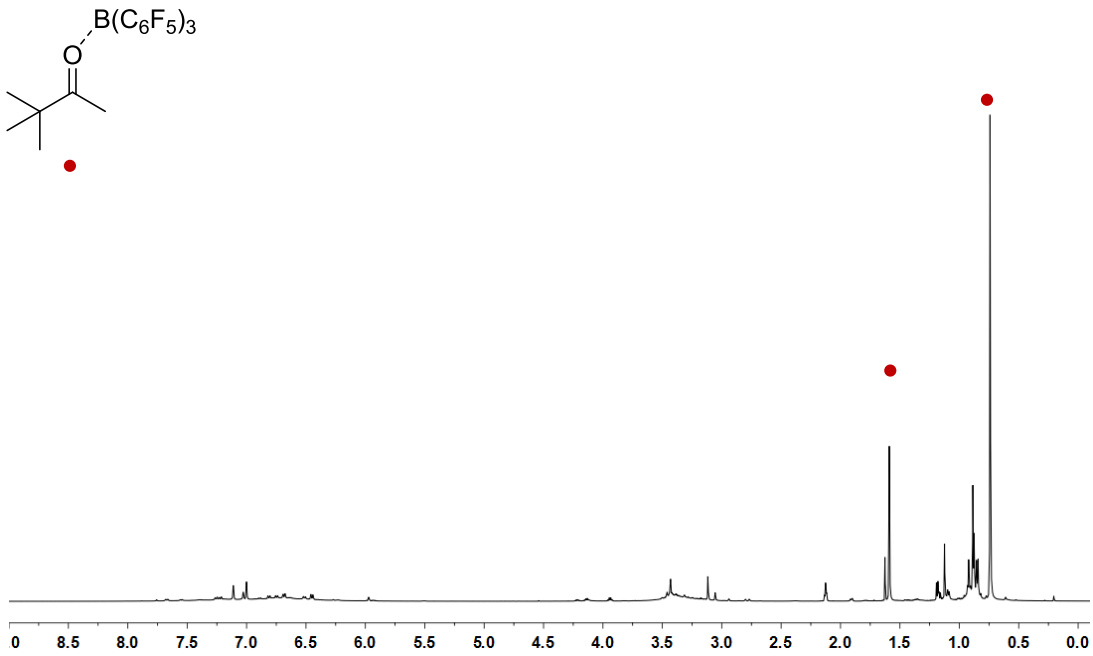

*^{1}H NMR (500MHz, toluene-d_8) spectrum of **32k** and H-Bpin.*

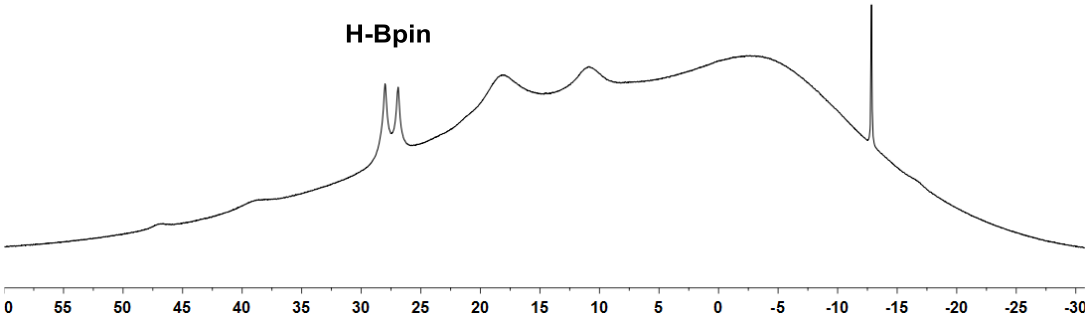

*^{11}B NMR (160 MHz, toluene-d_8) of **32k** and H-Bpin.*

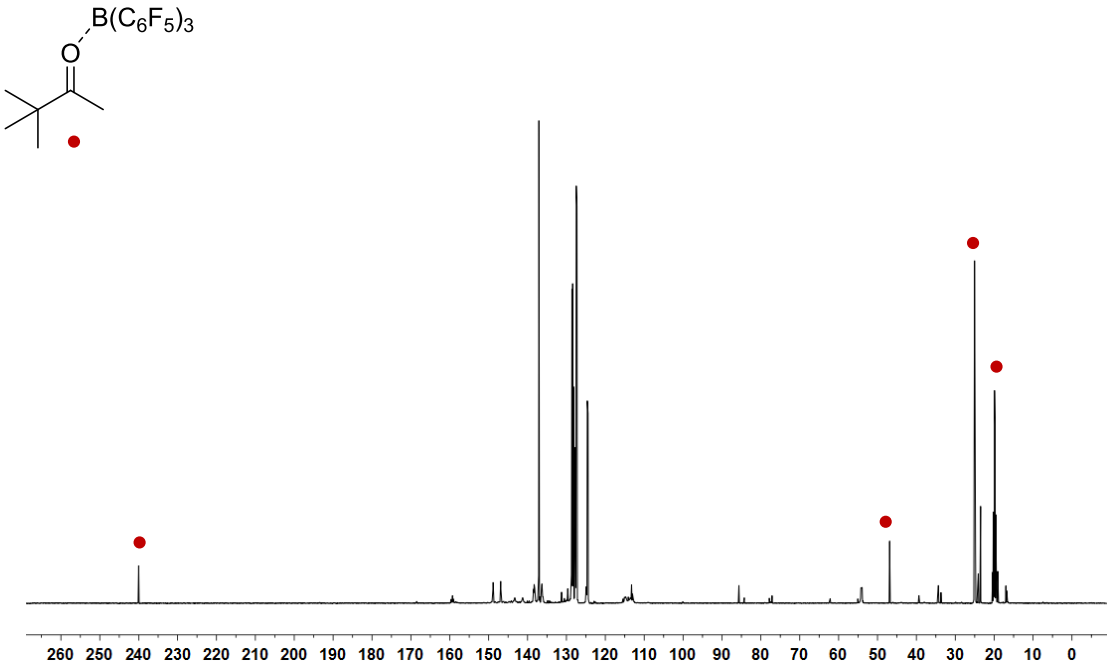

*^{13}C{H} NMR (160 MHz, 298 K, toluene-d_8) of **32k** and H-Bpin.*

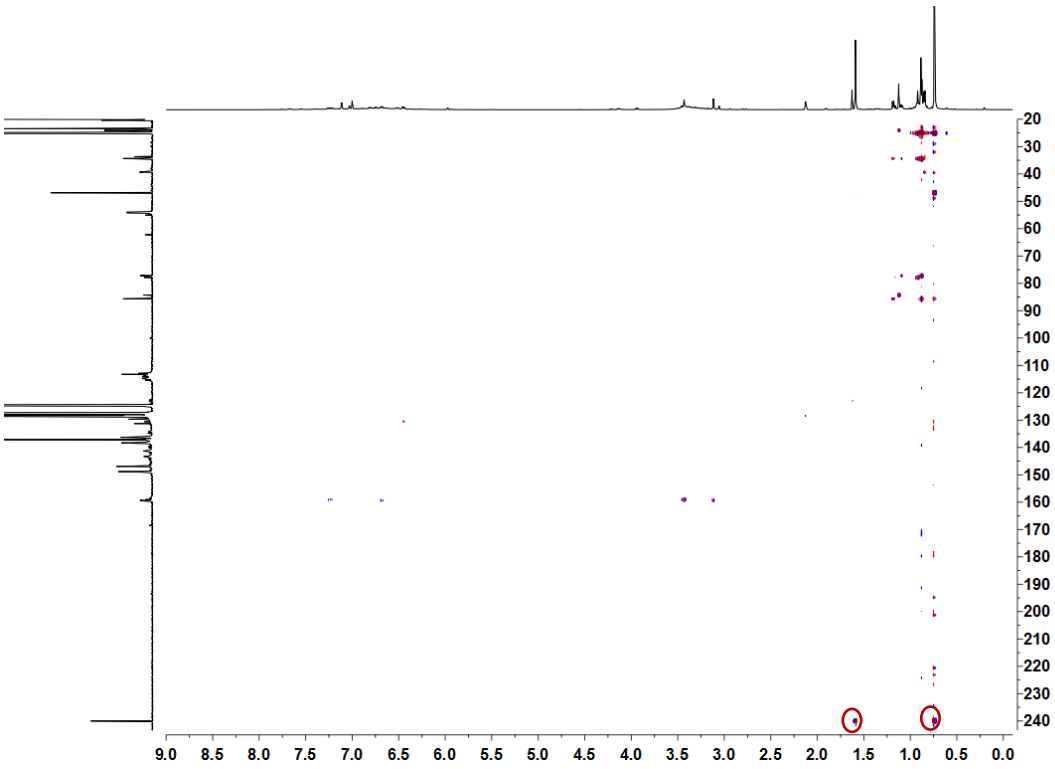

*2D HMBC ^{1}H ^{13}C NMR of **32k** and H-Bpin.*

Catalysis using the zwitterion (32k)

A solution of paramethoxy-phenyl acetylene (0.04 mmol, 5.0 mg) in 0.60 mL of toluene-d_8 was added at 195 K to $B(C_6F_5)_3$ (0.04 mmol, 20.0 mg) in an NMR tube. The solution was allowed to warm up to room temperature and NMR spectra were recorded to confirm the formation of the Zwitterion. After paramethoxy-phenyl acetylene (40 eq., 200 mg) and HBpin (48 eq., 0.280 mL) were added and the reaction was heated for 2 h at 60 °C.

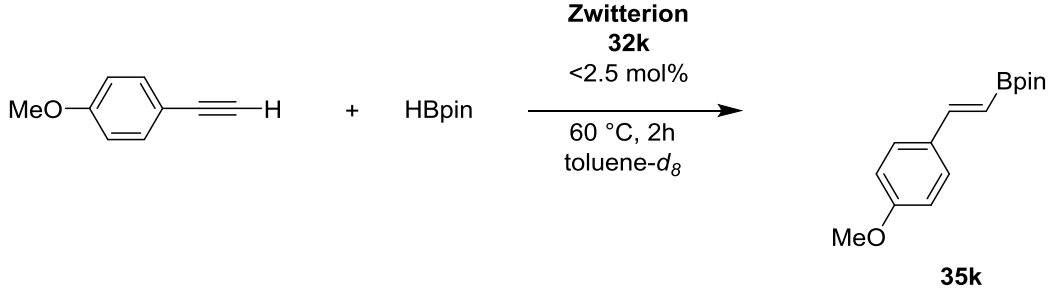

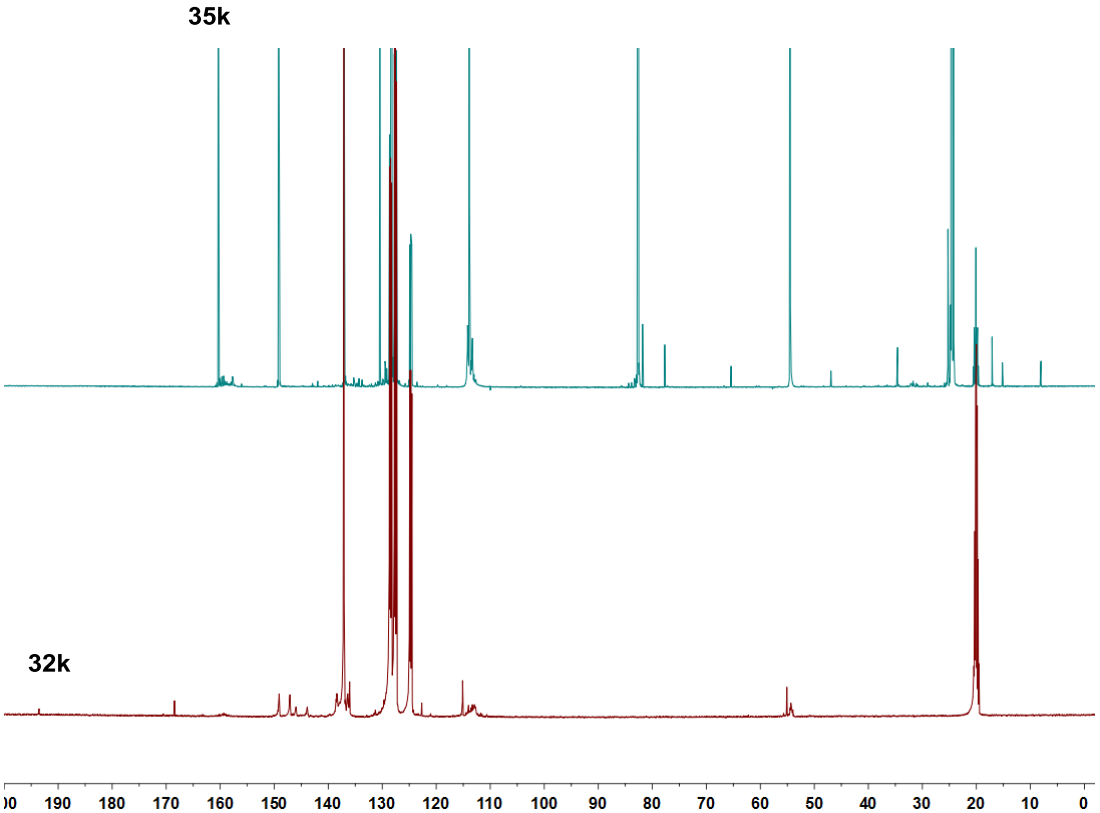

*Comparison of $^{13}C\{H\}$ NMR (500 MHz, toluene-d_8) spectra of the catalysis using zwitterion (**32k**).*

5.26 References

[1] J. Wang, A. K. Dash, M. Kapon, J. C. Berthet, M. Ephritikhine, M. S. Eisen, *Chem. Eur. J.,* 2002, **8**, 5384–2396.

[2] F. Labre, Y. Gimbert, P. Bannwarth, S. Olivero, E. Duñach, P. Y. Chavant, *Org. Lett.,* 2014, **16**, 2366–2369.

[3] J. Zhao, Z. Niu, H. Fu, Y. Li, *Chem. Commun.,* 2014, **50**, 2058–2060.

[4] K. Shirakawa, A. Arase, M. Hoshi, *Synthesis*, 2004, **11**, 1814–1820.

[5] M. D. Greenhalgh, S. P. Thomas, *Chem. Commun.,* 2013, **49,** 11230–11232.

[6] H. R. Kim, J. Yun, *Chem. Commun.,* 2011, **47**, 2943–2945.

[7] H. Y. Wang, L. L. Anderson, L. L. *Org. Lett.,* 2013, **15**, 3362–3365.

[8] C. Feng, H. Hong Wang, L. Liang Xu, P. Li, *Org. Biomol. Chem.* 2015, **13**, 7136–7139.

[9] M. V. Joannou, B. S. Moyer, M. J. Goldfogel, J. Simon, S. J. Meek, *Angew. Chem. Int. Ed*., 2015, **54**, 14141–14145.

[10] D. Peng, M. Zhang, Z. Huang, Z. *Chem. Eur. J.,* 2015, **21**, 14737–14741.

[11] W. Uhl, E. Er, A. Hepp, J. Kösters, M. Layh, M. Rohling, A. Vinogradov, E. U. Würthwein, N. Ghavtadze, *Eur. J. Inorg. Chem*., 2009, 3307–3316.

[12] H. C. Brown, B. Singaram, *Inorg. Chem.,* 1980, **19**, 451–455.

[13] J. V. Obligacion, P. J. Chirik, *J. Am. Chem. Soc.*, 2013, **135**, 19107–19110.

[14] L. Zhang, Z. Zuo, X. Leng, Z. Huang, *Angew. Chem. Int. Ed*., 2014, **53**, 2696-2700.

[15] M. Toure, O. Chuzel, J. Parrain, *Dalton Trans.*, 2015, **44**, 7139–7143.

[16] J. Lee, M. M. Joullie', M. Hoshi, *Tetrahedron*, 2015, **71**, 7620–7629.

[17] Q. Yin, S. Kemper, H. F. T. Klare, M. Oestreich, *Chem. Eur. J.,* 2016, **22**, 13840–13844.

[18] K. Yang, Q. Song, *Green Chem*., 2016, **18**, 932–936.

[19] M. Espinal-Viguri, C. R. Woof, R. L. Webster, *Chem. Eur. J.,* 2016, **22**, 11605–11608.

[20] J. Schneider, C. P. Sindlinger, S. M. Freitag, H. Schubert, L. Wesemann, *Angew. Chem. Int. Ed*., 2017, **56**, 333–337.

[21] D. Mukherjee, A. Ellern, A. D. Sadow, *Chem. Sci.,* 2014, **5**, 959–964.

[22] C. Weetman, M. D. Anker, M. Arrowsmith, M. S. Hill, G. Kociok-Köhn, D. J. Liptrot, M. F. Mahon, *Chem. Sci.,* 2016, **7**, 628–641.

[23] DOI: 10.1039/SP215.

[24] A. Bismuto, S. P. Thomas, M. J. Cowley, *Angew. Chem. Int. Ed.,* 2016, **55**, 15356.

[25] M. Fleige, J. Möbus, T. vom Stein, F. Glorius and D. W. Stephan, *Chem. Commun.*, 2016, **52**, 10830–10833.

[26] H. Yoshida, I. Kageyuki, K. Takaki, *Org. Lett.* 2014, **16**, 3512.

[27] D. Janssen-Müller, M. Schedler, M. Fleige, C. G. Daniliuc, F. Glorius, *Angew. Chem. Int. Ed.,* 2015, **54**, 12492–13844.

Appendix 1: Publications

A. Bismuto, S. P. Thomas, M. J. Cowley, *Angew. Chem. Int. Ed*., 2016, **55**, 15356–15359.

A. Bismuto, M. J. Cowley, S. P. Thomas, *ACS Catal*., 2018, **8**, 2001–2005.

Nate W. J. Ang, C. S. Buettner, S. Docherty, A Bismuto, J. R. Carney, J. H. Docherty, M. J. Cowley, S. P. Thomas, Synthesis, 2018, **50**, 803.

Appendix 2: NMR Spectra

Please find copies of the NMR spectra on attached USB stick

Appendix 3: X-ray Crystallographic Data

Please find copies of X-ray crystallographic reports, CIF files on attached USB stick